

1996

Experimental and analytical study of galloping forces on support structures

Mingche Wu
Iowa State University

Follow this and additional works at: <https://lib.dr.iastate.edu/rtd>

 Part of the [Civil Engineering Commons](#)

Recommended Citation

Wu, Mingche, "Experimental and analytical study of galloping forces on support structures " (1996). *Retrospective Theses and Dissertations*. 11347.
<https://lib.dr.iastate.edu/rtd/11347>

This Dissertation is brought to you for free and open access by the Iowa State University Capstones, Theses and Dissertations at Iowa State University Digital Repository. It has been accepted for inclusion in Retrospective Theses and Dissertations by an authorized administrator of Iowa State University Digital Repository. For more information, please contact digirep@iastate.edu.

INFORMATION TO USERS

This manuscript has been reproduced from the microfilm master. UMI films the text directly from the original or copy submitted. Thus, some thesis and dissertation copies are in typewriter face, while others may be from any type of computer printer.

The quality of this reproduction is dependent upon the quality of the copy submitted. Broken or indistinct print, colored or poor quality illustrations and photographs, print bleedthrough, substandard margins, and improper alignment can adversely affect reproduction.

In the unlikely event that the author did not send UMI a complete manuscript and there are missing pages, these will be noted. Also, if unauthorized copyright material had to be removed, a note will indicate the deletion.

Oversize materials (e.g., maps, drawings, charts) are reproduced by sectioning the original, beginning at the upper left-hand corner and continuing from left to right in equal sections with small overlaps. Each original is also photographed in one exposure and is included in reduced form at the back of the book.

Photographs included in the original manuscript have been reproduced xerographically in this copy. Higher quality 6" x 9" black and white photographic prints are available for any photographs or illustrations appearing in this copy for an additional charge. Contact UMI directly to order.

UMI

A Bell & Howell Information Company
300 North Zeeb Road, Ann Arbor MI 48106-1346 USA
313/761-4700 800/521-0600

**Experimental and analytical study of galloping forces on
support structures**

by

Mingche Wu

**A dissertation submitted to the graduate faculty
in partial fulfillment of the requirements for the degree of
DOCTOR OF PHILOSOPHY**

Department: Civil and Construction Engineering

Major: Civil Engineering (Structural Engineering)

Major Professors: Terry J. Wipf and Mardith A. Baenziger

Iowa State University

Ames, Iowa

1996

UMI Number: 9626076

**UMI Microform 9626076
Copyright 1996, by UMI Company. All rights reserved.**

**This microform edition is protected against unauthorized
copying under Title 17, United States Code.**

UMI
300 North Zeeb Road
Ann Arbor, MI 48103

**Graduate College
Iowa State University**

**This is to certify that the doctoral dissertation of
Mingche Wu
has met the dissertation requirements of Iowa State University**

Signature was redacted for privacy.

Committee Member

Signature was redacted for privacy.

Committee Member

Signature was redacted for privacy.

Committee Member

Signature was redacted for privacy.

Co-Major Professor

Signature was redacted for privacy.

Co-Major Professor

Signature was redacted for privacy.

For the Major Department

Signature was redacted for privacy.

For the Graduate College

TABLE OF CONTENTS

ACKNOWLEDGEMENTS	vi
1. INTRODUCTION	1
1.1 Transmission/Distribution Line Systems	1
1.1.1 Structural Systems	1
1.1.2 Characteristic	5
1.1.3 Damage/Failure of the Transmission Line	7
1.2 Conductor Galloping	9
1.2.1 Characteristics of Conductor Galloping	9
1.2.2 Time of Occurrence	9
1.2.3 Cause of Galloping	10
1.3 Significance of Galloping Study	12
1.3.1 Damage Caused by Conductor Galloping	12
1.3.2 Ice Storm Example	13
1.4 Current Design Problem of the Transmission Line	13
1.4.1 Current Design Criteria	13
1.4.2 Lack of Information for Dynamic Loads from Code and Design Guide	14
1.5. The Scope of the Project	15
2. LITERATURE REVIEW	16
2.1 Aerodynamics of Iced Line	16
2.2 Field Observations	17
2.3 Modelling and Assessment	19
3. EXPERIMENTAL RESEARCH	23
3.1 Modelling	23
3.1.1 Model Description/Construction	23
3.1.1.1 Comparison between Real Transmission Line and Experimental Model	23
3.1.1.2 Experimental Arrangement	28
3.1.2 Justification of Excitation Mechanism	35
3.1.3 Comparison between Laboratory Prototype and Laboratory Model	36
3.1.3.1 Selection of Variables	38
3.1.3.2 Dimensional Analysis	38
3.1.3.3 Model Design Condition	39
3.1.3.4 Laboratory Prototype and Model Wires	40
3.1.4 Measurement Apparatus	41
3.1.4.1 MTS Dynamic System	41
3.1.4.2 Load Cell and Plotting Recorder	42
3.1.4.3 Stick Scale and Video Camera	42
3.2 Test Procedure	44
3.2.1 Calibration of the Load Cell	44
3.2.2 Wire Cutoff	49
3.2.3 Simulation of Ice Load	51
3.2.4 Measurement of Dynamic Load/Amplitude/Static Load	51
3.3 Error Analysis	52
3.3.1 Selection of Relevant Parameters	52

3.3.2	Method of Analysis	52
3.3.3	Results of the Average Maximum Percentage Measurement Error	54
3.3.4	Effects of Measurement Errors of Various Parameters on Support Forces	55
3.3.4.1	Effect of Measurement Error of Unit Weight on Support Forces	55
3.3.4.2	Effect of Measurement Error of Cross-sectional Area on Support Forces	70
3.3.4.3	Effect of Measurement Error of Wire Length on Support Forces	75
3.4	Results and Discussions	82
3.4.1	Laboratory Prototype and Model Wires	82
3.4.1.1	Forces Comparison	82
3.4.1.2	Explanation of the Discrepancy	85
3.4.1.3	Reconstruction of the Prototype-Model Comparison after Considering the Length Measurement Error	87
3.4.1.4	Estimation of the Actual Length	88
3.4.2	Usefulness of the Collected Data	92
3.4.3	Other Experimental Conclusions	95
4.	ANALYTICAL STUDY	97
4.1	Assumptions	97
4.2	Governing Equations of Motion	98
4.2.1	Derivation of Equations of Motion	98
4.2.2	Characteristic of Governing Equations of Motion	109
4.3	Solution Strategy	112
4.4	Results and Discussions	115
4.4.1	Comparison of the Analytical and Experimental Results	115
4.4.2	Discussions of the Analytical Solution	119
5.	SUMMARY AND CONCLUSION	122
5.1	Summary	122
5.2	Conclusions	123
5.2.1	Experimental Study	123
5.2.2	Analytical Study	124
5.3	Contribution	125
5.4	Recommendation for Further Research	126
APPENDIX A: TEST WIRE INFORMATION		128
APPENDIX B: JUSTIFICATION OF EXCITATION MECHANISM		131
APPENDIX C: SCALES OF THE PARAMETERS OF THE SIMILARITY PAIRS		139
APPENDIX D: STATISTICAL METHOD		140

APPENDIX E: SPRING CONSTANT OF LOAD CELL LC1	145
APPENDIX F: MEASUREMENT ERROR	146
APPENDIX G: SIMILARITY PAIRS	227
APPENDIX H: IRVINE'S AND SIMPSON'S FORMULAE	231
APPENDIX I: FIGURES OF SIMILARITY PAIRS OF WIRES	235
REFERENCES	242

ACKNOWLEDGEMENTS

I thank God for enabling me to complete this work, and seek His help and guidance in all my efforts, and I attribute any success that I attain in my life to His grace and guidance.

I wish to express my deepest appreciation to my major professors Dr. Terry J. Wipf and Dr. Mardith Baenziger for their help and support throughout this work. I would also like to thank Dr. Robert E. Abendroth, Dr. Donald F. Young, and Dr. William D. James for serving on my graduate committee and their help in this research.

I express my utmost gratitude and my deepest appreciation to my parents for their patience, care and advice, and would like to thank all the people who encouraged me throughout my work. I share all my accomplishments to my beautiful wife, Fenning Dyer, and my two handsome sons, Samuel and Enoch Wu.

1. INTRODUCTION

1.1 Transmission/Distribution Line Systems

1.1.1. Structural Systems

The use of electricity has revolutionized the world since its invention. The daily essential appliances such as lamps, TVs, refrigerators, and washing machines all need electricity. Electricity is also important to industrial productions and social activities. History has shown that the more industrialized a nation is, the higher its citizens consume electricity. Therefore, the density of transmission/distribution lines is, in some respect, an index of the degree of the development of a nation. By definition, the transmission lines are the overhead conductors which transport the electricity from a power station to a substation or from one substation to another substation. On the other hand, the distribution lines transport the electricity from a substation to areas of service. From a mechanical, structural, and topographical point of view, the transmission lines which carry high-voltage power would use larger conductors and are built with longer spans. As an example, the aluminum-conductor-steel-reinforced (ACSR) "Drake" with overall diameter of 1.108 inches is most intensively used in Iowa's 345-kV transmission lines with typical span of 1200 feet. The distribution line will use smaller ACSR such as "Sparate" (0.325 inch in diameter with 300-foot span length).

The transmission/distribution line structural system

consists of three basic elements, i.e., support structure, suspension insulator, and the wires as shown in Fig. 1-1. The support structures are usually made of wood, concrete, or steel. Some will use aluminum when weight savings, as when construction is done by a helicopter, are significant as compared to steel structures. Wood poles are most commonly used for the support of distribution lines. They require a type of wood (such as pine) that provides strength, durability, lightness in weight, straightness, and accessible supply. Concrete pole is the choice for areas with diminishing supply of wood pole. Solid and hollow types are used for concrete poles. The former is more easily manufactured while the latter could provide connections of the aerial lines to the underground cables through the core. The steel poles and towers are divided into five categories, i.e., tubular steel poles, expanded steel truss poles, latticed steel poles, flexible steel structure, and fabricated steel tower [1]. The structural components of an H-frame steel structure, as commonly seen in Iowa, are shown in Fig. 1-2.

An insulator consisting of glass, porcelain or composition of both is used to hang the lines from the support structure while preventing the transmission of electricity to the support structure. Generally, insulators can be divided into three classes [1], i.e., post type, suspension type, and dead-end type. The post-type insulator, being of a pedestal form, is designed to carry the conductor above the crossarm of

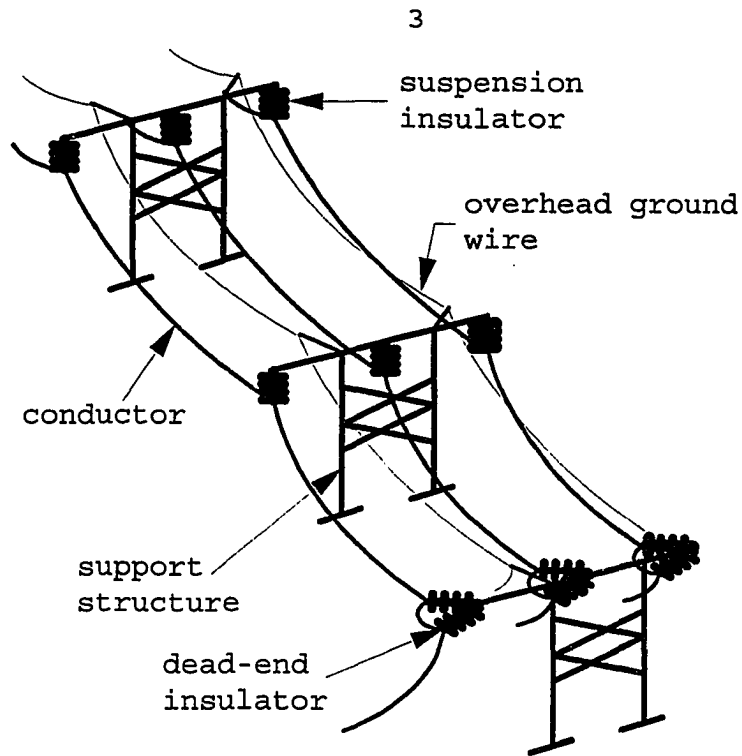


Fig. 1-1: A segment of the transmission line system.

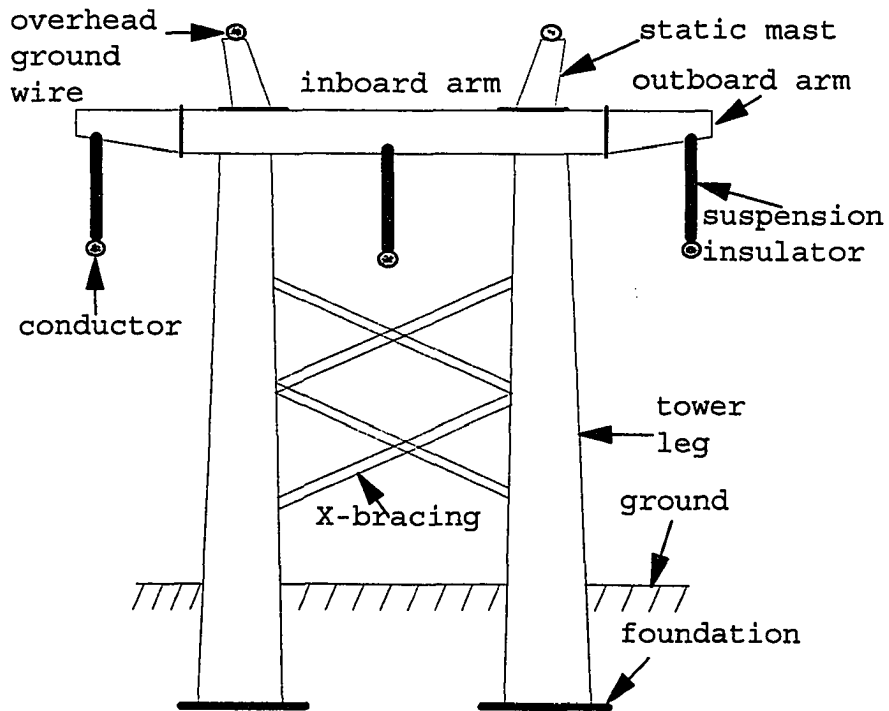


Fig. 1-2: A typical H-frame flexible steel structure.

the support structure, i.e., it is designed to resist the load perpendicular to its axes. The other two classes as shown in Fig. 1-1 would support the conductors below the crossarms of the support structure. Since the insulators would swing as the conductors move, they are designed to resist the load along their axes. Note that the dead-end type which includes two suspension insulators is used when the transmission line changes direction.

The wires include the conductors and overhead ground wires (or shield wires). The principal kind of composite conductors used recently in transmission lines are 1350-H19 grade aluminum, stranded conductors that are reinforced by a core of steel wires (aluminum conductor, steel reinforced or ACSR). Since aluminum strands have higher conductivity coefficients and greater cross-sectional area than steel strands, they have higher conductivity than steel strands. Also alternating current tends to concentrate on the outer loop of the cross section. Due to the above reasons, the aluminum strands will carry most of the electricity. The purpose of the steel strands is to reinforce the strength of the composite material. The overhead ground wires which do not transmit electrical power are not insulated from the support towers. The ground wires are used to avoid damage to the conductors and to the support structure in case of lightning. Note that the ground wires are installed above the power-carrying conductors as shown in Fig. 1-1 so that they can act

as lightning rods.

Secondary elements in the transmission line systems which serve a structural purpose include the crossarms, dampers, and foundations of the support structures. The size of a crossarm should be designed in accordance with the number, size, voltage and span length of the conductor to be installed. If necessary, the arm should be reinforced by bracing to avoid a bending failure.

1.1.2 Characteristic

The study of cable dynamics can be traced back to the ancient Greeks who investigated the small-amplitude vibration (aeolian vibration) in musical instruments. The behavior of a taut string vibration, described by the wave equation, was thoroughly understood by Taylor, D'Alembert, Euler, and Bernoulli early in the eighteen century. However, cables possess some level of sag in most practical application. Their dynamic behavior are found to be distinctly different from those of taut wires.

In spite of numerous efforts [2, 3, 4] being made in the analytical solution of the latter problem, a complete understanding of cable dynamics has not been achieved. The reason for the difficulty, especially in the field of transmission lines, is due to several aspects. The conductors are manufactured of spiral-wrapped strands, some of them being aluminum strands in the outer loop and others being steel

strands in the center. The mechanical behavior of such a combination is very complex. The report from Aluminum Association shows that the stress-strain relationship of an ACSR conductor is nonlinear and is described by a cubic polynomial [5]. Also, the flexural rigidity EI , expressed as the product of the modulus of elasticity E of the conductor and the section moment of inertia I , is complicated in the case of spiral-wrapped, stranded conductors. Two extreme cases for the values of moment of inertia might exist. If all strands act independently when stretched, a minimum moment of inertia I_{\min} is obtained; and a maximum moment of inertia I_{\max} will be obtained if all strands act compositely as a single unit. The difference of moment of inertias between the two cases would vary as much as 70 to 1 [6]. Practically, the interaction within the strands should be between the above two cases. In addition, the interstrand motion within the strands would vary along a vibrating conductor, and would also vary with time during vibration cycle. Therefore, the rigidity EI is a function of both length coordinate and the time. By adding this variation into the analysis of cable dynamics when the flexural behavior is considered, the equations become very complicated.

Unlike the axial vibration of a bar or lateral vibration of a beam in which the amplitude of oscillation is small with respect to the entire length of the member, the amplitude of oscillation in conductor dynamics is large. This large-

amplitude motion can be observed in either broken or galloping conductors. The former occurs when the unbalancing forces resulting from the sudden breaking of one conductor cause the adjacent ones into violent and irregular vibration. The latter will be discussed in details in Section 1.2.

1.1.3 Damage/Failure of the Transmission Line

The damage/failure of the transmission lines will result in power outage which would be either inconvenient or even economically devastating to the residence community and the industrial area in modern society. The possible causes for the damage/failure include lightning, tree falling, ice deposition, fatigue of transmission line and structural component of support, and conductor galloping.

Lightning damage to the transmission lines results from a sudden voltage and current surge produced by the stroke. The damage includes malfunctioning and even permanent failure to the electrical power system [7]. To improve the protection from damage, high priority should be given to the understanding of basic physics of atmospheric electricity as well as steps to lessen the vulnerability of electric equipment such as use of solid-state circuits.

Damage of a transmission line by falling trees, freezing rain storms or both are occasionally seen. For instance, a 420-kV line spanning between Keban and Istanbul, Turkey was put into operation in 1974. During the first five years of

operation, 114 towers out of 6658 towers were destroyed in 14 incidents. Among those incidents, all the winter ones were caused by heavy ice, generally in combination with strong wind load [8].

Aeolian vibration of the transmission lines over a long period of time could cause a fatigue failure. These points in the transmission line system include support location, suspension clamps, clamp-top, pin insulators, and deadends. Several special devices such as Armor-Grip suspension and long-radius clamps can permit higher vibration levels without fatigue [6]. Control of vibration with the addition of vibration dampers can also reduce the occurrence of fatigue.

Galloping damage can be seen occasionally in the freezing rain areas. As a result of ice deposition on the conductor under the wind flow, galloping can break conductor strands and destroy tower hardware. A 1990 ice storm in central Iowa caused a domino collapse of sixty-eight support towers in a portion of Lehigh-Sycamore 345 kV line [9], resulting in power outage for thousands of residents and high costs of repair.

Some other causes of damage and failure to the transmission line system include design error and defective material so that the support structure will fail in the severe weather condition. In addition, tornadoes, earth movement , or even errant aircraft can also damage the power line.

1.2 Conductor Galloping

1.2.1 Characteristics of Conductor Galloping

Conductor galloping, also called "conductor dancing", is an unusual aerodynamic phenomenon of the electrical transmission line. It is characterized by a primarily vertical motion of low frequency and high amplitude. The horizontal (along-the-line) and out-of-plane motions do exist when galloping occurs, but the motions are significantly smaller than the vertical oscillation. The frequency of the vibration is between 0.08 and 3 Hz. The range of vibration amplitude (peak-to-peak) varies from 0.5 to 30 feet, depending on the span of the conductors [6].

1.2.2 Time of Occurrence

Conductor galloping has rarely been observed in warm or hot countries, but it occurs occasionally in regions which have freezing rain. Galloping occurs as the result of irregular ice deposition on the surface of the conductor when temperature hovers around 32°F or lower and steady transverse wind flow on conductor surface. The equivalent radial thickness of ice deposition is from 0.1 to 1 inch and the average wind velocity is approximately between 15 and 40 mph [6]. Note that early studies of conductor galloping [10] associated it with rather strong windspeeds, e.g. in excess of 56 mph. More recent studies, however, show that well-ordered winds at about 34 mph are perhaps the most troublesome [11].

Once started, the disturbance is very persistent and continues sometimes for up to 2 days [6].

1.2.3 Cause of Galloping

The actual cause of conductor galloping is still a topic of research. A popular explanation is called "airfoil analogy". It states that the asymmetrical cross-sectional shape of an iced conductor resembles an airfoil. The eccentricity between the center of gravity of the conductor itself and that of the iced conductor causes periodic twisting of the conductor as air current flows past the conductor [12]. When the airfoil-shape section orients to such a position that the aerodynamic force induced from the transverse wind flow moves the conductor upward, galloping of the conductor occurs. The phenomenon is similar to the takeoff of an airplane in which the speed of air flow increases on the longer side of the wing, resulting in a low pressure region according to Bernoulli's principle. The unbalance between the high pressure region on the under side and the low pressure region on the upper side results in an upward force, which lifts the plane.

Once galloping starts, Den Hartog [10] proposed that sustained vibrations occur at the angle of attack for which the negative slope of lift curve exceeds the drag force, or mathematically,

$$\frac{dL}{d\alpha} + D < 0$$

$$, \text{ or } \frac{dC_L}{d\alpha} + C_D < 0 \quad (1-1)$$

where L and D are the magnitude of the aerodynamic lift and drag forces acting on the conductor per unit length of the conductor (The aerodynamic drag force acts in the direction of the relative wind velocity, i.e., the relative velocity between wind and conductor velocity, and lift force acts perpendicular to it). C_L and C_D are the lift and drag coefficients of the section, and α is the angle of incidence of the wind in the vertical plane measured from some (arbitrary) reference axis. In other word, for some interval in α if the upward motion is coincident with a positive aerodynamic lift force, and if the downward motion is coincident with a negative lift force, accelerating gallop will result. On the other hand, if the upward conductor motion coincides with a negative aerodynamic lift force, and if the downward motion coincides with a positive lift force, the motion will be suppressed, and the conductor will not gallop. Note that the generalized instability criterion in Equation 1-1 is usually the case when the cross section of the conductor take the form of an ellipse (or similar shapes). For this reason, conductors of circular section which have accreted ice are usually prone to galloping. Likewise, cables with some other shapes such as square sections and certain rectangular sections will also gallop readily if they are

positioned a suitable orientation to the wind.

1.3 Significance of Galloping Study

1.3.1 Damage Caused by Conductor Galloping

Conductor galloping has long been the concern of the transmission line designers because of the costly damage that can result from this type of behavior. Galloping reduces the vertical and horizontal clearances between the lines, and then increases the possibility of conductors' contact with each other which would cause flashover and consequent outage of the circuit. Also, galloping could break conductor strands and damage dampers, insulator pins, suspension and crossarm hardware, and even the towers due to whipping effect of downward motion. If no immediate damage occurs due to conductor galloping, the sustained periodic motion of overhead lines may lead to conductor fatigue and hence to line failure. Because of the voltage involved, the type of close-range inspection desired for early detection of such damage is possible only when the line is taken out of service. The difficulty encountered in arranging for scheduled outage makes the study of galloping behavior important: problems caused by conductor motion must be either anticipated and prevented during the design and construction stages or resolved at higher costs after visible damage has occurred. Therefore, it is important to be familiar with the galloping loads to

improve the design of transmission line structural systems.

1.3.2 Ice Storm Example

A freezing rain storm moved into southwestern and central Iowa on March 7, 1990. This storm caused severe damage in a portion of Lehigh-Sycamore 345 kV electric transmission line. The storm had average wind speed of 12.1 mph, a peak wind gust of 31 mph, and accumulated radial thickness of ice on the conductors 1.25 to 1.5 inches. As the result of these heavy loads and subsequent conductor galloping, sixty-eight H-frame steel towers collapsed. Strands of conductors and shield wires were stretched to failure. The X-bracings and tower legs buckled and insulators were separated from the crossarms of the towers and fell to pieces on ground [9]. Consequently, thousands of residents lost power for days and millions of dollars were spent to restore the system.

1.4. Current Design Problem of the Transmission Line

1.4.1 Current Design Criteria

The National Electrical Safety Code (NESC) is widely used by utilities as a design guide. It states that the mechanical strength of a conductor must be so strong that [13]

- (a) tension under maximum loading conditions, i.e., wind plus ice loads, shall not exceed 60% of the ultimate strength,
- (b) tension at 60°F and without external load shall not exceed one quarter of the ultimate strength after the conductor

has assumed its final sag, e.g. creep factor is considered after ten years installation, and

(c) tension at 60°F and under initial no-load conditions shall not exceed 35% of the ultimate strength.

The NESC also specifies the combined wind and ice loading for different areas of the United States. For instance, Iowa, designated as the heavy loading area, is expected to receive 0.5 inch radial thickness of ice and 4 lb/ft² horizontal wind pressure on the conductor at temperature 0°F in winter season.

1.4.2 Lack of Information for Dynamic Loads from Code and Design Guide

Until recently, the design of the transmission lines and the structures supporting them have been primarily based on static loads with a conservative safety factor. For instance, the NESC [13] specifies the overload capacity factors for support structure, foundation, guy wires, crossarm, bracing, and conductor. However, no information is provided for the dynamic loads on support structures due to conductor galloping. Similarly, other commonly used publications such as "Guidelines for Transmission Line Structure Loading" [14] and "Transmission Line Design Manual" [15] contain no formulas for the forces transmitted to the support structure by galloping conductors. Therefore, the project under investigation seeks to develop a reliable method to predict galloping conductor forces.

1.5. The Scope of the Project

The objective of this study is to (1) develop an experimental procedure to simulate galloping and to measure amplitude and dynamic forces on support structures, and (2) develop an analytic procedure to predict more accurately the forces on the support structures.

The experimental portion of the project included the excitation of a single-span wire line into galloping motion by hydraulic actuators in the Iowa State University Structural Laboratory. Fabrication of the experimental arrangement included the connection between the wire and load cell which measured the force, the steel box which housed the load cell, the triangular truss which connected the steel box and the actuator, and the stick scale which was used to measure the amplitude.

The analytic portion included derivation of the governing equations of motion for both linear and nonlinear cases. Since the equation development did not contain as many simplified assumptions as the expressions developed by other authors, they were more general for the application to the real transmission line. An algorithm for the numerical solution was adopted to obtain the tension along the line. The results were compared to those obtained from the experiment.

2. LITERATURE REVIEW

2.1 Aerodynamics of Iced Line

J.J. Ratkowski [16] tested nineteen models with different ice shapes both analytically by computer simulation and experimentally in a wind tunnel by rotating the models through angular steps. Note that the rotation of the model is not a prerequisite to cause, but to facilitate, galloping. This is because, as the model moves vertically under horizontal wind force, the angle of attack varies with the location of the model. Therefore, there is enough chance to generate the lift force for the model against gravity without rotation. Results showed that seventeen models, when suitably oriented to cause instability, would gallop. Ratkowski found that only a limited number of airfoil positions exist where galloping could occur. In addition, the airfoil critical orientation must exist over a major portion of the span otherwise the atmospheric forces will act to damp the galloping motion in the portion of the span that is not critically oriented. He further explained in another paper [17] using an energy method that he found three general types of galloping, each exists due to different conditions which start the galloping. The first type is the vertical torsion-free galloping, which does not require torsional rotation either to start or to maintain vibration. The second type is the elliptical torsionally modified galloping, which does not require torsional motion either to start or to maintain vibration, but which, because of an

eccentric cross section, develops torsional motion which modifies the motion of the conductor. The third type is the elliptical, torsionally controlled galloping, which requires torsional motion to start and to maintain galloping.

2.2 Field Observations

Due to technical difficulties involved, there are few field-collected data about conductor galloping. One difficulty relates to the equipment needed to accurately measure the amplitude of galloping under severe weather condition. One possible approach is to use a video camera and a scale, as proposed in this project. However, the visibility during the storm, the unknown out-of-plane displacement, and even the physical endurance of the researcher to operate the camera are the obstacles to overcome. In addition, galloping occurs so sporadically that a researcher might spend all winter without recording any incident. The varied characters and shapes of ice deposition from one occasion to another also makes generalization of a few observations inaccurate.

Krishnasamy [18] presented one of the few papers with field-collected data about galloping. Measurement equipments at five locations in South Ontario were used to monitor the wind and ice loads on the conductors. Data collected at three of these sites are useful for analysis. The report recorded mean/maximum wind speed and direction during icing, equivalent radial ice thickness, air temperature, insulator swing angle,

and the vertical and along-the-line (longitudinal) dynamic forces for four incidents of galloping. He found that the insulator swing angle which determines the clearance between the support tower and the energized conductor increases nonlinearly with wind velocity above 56 mph and that this relationship is approximately linear for wind speed below 56 mph. Krishnasamy established that the vertical dynamic loads ranged from 1.2 to 2 times of the conductor weight. The additional along-the-line dynamic force is between 270 and 900 lb, which is considered negligible with respect to the original static tension of 12900 lb.

C.B. Rawlins [19] studied the peak-to-peak amplitude of vibration from observed galloping incidents of several single, but not bundled, electrical transmission lines. Statistical analysis was used to set up guides for obtaining the expected amplitude for a particular conductor line with galloping. The information could be used to select the required clearances between the lines to prevent outage of power due to flashover between phases and between phase and ground wire. The parameters involved to obtain the amplitude include the line tension, unit weight, axial stiffness, and span length. Rawlins found that when amplitude to span length ratio is smaller than 0.01 or the tension to unit weight ratio is greater than 6500 lb/(lb/ft), galloping is not likely to occur or the amplitude is too small to be of any significance. The data he compiled and summarized such as ice shape and

thickness, wind speed, and amplitude of oscillation were made from the ground so that some errors are expected. However, because of large numbers of galloping cases, the results of Rawlins' study might have value to the transmission line design process.

2.3 Modelling and Assessment

E. W. Lee [2] excited a wire into motion by applying a magnetic field at a right angle to a small portion of the wire and then passing an alternating current through it. The wire is thus set into vertical motion at the frequency of the electric current. The amplitude of vibration was measured by placing a paper scale behind the wire. Under such a setup, Lee studied the amplitude response of the wire near its fundamental resonance frequency. He observed the discontinuities, a phenomenon called "jump", in the amplitude as the driving frequency is changed. He further found that the frequency at which these jumps occur depends on whether the frequency is being increased or decreased, i.e., the amplitude response shows a sudden drop while the driving frequency is being increased and an upward jump at a different frequency while the frequency is being decreased. In Lee's experiment, the magnetic field used to drive the wire into motion only acted on a short portion of the wire. As a result, uniform stretching, as observed in the case of overhead transmission line galloping, does not occur. Also the amplitude was limited

between 0.002 and 0.354 inch, a motion more like the aeolian vibration than the large-amplitude galloping.

W.D. James, et al. [20] used 40-inch long plastic tubings with the ice shape formed directly on the surface in wind tunnel tests. The ice shape was constructed by placing 2-inch segments of straws in a line along one side of the tubing. The straws were positioned with a 1/4-inch space between them to prevent any contact during galloping. Nine models with changes in spring stiffness, distributed weight, static tension and eccentricity among them were tested to study the forces on the supports . The angle of attack which resulted in instability of test model was also recorded. The results show that the dynamic forces of some models compare well with those calculated from Li Li's simplified formula [3], while others show large error. The latter could be attributed to a physical difference between the wind tunnel model and the assumptions of the analytical model.

A. Simpson [4] derived an analytical model for a shallow elastic catenary cable oscillating freely with a small amplitude. He obtained the force and frequency equations for various types of end supports. A successful comparison was made between the results by his method and those obtained from a "lumped parameter" method for a practical 3-span system. However, Simpson neglected a series of terms in the process of derivation to obtain a closed-form solution of the equation. The accumulated error is found to be large, especially in the

high order vibration modes. For instance, a Drake conductor, hanging on a 1200 feet span and stringing 6000 lb at both ends at 60°F initially, has 1/2 inch ice deposition at 32°F. The ratio of support tension from the equations after and before simplification are 1.86, 2.05, 2.69 for the first three modes, respectively. In addition, He neglected the slope of the horizontal displacement in his derivation. Since that term is approximately one-eighth of the slope of the vertical displacement for the aforementioned example, there exists significant error. Finally, Simpson's formula only applies to the free-vibration case, not to the forced-vibration case in galloping.

Li Li [3] formulated a simplified formula for an elastic catenary cable under the conditions of i) free oscillation in small amplitude only, ii) constant additional horizontal tension, and iii) harmonic vertical deflection shape. He obtained the vertical and horizontal tensions at the support of the transmission line due to galloping. Li concluded that the use of suspension insulators reduces both the vertical and horizontal tensions in the conductor. He also found that the dynamic forces increase as wind velocities increase, but a limit for wind speed exists above which galloping is prevented. Comparison of Li's and Simpson's works shows that, in addition to Simpson's assumptions, Li made further ones such as replacing the coordinate s along the catenary by horizontal coordinate x and assuming harmonic vertical

deflection shape to achieve his simplified formula. As a result, his formula is limited to the case of a very taut cable (sag to span ratio approaches zero) which does not represent a typical electrical transmission line (sag to span ratio is around 3%). Therefore, errors exist when applying it to a transmission line.

3. EXPERIMENTAL RESEARCH

3.1 Modelling

3.1.1 Model Description/Construction

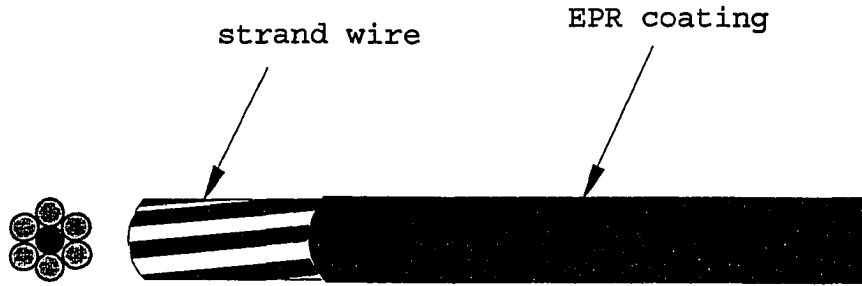
3.1.1.1 Comparison between Real Transmission Line and Experimental Model

A study conducted by the author concludes that the sag-to-span ratio for a typical transmission line is around 0.02 for a 700 feet span line and is around 0.035 for a 1000-1400 feet span line. The ratio for a typical distribution line of 300 feet span is around 0.01. A "parabolic formula" which is a good approximation to the exact elastic catenary could be used to find the static horizontal tension when the sag-to-span ratio is lower than 5% [21]. Unlike structural steel with yield strength of 65 ksi or less, in which the stress-strain relation can be clearly simplified into elastic and perfectly plastic regions, a typical ACSR used in the electrical transmission line does not have a distinctive transition point which separates the two regions. In general, the relation for an ACSR, which consists of aluminum and steel strands can be expressed by a cubic polynomial [5]. However, the nonlinear terms in that expression are much smaller than the linear ones at the low stress region. Therefore, the stress-strain relation is approximately linear for an overhead conductor oscillating at a small amplitude. In addition, when the conductor is galloping, the distribution of deposited ice along the transmission line varies with changing time since

some of the ice will be whipped away as the conductor moves up and down. Also, the ice coating will add slight axial strength to the conductor due to the bond between them.

The experimental model for the conductor included nine classes of wires. They were:

1. **No.2 bare steel wire:** Single wires with nominal diameter of 0.1 inch.
2. **No.4 bare steel wire:** Single wires with nominal diameter of 0.08 inch.
3. **No.6 bare steel wire:** Single wires with nominal diameter of 0.06 inch.
4. **No.2 USE strand copper wire:** This is a seven-strand wire covered with EPR as shown in Fig. 3-1. The nominal diameter for a single strand is 0.1 inch.
5. **No.4 USE strand copper wire:** The wire is similar with No.2 USE strand copper wire except with a smaller diameter. The nominal diameter for a single strand is 0.08 inch.
6. **No.6 USE bare copper wire:** This is a single-strand USE copper wire with nominal diameter of 0.6 inch.
7. **No.2 USE strand aluminum wire:** This is a seven-strand wire covered with EPR as shown in Fig. 3-1. The nominal diameter for a single strand is 0.1 inch.
8. **No.4 USE strand aluminum wire:** The wire is similar with No.2 USE strand aluminum wire except with a smaller diameter. The nominal diameter for a single strand is 0.08 inch.



Bare steel

#1: 0.1"

#2: 0.08"

#3: 0.06"

copper

#4: 0.1" for each strand

#5: 0.08" for each strand

#6: 0.06"

aluminum

#7: 0.1" for each strand

#8: 0.08" for each strand

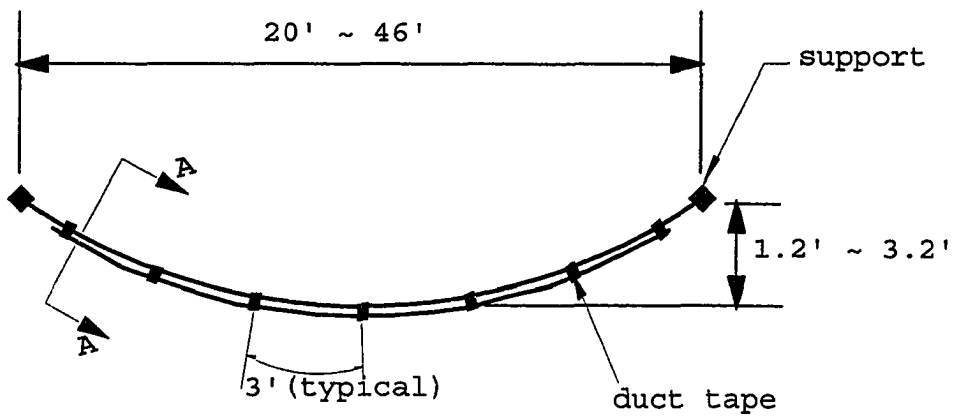
#9: 0.06" for each strand

Fig. 3-1: Strand wire used in the test.

9. **No.6 USE strand aluminum wire:** The wire is similar with No.2 USE strand aluminum wire except with a smaller diameter. The nominal diameter for a single strand is 0.06 inch.

The strand wires in classes 4, 5, 7, 8, and 9 were first stripped of the EPR coating and then were separated into single wires before testing. The nine wires from class 1 to 9 are denoted as S1, S2, S3, C1, C2, C3, A1, A2, and A3, respectively, and, therefore, subsequent reference to the wires will be with the above denotations. The wires were combined and classified in groups depending on wire type, wire length, and span length. Two hundred and twenty-one experiments were performed in which various combination of the nine classes of wires were tested. The type, wire length, and span length information about the wires for each experiment are recorded in Appendix A.

The sag-to-span ratios of the experimental models in Appendix A were between 0.045 and 0.07. The dynamic forces experienced during the test were within the linear regions of the stress-strain relationship for the respective wires. The superimposed load was simulated by imposing an attached wire or wires on the loading wire(s). The loading wires which are stressed during galloping are continuous to the support while the attached wires are continuous but are cut near the support as shown in Fig. 3-2. Duct tape strips of approximately 1/8 inch in width were used to bind those wires together in



loading wire (continuous to the support)

attached wire (served as superimposed load)



Section A-A

Fig. 3-2: The loading and attached wires are bound together by duct tape.

approximately 3 feet intervals along the length. This allows the composite wires to function together when they are excited by the hydraulic actuators. The binding effect from the duct tape produced additional resistance against stretching to the loading wires. The phenomenon is qualitatively similar to the effect of deposited ice on the conductor.

As a result, the model under investigation simulates the kind of overhead conductor of a slightly larger sag-to-span ratio, under uniform ice load, and linear mechanical behavior during galloping.

3.1.1.2 Experimental Arrangement

A support movement method was used to obtain a large-amplitude motion in the experimental approach for the galloping test. A single-span wire line, symmetrical with respect to midspan, was subjected at both ends to support motion driven by hydraulic actuators. The configuration of the equipment is shown in Fig. 3-3. The left end of the wire was connected to two load cells, one in the top measuring the vertical tension through a vertical wire rope and another in the left measuring the horizontal tension through a horizontal wire rope. The right end of the wire was connected to a third load cell through another vertical wire rope. Since the wire rope passed through a pulley to the load cell, the force recorded was then the tension force at the right end of the wire. The two load cells on the left hand side and the one on

the right hand side were mounted inside steel boxes. Each box had two opening faces, one in front and one facing each other. At each side, the box was excited by a hydraulic actuator through a triangular truss pivoted at one-thirteenth point of the top side of the truss to the side of the actuator. The amplification of the excitement through the pivoted point was necessary because, if the box was connected directly to the hydraulic actuator, the stroke was too small to make the wire develop galloping motion. Once excited, the steel boxes moved up and down along the vertical stainless steel rails at both sides. This ensured the forces recorded at the left end of the wire were horizontal and vertical tensions while that recorded at the right end was wire's tension force. Fig. 3-4 demonstrates how this system works. Detailed descriptions at each critical connection are as follows.

Fig. 3-5 shows the connection at the left end of the wire. Three connection adapters were joined by a bolt at the position right below the top load cell and to the right of the other load cell. The top and front views of the connection adapter were shown in the right hand side of Fig. 3-5. The bolt connecting the three adapters together was lubricated so that the adapter joining the wire was free to rotate. Fig. 3-6 shows the connection at the right end of the wire.

Theoretically, the right end of the wire should extend to the right-most point of the pulley, i.e., point A in Fig. 3-6. However, because of practical difficulties of connecting the

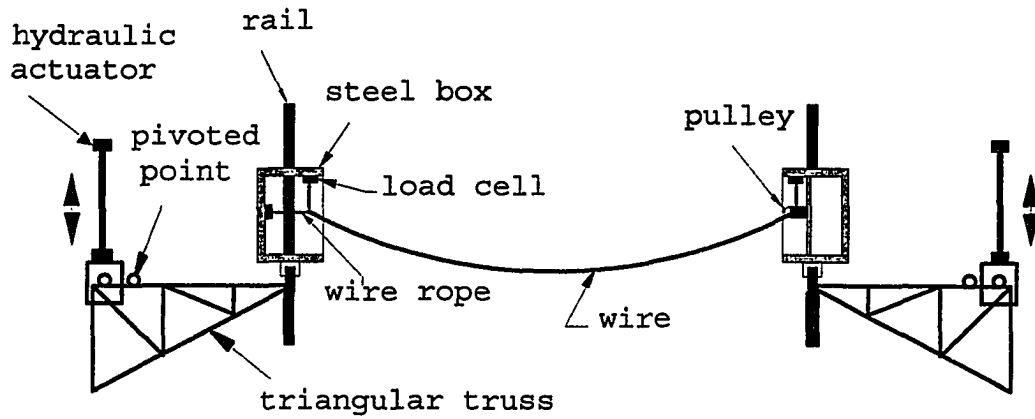


Fig. 3-3: Configuration of the equipment to test wire galloping using a single-span wire line.



Fig. 3-4: Configuration of a single-span wire and its supporting equipments in motion.

test wire and wire rope at point A, the connection adapters were joined at the lower left side. The pulley was lubricated so that the friction between the wire and the pulley was reduced to the minimum. Fig. 3-7 shows the arrangement of the steel box, the guide sleeve, and the stainless rail. The guide sleeve was fixed to the box so that both could move together. On the other hand, the rail was bolted vertically to the support frame so that the box was allowed to move only in the vertical direction. Fig. 3-8 shows the connection between the steel box and the triangular truss. A yoke end was bolted with a pin to the box so that the box was able to move vertically instead of rotating about the pivoted point. In Fig. 3-9, two bearings, one for the support frame and the other for the hydraulic actuator, were provided at the connection points of the triangular truss. The right bearing was connected to the support frame through a bolt to serve as the pivoted point for the truss while the left bearing that served as the the exciting point was connected to a hydraulic actuator with another bolt. To prevent out-of-plane movement of the truss, two shaft collars, one at each side of the bearing, were used as shown in section A-A of Fig. 3-9. A survey stick scale mounting on a W-shape steel section as shown in Fig. 3-10 was placed 30.5~33.2 inches behind the midspan of the wire to measure the amplitude.

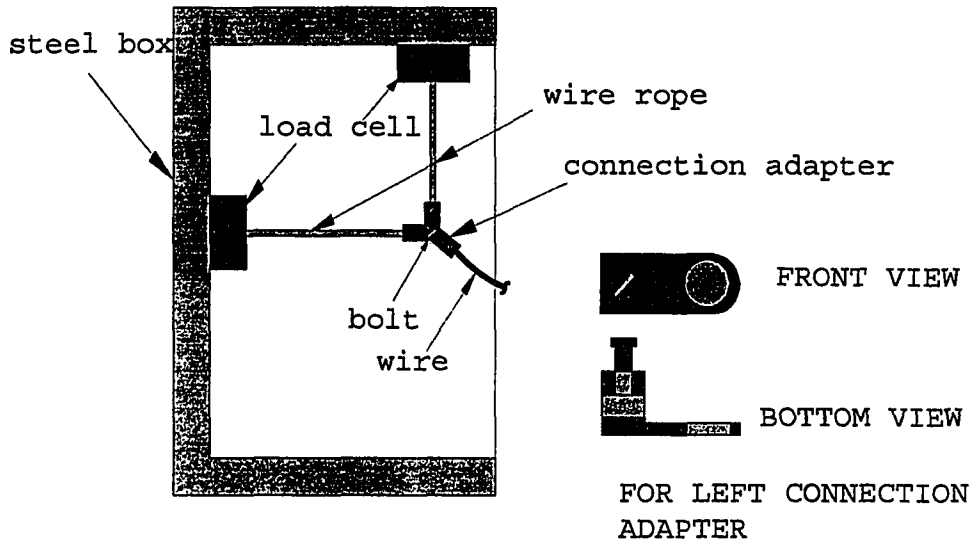


Fig. 3-5: Connection at left end of the wire. The configuration of a connection adapter is shown at the right hand side.

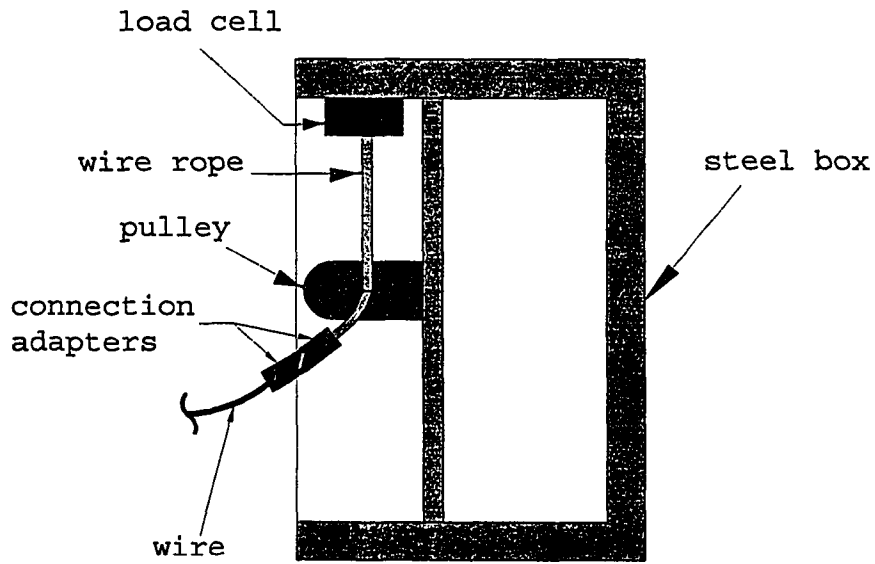


Fig. 3-6: Connection at right end of the wire.

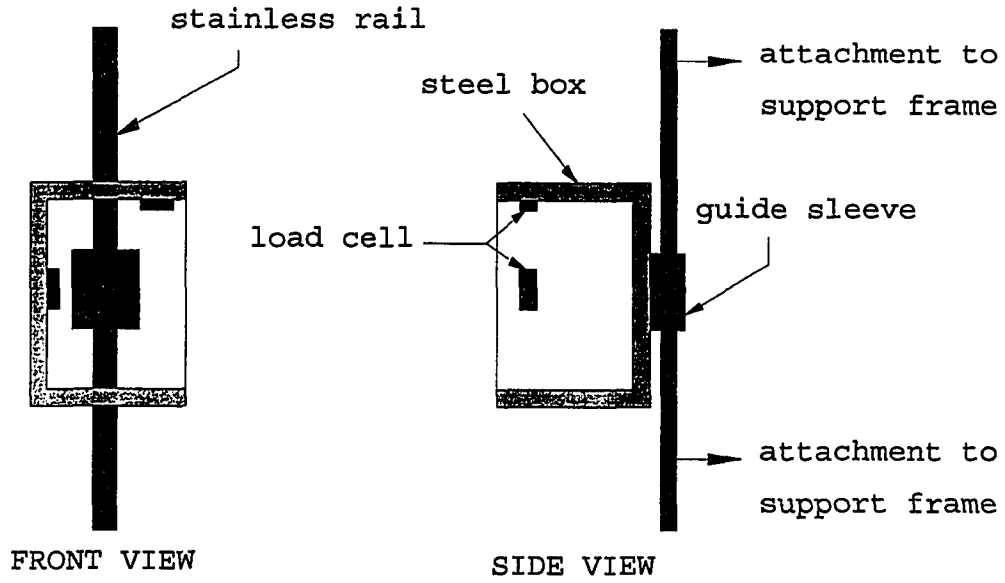


Fig. 3-7: Arrangement of guide track and stainless rail with respect to the steel box.

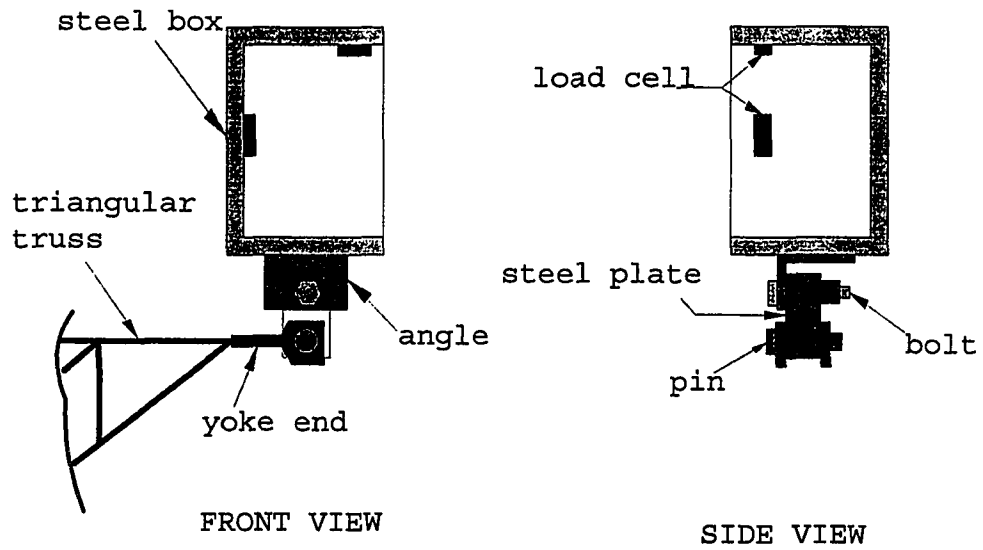


Fig. 3-8: Connection between the steel box and the triangular truss.

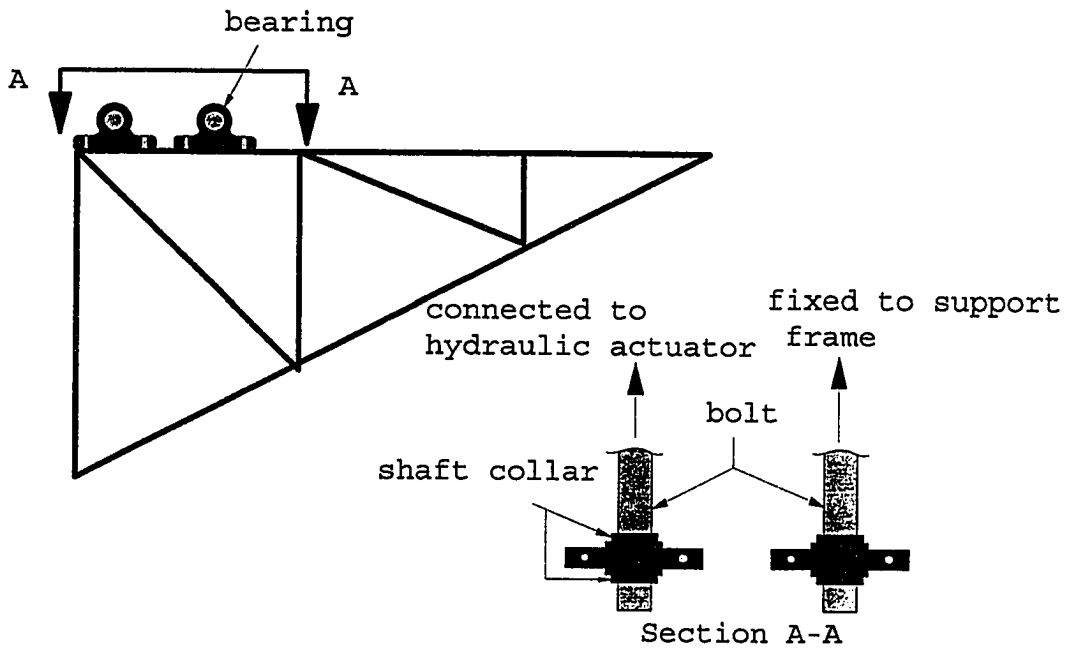


Fig. 3-9: Connections of triangular truss to a hydraulic actuator and a support frame.

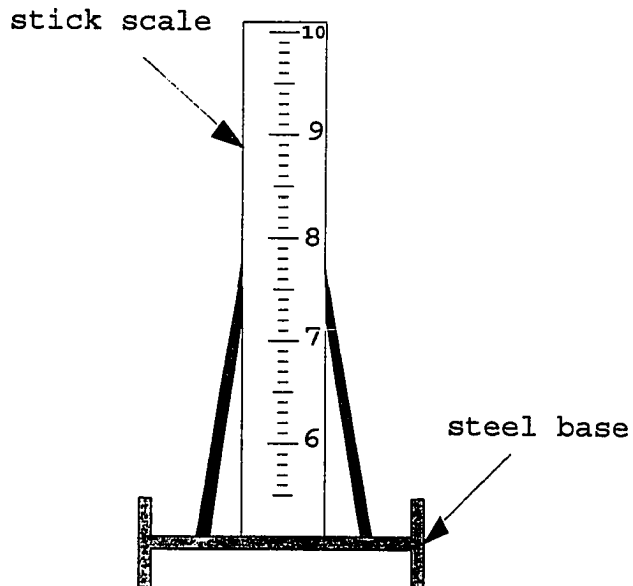


Fig. 3-10: Stick scale used to measure the amplitude.

3.1.2 Justification of Excitation Mechanism

As described in Section 3.1.1.2, the experimental model is subjected to support motion at both ends, while an overhead conductor for distribution lines in the field that have both ends simply supported to the support towers is excited into galloping motion by the assumed uniform aerodynamic lift force. The relative motion of a base-excitation wire is verified in Appendix B to be equivalent to the absolute motion of a simply-supported wire under uniform external load of the magnitude $m\Omega^2 Z$, where

m =unit mass, i.e., mass per unit length of the wire,
 Ω =frequency of the base motion, and
 Z =amplitude of the base motion.

The result is not surprising since similar phenomenon can be found in other continuous structural system. For instance, the steady-state response $v(x,t)$ of a simply-supported beam under base excitation $z(t)=Z\cos(\Omega t)$ at both ends is [22]

$$v(x, t) = \frac{Z}{2} \left[-\text{TANh}\left(\frac{\lambda l}{2}\right) \text{SIN}(\lambda x) + \text{COSH}(\lambda x) + \text{TAN}\left(\frac{\lambda l}{2}\right) \text{SIN}(\lambda x) + \text{COS}(\lambda x) \right] * \text{COS}(\Omega t)$$

where

v =transverse displacement,
 x =coordinate along the length,
 t =time,
 Z =amplitude of the base motion,
 l =beam length,
 Ω =frequency of the base motion,

$$\lambda = m\Omega^2/EI,$$

m =unit mass,

E =modulus of elasticity, and

I =moment of inertia.

Then the relative displacement $w(x,t)$ of the beam motion with respect to the ends is obtained, i.e.,

$$\begin{aligned} w(x,t) &= v(x,t) - z(t) \\ &= \frac{Z}{2} \left[-\text{TANh}\left(\frac{\lambda l}{2}\right) \text{SIN}(\lambda x) + \text{COSh}(\lambda x) \right. \\ &\quad \left. + \text{TAN}\left(\frac{\lambda l}{2}\right) \text{SIN}(\lambda x) + \text{COS}(\lambda x) - 2 \right] \text{COS}(\Omega t) \end{aligned} \quad (3-1)$$

On the other hand, the steady-state response $u(x,t)$ of a simply-supported beam under uniform external load $P\cos(\Omega t)$ is [22]

$$\begin{aligned} u(x,t) &= \frac{P}{2m\Omega^2} \left[-\text{TANh}\left(\frac{\lambda l}{2}\right) \text{SIN}(\lambda x) + \text{COSh}(\lambda x) \right. \\ &\quad \left. + \text{TAN}\left(\frac{\lambda l}{2}\right) \text{SIN}(\lambda x) + \text{COS}(\lambda x) - 2 \right] \text{COS}(\Omega t) \end{aligned} \quad (3-2)$$

Note that, if $P = m\Omega^2 Z$, then Equation 3-1 and Equation 3-2 are basically the same. Therefore, the relative motion of a simply-supported beam under base excitation $Z\cos(\Omega t)$ is equivalent to the absolute motion of the same beam under uniform harmonic load of magnitude $m\Omega^2 Z$.

3.1.3. Comparison between Laboratory Prototype and Laboratory Model

When designed properly, the behavior of a prototype in the field can be predicted by that of a model in the lab. However, because of the limitation of lab space, equipment

capacity, availability of the suitable material for the model, modelling all types of distribution and transmission lines is difficult. For instance, a 1201.615 feet ACSR Drake of 1.094 lb/ft in weight, 0.7261 in² in cross-sectional area, and 1.28×10^7 psi in modulus of elasticity is stretched to 6000 lb at the ends among a 1200 feet level span at temperature 60°F. It gallops at 0.5 Hz with ice deposition of 1 inch in radial thickness, or equivalently, 2.575 lb/ft of ice load at 32°F. To simulate the prototype in the lab, a steel wire S2 of 0.015 lb/ft in weight, 0.0044 in² in cross-sectional area, and 2.48×10^7 psi in modulus of elasticity is used as the model. It is loaded by another steel wire S2 as shown in Fig. 3-2 which takes negligible load (due to the binding effect of the duct tape) and serves as a superimposed load. The similitude law requires that a 93.73 feet steel wire S2 to be hung between a 93.63 feet level span at temperature 60°F. The forces at the ends corresponding to the vibration at 7.73 Hz at 32°F will be used to predict that of the prototype conductor. For this simulation the Iowa State University Structural Laboratory did not allow for a 93.63 feet span length, a capacity of the hydraulic actuator to vibrate at 7.73 Hz at the appropriate amplitude, and a strength of the connection between the wire and the connection adapter as shown in Fig. 3-5 to avoid breaking at the connection point.

In spite of this limitation, the prototype/model comparison can still be made by arranging some of the tests as

the laboratory prototypes and the others as the laboratory models. Both are required to satisfy the design conditions, as will be discussed later, so that the results obtained from the laboratory model can be used to describe the behavior of the laboratory prototype. Since the behavior of the latter is also recorded in the lab, the prediction can then be checked from the analytical and experimental results.

3.1.3.1 Selection of Variables

Based on the work of others [2 ,3 ,4] on conductor galloping, the dynamic force (F) of an overhead conductor, either the tension force or its vertical and horizontal components, is modeled to be a function (g) of the unit mass (m); cross-sectional area (A); modulus of elasticity (E) of the conductor; conductor length (L_0); span length (l); frequency of excitation (Ω); amplitude (y_0) of vertical motion; and time (t). F can be written as:

$$F = g(m, A, E, L_0, l, \Omega, y_0, t) \quad (3-3)$$

3.1.3.2 Dimensional Analysis

Dimensional analysis [23] is used to combine the variables relevant to a particular phenomenon into several groups which have the same units. Usually the variables are combined into dimensionless terms, or pi terms. In this case, Equation 3-3 could be rewritten in terms of six pi terms as:

$$\frac{R}{EA} = f \left(\frac{L_o}{l}, \frac{y_o}{l}, \frac{A}{l^2}, \frac{m\Omega^2}{E}, \Omega t \right) \quad (3-4)$$

3.1.3.3 Model Design Condition

Consider two sets of wires **X** and **Y** that are galloping for which, from Equation 3-4, their respective support forces in pi terms are

$$\left(\frac{R}{EA} \right)_x = f \left[\left(\frac{L_o}{l} \right)_x, \left(\frac{y_o}{l} \right)_x, \left(\frac{A}{l^2} \right)_x, \left(\frac{m\Omega^2}{E} \right)_x, (\Omega t)_x \right]$$

and

$$\left(\frac{R}{EA} \right)_y = f \left[\left(\frac{L_o}{l} \right)_y, \left(\frac{y_o}{l} \right)_y, \left(\frac{A}{l^2} \right)_y, \left(\frac{m\Omega^2}{E} \right)_y, (\Omega t)_y \right].$$

Then, if the wires **X** and **Y** are designed and operated under the following conditions:

$$\begin{aligned} \left(\frac{L_o}{l} \right)_x &= \left(\frac{L_o}{l} \right)_y \\ \left(\frac{y_o}{l} \right)_x &= \left(\frac{y_o}{l} \right)_y \\ \left(\frac{A}{l^2} \right)_x &= \left(\frac{A}{l^2} \right)_y \\ \left(\frac{m\Omega^2}{E} \right)_x &= \left(\frac{m\Omega^2}{E} \right)_y \\ (\Omega t)_x &= (\Omega t)_y, \end{aligned} \quad (3-5)$$

the result is expected to be

$$\left(\frac{R}{EA} \right)_x = \left(\frac{R}{EA} \right)_y \quad (3-6)$$

Therefore, the larger diameter wire could be called the laboratory prototype and the other is the laboratory model.

3.1.3.4 Laboratory Prototype and Model Wires

Of the 221 tests listed in appendix A, there are 17 pairs which satisfy the similarity requirements in Equation 3-5 between the two sets of the wires in the defined pair. For instance, the pair of the 46.4 feet composite aluminum wire 4A2+(2A2) (see the note in Appendix A) hanging on 46 feet span (Test No.44 in Appendix A) and the 23.2 feet composite aluminum wire 1A2+(2A2) hanging on 23 feet span (Test No.193 in Appendix A) satisfies the similarity requirements. This is because, as designating the former as the laboratory prototype and the latter as the laboratory model, the nominal unit mass scale $n_m=2$, the nominal area scale $n_A=4$, the nominal modulus of elasticity scale $n_E=1$, and the nominal length scale $n_l=2$. Then if selecting nominal frequency scale as $1/\sqrt{2}$, i.e., to compare the support force of the laboratory prototype at frequency Ω to that of the laboratory model at frequency $(\sqrt{2})\Omega$, the similarity requirements in Equation 3-5 are satisfied. Therefore, from Equation 3-6,

$$\left(\frac{R}{EA}\right)_p = \left(\frac{R}{EA}\right)_m$$

, where p and m represent the laboratory prototype and the laboratory model, respectively.

Rearranging the above equation produces

$$\frac{R_p}{R_m} = \frac{E_p}{E_m} \frac{A_p}{A_m} = n_E n_A = 1 * 4 = 4 \quad (3-7)$$

which means the support force of the laboratory prototype is

expected to be four times of that of the laboratory model.

The 17 pairs of wires along with their unit mass, cross-sectional area, modulus of elasticity, and length scales are listed in Appendix C.

3.1.4 Measurement Apparatus

3.1.4.1 MTS dynamic System

The wire was excited into galloping motion by an electro-hydraulically operated dynamic system designed by MTS (Materials Test Systems) Systems Corporation. The system uses an analog computer to send signals to control the servovalve located on the hydraulic actuators. The servovalve controls the hydraulic distribution system to regulate the flow of hydraulic fluid to achieve the desired motion of the actuator. The test began by slowly increasing the motion frequency of the hydraulic actuator from 1 Hz to the frequency that caused until the load wire to start galloping. Then, the frequency was raised at an interval of 0.05 Hz until the galloping motion stopped. At each interval, the reaction forces at the ends and the corresponding amplitude in the midspan of the load wire(s) were recorded.

For some support displacements, the wire translated up and down but did not gallop. As the actuator movement increased, a point was reached when galloping occurred. Therefore, it turned out that Test No. 1-143 and 148-149 in Appendix A were conducted with 3-11/16 inches amplitude of the

actuator movement while the others required a 1-13/16 inches amplitude of movement in order to gallop.

3.1.4.2 Load Cell and Plotting Recorder

Three load cells of model MLP-100 as shown in Fig. 3-3 were used to measure the support forces. Two of them mounted inside the left steel box were used to measure the vertical and horizontal tensions at the left end of the wire. The third load cell mounted inside the right steel box was used to measure the wire's tension force at the right end. They are denoted as LC1, LC2, and LC3, respectively, which will be used later in Section 3.2.1. The load cells are products of Transducer Technique and can measure to within an accuracy of 0.1 lb. Once the wire started galloping, the force signals from the load cells were enlarged through an amplifier since otherwise they were too weak to be read from the stripchart. A Gould's recorder of model 2400S as shown in Fig. 3-11 was used to plot the amplified signals on the stripchart. A typical plotting is shown in Fig. 3-12.

3.1.4.3 Stick Scale and Video Camera

A survey stick scale mounted on a wide W-shape steel was placed 30.5~33.2 inches behind the center of the wires to measure the amplitude. The scale could measure up to the accuracy of 0.1 foot. Two Sony video cameras, which were aimed at the locations where the wires reached the lowest possible

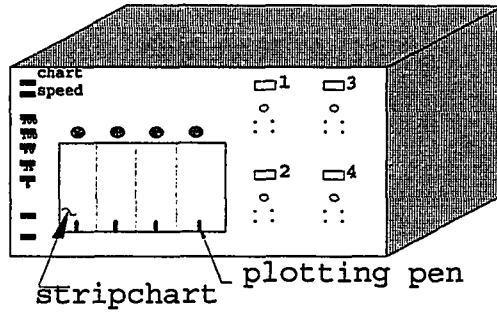


Fig. 3-11: A Gould's recorder used to plot the signals from the load cells.

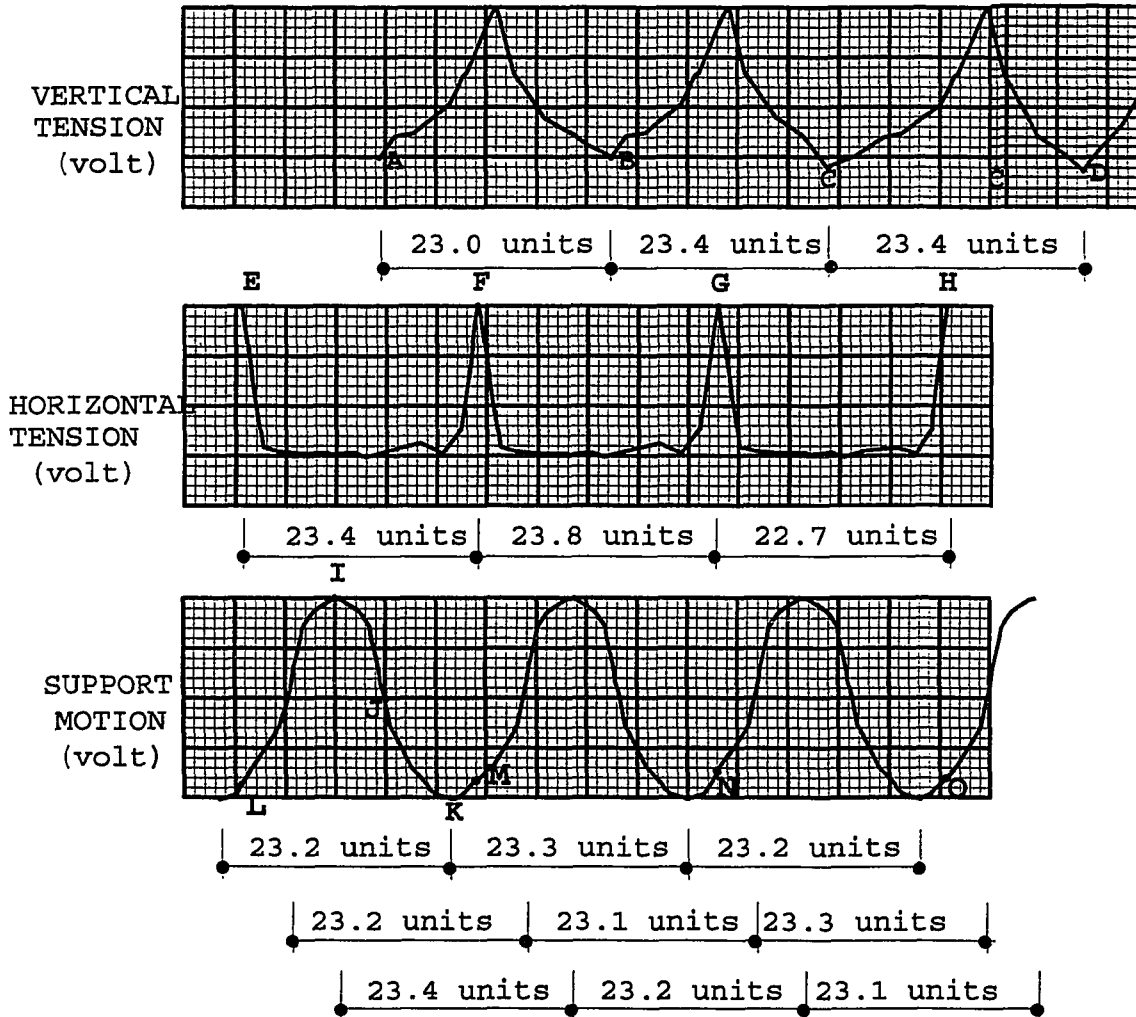


Fig. 3-12: Output for vertical tension, horizontal tension, and support motion (horizontal coordinate is time).

and highest possible points at galloping were placed on the other side to record the motion as shown in Fig. 3-13. Note that the cameras which recorded the motion at a speed of 30 frames per second were set at the elevations close to those of the wire when it reached the lowest and highest points. Since the actual elevations when the wire reached the peaks could not be known in advance and also those peak elevations changed from wire to wire and from one driving frequency to another, the elevations of the cameras were, therefore, adjusted several times by the operator during the test. Once galloping, the motion was recorded for about 10 seconds at each nominal frequency (see Section F.4 in Appendix F for the definition of nominal frequency) on a 120-minute VHS video cassette. Ten cassettes were used for the 221 tests listed in Appendix A.

3.2 Test Procedure

3.2.1 Calibration of the Load Cell

To calibrate the three load cells LC1, LC2, and LC3, a steel bucket and thirteen steel weights with the weights as shown in Table 3-1 were selected. The weights were measured with a Mettler P11N top-loading electronic balance. The load cell mounted to a steel beam in the top was connected to a voltmeter which was reset to zero in the beginning of the test. The bucket was then added to the bottom of the load cell and the steel weights were placed sequentially inside the bucket as shown in Fig. 3-14. To each load, the corresponding

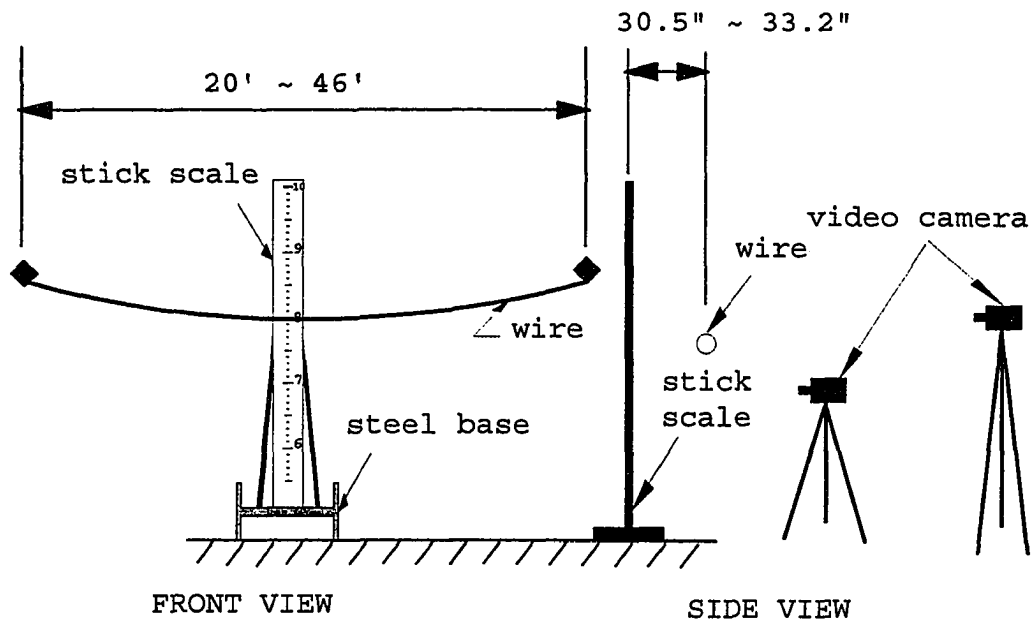


Fig. 3-13: The arrangement to record the amplitude of the wire.

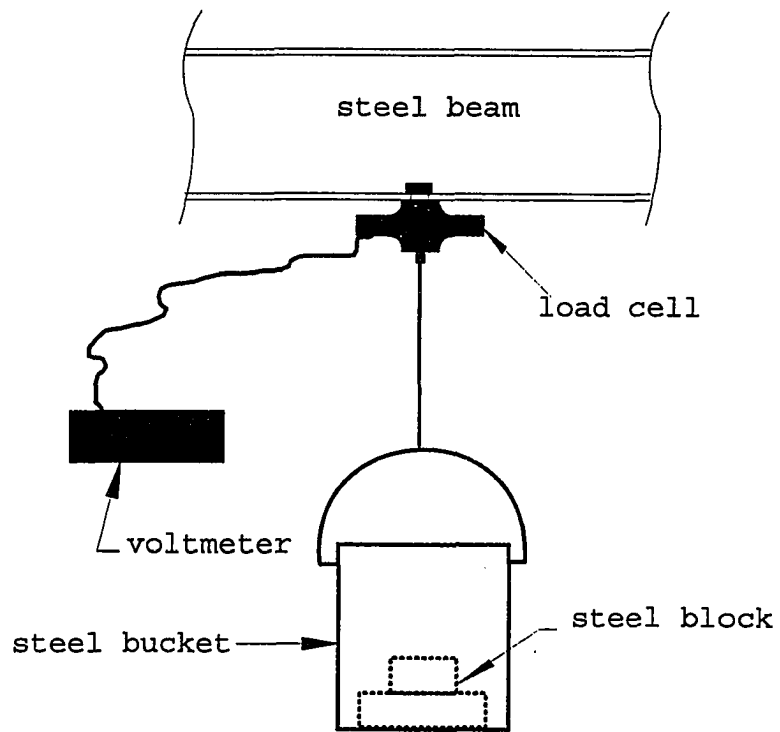


Fig. 3-14: The arrangement to calibrate the load cell.

Table 3-1

Weights of steel bucket and weights used to calibrate the load cells.

	Bucket	Steel weights No.1 to No.13
Weight(gram)	783	607 735 1006 1010 1015 1378 1342 1452 1988 2220 3414 3911 4582

elongation of the load cell in terms of voltage was recorded. The test was repeated three times by adding the steel weights in different order. The results are listed in Table 3-2.

The load-elongation relations for load cells LC1, LC2, and LC3 in Table 3-2 are plotted, respectively, as shown in Fig. 3-15. Also listed in the table is the corresponding coefficient of determination, R^2 , for a linear regression model. The coefficient of determination is a measure of accuracy of fit of a linear regression model to data [24]. Since the values of R^2 for all three cases are close to 1, there shows strong linear relationships between the loads and the elongations in those cases. Consequently, linear regression would be used to find the spring constants of the load cells. Referring to Appendix E which uses the statistical method as introduced in Appendix D, the means and standard errors of the spring constants of the three load cells are obtained as follows:

Load cell LC1: (4069.7±2.9) lb/volt

Load cell LC2: (4097.2±0.8) lb/volt

Load cell LC3: (4201.1±0.9) lb/volt

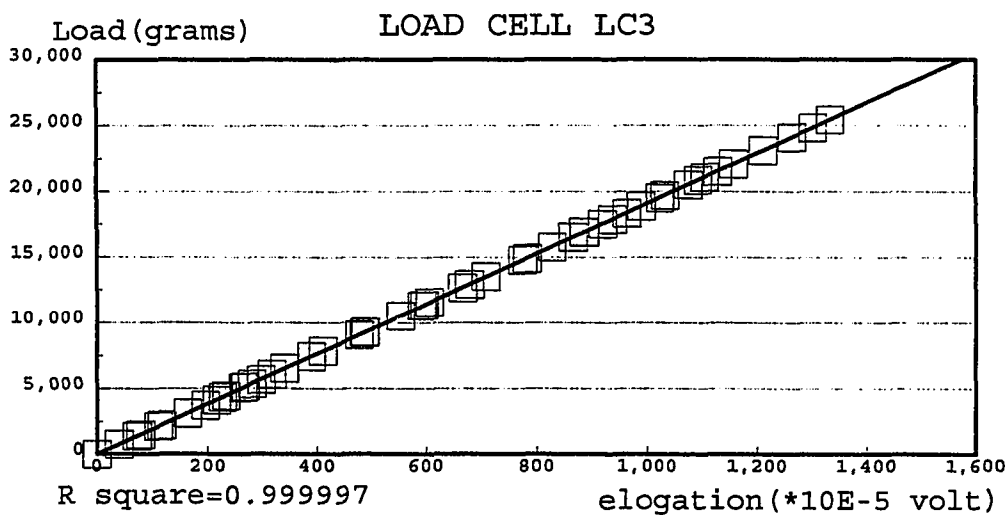
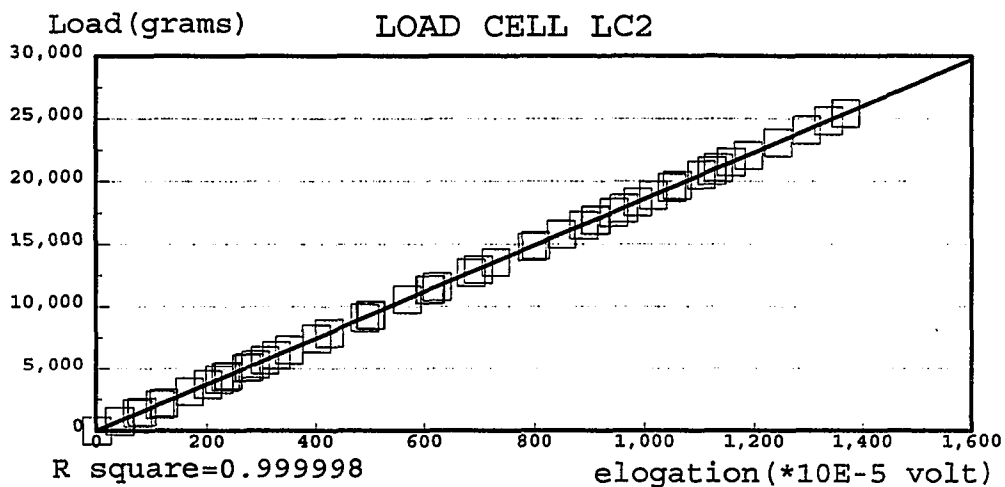
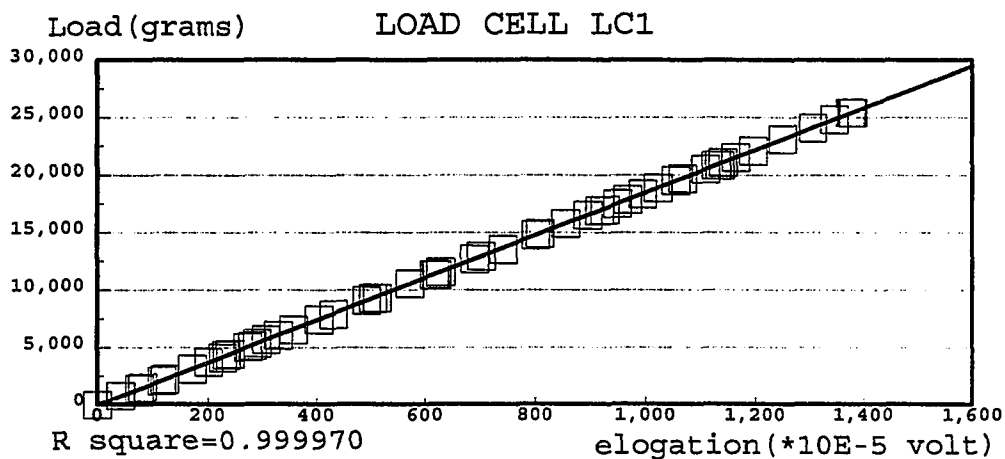


Fig. 3-15: Load-elongation relations for load cells LC1, LC2, and LC3.

Table 3-2

The loads and the corresponding elongations in terms of voltage recorded during the calibration of the load cells LC1, LC2, and LC3.

Load (gram)	Elogation(*1E-5 volt) for test1			Load (gram)	Elogation(*1E-5 volt) for test2		
	LC1	LC2	LC3		LC1	LC2	LC3
0	0	0	0	0	0	0	0
783	42	41	40	783	42	42	40
1390	76	74	72	5365	292	290	281
2125	116	114	110	9276	504	501	486
3131	172	168	163	12690	690	684	666
4141	228	223	216	14910	809	803	783
5156	283	278	269	16898	917	910	887
6534	359	352	341	18350	995	988	963
7876	432	425	411	19692	1068	1060	1033
9328	512	503	488	21070	1142	1135	1106
11316	621	609	592	22085	1197	1189	1158
13536	742	729	708	23095	1251	1243	1211
16950	927	912	886	24101	1306	1297	1264
20861	1136	1122	1094	24836	1346	1337	1302
25443	1381	1368	1333	25443	1379	1369	1334
	Test3				Test4		
0	0	0	0	0	0	0	0
783	42	42	40	783	41	42	40
2235	121	121	116	1518	81	82	78
4455	242	240	233	3738	202	202	195
5062	275	273	265	4345	235	235	227
6077	331	328	318	5687	308	307	298
7455	405	402	390	9101	493	491	477
11366	617	612	596	10553	572	569	553
14780	802	796	775	11568	628	623	606
15786	856	850	828	12946	702	698	678
16521	896	890	866	17528	949	944	919
17863	968	962	937	19516	1056	1050	1024
18873	1023	1016	990	20526	1110	1104	1076
20861	1130	1123	1094	21532	1164	1158	1129
25443	1378	1369	1334	25443	1375	1369	1334

3.2.2 Wire cutoff

A 50-foot long Stanley tape measurer which could measure up to the accuracy of 1/16 inch was first laid down along the corner of the lab basement with duct tape attaching intermittently along its length as shown in Fig. 3-16. The wire was then expanded along the measurer in which the left end was pressed down by a 50-lb weight with 6 inches extruding to the start mark of the measurer. The other end of the wire

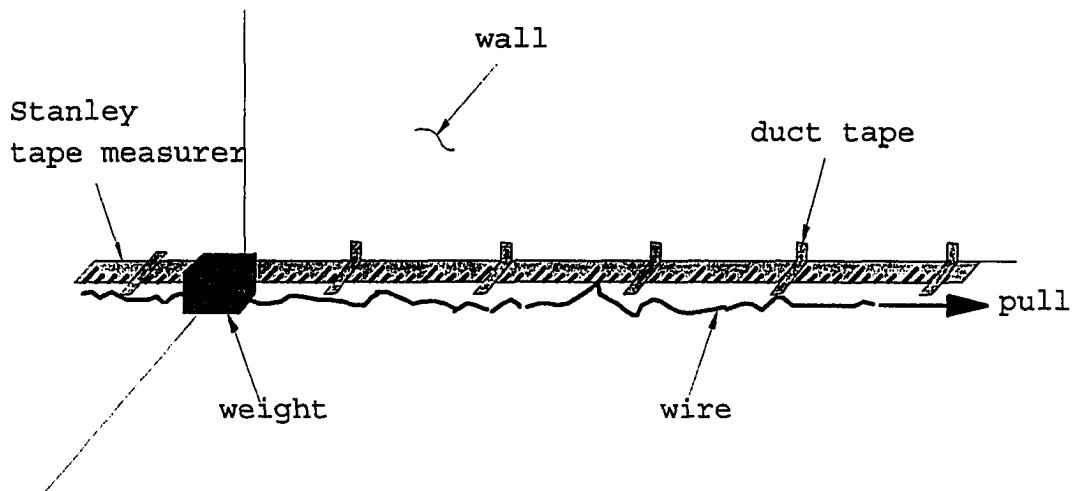


Fig. 3-16: Wire to be measured is pressed down at the left end by a weight and is then pulled from the other end.

was pulled straight with a reasonable force: a force not strong enough to move the wire under the weight but strong enough to reduce the kinks in the wire to the minimum. At the desired length, the wire was marked and then cut off. To ensure that the wire had the desired length, it was remeasured once following the same procedure.

Due to the kinks in the wire, the actual length of the wire is expected to be longer than the measured one. The difficulty of reducing the kink effect made the measured value include some obvious error which is discussed in detail in Section F.1.3 of Appendix F.

3.2.3 Simulation of Ice Load

As mentioned in Section 3.1.1.1, the attached wires which are continuous but are cut near the support were used to simulate the ice load on the transmission lines.

3.2.4 Measurement of Dynamic Load/Amplitude/Static Load

As mentioned in Section 3.1.4.1 to 3.1.4.3, the frequency of the vibrating hydraulic actuator was first increased slowly from 1 Hz until the wire started galloping. It was then raised at an interval of 0.05 Hz till galloping motion collapsed. At each interval, the forces at the ends were recorded on the stripchart and the corresponding amplitude was recorded on videotape.

When the wire rested in its static equilibrium position

after collapsing from galloping motion, the pointer of the Gould's recorder was set to the reference position. The wire was then taken off to the ground and the recorder was restarted to plot the signals from the three load cells in which one of them was shown by one force signal in Fig. 3-17. The differences was the static tension force and its vertical and horizontal components.

3.3 Error Analysis

3.3.1 Selection of Relevant Parameters

As mentioned in Section 3.1.3.1, the parameters involved in the test include unit weight, cross-sectional area of the wire, wire length, modulus of elasticity of the wire, span length, frequency of excitation, magnitude of external load, amplitude, support force, and passing time. The measurement error for all parameters except the last one will be examined.

3.3.2 Method of Analysis

The statistical methods to be briefly introduced in Appendix D will be used for the error analysis of the relevant parameters. The analysis is based on the "student's t-distribution" [24] for the means and standard errors of the parameters.

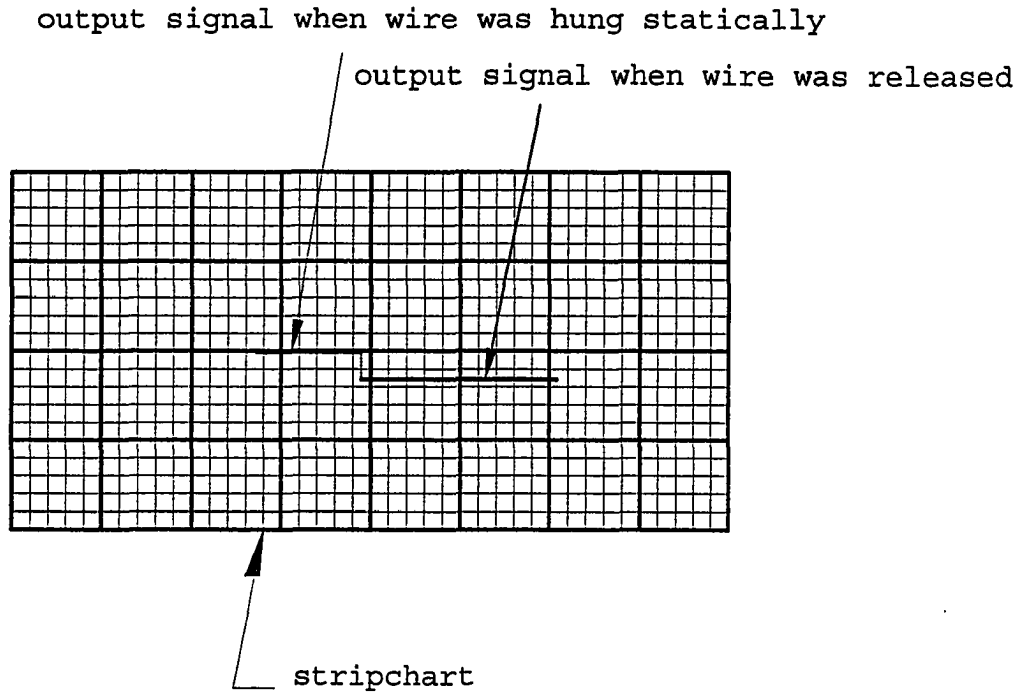


Fig. 3-17: output signal on the stripchart showing the static force.

3.3.3 Results of the Average Maximum Percentage Measurement Error

Define the maximum percentage measurement error of a parameter as the maximum measurement error, i.e. $t_{\alpha/2, n-1}SE$ in Equation D-1, divided by the corresponding mean of the measurements times 100. Then those errors for unit weight, cross-sectional area of the wire, wire length, modulus of elasticity of the wire, span length, frequency of excitation, magnitude of external load, amplitude, and support force are obtained as listed in Table 3-3. The detailed calculations are in Appendix F. Note that those errors in Table 3-3 mean that, for instance, if γ is the mean value of the unit weight of a wire, it is expected to have a $\pm 0.03\% \gamma$ of error in the maximum extreme.

Table 3-3

The maximum percentage error in the measurement of the various parameters.

	Maximum % measurement error
Unit weight	0.03%
Cross-sectional area	0.63%
Wire length	0.59%
Modulus of elasticity	2.41%
Span length	0.04%
Frequency	0.56%
Magnitude of external load	1.06%
Amplitude	0.84%
Support force	0.82%

3.3.4 Effects of Measurement Errors of Various Parameters on Support Forces

The effects of the measurement errors of the unit weight, cross-sectional area, and length of the wire on the recorded support vertical and horizontal tensions, both in static and dynamic cases, will be examined. The consequences of modulus of elasticity, span length, exciting frequency, and amplitude on those forces are unavailable due to lack of experimental information. However, the modulus of elasticity should have a similar effect on the support forces as that of the area since the product of both parameters, or the axial rigidity, usually appears together in the engineering equations. Also, the span length and wire length should have similar effects on the resulting support forces because both are used to describe the configuration of the wire.

3.3.4.1 Effect of Measurement Error of Unit Weight on Support Forces

From the 221 tests listed in Appendix A, 108 pairs of tests are selected in which, except the unit weight (and the amplitude in dynamic case), the values of other parameters are the same for the two sets of wires in the same pair. For instance, both the aluminum wires 4A2 (Test No.82 in Appendix A) and composite aluminum wire 4A2+(2A2) (Test No.81 in Appendix A) only differ in unit weight (ratio 4:6) while the other properties, i.e., cross-sectional area, modulus of

elasticity, wire length, and span length, are the same.

The 108 pairs of wires can be divided into six groups according to the unit weight ratios, which are 1:3, 1:2, 2:3, 3:4, 4:5, and 5:6. The unit weight ratio in each group is defined as the ratio between the two sets of wires in the defined pair. Table 3-4 lists the numbers of pairs in each group and the ratio of unit weight in each pair of that group. The detailed information regarding the wire type, wire length, and span length for each of the 108 wire pairs are listed in Part I of Appendix G.

Table 3-4

The numbers of pairs in each group and the ratio of unit weight in each pair of that group.

Group	Unit weight ratio	Number of pairs
1	1:3	11
2	1:2	35
3	2:3	40
4	3:4	14
5	4:5	4
6	5:6	4
		TOTAL 108

(A) Static Case

Taking the pair 4A2 vs. 4A2+(2A2) (Pair No.56 in Part I of Appendix G) for instance, the measured static vertical and horizontal tensions are listed in the first four columns of Table 3-5. Define the percentage change of forces as the difference between the forces in both sets of wires divided by the one in the lighter set, i.e., aluminum wires 4A2 in this case, expressed as percentage. Then the percentage changes of

static vertical and horizontal tensions are $(0.7-0.5)/0.5$, or 40%, and $(3.0-2.0)/2.0$, or 50%, respectively, as listed in the last two columns of Table 3-5. In the same manner, the percentage changes of the static vertical and horizontal tensions for the other 107 pairs are obtained and the results are plotted in Fig. 3-18a to Fig. 3-18f. The 95% confidence intervals for the true means of the static vertical and horizontal tensions, obtained from Equation D-1, are listed in the bottom of the respective figures. These intervals indicate that the true means, not the test data, have 95% confidence within those ranges. The data points which fall outside three standard deviations from the mean are usually referred to as outliers. After discarding the outliers, the adjusted confidence interval for each group of wires was calculated and is listed in the third and fourth columns of Table 3-6.

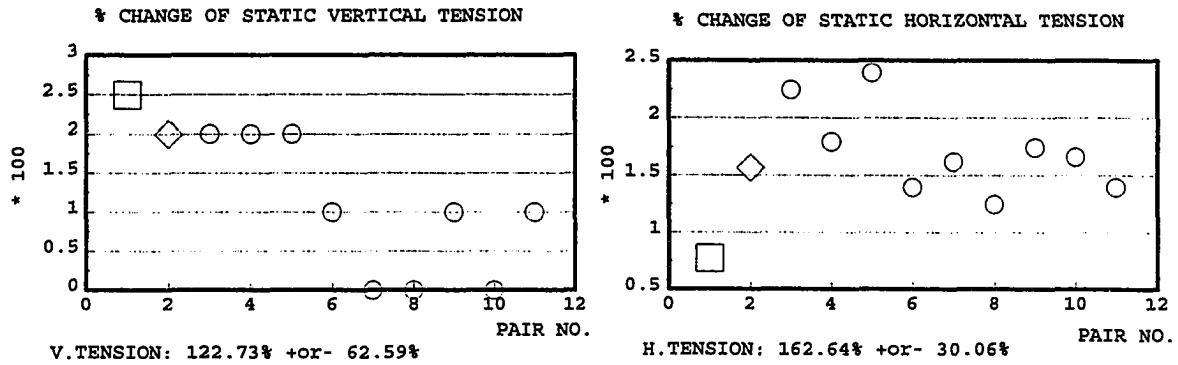
Table 3-5

Changes in static tensions between two sets of wires.

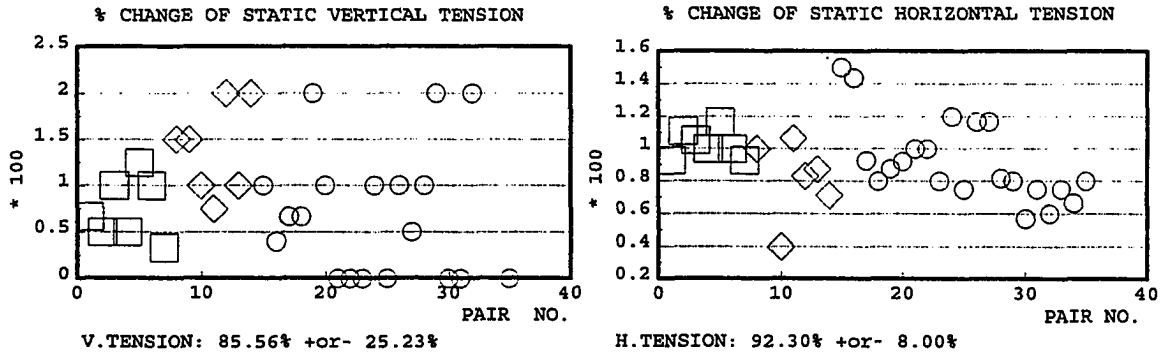
40.4' ALUMINUM WIRES 4A2		40.4' COMPOSITE WIRE 4A2+(2A2)		PERCENTAGE CHANGE	
VERTICAL TENSION (lb)	HORIZONTAL TENSION (lb)	VERTICAL TENSION (lb)	HORIZONTAL TENSION (lb)	VERTICAL	HORIZONTAL
0.5	2.0	0.7	3.0	40%	50%

For comparison with the theoretical expectations, the 40.4 feet composite aluminum wire 4A2+(2A2) hanging on 40 feet span of the same level (Test No. 81 in Appendix A) will be used for investigation. Due to the increases in unit weight as

a. UNIT WEIGHT RATIO=1:3



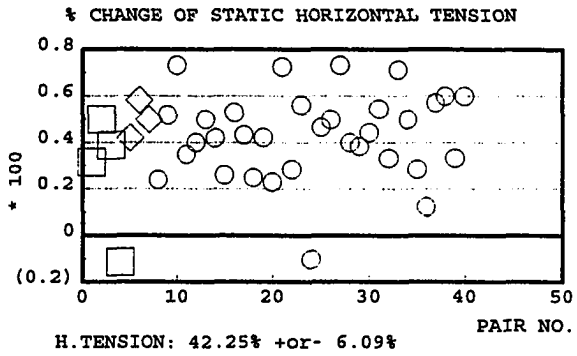
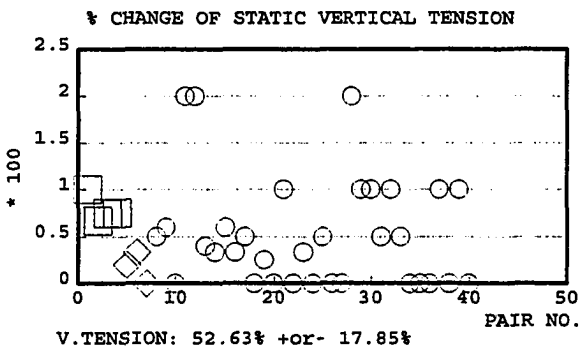
b. UNIT WEIGHT RATIO=1:2



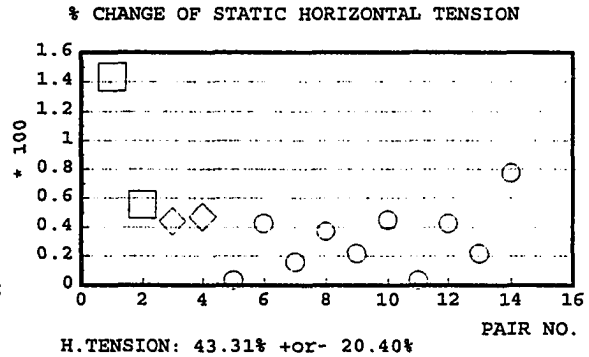
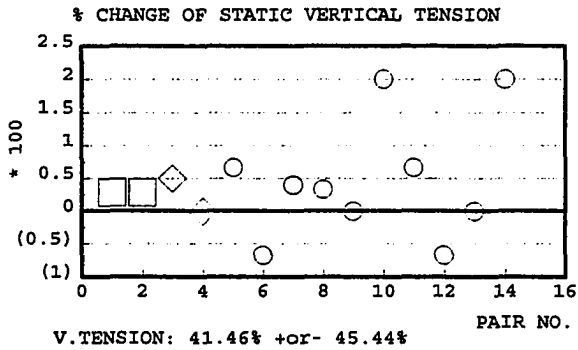
STEEL COPPER ALUMINUM

Fig. 3-18: Percentage changes of static vertical and horizontal tensions for wires with the unit weight ratio a)1:3 and b)1:2 in the same pair.

c: UNIT WEIGHT RATIO=2:3



d. UNIT WEIGHT RATIO=3:4

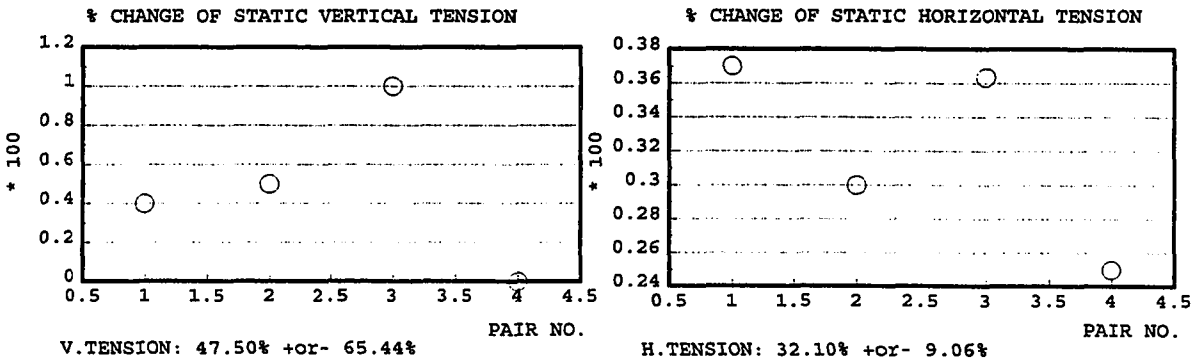


STEEL COPPER ALUMINUM

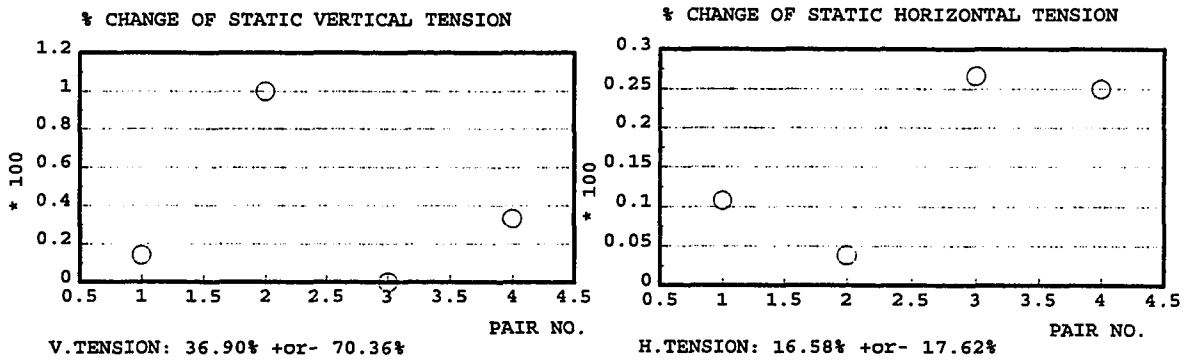
□ ◇ ○

Fig. 3-18: (continued) Unit weight ratio c)2:3 and d)3:4 in the same pair.

e. UNIT WEIGHT RATIO=4:5



f. UNIT WEIGHT RATIO=5:6



ALUMINUM
○

Fig. 3-18: (continued) Unit weight ratio e)4:5 and f)5:6 in the same pair.

listed in the second column of Table 3-6, the corresponding changes in theoretical vertical and horizontal tensions are calculated using Irvine's static equation as shown in Part I of Appendix H. The results are listed in the fifth and sixth columns of Table 3-6. The difference between the theoretical and experimental values divided by the theoretical one in percentage is listed in the last two column of Table 3-6. It is found that the theoretical expectations fall into the ranges of the experimental results but with large margin of errors. (The large margin of error in the experimental results of the last two groups is because only four data were collected, as found in Fig. 3-18e and Fig. 3-18f. Therefore, they are presented only as the references.)

Table 3-6

Changes in static tensions due to changes of unit weight.

Unit weight ratio	Increase in unit weight	EXPERIMENT		THEORY		(T-E)/T*100%	
		% change in V. tension	% change in H. tension	% change in V. tension	% change in H. tension	V. tension (%)	H. tension (%)
1:3	200%	169%±50%	171%±26%	200%	199.48%	-9~ 41	1~ 27
1:2	100%	92%±14%	92%± 6%	100%	99.83%	-6~ 22	2~ 14
2:3	50%	47%± 8%	46%± 5%	50%	49.93%	-10~ 22	-2~ 18
3:4	33.3%	31%±18%	32%±11%	33.33%	33.29%	-47~ 61	-29~ 37
4:5	25%	30%±66%	32%± 9%	25%	24.97%	-284~244	-64~ 8
5:6	20%	16%±42%	17%±18%	20%	19.98%	-190~230	-75~105

The large margins of errors for the vertical tensions of the first four groups and the horizontal tensions for the first and fourth groups of Table 3-6 are due to the following two reasons:

(i) Very small static support forces with the order close to load cell's least accuracy:

Considering the two sets of wires in Table 3-5 again, the measured static vertical tensions are 0.5 lb and 0.7 lb, respectively, as seen in the first and third columns. Since the load cells are only accurate to 0.1 lb, the inability to measure more numbers after the decimal point would cause relatively large errors. As an example, if the actual static vertical tensions for the two sets of wires are (0.4500, 0.7499) lb, or (0.5499, 0.6500) lb, respectively, the load cell would record both as (0.5, 0.7) lb. Then the percentage changes of static vertical forces between the two sets of wires for the two cases are

$$(0.7499-0.4500)/0.4500 \text{ ,or } 67\% \text{ , and}$$

$$(0.6500-0.5499)/0.5499 \text{ ,or } 18\% \text{ ,}$$

respectively. This lack of accuracy in load measurement causes a big difference.

(ii) Reading errors from the output in the stripchart:

The signals recorded from the load cells were plotted on the stripchart as discussed in Section 3.1.4.2. An output is shown in Fig. 3-17 for the static horizontal tension of the 40.4 feet aluminum wires 4A2, hanging on 40 feet span. The signal shown in that figure is read as 1.5 units so that the force is calculated as

$$0.0005 \text{ volt} * 1.5 \text{ units} / (1.5 \text{ amplification factors}) * 4097.2$$

lb/volt, or 2.0 lb where,

- (a) 0.0005 is the chart unit voltage value based on the full scale setting of the recorder,
- (b) 1.5 is the amplification factor of the signals from the load cell (so that the output is more readable), and
- (c) 4097.2 is the calibrated slope of the load-strain relation of the load cell which relates the signal(in voltage) to the forces (in pound).

However, one might read the output as 1.6 units so that the force becomes $0.0005 \times 1.6 / 1.5 \times 4097.2$, or 2.2 lb. Assume similar reading error occurs for the 40.4 feet composite aluminum wire 4A2+(2A2) so that the static horizontal tension is calculated as 2.8 lb instead of 3.0 lb which is listed in the fourth column of Table 3-5. Thus the percentage changes of horizontal tensions between the two sets of wires for the two reading cases are, respectively,

$$(3.0-2.0)/2.0 \text{ ,or } 50\% \text{ , and}$$

$$(2.8-2.2)/2.2 \text{ ,or } 27\%.$$

Therefore, as the result of small support forces and reading error from stripchart, the resulting percentage change of support forces might deviate greatly from the actual one.

Since Irvine's static formula is acceptable for the prediction of the wire with increases of unit weight as shown in the second column of Table 3-6, it is reasonable to use it again to extrapolate the effect of 0.03% measurement error in unit weight (see Table 3-3) upon the support forces. Taking the aforementioned 40.4 feet composite aluminum wires

4A2+(2A2) for investigation, the changes of static vertical and horizontal tensions at ends are both calculated as 0.03%.

(B) Dynamic case

During the galloping test, the amplitude cannot be controlled by the operator and, therefore, is not a constant within the two sets of wires in the defined pair. However, the comparison can still be made since, relative to the changes of support forces, the changes of amplitudes are found to be small. Therefore, taking again the pair 4A2 vs. 4A2+(2A2) of 40.4 feet in length for instance, the frequencies in which the wire gallops and the corresponding vertical tensions, horizontal tensions, and amplitudes are listed in the first seven columns of Table 3-7. At 1.15 Hz frequency, the percentage changes of vertical tension, horizontal tension, and amplitude are, respectively,

$$(4.8-3)/3, \text{ or } 60\%,$$

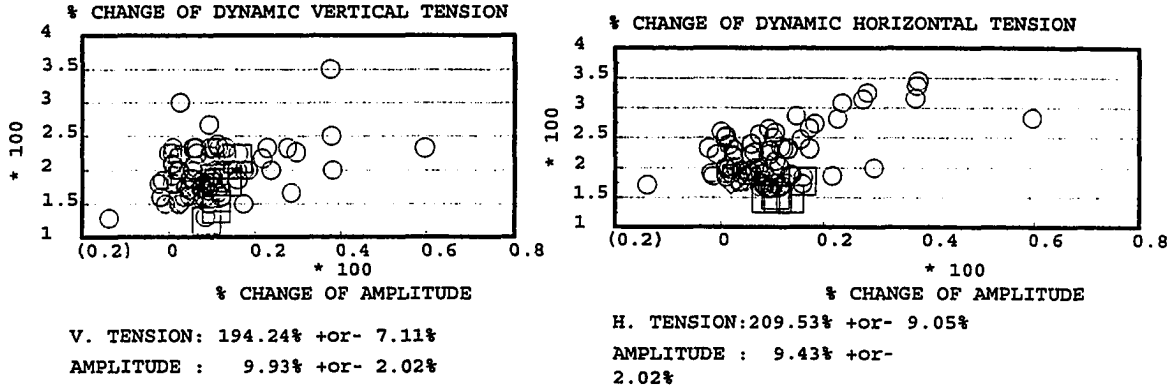
$$(35.5-22.5)/22.5, \text{ or } 58\%, \text{ and}$$

$$(2.06-1.94)/1.94, \text{ or } 6\%,$$

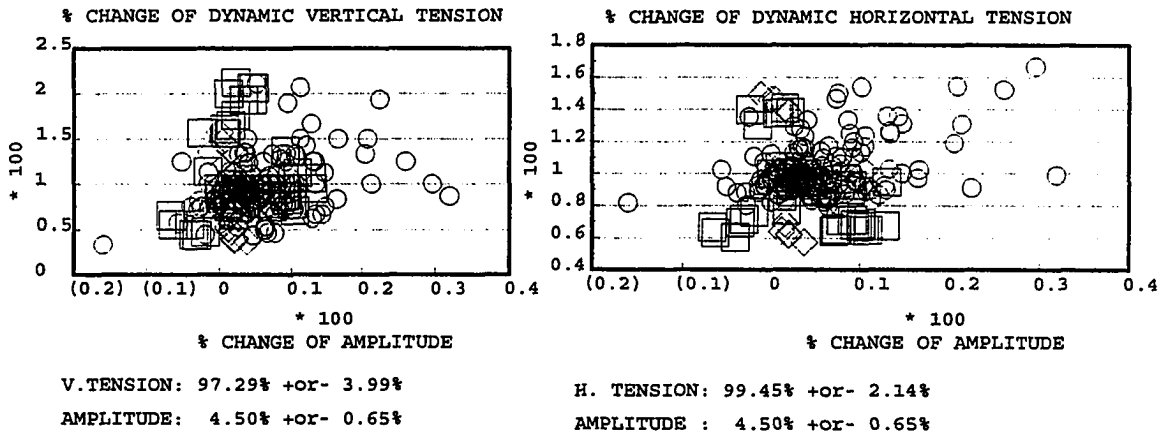
as listed in the last three columns of Table 3-7.

In the same manner, the percentage changes of the dynamic vertical and horizontal tensions and the corresponding amplitudes for the other 107 pairs were obtained. The results are plotted in Fig. 3-19a to Fig. 3-19f with the respective 95% confidence intervals for the true means of vertical tensions, horizontal tensions and the corresponding amplitudes

a. UNIT WEIGHT RATIO=1:3



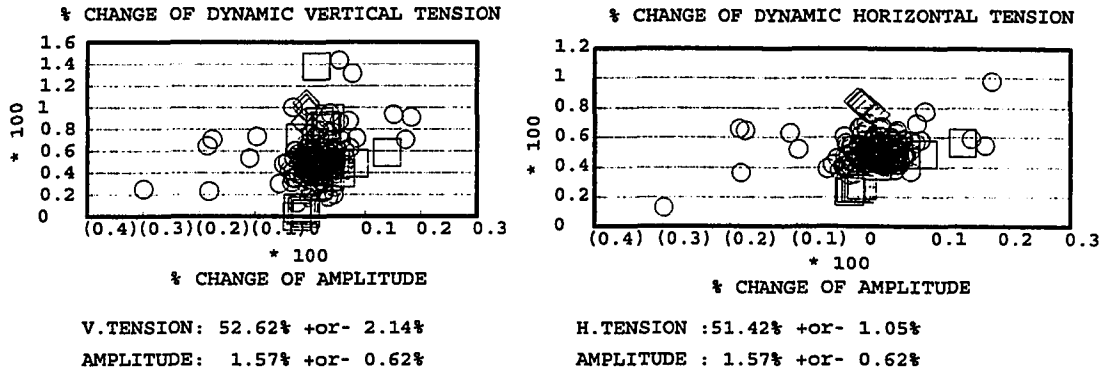
b: UNIT WEIGHT RATIO=1:2



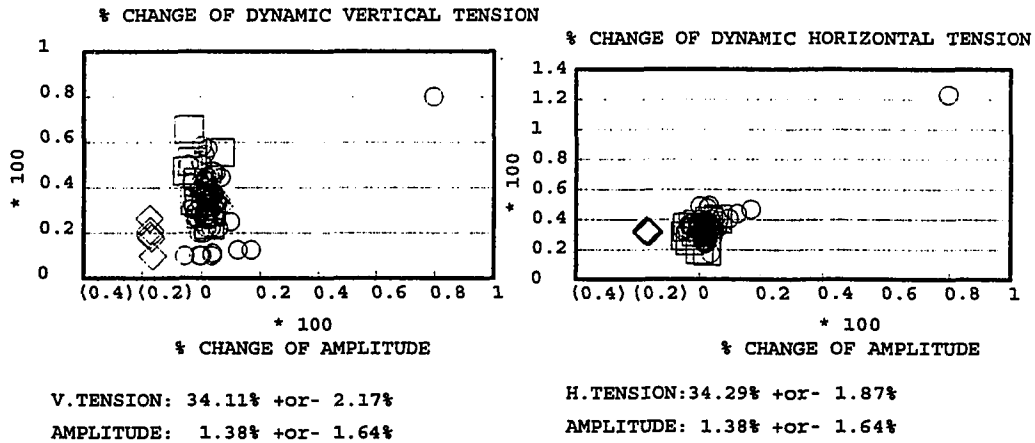
STEEL COPPER ALUMINUM

Fig. 3-19: Percentage changes of dynamic vertical and horizontal tensions with respect to percentage change of amplitude for wires with unit weight ratio a) 1:3 and b) 1:2 in the same pair.

c. UNIT WEIGHT RATIO=2:3



d. UNIT WEIGHT RATIO=3:4

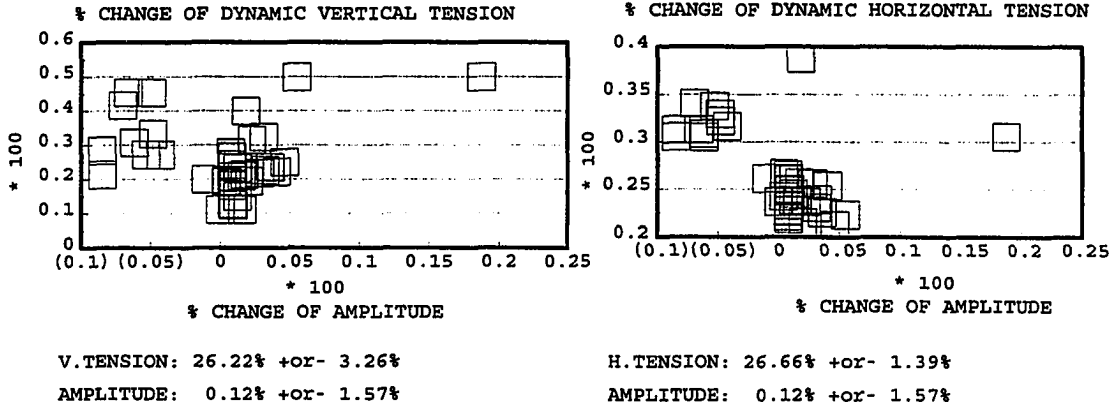


STEEL COPPER ALUMINUM

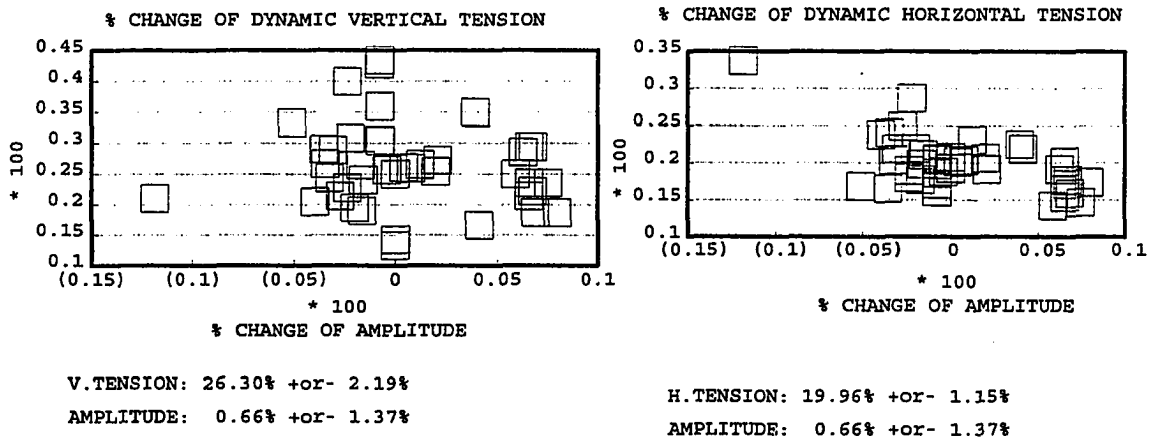
□ ◇ ○

Fig. 3-19: (continued) Unit weight ratio c) 2:3 and d) 3:4 in the same pair.

e. UNIT WEIGHT RATIO=4:5



f. UNIT WEIGHT RATIO=5:6



ALUMINUM
 □

Fig. 3-19: (continued) Unit weight ratio e) 4:5 and f) 5:6 in the same pair.

Table 3-7

Changes in tensions and amplitudes between two sets of wires.

FREQUENCY (Hz)	40.4' ALUMINUM WIRE 4A2			40.4' COMPOSITE WIRE 4A2+(2A2)			PERCENTAGE CHANGE		
	VERT TENSION (lb)	HORI TENSION (lb)	AMPLI (ft)	VERT TENSION (lb)	HORI TENSION (lb)	AMPLI (ft)	VERT TENSION	HORI TENSION	AMPLI
1.15	3.0	22.5	1.94	4.8	35.5	2.06	60%	58%	6%
1.20	3.4	24.9	2.08	5.5	39.2	2.18	62%	57%	5%
1.25	3.8	26.7	2.18	5.7	41.7	2.22	50%	56%	2%
1.30	3.8	27.9	2.19	6.0	42.9	2.26	58%	54%	3%
1.35	4.0	29.2	2.27	6.4	44.3	2.28	60%	52%	0%
1.40	4.3	30.2	2.27	6.5	46.2	2.36	51%	53%	4%
1.45	4.3	30.8	2.30	6.5	47.2	2.23	51%	53%	-3%
1.50	4.3	31.6	2.21	6.8	47.8	2.31	58%	51%	5%

listed in the bottom of the figures. By discarding the "outliers" and then recalculating the 95% confidence interval, the adjusted results are listed in the last three columns of Table 3-8.

For comparison with the theoretical expectations, the aforementioned 40.4 feet composite aluminum wire 4A2+(2A2) are used again for investigation. Due to the increases of unit weights and amplitudes as listed in the second and third columns of Table 3-8, the corresponding changes in theoretical dynamic vertical and horizontal tensions are calculated using both Simpson's and Irvine's dynamic formulae as shown in Part II and III of Appendix H. The results are listed in Table 3-9. It is found from Table 3-8 and Table 3-9 that the theoretical expectations fall into or are close to the ranges of the experimental results.

Table 3-8

Experimental changes in dynamic tensions due to changes of unit weights and amplitudes.

Unit weight ratio	Percentage Increase of unit weight	Percentage change in amplitude	Percentage change in vertical tension	Percentage change in horizontal tension
1:3	200%	7%±1%	191%±6%	202%±7%
1:2	100%	4%±1%	93%±3%	97%±2%
2:3	50%	1%±0.4%	51%±2%	50%±1%
3:4	33.3%	1%±0.5%	36%±2%	33%±1%
4:5	25%	2%±0.5%	21%±2%	24%±1%
5:6	20%	1%±1%	25%±1%	20%±1%

Table 3-9

Theoretical changes in dynamic tensions due to changes of unit weights and amplitudes.

% increase in unit weight	% change of amplitude (%)	Simpson's method		Irvine's method		(T-E)/T*100%	
		% change in vert. tension (%)	% change in hori. tension (%)	% change in vert. tension (%)	% change in hori. tension (%)	vert. tension (%)	hori. tension (%)
200%	7	203	209	214	209	3- 9	0- 7
100%	4	101	104	105	104	5- 11	5- 9
50%	1	50	51	51	51	-6- 2	0- 4
33.3%	1	34	34	34	34	-12- 0	0- 6
25%	2	25	26	27	26	8- 24	4-12
20%	1	20	21	21	21	-30--20	0-10

Since both Simpson's and Irvine's dynamic formulae predict the increase in vertical and horizontal tensions of the wire with increases of unit weight and amplitude, as listed in the first two columns of Table 3-9, it is reasonable to use them to extrapolate the effect of 0.03% measurement error in unit weight upon the support forces. Note that the percentage changes of amplitudes are far smaller than those of unit weights as found in Table 3-9 and, therefore, will be considered as unchanged during the comparison. Taking the aforementioned 40.4 feet composite aluminum wire 4A2+(2A2)

hanging on 40 feet span of the same level for instance, the changes of dynamic vertical and horizontal tensions at ends, whatever either Simpson's or Irvine's formula is used, are both calculated as 0.03%.

As a summary from the analytical investigations of both static and dynamic cases above, the 0.03% measurement error in the unit weight of the wire was found to be having almost no effects on the recorded support forces.

3.3.4.2 Effect of Measurement Error of Cross-sectional Area on Support Forces

From the two hundred and twenty one tests listed in Appendix A, sixty pairs of tests are selected in which, except the cross-sectional area (and the amplitude in dynamic case), the values of other parameters are the same for the two sets of wires in the same pair. For instance, both the composite aluminum wire 1A2+(2A2) (Test No.54 in Appendix A) and three single aluminum wires 3A2 (Test No.48 in Appendix A) only differ in cross-sectional area (ratio 1:3) while the other properties, i.e., modulus of elasticity, unit weight, wire length, and span length, are the same.

The sixty pairs of wires can be divided into four groups according to the area ratios, which are 1:3, 1:2, 2:3, and 3:4. Table 3-10 lists the numbers of pairs in each group and the ratio of area in each pair of that group. The detailed informations regarding the wire type, wire length, and span

Table 3-10

The numbers of pairs in each group and the ratio of cross-sectional area in each pair of that group.

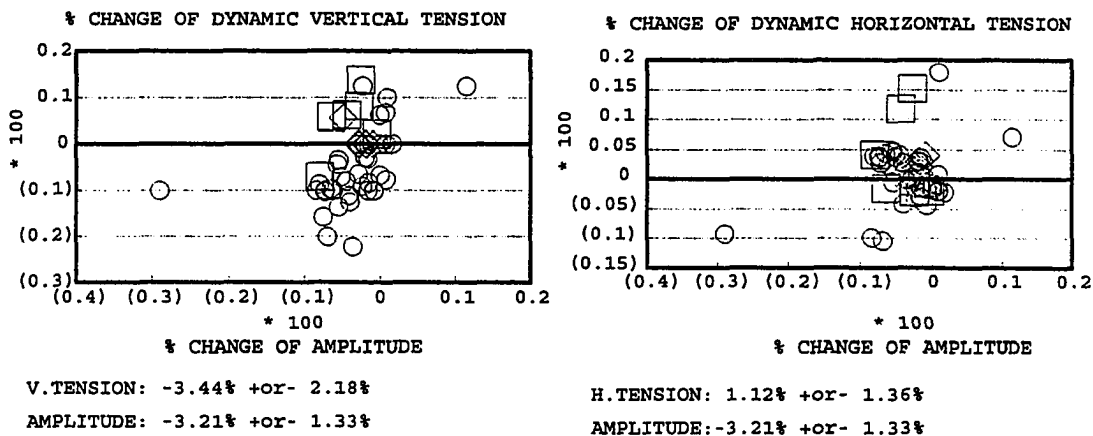
Group	Cross-sectional area ratio	Number of pairs
1	1:3	6
2	1:2	29
3	2:3	16
4	3:4	9
		TOTAL 60

length for each of the 60 wire pairs are listed in Part II of Appendix G.

The static support forces for the two sets of wires in the defined pair were mistakenly considered the same and, therefore, were not recorded during the test. Therefore, the effect of measurement error of cross-sectional area on the support forces can only be made in dynamic case as discussed in the following paragraphs.

Following the same procedures as those in Section 3.3.4.1(B), the percentage changes of the dynamic vertical and horizontal tensions and the corresponding amplitudes for the four groups of wires are obtained and are plotted in Fig. 3-20a to Fig. 3-20d, respectively. Again, by discarding the "outliers" in those figures, the adjusted 95% confidence intervals of the percentage changes of vertical tensions, horizontal tensions and their corresponding amplitudes are listed in the last three columns of Table 3-11, respectively.

a. CROSS-SECTIONAL AREA RATIO=1:3



b. CROSS-SECTIONAL AREA RATIO=1:2

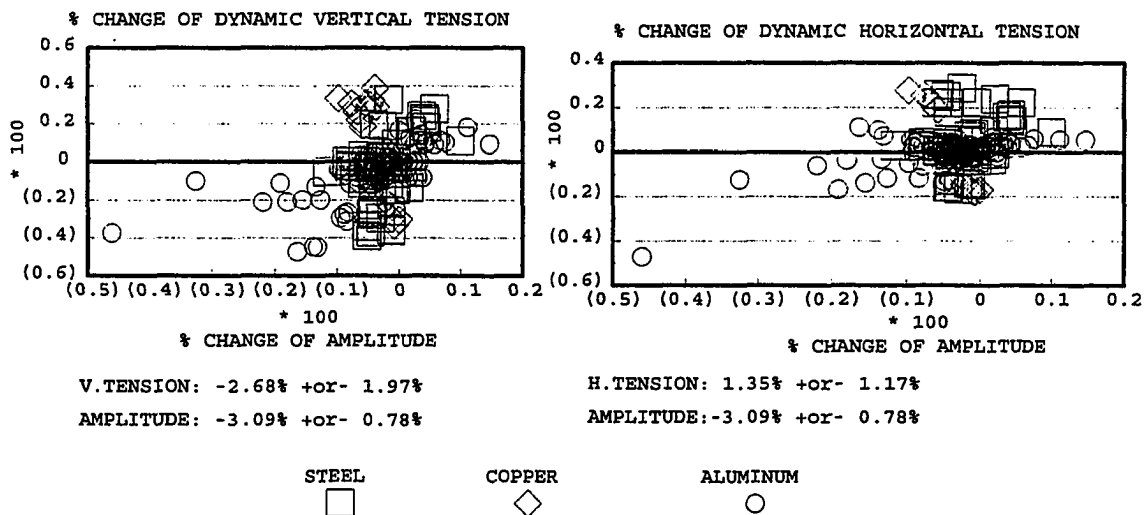
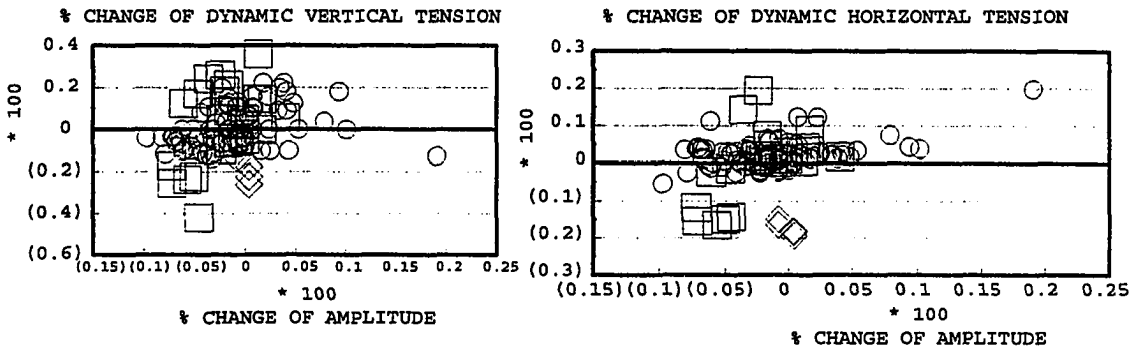


Fig. 3-20: Percentage changes of dynamic vertical and horizontal tensions with respect to percentage change of amplitude for wires with area ratio a) 1:3 and b) 1:2 in the same pair.

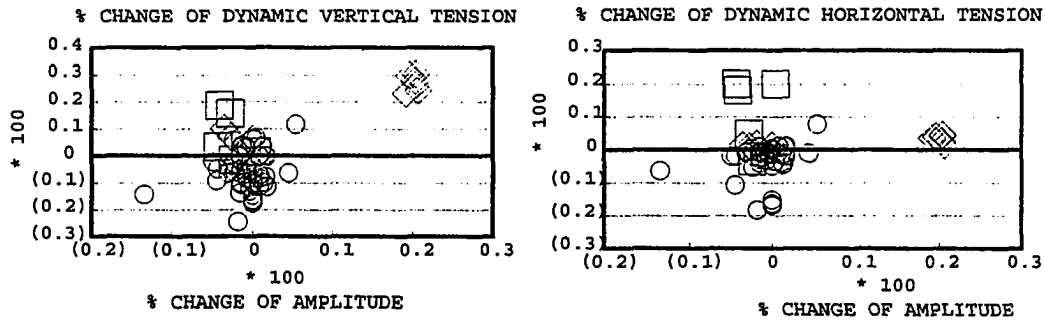
c. CROSS-SECTIONAL AREA RATIO=2:3



V.TENSION: 0.49% +or- 2.12%
 AMPLITUDE: -1.30% +or- 0.70%

H.TENSION: 1.10% +or- 1.10%
 AMPLITUDE: -1.30% +or- 0.70%

d. CROSS-SECTIONAL AREA RATIO=3:4



V.TENSION: -0.67% +or- 2.86%
 AMPLITUDE: 0.88% +or- 1.58%

H.TENSION: -0.54% +or- 1.55%
 AMPLITUDE: 0.88% +or- 1.58%

STEEL COPPER ALUMINUM
 □ ◇ ○

Fig. 3-20: (continued) Area ratio c) 2:3 and d) 3:4 in the same pair.

Table 3-11

Experimental changes in dynamic tensions due to changes of cross-sectional areas and amplitudes.

Area ratio	Percentage Increase in cross-sectional area	Percentage change in amplitude	Percentage change in vertical tension	Percentage change of horizontal tension
1:3	200%	-3%±1%	-3%±2%	1%±1%
1:2	100%	-2%±1%	-2%±2%	0%±1%
2:3	50%	-2%±1%	0%±2%	2%±0.4%
3:4	33.3%	-1%±0.5%	-4%±2%	-1%±1%

Applying both Simpson's and Irvine's dynamic formulae on the aforementioned 40.4 feet composite aluminum wire 4A2+(2A2), the changes in dynamic vertical and horizontal tensions at both ends as the result of the increases of cross-sectional areas and amplitudes, as listed in the second and third columns of Table 3-11, are obtained. The results are listed in Table 3-12.

It can be seen from the last two columns of Table 3-12 that there are large percentage differences between the theoretical and experimental values. This difference is the

Table 3-12

Theoretical changes in dynamic tensions due to changes of cross-sectional areas and amplitudes.

% increase in cross-sectional area	% change of amplitude (%)	Simpson's method		Irvine's method		(T-E)/T*100%	
		% change in vert. tension (%)	% change in hori. tension (%)	% change in vert. tension (%)	% change in hori. tension (%)	vert. tension (%)	hori. tension (%)
200%	-3	-1	-0.3	-1	-2	- 400~ 0	100~ 767
100%	-2	-0.9	-0.2	-0.9	-1	- 344~100	- 400~ 600
50%	-2	-0.9	-0.1	-0.9	-1	- 122~322	1700~2500
33.3%	-1	-0.4	-0.1	-0.4	-0.7	-1400~400	-1900~ 100

result of small change in forces due to large change in cross-sectional area. Since the area change of 200% has little effect on the forces, a measurement error of 0.63% will have no effect.

3.3.4.3 Effect of Measurement Error of Wire Length on Support Forces

From the two hundred and twenty one tests listed in Appendix A, twenty-four pairs of tests are selected in which, except the wire length (and the amplitude in dynamic case), the values of other parameters are the same for the two sets of wires in the same pair. For instance, both a steel wire S2 (Test No.21 in Appendix A) and another steel wire S2 (Test No.4 in Appendix A) only differ in length(ratio 46.4:46.6) while the other properties, i.e., unit weight, cross-sectional area, modulus of elasticity, and span length, are the same.

The 24 pairs of wires can be divided into two groups according to the length ratios, which are 40.2:40.4 and 46.4:46.6. Table 3-13 lists the numbers of pairs in each group and the ratio of length in each pair of that group. The detailed informations regarding the wire type, wire length, and span length for each of the 24 wire pairs are listed in Part III of Appendix G.

Table 3-13

The numbers of pairs in each group and the ratio of length in each pair of that group. Also listed are the percentage change of length and sag.

Group	Length ratio	Number of pairs	Percentage Increase in length	Percentage changes of sag
1	40.2:40.4	13	0.498%	41%
2	46.4:46.6	11	0.431%	23%
		TOTAL 24		

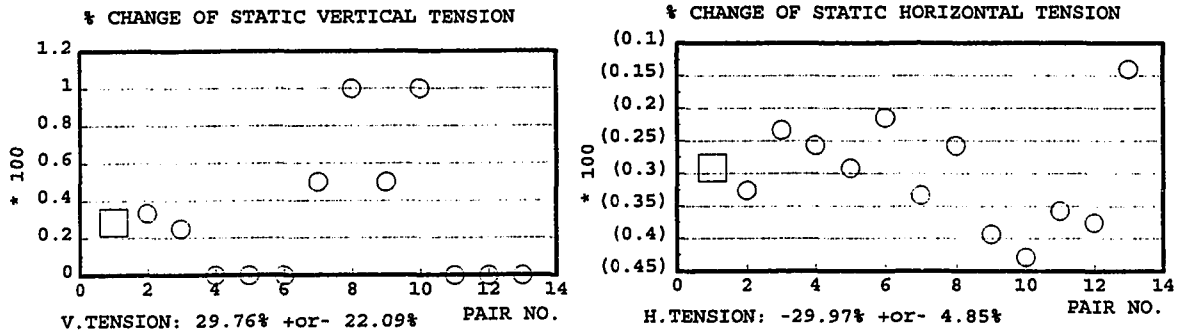
(A) Static Case

Following the same procedures as those in Section 3.3.4.1(A), the percentage changes of the static vertical and horizontal tensions for the two groups of wires are obtained and are plotted in Fig. 3-21a and Fig. 3-21b, respectively. Again by discarding the "outliers" in those figures, the adjusted 95% confidence intervals of the percentage changes of vertical and horizontal tensions are obtained and are listed in the third and fourth columns of Table 3-14, respectively.

By applying Irvine's static formula on the aforementioned 40.4 feet composite aluminum wire 4A2+(2A2) again, the changes in vertical and horizontal tensions at both ends as the result of increases of length as listed in the second column of Table 3-14 were obtained and are listed in the fifth and sixth columns, respectively.

It is found from observation of the results listed in the last two columns of Table 3-14 that the experimental results do not closely match the theoretical predictions. Again, the discrepancy in static forces is considered the results of the

a. LENGTH RATIO=40.2:40.4



b. LENGTH RATIO=46.4:46.6

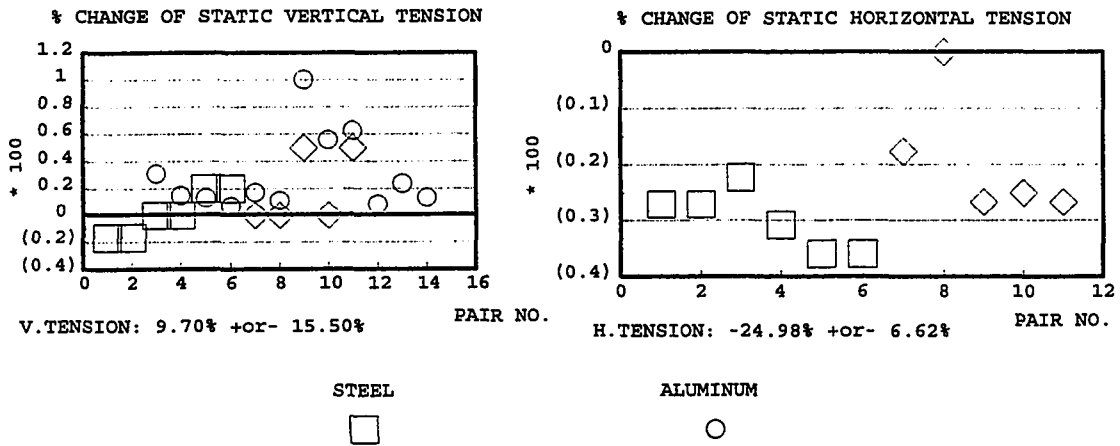


Fig. 3-21: Percentage changes of static vertical and horizontal tensions for wires with the length ratio a) 40.2:40.4 and b) 46.4:46.6 in the same pair.

Table 3-14

Changes in static tensions due to changes of length.

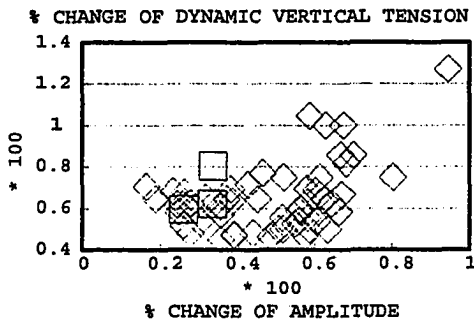
Length ratio	Increase in length	EXPERIMENT		THEORY		(T-E)/T*100%	
		% change in V. tension	% change in H. tension	% change in V. tension	% change in H. tension	V. tension (%)	H. tension (%)
40.2:40.4	0.498%	10%±11%	-31%±4%	0.50%	-18.33%	-4100-300	-91--47
46.4:46.6	0.431%	1%±10%	-27%±4%	0.43%	-16.45%	-2458-2193	-88--40

small forces and reading errors from the stripchart as mentioned in Section 3.3.4.1. Consequently, it is assumed that the experimental and theoretical results would closely match in Table 3-14 if no aforementioned errors occur. Then Irvine's static formula will be used again to investigate the changes of support forces due to 0.59% measurement error in wire length (see Table 3-3). Taking the aforementioned 40.4 feet composite aluminum wires 4A2+(2A2) for instance, it is calculated that the changes of static vertical and horizontal tensions at ends are 0.59% and -20.74%, respectively, where the minus sign means decrease in forces.

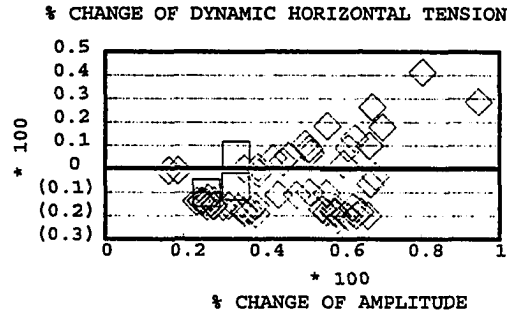
(B) Dynamic Case

Following the same procedures as those in Section 3.3.4.1(B), the percentage changes of the dynamic vertical and horizontal tensions and the corresponding amplitudes for the two groups of wires are obtained and are plotted in Fig. 3-23a and Fig. 3-23b, respectively. Again, by discarding the "outliers" in those figures, the adjusted 95% confidence intervals of the percentage changes of vertical tensions,

a. WIRE LENGTH RATIO=40.2:40.4

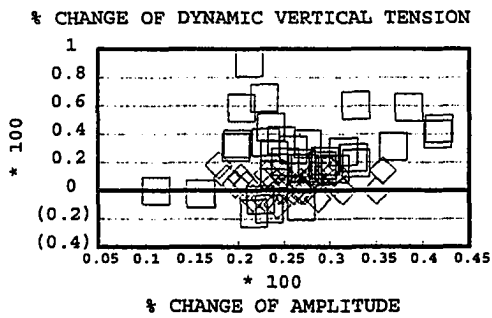


V.TENSION: 64.83% +or- 4.01%
 AMPLITUDE: 47.20% +or- 4.39%

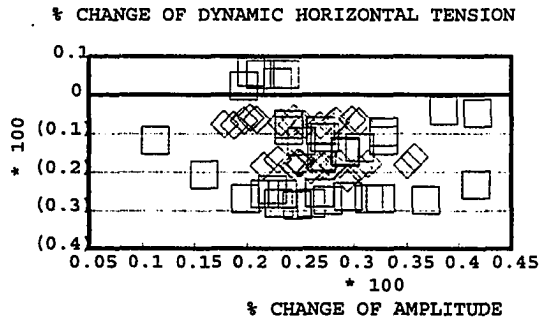


H.TENSION: -6.34% +or- 3.65
 AMPLITUDE: 47.20% +or- 4.39%

b. WIRE LENGTH RATIO=46.4:46.6



V.TENSION: 16.38% +or- 5.07%
 AMPLITUDE: 26.45% +or- 1.41%



H.TENSION: -14.02% +or- 2.27%
 AMPLITUDE: 26.45% +or- 1.41%

STEEL


ALUMINUM


Fig. 3-23: Percentage changes of dynamic vertical and horizontal tensions w.r.t. percentage change of amplitude for wires with length ratio a) 40.2:40.4 and b) 46.4:46.6 in the same pair.

horizontal tensions and the corresponding amplitudes are obtained and are listed in the last three columns of Table 3-16, respectively.

Applying both Simpson's and Irvine's dynamic formulae on the aforementioned 40.4 feet composite aluminum wire 4A2+(2A2) again, the changes in vertical and horizontal tensions at both ends as the result of increases of lengths and amplitudes as listed in the second and third columns of Table 3-16 are obtained and are listed in middle four columns of Table 3-17.

Table 3-16

Experimental changes in dynamic tensions due to changes in wire lengths and amplitudes.

Length ratio	Percentage Increase in wire length	Percentage change in amplitude	Percentage change in vertical tension	Percentage change in horizontal tension
40.2:40.4	0.498%	44%±4%	60%±2%	-11%±3%
46.4:46.6	0.431%	26%±1%	10%±4%	-16%±2%

Table 3-17

Theoretical changes in dynamic tensions due to changes of lengths and amplitudes.

% increase in wire length	% change of amplitude (%)	Simpson's method		Irvine's method		(T-E)/T*100%	
		% change in vert. tension (%)	% change in hori. tension (%)	% change in vert. tension (%)	% change in hori. tension (%)	vert. tension (%)	hori. tension (%)
0.498%	44	0.3	-11	8	-12	-192332-20566	-27-27
0.431%	26	0.3	-14	0.5	-15	-4567--1900	-29-0

From Table 3-16 and Table 3-17, the theoretical expectations of the percentage changes of dynamic horizontal tensions are found to fall into the range of the experimental results. However, there shows significant errors for those of the dynamic vertical tensions. This is because the responses of the vertical forces for the thirteen pairs of wires listed in Part III of Appendix G show a random nature of excitation. The erratic behavior of vibration was not typical throughout the experiments but occurred once in a while in some of the tests. Therefore, the recorded forces involved large margins of errors.

Note from Table 3-16 that, unlike the previous cases, the percentage changes of amplitudes are relatively larger than those of the lengths. It is suspicious that the magnitude of the amplitude in dynamic case relates to that of the wire sag in static case which is listed in the last column of Table 3-13. Comparison the third column of Table 3-16 to the last column of Table 3-13 reinforces that idea. Therefore, the change of static sag was used to replace that of the amplitude in dynamic case. Then by applying Irvine's static formula on the aforementioned 40.4 feet composite aluminum wire 4A2+(2A2) as an example, the percentage change of static sag is calculated as 26.54% due to 0.59% measurement error in wire length (see Table 3-3). Therefore, the change in dynamic horizontal tensions at both ends is -19.91% by Simpson's method and would be -20.71% if Irvine's method is used.

In summary, the support force is very sensitive to the length measurement error, i.e. the plotting of force vs. length is very steep so that a small change of length will result in a large change of forces. Therefore, straighter wires and better length measurement instrument should be used to ensure the accuracy of the force.

3.4 Results and Discussions

3.4.1 Laboratory Prototype and Model Wires

3.4.1.1 Forces Comparison

As mentioned in Section 3.1.3.4, there are seventeen pairs of wires which satisfy the similarity requirements between the two sets of wires in the same pair. The nominal properties such as unit weight, cross-sectional area, modulus of elasticity, wire length, and span length for those pairs are listed in Table 3-18.

To compare the laboratory prototype's forces predicted by the model to those obtained from the experiment, Pair No.1 in Table 3-18 will be used for investigation. The measured vertical and horizontal tensions of the laboratory model wire $1A2+(2A2)$ are listed in the second column of Table 3-19. Multiplying those forces by four (see Equation 3-7) yields the predicted prototype's forces as listed in the fourth column. Note that the corresponding frequency is obtained by dividing the model's one by $\sqrt{2}$ according to similarity requirement. On the other hand, the actual vertical and horizontal tensions of

Table 3-18

Physical properties of the seventeen pairs of wires which satisfy the similarity requirements.

Pair #	Wire-type (prototype)	unit-weight (lb/ft)	area (in ²)	Mod. (ksi)	Len. (ft)	Span (ft)	Wire type (model)	unit weight (lb/ft)	area (in ²)	Mod. (ksi)	Len. (ft)	Span (ft)
1	4A2+(2A2)	0.036	0.020	10510	46.4	46.0	1A2+(2A2)	0.018	0.005	10510	23.2	23.0
2	4A2	0.024	0.020	10510	46.4	46.0	1A2+(1A2)	0.012	0.005	10510	23.2	23.0
3	4A2+(2A3)	0.031	0.020	10450	46.4	46.0	1A2+(1A2+1A3)	0.015	0.005	10450	23.2	23.0
4	4A3+(2A3)	0.020	0.012	10450	46.4	46.0	1A3+(2A3)	0.010	0.003	10450	23.2	23.0
5	4A3	0.014	0.012	10450	46.4	46.0	1A3+(1A3)	0.007	0.003	10450	23.2	23.0
6	4A2+(2A3)	0.031	0.020	10450	43.4	43.0	1A2+(1A2+1A3)	0.015	0.005	10450	21.7	21.5
7	4A2	0.024	0.020	10510	43.4	43.0	1A2+(1A2)	0.012	0.005	10510	21.7	21.5
8	4A2+(2A2)	0.036	0.020	10510	43.4	43.0	1A2+(2A2)	0.018	0.005	10510	21.7	21.5
9	4A3+(2A3)	0.020	0.012	10450	43.4	43.0	1A3+(2A3)	0.010	0.003	10450	21.7	21.5
10	4A3	0.014	0.012	10450	43.4	43.0	1A3+(1A3)	0.007	0.003	10450	21.7	21.5
11	4A2+(2A2)	0.036	0.020	10510	40.4	40.0	1A2+(2A2)	0.018	0.005	10510	20.2	20.0
12	4A2	0.024	0.020	10510	40.4	40.0	1A2+(1A2)	0.012	0.005	10510	20.2	20.0
13	4A2+(2A3)	0.031	0.020	10450	40.4	40.0	1A2+(1A2+1A3)	0.015	0.005	10450	20.2	20.0
14	4A3+(2A3)	0.020	0.012	10450	40.4	40.0	1A3+(2A3)	0.010	0.003	10450	20.2	20.0
15	4A3	0.014	0.012	10450	40.4	40.0	1A3+(1A3)	0.007	0.003	10450	20.2	20.0
16	4C3	0.050	0.012	14160	40.4	40.0	1C3+(1C3)	0.025	0.003	14160	20.2	20.0
17	4A1	0.042	0.036	7820	40.4	40.0	1A1+(1A1)	0.021	0.009	7820	20.2	20.0

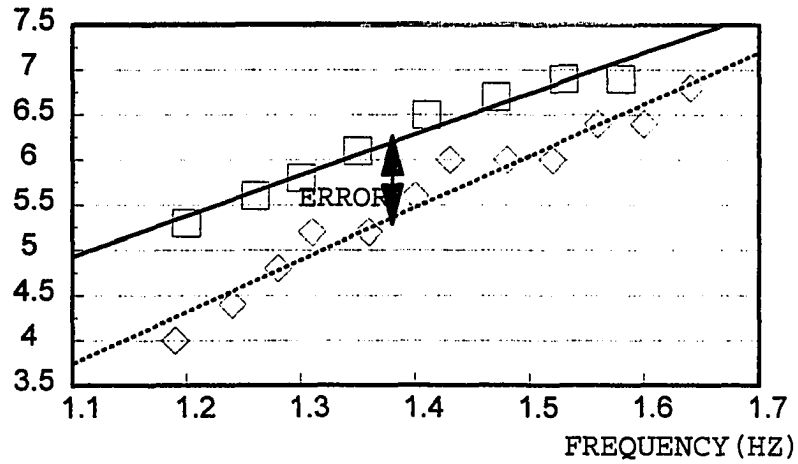
the prototype wire 4A2+(2A2) obtained from the experiment are listed in the last column of Table 3-19. The results are plotted in Fig. 3-24. Similar comparisons can be made for the other sixteen pairs and the results are plotted from Fig. I-1 of Appendix I.

In Fig.3-24 and Fig.I-1, the squares represent the prototype forces obtained from the experiment. On the other hand, the diamonds represent the predicted prototype forces

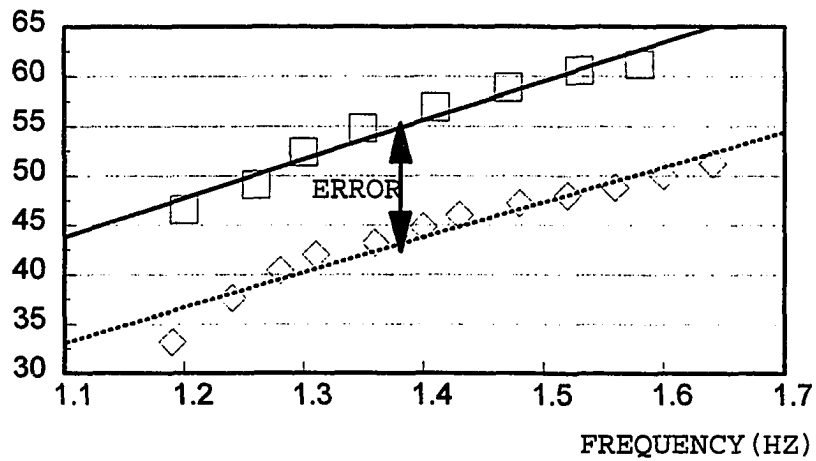
46.4' 4A2+(2A2) --PROTOTYPE

23.2' 1A2+(2A2) --MODEL

VERTICAL TENSION (lb)



HORIZONTAL TENSION (lb)



From testing prototype experimentally 4*(experimentally obtained model forces)



Fig. 3-24: Comparison of the vertical and horizontal tensions of the prototype both obtained from the experiment and predicted by the model.

Table 3-19

Tensions of the prototype wire both predicted by the model wire and obtained from the experiment.

MODEL:23.2' 1A2+(2A2)			PROTOTYPE:46.4' 4A2+(2A2)					
Measured from experiment			Predicted by model			Measured from experiment		
Frequency(Hz)	Ver	Hor(lb)	Frequency(Hz)	Ver	Hor(lb)	Frequency(Hz)	Ver	Hor(lb)
1.69	1.0	8.3	1.19	4.0	33.2	1.20	5.3	46.6
1.75	1.1	9.4	1.24	4.4	37.6	1.26	5.6	49.1
1.81	1.2	10.1	1.28	4.8	40.4	1.30	5.8	52.4
1.86	1.3	10.5	1.31	5.2	42.0	1.35	6.1	54.8
1.92	1.3	10.8	1.36	5.2	43.2	1.41	6.5	56.9
1.98	1.4	11.2	1.40	5.6	44.8	1.47	6.7	58.9
2.03	1.5	11.5	1.43	6.0	46.0	1.53	6.9	60.6
2.09	1.5	11.8	1.48	6.0	47.2	1.58	6.9	61.2
2.15	1.5	12.0	1.52	6.0	48.0			
2.20	1.6	12.2	1.56	6.4	48.8			
2.26	1.6	12.5	1.60	6.4	50.0			
2.32	1.7	12.8	1.64	6.8	51.2			

obtained by multiplying the model forces by four according similitude law. It can be seen that, except the last two pairs in Fig.I-1c, there are discrepancies between the predicted and measured forces of the prototype wire.

3.4.1.2 Explanation of the Discrepancy

The analysis in Section 3.3.4 shows that the support forces are very sensitive to the length measurement error (including wire length, and possibly, span length) while the measurement errors in other parameters with the amounts as listed in Table 3-3 have virtually no effects on the forces. Since the measurement error of span length is far smaller than that of the wire length (also see Table 3-3), the latter is concluded to be the main reason for the discrepancy of the prototype forces between the one predicted by the model and the one measured from the experiment. Note that the

combination of both change of the wire length and the resulting amplitude cause the large change in the dynamic support force.

Re-examining Fig. 3-24 and Fig. I-1 indicates that all fifteen pairs of wires which exhibit discrepancies are made of either aluminum wires A2 or A3. The other two pairs which match well are made of copper wire C3 and aluminum wire A1. The consistent pattern of discrepancy in tests involving wire A2 or A3 is understandable because basically the same wires were used for those tests. For instance, after the test using the 46.4 feet composite aluminum wire 4A2+(2A2) (prototype wire of Pair No.1 in Table 3-18) , the two attached wires A2 were taken off so that the remaining four 46.4 feet aluminum wires A2 (prototype wire of Pair No.2 in Table 3-18) were used to perform another test. Then the aforementioned 46.4 feet composite aluminum wire 4A2+(2A2) was re-combined and cut by 3 feet (becoming prototype wire of Pair No.8 in Table 3-18) to perform the subsequent test. Therefore, approximately the same amount of length measurement errors for the tests using the same type of wires are expected. As a result, if the discrepancy exists in any of the fifteen pairs of wires, the other fourteen pairs are expected to show similar trends.

3.4.1.3 Reconstruction of the Prototype-Model Comparison after Considering the Length Measurement Error

In order to reconstruct the prototype-model comparison, the forces corresponding to the nominal lengths of the first 15 pairs of wires in Table 3-18 need to be first obtained. Taking Pair No.1 of Table 3-18 again for instance, the percentage length measurement error for the 23.2 feet (nominal length) model wire 1A2+(2A2) is $(0.59 \pm 0.43)\%$, or 0.16% to 1.02%, according to Table F-5, i.e., the actual length ranges from 23.24 feet to 23.44 feet. Considering the case when the model wire gallops at 1.69 Hz, the horizontal tension measured as 8.3 lb as listed in the second column of Table 3-19 will be the one corresponding to a particular length ranging between 23.24 feet and 23.44 feet. Thus,

- (i) if that length=23.24 feet, then the horizontal tension corresponding to the nominal 23.2 feet wire will be 8.9 lb according to Simpson's dynamic formula in Appendix H, and
- (ii) if that length=23.44 feet, then the horizontal tension corresponding to the nominal 23.2 feet wire will be 11.8 lb.

Consequently, since the actual wire length is between 23.24 feet and 23.44 feet, the horizontal tension corresponding to 23.2 feet model wire 1A2+(2A2) at 1.69 Hz is between 8.9 lb (lower bound) and 11.8 lb (upper bound).

Similarly, the lower and upper bounds of horizontal tensions of the 23.2 feet model wire 1A2+(2A2) at other frequencies and those of the 46.4 feet prototype wire

$4A^2+(2A)^2$ can be obtained. The results are listed in the second and last columns of Table 3-20, respectively. Multiplying the forces of the model wire by four and dividing the corresponding frequencies by $\sqrt{2}$ as demanded by the similarity requirements yield the predicted forces for the 46.4 feet prototype wire as listed in the fourth column. The results from Table 3-20 are plotted in Fig. 3-25, in which the circles and solid stars represent the lower and upper bounds of horizontal tensions, respectively, for the 46.4 feet prototype wire $4A^2+(2A)^2$ predicted by the model. The squares and solid squares represent the lower and upper bounds of horizontal tensions, respectively, obtained from the experiment. The overlapped region marked by the zigzag line will be the one in which the prototype and model satisfy the similitude prediction. In the same manner, the lower and upper bounds of the horizontal tensions for the other fourteen pairs are plotted from Fig. I-2a to Fig. I-2c of Appendix I. Consequently, the similitude predictions are confirmed once the length measurement error is considered.

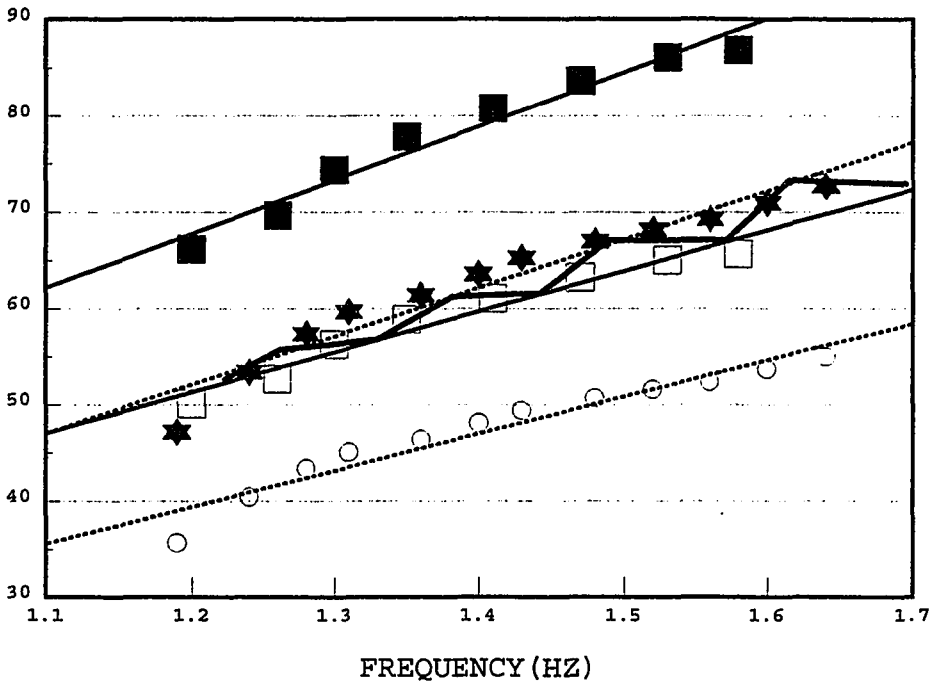
3.4.1.4 Estimation of the Actual Length

It is intended to estimate the actual length of the first 15 pairs of wires in Table 3-18 based on the assumption that the prototype forces both predicted by the model and measured from the experiment match exactly. Consider the Pair No.1 of Table 3-18 again in which the nominal lengths of the prototype

46.4' 4A2+(2A2) -- PROTOTYPE

23.2' 1A2+(2A2) -- MODEL

HORIZONTAL TENSION (lb)



From testing prototype experimentally		4* (experimentally obtained model forces)	
lower bound	upper bound	lower bound	upper bound
—□—	—■—○.....★.....

Fig. 3-25: Lower and upper bounds of the prototype's horizontal tensions obtained by experiment and prediction, respectively, after considering length measurement error.

Table 3-20

The lower and upper bounds of horizontal tensions of the prototype wire both predicted by the model wire and obtained from the experiment.

Horizontal Tension								
MODEL:23.2' 1A2+(2A2)			PROTOTYPE:46.4' 4A2+(2A2)					
Measured from experiment			Predicted by model			Measured from experiment		
Frequency (Hz)	Lower bound	upper(lb) bound	Frequency (Hz)	Lower bound	upper(lb) bound	Frequency (Hz)	Lower bound	upper(lb) bound
1.69	8.9	11.8	1.19	35.7	47.2	1.20	50.1	66.2
1.75	10.1	13.4	1.24	40.4	53.4	1.26	52.7	69.7
1.81	10.9	14.4	1.28	43.4	57.4	1.30	56.3	74.4
1.86	11.3	14.9	1.31	45.1	59.7	1.35	58.9	77.8
1.92	11.6	15.4	1.36	46.4	61.4	1.41	61.1	80.8
1.98	12.0	15.9	1.40	48.1	63.6	1.47	63.3	83.7
2.03	12.4	16.3	1.43	49.4	65.3	1.53	65.1	86.1
2.09	12.7	16.8	1.48	50.7	67.0	1.58	65.7	86.9
2.15	12.9	17.1	1.52	51.6	68.2			
2.20	13.1	17.3	1.56	52.4	69.3			
2.26	13.4	17.8	1.60	53.7	71.0			
2.32	13.8	18.2	1.64	55.0	72.7			

and model are 46.4 feet and 23.2 feet, respectively. Assume the actual lengths of the model and prototype wires are such that the horizontal tensions both predicted by the model and obtained from the experiment match exactly and fall into the region marked by the zigzag line as shown in the upper left corner of Fig. 3-25a. Then those lengths can be obtained from the following two parts:

(i) If the horizontal tension of the prototype wire 4A2+(2A2) predicted by the model wire 1A2+(2A2) matches the lower bound of the overlapped region, the actual length of the model wire is, as obtained by trial and error from Simpson's dynamic formula in Appendix H, 23.35 feet. On the other hand, if that force matches the upper bound of the overlapped region, the actual length of the model is 23.44 feet. Therefore, the

actual length of the model wire will be between 23.35 feet and 23.44 feet if that predicted force is within the region marked by the zigzag line.

(ii) Similarly, the actual lengths of the prototype wire $4A_2+(2A_2)$ are 46.47 feet and 46.52 feet if the corresponding horizontal tensions measured from the experiment agree with the lower and upper bounds, respectively, of the overlapped region. Consequently, the actual length of the prototype wire will be between 46.47 feet and 46.52 feet if the measured force is within the region marked by the zigzag line.

Therefore, if the actual length of the model wire $1A_2+(2A_2)$ is the one between 23.35 feet and 23.44 feet and that of the prototype wire $4A_2+(2A_2)$ has a corresponding value which is between 46.47 feet and 46.52 feet (say model=23.39 feet, prototype=46.49 feet) such that the prototype's forces both predicted by the model and obtained from the experiment match exactly and fall into the region marked by the zigzag line as shown in the upper left corner of Fig. 3-25a, the similitude prediction is perfectly matched. In the same manner, the actual length of the other fourteen pairs can be obtained and the results are listed in Table 3-21.

It is not surprising to find from Table 3-21 that the actual length is longer than the measured (nominal) one, which is to be expected due to the kinks in the wire.

Table 3-21

The actual lengths of the prototype and model wires.

Pair #	Wire type (prototype)	Nominal length (ft)	Actual length (ft)	Wire type (prototype)	Nominal length (ft)	Actual length (ft)
1	4A2+(2A2)	46.4	46.47-46.52	1A2+(2A2)	23.2	23.35-23.44
2	4A2	46.4	46.47-46.51	1A2+(1A2)	23.2	23.42-23.44
3	4A2+(2A3)	46.4	46.47-46.52	1A2+(1A2+1A3)	23.2	23.35-23.44
4	4A3+(2A3)	46.4	46.47-46.51	1A3+(2A3)	23.2	23.36-23.44
5	4A3	46.4	46.47-46.53	1A3+(1A3)	23.2	23.42-23.44
6	4A2+(2A3)	43.4	43.47-43.58	1A2+(1A2+1A3)	21.7	21.79-21.92
7	4A2	43.4	43.47-43.61	1A2+(1A2)	21.7	21.79-21.92
8	4A2+(2A2)	43.4	43.47-43.59	1A2+(2A2)	21.7	21.79-21.92
9	4A3+(2A3)	43.4	43.47-43.48	1A3+(2A3)	21.7	21.87-21.92
10	4A3	43.4	43.47-43.52	1A3+(1A3)	21.7	21.89-21.92
11	4A2+(2A2)	40.4	40.46-40.48	1A2+(2A2)	20.2	20.35-20.41
12	4A2	40.4	40.46-40.54	1A2+(1A2)	20.2	20.29-20.41
13	4A2+(2A3)	40.4	40.46-40.54	1A2+(1A2+1A3)	20.2	20.30-20.41
14	4A3+(2A3)	40.4	40.46-40.51	1A3+(2A3)	20.2	20.33-20.41
15	4A3	40.4	40.46-40.52	1A3+(1A3)	20.2	20.36-20.41

3.4.2 Usefulness of the Collected Data

As discussed in Section 3.3.4.3(B), the support horizontal tensions may need to be adjusted as much as 20% as a result of the 0.59% length measurement error. Then are they still useful in the extreme case? The answer is yes, if the collected data are uniformly distributed around the theoretical solutions.

Consider a motion which is governed by the equation $y=x^5$, where x and y are the independent and dependent variables, respectively. This equation was selected since y is very sensitive to the changes of x as being seen similarly in the

galloping case for the support force with respect to wire length. Assume the measured x 's and y 's during a series of tests are such as listed in the second and fifth columns of Table 3-22, respectively. Also if the actual values of x 's are the ones as listed in the first column, the actual values of y 's, as obtained by $y=x^5$, will be the ones as listed in the fourth column. Define the percentage change of x or y as the difference between the measured and actual values divided by the measured value. Then the percentage changes of x and y are obtained as listed in the third and sixth columns, respectively.

Note that, from Table 3-22, the actual x 's is designated to be larger than the measured one to simulate the case of the wire length as discussed in the previous section. Then using the linear regression model of $y=\beta_0+\beta_1x'$ where $x'=x^5$ for measured x 's and y 's in Table 3-22, the governing equation is calculated from Equation D-4 of Appendix D as

$$y=4.303012+1.011886x^5 \quad (3-8)$$

and R^2 , the coefficient of determination, is 0.998739. Note that since that value is close to 1, there shows strong evidence of accuracy of fit of Equation 3-8 to the data.

Using Equation 3-8 to predict the y -value corresponding to x 's from 20 to 25 which are outside the experimental ranges, the results are listed in the ninth column of Table 3-22. Also listed in the eighth column are the actual y corresponding to x using the actual governing equation $y=x^5$.

Table 3-22

Measured and actual x's and their corresponding y's.

x-actual	x-measured	% change	y-actual	y-measured	% change	x	y	y-regression	%change
1.00	0.99	-1.01%	1.00 ⁵	1.02 ⁵	9.43%	20.0	20.0 ⁵	3238042	1.17%
1.10	1.08	-1.85%	1.10 ⁵	1.12 ⁵	8.62%	20.1	20.1 ⁵	3319806	1.17%
1.20	1.19	-0.84%	1.20 ⁵	1.17 ⁵	-13.50%	20.2	20.2 ⁵	3403214	1.17%
1.30	1.28	-1.56%	1.30 ⁵	1.32 ⁵	7.35%	20.3	20.3 ⁵	3488290	1.17%
1.40	1.38	-1.45%	1.40 ⁵	1.38 ⁵	-7.46%	20.4	20.4 ⁵	3575059	1.17%
1.50	1.49	-0.67%	1.50 ⁵	1.52 ⁵	6.41%	20.5	20.5 ⁵	3663547	1.17%
1.60	1.60	0.00%	1.60 ⁵	1.63 ⁵	8.87%	20.6	20.6 ⁵	3753777	1.17%
1.70	1.67	-1.80%	1.70 ⁵	1.68 ⁵	-6.10%	20.7	20.7 ⁵	3845777	1.17%
1.80	1.78	-1.12%	1.80 ⁵	1.82 ⁵	5.38%	20.8	20.8 ⁵	3939572	1.17%
1.90	1.88	-1.06%	1.90 ⁵	1.89 ⁵	-2.67%	20.9	20.9 ⁵	4035188	1.17%
2.00	1.99	-0.50%	2.00 ⁵	2.02 ⁵	4.85%	21.0	21.0 ⁵	4132652	1.17%
2.10	2.08	-0.96%	2.10 ⁵	2.11 ⁵	2.35%	21.1	21.1 ⁵	4231990	1.17%
2.20	2.17	-1.38%	2.20 ⁵	2.17 ⁵	-7.11%	21.2	21.2 ⁵	4333229	1.17%
2.30	2.28	-0.88%	2.30 ⁵	2.32 ⁵	4.24%	21.3	21.3 ⁵	4436396	1.17%
2.40	2.38	-0.84%	2.40 ⁵	2.39 ⁵	-2.11%	21.4	21.4 ⁵	4541520	1.17%
2.50	2.49	-0.40%	2.50 ⁵	2.52 ⁵	3.91%	21.5	21.5 ⁵	4648626	1.17%
2.60	2.60	0.00%	2.60 ⁵	2.62 ⁵	3.76%	21.6	21.6 ⁵	4757744	1.17%
2.70	2.67	-1.12%	2.70 ⁵	2.68 ⁵	-3.79%	21.7	21.7 ⁵	4868901	1.17%
2.80	2.78	-0.72%	2.80 ⁵	2.78 ⁵	-3.65%	21.8	21.8 ⁵	4982127	1.17%
2.90	2.88	-0.69%	2.90 ⁵	2.92 ⁵	3.38%	21.9	21.9 ⁵	5097449	1.17%
3.00	2.99	-0.33%	3.00 ⁵	2.99 ⁵	-1.68%	22.0	22.0 ⁵	5214896	1.17%
3.10	3.08	-0.65%	3.10 ⁵	3.12 ⁵	3.16%	22.1	22.1 ⁵	5334499	1.17%
3.20	3.20	0.00%	3.20 ⁵	3.21 ⁵	1.55%	22.2	22.2 ⁵	5456286	1.17%
3.30	3.28	-0.61%	3.30 ⁵	3.27 ⁵	-4.67%	22.3	22.3 ⁵	5580287	1.17%
3.40	3.37	-0.89%	3.40 ⁵	3.42 ⁵	2.89%	22.4	22.4 ⁵	5706533	1.17%
3.50	3.48	-0.57%	3.50 ⁵	3.49 ⁵	-1.44%	22.5	22.5 ⁵	5835053	1.17%
3.60	3.58	-0.56%	3.60 ⁵	3.62 ⁵	2.73%	22.6	22.6 ⁵	5965879	1.17%
3.70	3.69	-0.27%	3.70 ⁵	3.73 ⁵	3.96%	22.7	22.7 ⁵	6099040	1.17%
3.80	3.80	0.00%	3.80 ⁵	3.78 ⁵	-2.67%	22.8	22.8 ⁵	6234569	1.17%
3.90	3.87	-0.78%	3.90 ⁵	3.87 ⁵	-3.94%	22.9	22.9 ⁵	6372497	1.17%
4.00	3.98	-0.50%	4.00 ⁵	4.02 ⁵	2.46%	23.0	23.0 ⁵	6512855	1.17%
4.10	4.08	-0.49%	4.10 ⁵	4.09 ⁵	-1.23%	23.1	23.1 ⁵	6655675	1.17%
4.20	4.19	-0.24%	4.20 ⁵	4.24 ⁵	4.63%	23.2	23.2 ⁵	6800990	1.17%
4.30	4.28	-0.47%	4.30 ⁵	4.33 ⁵	3.42%	23.3	23.3 ⁵	6948832	1.17%
4.40	4.38	-0.46%	4.40 ⁵	4.38 ⁵	-2.30%	23.4	23.4 ⁵	7099234	1.17%
4.50	4.47	-0.67%	4.50 ⁵	4.52 ⁵	2.19%	23.5	23.5 ⁵	7252229	1.17%
4.60	4.58	-0.44%	4.60 ⁵	4.58 ⁵	-2.20%	23.6	23.6 ⁵	7407850	1.17%
4.70	4.68	-0.43%	4.70 ⁵	4.73 ⁵	3.13%	23.7	23.7 ⁵	7566132	1.17%
4.80	4.79	-0.21%	4.80 ⁵	4.79 ⁵	-1.05%	23.8	23.8 ⁵	7727107	1.17%
4.90	4.87	-0.62%	4.90 ⁵	4.87 ⁵	-3.12%	23.9	23.9 ⁵	7890811	1.17%
5.00	4.98	-0.40%	5.00 ⁵	4.97 ⁵	-3.05%	24.0	24.0 ⁵	8057278	1.17%
5.10	5.08	-0.39%	5.10 ⁵	5.12 ⁵	1.94%	24.1	24.1 ⁵	8226543	1.17%
5.20	5.18	-0.39%	5.20 ⁵	5.16 ⁵	-3.94%	24.2	24.2 ⁵	8398640	1.17%
5.30	5.30	0.00%	5.30 ⁵	5.31 ⁵	0.94%	24.3	24.3 ⁵	8573606	1.17%
5.40	5.38	-0.37%	5.40 ⁵	5.36 ⁵	-3.79%	24.4	24.4 ⁵	8751475	1.17%
5.50	5.49	-0.18%	5.50 ⁵	5.51 ⁵	0.90%	24.5	24.5 ⁵	8932285	1.17%
5.60	5.57	-0.54%	5.60 ⁵	5.58 ⁵	-1.81%	24.6	24.6 ⁵	9116070	1.17%
5.70	5.68	-0.35%	5.70 ⁵	5.67 ⁵	-2.67%	24.7	24.7 ⁵	9302869	1.17%
5.80	5.78	-0.35%	5.80 ⁵	5.84 ⁵	3.38%	24.8	24.8 ⁵	9492717	1.17%
5.90	5.90	0.00%	5.90 ⁵	5.87 ⁵	-2.58%	24.9	24.9 ⁵	9685652	1.17%
6.00	5.98	-0.33%	6.00 ⁵	6.03 ⁵	2.46%	25.0	25.0 ⁵	9881711	1.17%

The corresponding percentage changes of y as listed in the last column are almost 1.17% for all cases which are smaller than those listed in the sixth column.

Therefore, if the recorded support forces of the galloping test are uniformly distributed around the actual ones as in the case of the variable y in Table 3-22, the regression model will have good chance to produce satisfactory results when applying to the real transmission line. However, if those forces are distributed too widely, the prediction will have large standard deviation.

3.4.3 Other Experimental Conclusions

Unlike the lateral motion of a simply-supported beam or a very taut guitar chord, the wire galloped asymmetrically with respect to its static equilibrium position with large amplitude above and small movement below that position. More than three-fifths of the time during a period was spent for the motion above the static equilibrium position in which the wire would pass the horizon and became concave downward when it reached the highest position. The support forces were found to be trivial because of the slackness of the wire at that time. On the other hand, due to the whipping effect of downward motion and the pull-back restraint at both ends, large support forces were recorded when the wire reached the lowest peak.

Results of the experiment showed that for frequencies far

from the natural frequency, the wire only translated up and down in accordance with the motion of support actuators. However, the wire started galloping when the driving frequency was near the wire's natural frequency and kept galloping with higher amplitude as the driving frequency increased. The motion suddenly collapsed at a particular frequency and returned to the translated motion thereafter. Note that only the first mode was excited in the test.

Out-of-plane motion was observed during the test which coincided with the field reports. That motion was observed visually and was found to be negligible in comparison with the in-plane motion.

The relationship between the support force (either vertical or horizontal) and unit weight of the wire, as found from Table 3-8, seems to be linearly proportional in dynamic case. That relationship is similar in the static case as indicated in Table 3-6. On the other hand, the changes of cross-sectional area, and hence the axial rigidity by deduction, have little effect on the resulting force as found from Table 3-11. Also, a small increase in the wire length changes the wire's static configuration enormously and, therefore, decreases greatly the horizontal tension in static case. Similar behavior is also found in the dynamic case.

4. ANALYTICAL STUDY

Galloping is a three dimensional motion, coupled with torsional vibration resulting from the eccentricity between the gravity center of the conductor itself and that of the iced conductor. However, it is primarily a vertical motion as the result of the aerodynamic force in that direction as discussed in Section 1.2.1. The force is induced from transverse wind attack on the ice-deposit, airfoil-shape section. Due to the torsional motion, the angle of attack varies during the oscillation so that the resulting lift force alters the direction on the iced conductor periodically to provide the essential energy for motion.

4.1 Assumptions

Cable dynamics of a galloping conductor is characterized by a nonlinear and large-amplitude motion. In order to obtain an analytic solution, a series of assumptions are usually made to simplify the governing equations of motion. Unfortunately, the results obtained are often unsatisfactory. For instance, A. Simpson (7) derived an analytical model for a shallow elastic catenary cable oscillating freely with a small amplitude. To obtain a closed-form solution, he neglected a series of terms in the process of the derivation. The accumulated error is found to be large, especially in the high order vibration modes. Also, he neglected the slope of the horizontal displacement in his derivation. Since that term is

significant, the error is, therefore, high. In addition to Simpson's assumptions, Li Li (18) made further ones to achieve his simplified formula. Among them, the assumption of harmonic deflection shape limits his formula to the case of a very taut cable (sag-to-span ratio approaching zero) which does not represent a conductor in the typical transmission line with sag-to-span ratio of 3% or less. Therefore, significant error exists when applying it to a typical one.

In order to more realistically characterize the cable dynamics of a typical transmission line, an analytical expression was developed that does not contain as many restrictions as the expressions mentioned above do. In the current work in developing equations of motion which include both linear and nonlinear behavior, vertical motion only without torsional vibration was considered. The external forces resulting from the aerodynamic lift and drag forces have been expressed by analytic functions. Second and higher order terms in Taylor series expansion for forces and displacements have been neglected.

4.2 Governing Equations of Motion

4.2.1 Derivation of Equations of Motion

Consider a catenary conductor oscillating in its own plane under the external load as shown in Fig. 4-1. The dashed curve is the conductor's static equilibrium position and the solid one is the conductor's position at the time of interest.

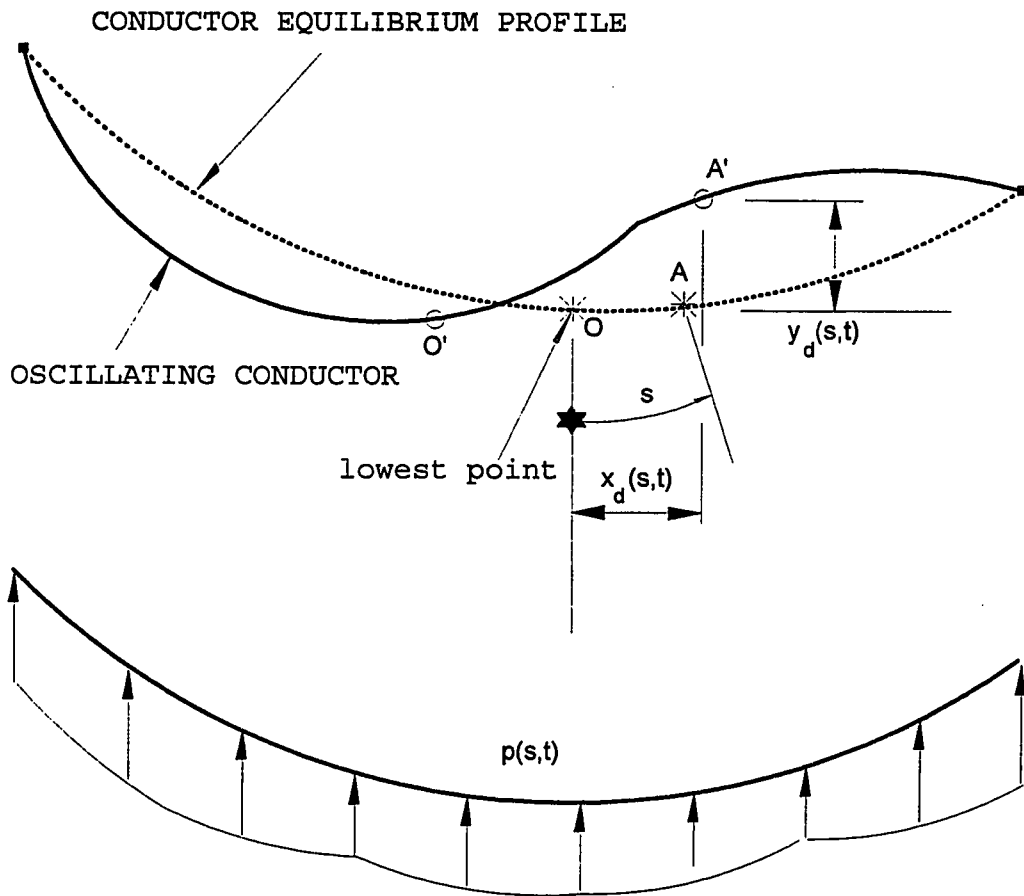


Fig.4-1: A conductor oscillating in its own plane.

Note that the end supports of the conductor are not required to be at the same level. Also the type of end support is not restricted to a particular one. It can be either fixed-fixed, horizontally free-horizontally free, or others.

Locate the origin O at the lowest point of the static equilibrium position as shown in Fig. 4-1 in which the conductor is loaded by its own weight as well as the deposited ice (not shown). It moves to point O' at time t under the external load $p(s,t)$. Let

s = length coordinate along the unstretched configuration

E = modulus of elasticity of the conductor in linear case

σ = stress of the conductor

ϵ = strain of the conductor

c_0, c_1, c_2, c_3 = constant coefficients so that the stress-strain of the conductor is expressed as $\epsilon = c_0 + c_1\sigma + c_2\sigma^2 + c_3\sigma^3$ in the non-linear case

A = cross-sectional area of the conductor

$m(s)$ = mass per unit unstretched length of the iced conductor.

The variable $m(s)$ is a function of length s due to the fact that the ice is deposited irregularly along the conductor.

$s_d(s,t)$ = length coordinate along the stretched configuration in the dynamic case

$x_d(s,t)$ = horizontal coordinate in the dynamic case

$y_d(s,t)$ = vertical coordinate in the dynamic case

$T_d(s,t)$ = dynamic tension

$p(s,t)$ = external load per unit unstretched length of the conductor

(A) Linear Case

Consider the case of small-amplitude vibration so that the conductor behaves linearly, i.e., the stress-strain relation can be expressed as $\sigma = E\epsilon$. A small element AB with an unstretched length δs in its static equilibrium position has the unstretched length coordinates s and $s + \delta s$ at ends A and B, respectively, as shown in Fig. 4-1. It then moves to A'B' at time t under the external load $p(s,t)$ in which the stretched length coordinates at ends A' and B' are $s_d(s,t)$ and $s_d(s + \delta s, t)$, respectively. In the meantime, the horizontal and vertical components are $x_d(s,t)$ and $y_d(s,t)$, respectively, for point A' and $x_d(s + \delta s, t)$ and $y_d(s + \delta s, t)$, respectively, for point B'. Also the tension at points A' and B' are $T_d(s,t)$ and $T_d(s + \delta s, t)$, respectively.

As a result, the stretched length coordinate at point B', i.e., $s_d(s + \delta s, t)$, can be expressed by that at point A' using the Taylor series expansion, i.e.,

$$s_d(s + \delta s, t) = s_d(s, t) + \delta s \frac{\partial s_d(s, t)}{\partial s} + \frac{(\delta s)^2}{2} \frac{\partial^2 s_d(s, t)}{\partial s^2} + \dots$$

As the element shrinks to be infinitesimally small, the second and higher order terms can be neglected. Then the stretched length coordinate at point B' becomes $s_d(s, t) + \delta s \{ \partial s_d(s, t) / \partial s \}$. Since the stretched length coordinate at point A' is $s_d(s, t)$,

the element AB is found to be stretched into $\delta s \{\partial s_d(s, t) / \partial s\}$ in length under the tension $T_d(s, t)$ as shown in Fig. 4-2a. Consider the forces in the tangential direction with the knowledge that as the element becomes infinitesimally small, the curve segment can be replaced by a straight one as shown in Fig. 4-2b in which $T_d(s+\delta s, t)_t$ and $\{[m(s)g-p(s, t)]\delta s\}_t$ are the tangential components of the respective forces. Because the body force $m(s)g\delta s$ and the external load $p(s, t)\delta s$ approach zero as the element becomes very small, the tensions at both ends of the element can be treated to be the same, i.e., $T_d(s, t)$, as far as the elongation is concerned [25]. Also the stretched length $\delta s \{\partial s_d(s, t) / \partial s\}_t$ approaches $\delta s \{\partial s_d(s, t) / \partial s\}$ for very small A'B'. Then from Hooke's law,

$$\sigma(s, t) = E\epsilon(s, t)$$

where the stress $\sigma(s, t)$ and the strain $\epsilon(s, t)$ can be expressed by

$$\sigma(s, t) = \frac{T_d(s, t)}{A}$$

$$\text{and } \epsilon(s, t) = \frac{\delta s \frac{\partial s_d(s, t)}{\partial s} - \delta s}{\delta s} = \frac{\partial s_d(s, t)}{\partial s} - 1.$$

As a result,

$$\frac{T_d(s, t)}{A} = E \left[\frac{\partial s_d(s, t)}{\partial s} - 1 \right]$$

or equivalently,

$$\frac{\partial s_d(s, t)}{\partial s} = 1 + \frac{T_d(s, t)}{EA} \quad (4-1)$$

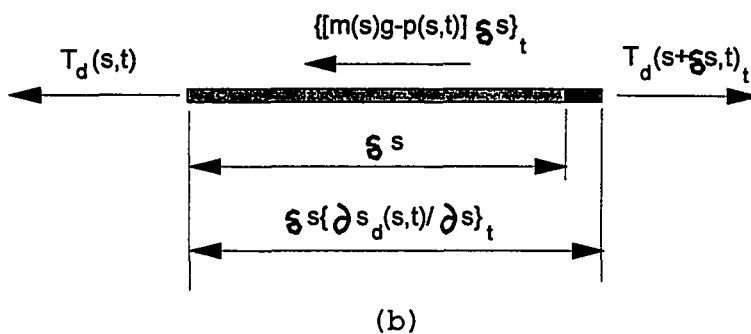
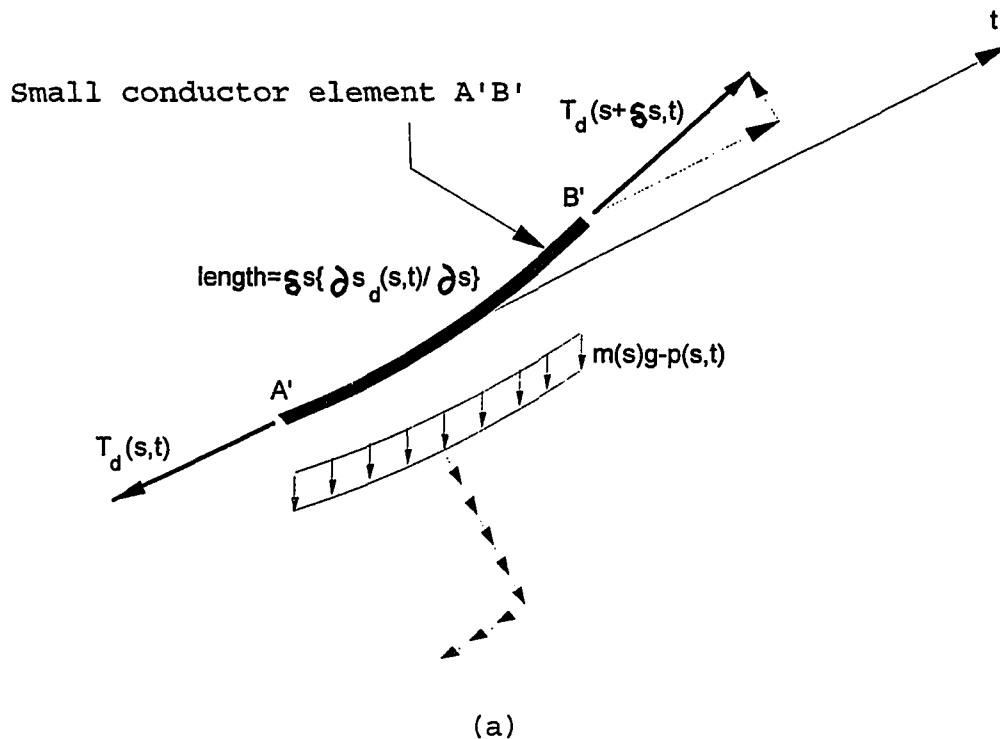


Fig. 4-2: The free body diagram showing (a) the forces on the small conductor A'B' (The dotted lines with arrows are the components of the respective forces), and (b) the forces and elongation in the tangential direction.

In the same manner, the stretched horizontal and vertical coordinates at point B', i.e., $x_d(s+\delta s, t)$ and $y_d(s+\delta s, t)$, respectively, can be approximated by $x_d(s, t) + \delta s \{ \partial x_d(s, t) / \partial s \}$ and $y_d(s, t) + \delta s \{ \partial y_d(s, t) / \partial s \}$, respectively. Since those at point A' are $x_d(s, t)$ and $y_d(s, t)$, respectively, the horizontal and vertical components of the element A'B' will be $\delta s \{ \partial x_d(s, t) / \partial s \}$ and $\delta s \{ \partial y_d(s, t) / \partial s \}$, respectively, as shown in Fig. 4-3. As a result, the horizontal and vertical components of the tension $T_d(s, t)$ at point A' are found to be

$$\left\{ \begin{array}{l} T_d(s, t) \frac{\delta s \frac{\partial x_d(s, t)}{\partial s}}{\delta s \frac{\partial s_d(s, t)}{\partial s}}, \text{ or } T_d(s, t) \frac{\frac{\partial x_d(s, t)}{\partial s}}{\frac{\partial s_d(s, t)}{\partial s}} \end{array} \right\}, \text{ and}$$

$$\left\{ \begin{array}{l} T_d(s, t) \frac{\delta s \frac{\partial y_d(s, t)}{\partial s}}{\delta s \frac{\partial s_d(s, t)}{\partial s}}, \text{ or } T_d(s, t) \frac{\frac{\partial y_d(s, t)}{\partial s}}{\frac{\partial s_d(s, t)}{\partial s}} \end{array} \right\}, \text{ respectively.}$$

Then using Taylor series expansion again and neglecting the second and higher order terms, the horizontal and vertical tension at point B' will be

$$T_d(s, t) \frac{\frac{\partial x_d(s, t)}{\partial s}}{\frac{\partial s_d(s, t)}{\partial s}} + \frac{\partial}{\partial s} \left[T_d(s, t) \frac{\frac{\partial x_d(s, t)}{\partial s}}{\frac{\partial s_d(s, t)}{\partial s}} \right] \delta s, \text{ and}$$

$$T_d(s, t) \frac{\frac{\partial y_d(s, t)}{\partial s}}{\frac{\partial s_d(s, t)}{\partial s}} + \frac{\partial}{\partial s} \left[T_d(s, t) \frac{\frac{\partial y_d(s, t)}{\partial s}}{\frac{\partial s_d(s, t)}{\partial s}} \right] \delta s, \text{ respectively,}$$

as shown in Fig. 4-3. Therefore, by Newton's second law of motion, the summation of all forces in the horizontal

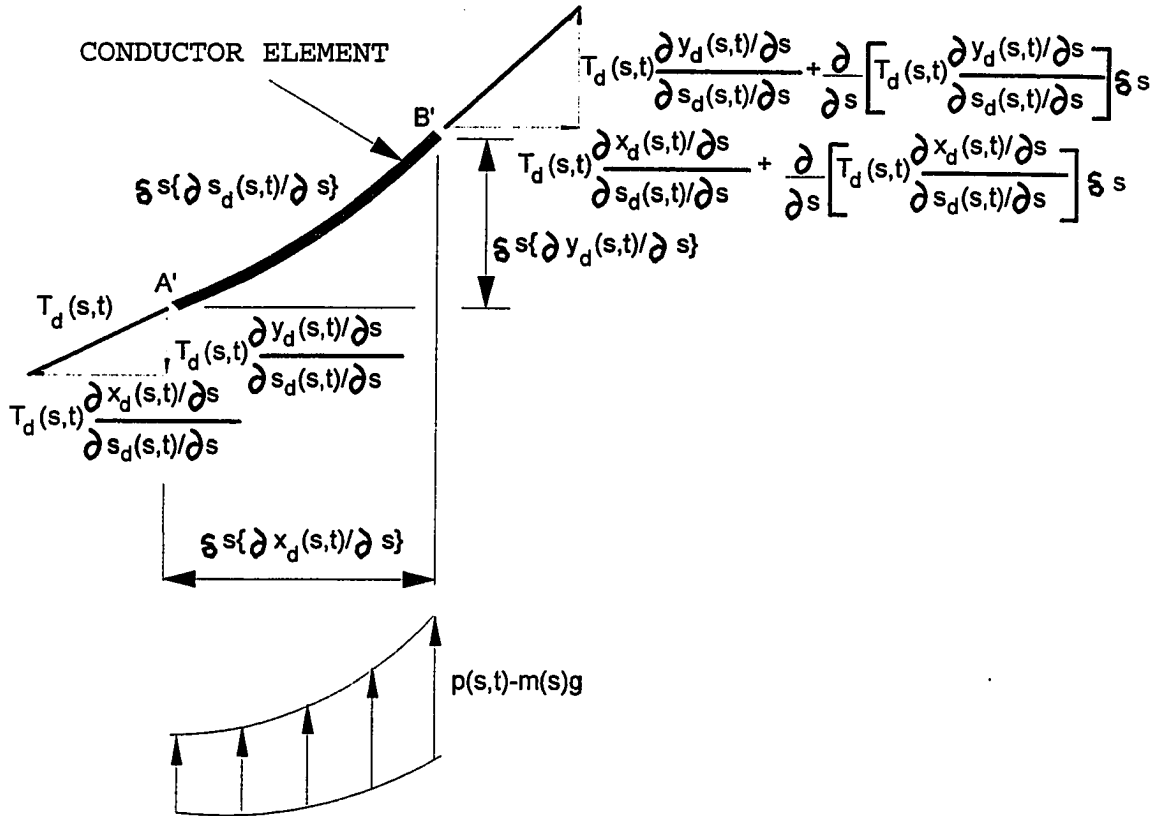


Fig. 4-3: Tension components at both ends of the conductor element A'B' in dynamic case.

direction should equal the product of the mass of the iced conductor element and the acceleration in that direction, i.e.,

$$\left\{ T_d(s, t) \frac{\frac{\partial x_d(s, t)}{\partial s}}{\frac{\partial s_d(s, t)}{\partial s}} + \frac{\partial}{\partial s} \left[T_d(s, t) \frac{\frac{\partial x_d(s, t)}{\partial s}}{\frac{\partial s_d(s, t)}{\partial s}} \right] \delta s \right\} - T_d(s, t) \frac{\frac{\partial x_d(s, t)}{\partial s}}{\frac{\partial s_d(s, t)}{\partial s}} = [m(s) \delta s] \frac{\partial^2 x_d(s, t)}{\partial t^2}$$

which can be reduced to

$$\frac{\partial}{\partial s} \left[T_d(s, t) \frac{\frac{\partial x_d(s, t)}{\partial s}}{\frac{\partial s_d(s, t)}{\partial s}} \right] = m(s) \frac{\partial^2 x_d(s, t)}{\partial t^2} \quad (4-2)$$

Substitution of Equation 4-1 into Equation 4-2 gives the equation of motion in the horizontal direction, i.e.,

$$\frac{\partial}{\partial s} \left\{ \frac{T_d(s, t)}{1 + \frac{T_d(s, t)}{EA}} \frac{\partial x_d(s, t)}{\partial s} \right\} = m(s) \frac{\partial^2 x_d(s, t)}{\partial t^2} \quad (4-3)$$

In the same manner, after summing up all forces in the vertical direction to be the product of the mass of the iced conductor element and the acceleration in that direction, it is readily obtained

$$\frac{\partial}{\partial s} \left\{ \frac{T_d(s, t)}{1 + \frac{T_d(s, t)}{EA}} \frac{\partial y_d(s, t)}{\partial s} \right\} = m(s) \frac{\partial^2 y_d(s, t)}{\partial t^2} + m(s) g - p(s, t) \quad (4-4)$$

Finally, consider the compatibility relation among the

stretched length $\delta s\{\partial s_d(s,t)/\partial s\}$ of the element A'B' and its horizontal and vertical components $\delta s\{\partial x_d(s,t)/\partial s\}$ and $\delta s\{\partial y_d(s,t)/\partial s\}$, respectively, as shown in Fig. 4-3. Since, as the element becomes very small,

$$\left[\delta s \frac{\partial x_d(s,t)}{\partial s} \right]^2 + \left[\delta s \frac{\partial y_d(s,t)}{\partial s} \right]^2 = \left[\delta s \frac{\partial s_d(s,t)}{\partial s} \right]^2$$

It follows that

$$\left[\frac{\partial x_d(s,t)}{\partial s} \right]^2 + \left[\frac{\partial y_d(s,t)}{\partial s} \right]^2 = \left[\frac{\partial s_d(s,t)}{\partial s} \right]^2 = \left[1 + \frac{T_d(s,t)}{EA} \right]^2 \quad (4-5)$$

Note that the relation between the second equality in Equation 4-5 is due to Equation 4-1. Then

$$T_d(s,t) = EA \left\{ \sqrt{\left(\frac{\partial x_d(s,t)}{\partial s} \right)^2 + \left(\frac{\partial y_d(s,t)}{\partial s} \right)^2} - 1 \right\} \quad (4-6)$$

Consequently, the displacements $x_d(s,t)$ and $y_d(s,t)$ can be obtained theoretically by solving Equation 4-3 and Equation 4-4 simultaneously, using the relation in Equation 4-6. However, the equations are too intractable to be solved analytically.

(B) Nonlinear Case

Consider now the nonlinear case in which the stress-strain relation is expressed by [5]:

$$\epsilon(s,t) = c_0 + c_1 \sigma(s,t) + c_2 \sigma^2(s,t) + c_3 \sigma^3(s,t)$$

Since,

$$\sigma(s, t) = \frac{T_d(s, t)}{A}$$

$$\text{and } \epsilon(s, t) = \frac{\delta s \frac{\partial s_d(s, t)}{\partial s} - \delta s}{\delta s} = \frac{\partial s_d(s, t)}{\partial s} - 1,$$

then

$$\frac{s_d(s, t)}{\partial s} - 1 = c_0 + c_1 \frac{T_d(s, t)}{A} + c_2 \left[\frac{T_d(s, t)}{A} \right]^2 + c_3 \left[\frac{T_d(s, t)}{A} \right]^3$$

or equivalently,

$$\frac{s_d(s, t)}{\partial s} = (1 + c_0) + c_1 \frac{T_d(s, t)}{A} + c_2 \left[\frac{T_d(s, t)}{A} \right]^2 + c_3 \left[\frac{T_d(s, t)}{A} \right]^3 \quad (4-7)$$

In the same manner as that in Part A, the equations of motion in the horizontal and vertical directions, respectively, are (see Equation 4-3 and Equation 4-4)

$$\frac{\partial}{\partial s} \left\{ \frac{T_d(s, t)}{(1 + c_0) + c_1 \frac{T_d(s, t)}{A} + c_2 \left[\frac{T_d(s, t)}{A} \right]^2 + c_3 \left[\frac{T_d(s, t)}{A} \right]^3} \frac{\partial x_d(s, t)}{\partial s} \right\}$$

$$= m(s) \frac{\partial^2 x_d(s, t)}{\partial t^2} \quad (4-8)$$

and

$$\frac{\partial}{\partial s} \left\{ \frac{T_d(s, t)}{(1 + c_0) + c_1 \frac{T_d(s, t)}{A} + c_2 \left[\frac{T_d(s, t)}{A} \right]^2 + c_3 \left[\frac{T_d(s, t)}{A} \right]^3} \frac{\partial y_d(s, t)}{\partial s} \right\}$$

$$= m(s) \frac{\partial^2 y_d(s, t)}{\partial t^2} + m(s) g - p(s, t) \quad (4-9)$$

The compatibility equation is (see Equation 4-5):

$$\left[\frac{\partial x_d(s, t)}{\partial s} \right]^2 + \left[\frac{\partial y_d(s, t)}{\partial s} \right]^2 = \left\{ (1+c_0) + c_1 \frac{T_d(s, t)}{A} + c_2 \left[\frac{T_d(s, t)}{A} \right]^2 + c_3 \left[\frac{T_d(s, t)}{A} \right]^3 \right\}^2 \quad (4-10)$$

Consequently, the displacements $x_d(s, t)$ and $y_d(s, t)$ and tension $T_d(s, t)$ can be obtained theoretically by solving Equation 4-8 and Equation 4-9, and Equation 4-10 simultaneously. However, the equations are too intractable to be solved analytically.

4.2.2 Characteristic of Governing Equations of Motion

The governing equations of motion for both linear and nonlinear case show two important characteristics of cable dynamics. They are: (i) asymmetrical motion with respect to the static equilibrium position, and (ii) symmetric vertical mode coupling with anti-symmetric longitudinal mode with respect to the origin, i.e., point O in Fig. 4-1. They will be verified for the linear case in the following paragraphs. The verification for the nonlinear case can be obtained in the same manner.

(i) Asymmetrical motion with respect to static equilibrium position

Consider point A with the unstretched length coordinate $(x(s), y(s))$ in Fig. 4-4 which is redrawn from Fig. 4-1. It moves $u(s, t)$ horizontally and $v(s, t)$ vertically to point A' at time t under disturbance. Assume the stretched length coordinate at point A' is $(x_d(s), y_d(s))$ so that

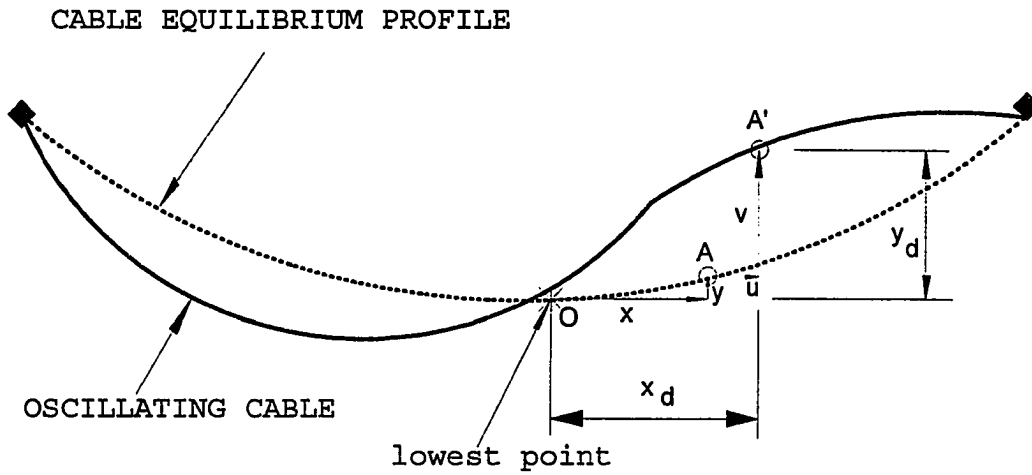


Fig. 4-4: Definition diagram showing components of displacement in disturbed profile (Point A in static case moves to point A' at time t in dynamic case).

$$\mathbf{x}_d(s) = \mathbf{x}(s) + \mathbf{u}(s, t)$$

$$\mathbf{y}_d(s) = \mathbf{y}(s) + \mathbf{v}(s, t).$$

Then, by substituting these relations into Equation 4-3, Equation 4-4, and Equation 4-6, respectively, gives

$$\begin{aligned} \frac{\partial}{\partial s} \left\{ \frac{T_d(s, t)}{1 + \frac{T_d(s, t)}{EA}} \left[\frac{dx(s)}{ds} + \frac{\partial u(s, t)}{\partial s} \right] \right\} &= m(s) \frac{\partial^2 u(s, t)}{\partial t^2} & (4-11) \\ \frac{\partial}{\partial s} \left\{ \frac{T_d(s, t)}{1 + \frac{T_d(s, t)}{EA}} \left[\frac{dy(s)}{ds} + \frac{\partial v(s, t)}{\partial s} \right] \right\} &= m(s) \frac{\partial^2 v(s, t)}{\partial t^2} + m(s) g - p(s, t) \\ T_d(s, t) &= EA \left\{ \sqrt{\left[\frac{dx(s)}{ds} + \frac{\partial u(s, t)}{\partial s} \right]^2 + \left[\frac{dy(s)}{ds} + \frac{\partial v(s, t)}{\partial s} \right]^2} - 1 \right\} \end{aligned}$$

Take the ordinary differential equation (ODE) $yy' = 0.5$ for instance in which one of the solution is a parabola $x = y^2$. It is found that the parabola is symmetrical with respect to the abscissa. The characteristic of symmetry can be re-confirmed by substituting $y = -y$ into the ODE which produces the same equation. However, by substituting $v = -v$ into the set of Equation 4-11 yields a different set of equations. Therefore, the cable vibration is not symmetrical to the static equilibrium position as also observed during the lab test (see Section 3.4.3).

(ii) Symmetric vertical mode coupling with anti-symmetric longitudinal mode with respect to the origin

The set of Equation 4-11 remains unchanged after substituting the relations $u = -u$, $v = v$, and $s = -s$. Therefore, the corresponding solution consists of symmetrical vertical mode as well as anti-symmetrical longitudinal mode with respect to

the origin.

4.3 Solution Strategy

As mentioned in Section 4.2.1, the equations of motion for both linear and nonlinear cases cannot be solved analytically. However, they can be solved numerically from the physical interpretation of the equations themselves. Consider Fig. 4-3 again in which $T_d(s,t) [\partial x_d(s,t)/\partial s] / [\partial s_d(s,t)/\partial s]$ is the horizontal tension at point A'. Then

$\delta \{T_d(s,t) [\partial x_d(s,t)/\partial s] / [\partial s_d(s,t)/\partial s]\}$ will be the difference of horizontal tension at both ends of the infinitesimal element A'B'. As a result, the physical interpretation of Equation 4-2 becomes

"the net horizontal force acting on the infinitesimal element A'B' equals the mass of that element times the resulting horizontal acceleration."

In the same manner, Equation 4-4 is interpreted as

"the net vertical force acting on the infinitesimal element A'B' equals the mass of that element times the resulting vertical acceleration."

Consequently, instead of solving the continuous model described by Equation 4-3 and Equation 4-4, the cable will be divided into discretized lumped masses for numerical analysis. In that regard, the finite difference form of Equation 4-6 is not applicable since it describes the tension of a very small straight element. Instead, the tensions at both ends of the

discretized mass will be obtained by using the static catenary formula of Equation H-2 in Appendix H. The procedures for solving the problem are as follows [26]:

(1) From Taylor series expansion, it is found that

$$x_d(s, t_0 + \Delta t) = x_d(s, t_0) + \Delta t \frac{\partial x_d(s, t_0)}{\partial t} + \frac{(\Delta t)^2}{2!} \frac{\partial^2 x_d(s, t_0)}{\partial t^2} + \frac{(\Delta t)^3}{3!} \frac{\partial^3 x_d(s, t_0)}{\partial t^3} + \frac{(\Delta t)^4}{4!} \frac{\partial^4 x_d(s, t_0)}{\partial t^4} + \dots$$

By neglecting the fourth and higher order terms, $x_d(s, t_0 + \delta t)$ or $x_d(s, t_1)$ is then approximated as

$$x_d(s, t_1) \approx x_d(s, t_0) + \Delta t \frac{\partial x_d(s, t_0)}{\partial t} + \frac{(\Delta t)^2}{2!} \frac{\partial^2 x_d(s, t_0)}{\partial t^2} + \frac{(\Delta t)^3}{3!} \frac{\partial^3 x_d(s, t_0)}{\partial t^3} \quad (4-12)$$

In the same manner, the following relations are established:

$$\begin{aligned} \frac{\partial x_d(s, t_1)}{\partial t} &\approx \frac{\partial x_d(s, t_0)}{\partial t} + \Delta t \frac{\partial^2 x_d(s, t_0)}{\partial t^2} + \frac{(\Delta t)^2}{2!} \frac{\partial^3 x_d(s, t_0)}{\partial t^3} & (4-13) \\ \frac{\partial^2 x_d(s, t_1)}{\partial t^2} &\approx \frac{\partial^2 x_d(s, t_0)}{\partial t^2} + \Delta t \frac{\partial^3 x_d(s, t_0)}{\partial t^3} \\ y_d(s, t_1) &\approx y_d(s, t_0) + \Delta t \frac{\partial y_d(s, t_0)}{\partial t} + \frac{(\Delta t)^2}{2!} \frac{\partial^2 y_d(s, t_0)}{\partial t^2} \\ &\quad + \frac{(\Delta t)^3}{3!} \frac{\partial^3 y_d(s, t_0)}{\partial t^3} \\ \frac{\partial y_d(s, t_1)}{\partial t} &\approx \frac{\partial y_d(s, t_0)}{\partial t} + \Delta t \frac{\partial^2 y_d(s, t_0)}{\partial t^2} + \frac{(\Delta t)^2}{2!} \frac{\partial^3 y_d(s, t_0)}{\partial t^3} \\ \frac{\partial^2 y_d(s, t_1)}{\partial t^2} &\approx \frac{\partial^2 y_d(s, t_0)}{\partial t^2} + \Delta t \frac{\partial^3 y_d(s, t_0)}{\partial t^3} \end{aligned}$$

The physical meanings of the terms $(x_d, \partial x_d / \partial t, \partial^2 x_d / \partial t^2)$ and $(y_d, \partial y_d / \partial t, \partial^2 y_d / \partial t^2)$ are (displacement, velocity, acceleration) in the horizontal and vertical directions, respectively. Thus, with given initial conditions, i.e., displacements,

velocities, and accelerations at time t_0 are known, those at time t_1 will be readily obtained from Equation 4-12 and Equation 4-13 once $\partial^3 x_d / \partial t^3$ and $\partial^3 y_d / \partial t^3$ at time t_0 , assuming to be constants, are known. Note that the designation of $\partial^3 x_d / \partial t^3$ and $\partial^3 y_d / \partial t^3$ at time t_0 to be constants means linear accelerations between time t_0 and t_1 in both directions are assumed. Therefore, the first step to solve the problem is to assume the values of $\partial^3 x_d / \partial t^3$ and $\partial^3 y_d / \partial t^3$ at time t_0 .

(2) Calculate the displacements, velocities and accelerations, respectively, at time t_1 from Equation 4-12 and Equation 4-13.

(3) Determine the cable element geometry from the displacements of Step 2 then use the static catenary formula in Equation H-2 to determine the cable forces at both ends.

(4) Determine the damping forces from the velocities obtained from Step 2. The horizontal and vertical damping forces at time t_1 are calculated as $c\{\partial x_d(s, t_1) / \partial t\}$ and $c\{\partial y_d(s, t_1) / \partial t\}$, respectively, where

c =damping coefficient, $c=2\xi\{\sqrt{(AEm)}\}$

ξ =dimensionless damping factor

A =cross-sectional area of the conductor

E =modulus of elasticity of the conductor

m =mass per unit unstretched length of the conductor.

(5) Compute the imbalance of forces on the lumped mass due to cable forces, damping forces, and external load to obtain the acceleration according to Newton's second law of motion.

(6) Compare the acceleration from Step 5 to that predicted in

Step 2. If the differences of both are within the convergence criteria, a new time interval is begun. Repeat Steps 1 to 6. Otherwise, compute new values for $\partial^3 x_d / \partial t^3$ and $\partial^3 y_d / \partial t^3$ from

$$\frac{\partial^3 x_d(s, t_0)}{\partial t^3} = \frac{\frac{\partial^2 x_d(s, t_1)}{\partial t^2} \Big|_{\text{Step 5}} - \frac{\partial^2 x_d(s, t_0)}{\partial t^2} \Big|_{\text{Step 1}}}{\Delta t}$$

$$\frac{\partial^3 y_d(s, t_0)}{\partial t^3} = \frac{\frac{\partial^2 y_d(s, t_1)}{\partial t^2} \Big|_{\text{Step 5}} - \frac{\partial^2 y_d(s, t_0)}{\partial t^2} \Big|_{\text{Step 1}}}{\Delta t}$$

Repeat Steps 2 to 6

4.4 Results and Discussions

4.4.1 Comparison of the Analytical and Experimental Results

From the eleven groups of wires in Appendix A in which the wire lengths in each group are the same, eleven representative wires, one from each group, are selected as shown in the first column of Table 4-1. Their vertical and horizontal tensions at ends when the galloping wires travel to the lowest peak will be compared between the analytical and experimental results.

With the physical properties and vibrating frequency as shown in the second column, the resulting amplitude, vertical tension (V), and horizontal tension (H) from experiment are listed in the first part of the third column. Note that the amplitudes are measured downward from the ends of the wires. Also with those amplitudes, the corresponding theoretical vertical and horizontal tensions at support are obtained as

shown in the middle of the third column. Define the percentage difference of forces as the difference between the theoretical and experimental forces divided by the theoretical one in percentage. Then the percentage difference of vertical and horizontal tensions for the eleven representative wires can be calculated and are listed in the last part of the third column of Table 4-1.

Table 4-1

Comparison of support vertical and horizontal tensions of galloping wires between the analytical and experimental results.

Wire type	Area (in ²)	Modulus (psi)	Unit WGT (lb/ft)	Length (ft)	Span (ft)	Freq (Hz)	Ampli (ft)	Experiment		Theory(lb)		Difference	
								V	H	V	H	V	H
1S1	.00757	2.201E7	.0255192	46.6	46.0	1.13	2.92	3.8	30.1	5.3	25.4	28%	-19%
1S2+(1S2)	.00442	2.482E7	.0297696	46.4	46.0	1.19	2.65	3.4	34.6	5.1	29.0	33%	-19%
4A2+(2A3)	.02116	1.045E7	.0310248	43.4	43.0	1.25	2.53	5.4	36.4	6.0	30.5	10%	-19%
4A2+(2A2)	.02116	1.051E7	.0360432	40.4	40.0	1.25	2.52	5.5	39.2	7.8	36.7	29%	-7%
4A1	.03640	7.820E6	.0417168	40.2	40.0	1.35	1.86	3.6	46.6	5.7	44.7	36%	-4%
1C1	.00813	1.395E7	.0308244	35.4	35.0	1.24	2.44	3.8	27.8	5.4	24.5	30%	-13%
1C2	.00505	1.401E7	.0190980	30.4	30.0	1.30	2.24	2.0	11.9	2.5	10.4	20%	-14%
1C3+(1C3)	.00320	1.416E7	.0246000	23.3	23.0	1.58	1.71	1.7	10.7	2.1	9.0	19%	-19%
1C3	.00320	1.416E7	.0123000	23.2	23.0	1.69	1.40	0.9	7.2	1.3	6.9	31%	4%
1A3+(1A3)	.00307	1.045E7	.0069960	21.7	21.5	1.69	1.34	0.5	2.7	0.6	2.8	17%	4%
1A2+(2A2)	.00529	1.051E7	.0180216	20.2	20.0	1.87	1.28	1.0	7.7	1.3	6.4	23%	-20%

It is found from Table 4-1 that there are approximately 20% errors between the theoretical and experimental values. The errors are considered to be the results of the following factors:

(a) **Discretization error:** The continuous wire is discretized into lumped masses and the passing time is divided into small time step (Δt) for numerical analysis, which produces the round-off and truncation errors. Also, the Δs -to- Δt ratio

where Δs is the distance along the wire between two consecutive lumped masses affect the accuracy of the results. The ratio for the best accuracy is unknown and, in general, one cannot assert that decreasing the mesh size always increases the accuracy.

(b) In Step 3 of the algorithm in Section 4.3, the tensions at both ends of the cable element are obtained by the static catenary formula in which the cable element is loaded by the distributed self-weight and the ice load. On the other hand, the inertia force is concentrated on the lumped mass which joins the neighboring two cable elements as mentioned in Step 5. The treatment of the system like this unavoidably produces errors.

(c) **Experimental error:** The measurement errors of the support forces also contribute to the differences in Table 4-1. For instance, from Table F-14 of Appendix F, the measured vertical and horizontal tensions of 46.6 feet steel wire 1S1 (Test No. 1) at 1.19 Hz (1.10 Hz of nominal frequency) is 3.8 ± 0.2 lb and 30.1 ± 0.7 lb, respectively. In the extreme case, those forces will be 4.0 lb and 29.4 lb, respectively, which are closer to the theoretical ones.

There are few field-collected data due to technical difficulties as mentioned in Section 2.2. However, the dynamic loads during four galloping events in South Ontario, Canada were recorded in Krishnasamy's paper [18]. The four events with relevant information are shown in the second and third

rows of Table 4-2. Note that in order to apply the analytical algorithm in Section 4.3 to the field test data, the length of insulator and the number of loop during conductor galloping needed to be assumed. However, based on typical design practice, the assumptions were realistic.

Table 4-2

Comparison between field-collected data and analytical results.

Field Test Number	1	2	3	4	
Line data:					
W_c , conductor's weight(lb/ft)	2.074	2.074	2.074	1.094	
d , overall diameter of conductor(inch)	1.602	1.602	1.602	1.102	
A_t , total area(in ²)	1.512	1.512	1.512	0.726	
A_a , area of aluminum strand(in ²)	1.398	1.398	1.398	0.624	
L , span length(feet)	709	709	709	1391	
L_i , insulator length(feet)	8	8	8	10	
W_i , weight of insulator(lb)	300	300	300	350	
Storm data:					
I_t , ice thickness (inch)	0.197	0.315	0.315	0.134	
V_w , mean wind velocity (ft/sec)	4.6	24.6	29.5	23.6	
Experimental	Y , peak-to-peak amplitude (ft)	4.4	23.4	28	38.6
	R , dynamic load/ static load	1.2	1.6	2.0	1.2
Analytical	Y , peak-to-peak amplitude (ft)	4.5	21.5	28.8	38.3
	R , dynamic load/ static load	1.5	2.6	2.9	2.2

In Table 4-2, the peak-to-peak amplitude in the experiment is obtained from the formula

$$Y_{\max} = 0.26V_w / f$$

, where Y_{\max} = peak-to-peak amplitude, ft

V_w = wind velocity, ft/sec, and

f = natural frequency, Hz.

Traditionally, the motion is assumed to be symmetrical with respect to the static equilibrium position, i.e. $Y_{\max}/2$ above

and $Y_{\max}/2$ below that position. On the other hand, the peak-to-peak amplitude in the analytical part is not symmetrical with respect to the static equilibrium position. The results showed that the displacements above and below that position were (2.5', 2.0'), (15.7', 5.8'), (22.3', 6.5'), and (30.1', 8.2'), respectively, for the four events

4.4.2 Discussions of the Analytical Solution

A typical transmission line (Drake conductor with 6000 lb stringing tension on 1200 feet span) under normal loading conditions of galloping (1/4" ice, 30 ft/s wind speed and 0.2 of lift coefficient) is found to only oscillate slightly away from the static equilibrium position when analyzed without damping. In order to produce a large-amplitude motion usually observed at galloping, the effect of negative damping will be considered. It is calculated that even a small amount of negative damping (-1% to -2%) will result in large-amplitude vibration. The derivation of negative damping coefficient is referred to Brent Wouters' work in which the total vertical aerodynamic force coefficient C_{Fv} is expressed as [27]

$$C_{Fv} = -\frac{1}{V_{rel}} \left(\frac{\partial C_L}{\partial \alpha} + C_D \right) \frac{dy_d}{dt} + \frac{\partial C_L}{\partial \alpha} \theta$$

where C_L , C_D , and α are referred to in Equation 1-1 and

V_{rel} = relative wind velocity between the wind and conductor

dy_d/dt = conductor's velocity in the vertical direction

θ = rotational angle of attack.

Then, when the damping coefficient $(\partial C_l / \partial \alpha + C_d) / V_{rel}$ is negative as mentioned by Den Hartog [10], an aerodynamic force in the same direction of the conductor's velocity will be produced to accelerate and maintain the vibration.

For practical application, an equivalent lift force will be assumed to produce the desired amplitude in the undamped case. The amplitude is determined by considering the required vertical clearance above and below the transmission line. Then the corresponding support forces will be used as the upper bound to the possible forces for design.

A typical time history of the conductor tension during a simulated galloping is not always a smooth curve, but a rather zigzag one. However, by including the (positive) damping, the curve is found to be much smoother. The effect of (positive) damping (for instance, 5%) significantly reduces the distortions from the curve in amplitude or support forces. On the other hand, only minor differences exist for different damping ratios (for instance, 10, 15, and 20%) on the time history of the conductor tensions, which coincides with Dr. M. Baenziger's investigation for the broken conductor case [26].

Finally, the program based on the algorithm in Section 4.3 fails to solve the vibration problem of the conductor with large sag-to-span ratio. This is because the profiles of that group of conductors become slack as they move to the level of supports. In that time, the forces in Step 5 of Section 4.3

always fail to converge since the algorithm is only applicable for a taut and stretched cable element.

5. SUMMARY AND CONCLUSION

5.1 Summary

Conductor galloping, known as a low-frequency, high-amplitude, and primarily vertical motion, has long been the concern of the transmission line designers. This is because the motion reduces the vertical clearance between the lines, and then increases the possibility of conductors' contact with each other which would cause flashover. Galloping can break conductor strands and damage dampers, insulator pins, suspension and crossarm hardwares, and even the towers. A 1990 ice storm in central Iowa caused a domino collapse of several support towers in a portion of Lehigh-Sycamore 345 kV line, resulting in power outage for thousands of residents and high costs of repair.

Until recently, the design of the transmission lines and the structures supporting the lines have been primarily based on static loads with a conservative safety factor. The project under investigation sought to improve the design by determining realistic forces for dynamic forces due to galloping by (1) developing an experimental procedure to simulate galloping and to measure amplitude and dynamic forces on support structures, and (2) developing an analytic procedure to predict more accurately the forces on the support structures.

A single-span wire line, symmetrical with respect to midspan, was subjected to support motion at both ends by

hydraulic actuators to excite galloping motion. Three load cells at the ends of the wire were used to measure tension forces. Two video cameras were used to measure the amplitude of galloping. Two hundred and twenty one tests were conducted on a variety of wire lengths, areas, unit weights, modulus of elasticity, external load, and span length. Seventeen pairs satisfied the similarity requirements between the two sets of wires in the defined pair. The results showed discrepancies between the prototype forces obtained from the experiment and those predicted by the model. The length measurement error was found to cause those discrepancies.

An analytical expression was developed that contained less restrictions than those obtained by other authors. The equations of motion including both linear and nonlinear cases were systems of complicated partial differential equations which were too intractable to be solved analytically. An algorithm based on the physical interpretation of the equations was developed to obtain the solution numerically.

5.2 Conclusions

5.2.1 Experimental Study

Experimental results showed that the wire galloped asymmetrically with respect to its static equilibrium position with large amplitude above and small movement below that position. The maximum dynamic force occurred when the wire moved to the lowest peak. That force was much larger than that

occurred when the wire reached the highest peak.

Results of experiment showed that for frequencies far from the natural frequency, the wire only translated up and down in accordance with the motion of support actuators. The wire started galloping when the driving frequency was near the wire's natural frequency and kept galloping with higher amplitude as the driving frequency increased. The motion suddenly collapsed at some particular frequency and returned to the translated motion thereafter.

The out-of-plane motion was observed during the test which coincided with the field reports. However, the in-plane motion was found to be dominant.

The relationship between the support force and unit weight of the wire seems to be linearly proportional in dynamic case. That relationship is similar in the static case. On the other hand, the change of cross-sectional area has little effect on the resulting force. However, a small increase in the wire length decreases tremendously the horizontal tension in static case. Similar behavior is also found in the dynamic case.

5.2.2 Analytical Study

Analytical study showed that the wire vibration is not symmetrical with respect to the static equilibrium position as observed during the lab test. Also, symmetrical vertical mode as well as anti-symmetrical longitudinal mode with respect to

the lowest point of the static equilibrium position coexist at galloping. A typical transmission line under normal loading conditions of galloping is found to only oscillate slightly away from the static equilibrium position when analyzed without damping. However, a large-amplitude motion is obtained when the negative damping is considered. For practical application, an equivalent lift force can be assumed to produce the desired amplitude in the undamped case. The resulting support forces will be used for design.

The results of laboratory test were compared to the analytical solutions and showed approximately 20% errors. Those errors are believed to be the results of measurement error from the experimental model and discretization error from the analytical model.

The analytical algorithm is limited to a conductor with small sag-to-span ratio(around 3% or smaller). A typical time history of the conductor tension during galloping is always not a smooth curve. However, by including the (positive) damping, the curve is found to be much smoother.

5.3 Contribution

The objective of this study was to develop an experimental procedure to simulate galloping and to measure amplitude and dynamic forces on support structures. In addition, the study intended to develop an analytic procedure to predict more accurately the forces on the support

structures. Those objectives were achieved through experimental and theoretical studies described in Chapters 3-4 which lead to the following contributions.

1. A pioneering experimental approach to excite the wire into galloping motion was adopted. This creative base-excitation method produced a large-amplitude motion in which the magnetic field method fails to achieve. As a result, conductor galloping in the field was more accurately simulated.
2. This is the first time that the equations of motion for conductor galloping were developed. The state-of-the-art equations contain fewer assumptions during the derivation and are more general for their application to the real transmission line.
3. A state-of-the-art algorithm for the solution of the equations is introduced. The algorithm will give the transmission line designers the magnitude of the support forces once the amplitude is specified.

5.4 Recommendation for Further Research

Further study is recommended for the solution of the governing partial differential equations by finite difference method or other numerical method. In this investigation, the stability of convergence criteria used with the equations need to be thoroughly studied.

The torsional effect in the derivation of equations of

motion for conductor galloping could be included. Since the vertical vibration is believed to be coupling with the torsional motion during galloping, the former will be more accurately described if the latter is considered.

The lift and drag forces are essential for the energy input of the conductor galloping in the field. Current works concentrating on the experiment of different shapes of conductors fail to give a general analytical expression among those forces and the relevant parameters such as wind velocity and angle of attack. A better understanding of the forcing function will be a great use to the galloping analysis.

Finally, the arrangement to measure the amplitude as shown in Fig. 3-13 needs to be improved. It has been considered to use the potentiometer displacement transducer with an attachment at the center of the wire to measure the amplitude directly. However, the pre-test study indicated that the wire's profile would be seriously distorted with a weight, even though very light, attached to it. Therefore, an improvement of the mechanism to measure the amplitude in future work is recommended.

APPENDIX A: TEST WIRE INFORMATION

The wire types, lengths, and spans for the two hundred and twenty-one tests performed in the experiments are listed as follows:

WIRE TYPE	WIRE LENGTH	SPAN	WIRE TYPE	WIRE LENGTH	SPAN
1. 1S1	46.6'	46.0'	53. 1A2	46.4'	46.0'
2. 2S2 (*)	46.6'	46.0'	54. 1A2+(2A2)	46.4'	46.0'
3. 1S2+(1S2)	46.6'	46.0'	55. 1A2+(1A2+1A3)	46.4'	46.0'
4. 1S2	46.6'	46.0'	56. 1A2+1A3+(1A2+1A3)	46.4'	46.0'
5. 1S2+(1C2) (**)	46.6'	46.0'	57. 1A2+1A3	46.4'	46.0'
6. 3S3	46.6'	46.0'	58. 4A2+(2A3)	46.4'	46.0'
7. 2S3+(1S3)	46.6'	46.0'	59. 4A2+(1A3)	46.4'	46.0'
8. 2S3	46.6'	46.0'	60. 4A3+(2A3)	46.4'	46.0'
9. 1S3+(1S3)	46.6'	46.0'	61. 4A3+(1A3)	46.4'	46.0'
10. 1S3	46.6'	46.0'	62. 4A3	46.4'	46.0'
11. 1S3+(1C3)	46.6'	46.0'	63. 3A3+(1A3)	46.4'	46.0'
12. 1C3+(1S3)	46.6'	46.0'	64. 3A3	46.4'	46.0'
13. 1C3	46.6'	46.0'	65. 2A3+(1A3)	46.4'	46.0'
14. 1C1	46.6'	46.0'	66. 2A3+(2A3)	46.4'	46.0'
15. 1C2+(1S2)	46.6'	46.0'	67. 2A3	46.4'	46.0'
16. 1C2	46.6'	46.0'	68. 1A3+(1A3)	46.4'	46.0'
17. 1C3+(1C3)	46.6'	46.0'	69. 1A3+(2A3)	46.4'	46.0'
18. 2C3	46.6'	46.0'	70. 1A3	46.4'	46.0'
19. 1S2+(1S2)	46.4'	46.0'	71. 4A2+(2A3)	43.4'	43.0'
20. 2S2	46.4'	46.0'	72. 4A2	43.4'	43.0'
21. 1S2	46.4'	46.0'	73. 4A2+(2A2)	43.4'	43.0'
22. 1S2+(1C2)	46.4'	46.0'	74. 1A2+(2A2)	43.4'	43.0'
23. 1C2+(1S2)	46.4'	46.0'	75. 1A2+(1A2)	43.4'	43.0'
24. 1C2	46.4'	46.0'	76. 1A2+(1A2+1A3)	43.4'	43.0'
25. 3S3	46.4'	46.0'	77. 4A3+(2A3)	43.4'	43.0'
26. 2S3+(1S3)	46.4'	46.0'	78. 4A3	43.4'	43.0'
27. 2S3	46.4'	46.0'	79. 1A3+(2A3)	43.4'	43.0'
28. 1S3+(1S3)	46.4'	46.0'	80. 1A3+(1A3)	43.4'	43.0'
29. 1S3	46.4'	46.0'			
30. 2C3	46.4'	46.0'	81. 4A2+(2A2)	40.4'	40.0'
31. 1C3+(1C3)	46.4'	46.0'	82. 4A2	40.4'	40.0'
32. 1C3	46.4'	46.0'	83. 4A2+(2A3)	40.4'	40.0'
33. 1S3+(1C3)	46.4'	46.0'	84. 1A2+(2A2)	40.4'	40.0'
34. 1C1	46.4'	46.0'	85. 1A2+(1A2)	40.4'	40.0'
35. 3A1	46.4'	46.0'	86. 1A2+(1A2+1A3)	40.4'	40.0'
36. 2A1+(1A1)	46.4'	46.0'	87. 4A3+(2A3)	40.4'	40.0'
37. 2A1	46.4'	46.0'	88. 4A3	40.4'	40.0'
38. 1A1+(1A1)	46.4'	46.0'	89. 1A3+(2A3)	40.4'	40.0'
39. 1A1	46.4'	46.0'	90. 1A3+(1A3)	40.4'	40.0'
40. 1A1+1A2	46.4'	46.0'	91. 1A3	40.4'	40.0'
41. 1A1+1A2+(1A1+1A2)	46.4'	46.0'	92. 1A2	40.4'	40.0'
42. 1A1+1A3+(1A1+1A3)	46.4'	46.0'	93. 4S3	40.4'	40.0'
43. 1A1+1A3	46.4'	46.0'	94. 3S3+(1S3)	40.4'	40.0'
44. 4A2+(2A2)	46.4'	46.0'	95. 2S3+(2S3)	40.4'	40.0'
45. 4A2+(1A2)	46.4'	46.0'	96. 2S3+(1S3)	40.4'	40.0'
46. 4A2	46.4'	46.0'	97. 1S3+(2S3)	40.4'	40.0'
47. 3A2+(1A2)	46.4'	46.0'	98. 3S3	40.4'	40.0'
48. 3A2	46.4'	46.0'	99. 2S3	40.4'	40.0'
49. 2A2+(1A2)	46.4'	46.0'	100. 1S3+(1S3)	40.4'	40.0'
50. 2A2+(2A2)	46.4'	46.0'	101. 1S3	40.4'	40.0'
51. 2A2	46.4'	46.0'	102. 4C3	40.4'	40.0'
52. 1A2+(1A2)	46.4'	46.0'	103. 3C3+(1C3)	40.4'	40.0'

WIRE TYPE	WIRE LENGTH	SPAN	WIRE TYPE	WIRE LENGTH	SPAN
104. 3C3	40.4'	40.0'	165. 1A1+(1A1)	23.2'	23.0'
105. 2C3+(1C3)	40.4'	40.0'	166. 1A1	23.2'	23.0'
106. 2C3	40.4'	40.0'	167. 1A1+1A2+(1A1+1A2)	23.2'	23.0'
107. 1C3+(1C3)	40.4'	40.0'	168. 1A1+1A2	23.2'	23.0'
108. 1C3	40.4'	40.0'	169. 1A1+1A3+(1A1+1A3)	23.2'	23.0'
109. 1S1	40.4'	40.0'	170. 1A1+1A3	23.2'	23.0'
110. 2S2	40.4'	40.0'	171. 4A3+(2A3)	23.2'	23.0'
111. 1S2+(1S2)	40.4'	40.0'	172. 4A3+(1A3)	23.2'	23.0'
112. 1S2	40.4'	40.0'	173. 4A3	23.2'	23.0'
113. 1C1	40.4'	40.0'	174. 3A3+(1A3)	23.2'	23.0'
114. 2C2	40.4'	40.0'	175. 3A3	23.2'	23.0'
115. 1C2+(1C2)	40.4'	40.0'	176. 2A3+(1A3)	23.2'	23.0'
116. 1C2	40.4'	40.0'	177. 2A3+(2A3)	23.2'	23.0'
117. 4A1	40.4'	40.0'	178. 2A3	23.2'	23.0'
118. 1A2+(1A2+1A3)	40.2'	40.0'	179. 1A3+(1A3)	23.2'	23.0'
119. 1A2+(1A2)	40.2'	40.0'	180. 1A3+(2A3)	23.2'	23.0'
120. 1A2+(2A2)	40.2'	40.0'	181. 1A3	23.2'	23.0'
121. 4A2	40.2'	40.0'	182. 4A2+(2A2)	23.2'	23.0'
122. 4A2+(2A2)	40.2'	40.0'	183. 4A2+(1A2)	23.2'	23.0'
123. 4A2+(2A3)	40.2'	40.0'	184. 4A2	23.2'	23.0'
124. 4A3+(2A3)	40.2'	40.0'	185. 4A2+(2A3)	23.2'	23.0'
125. 4A3	40.2'	40.0'	186. 4A2+(1A3)	23.2'	23.0'
126. 1A3+(2A3)	40.2'	40.0'	187. 3A2+(1A2)	23.2'	23.0'
127. 1A3+(1A3)	40.2'	40.0'	188. 3A2	23.2'	23.0'
128. 1A3	40.2'	40.0'	189. 2A2+(1A2)	23.2'	23.0'
129. 4S3	40.2'	40.0'	190. 2A2+(2A2)	23.2'	23.0'
130. 4A1	40.2'	40.0'	191. 2A2	23.2'	23.0'
131. 3A1+(1A1)	40.2'	40.0'	192. 1A2+(1A2)	23.2'	23.0'
132. 3A1	40.2'	40.0'	193. 1A2+(2A2)	23.2'	23.0'
133. 2A1+(1A1)	40.2'	40.0'	194. 1A2+(1A2+1A3)	23.2'	23.0'
134. 2A1	40.2'	40.0'	195. 4A2	21.7'	21.5'
135. 1A1+(1A1)	40.2'	40.0'	196. 4A2+(2A2)	21.7'	21.5'
136. 1A1	40.2'	40.0'	197. 4A2+(2A3)	21.7'	21.5'
137. 4A2+(2A3)	35.4'	35.0'	198. 1A2+(2A2)	21.7'	21.5'
138. 4A2	35.4'	35.0'	199. 1A2+(1A2)	21.7'	21.5'
139. 1A1	35.4'	35.0'	200. 1A2+(1A2+1A3)	21.7'	21.5'
140. 1C1	35.4'	35.0'	201. 1A2	21.7'	21.5'
141. 1C2	35.4'	35.0'	202. 1A3+(2A3)	21.7'	21.5'
142. 1S2	35.4'	35.0'	203. 1A3+(1A3)	21.7'	21.5'
143. 1C2	30.4'	30.0'	204. 1A3	21.7'	21.5'
144. 1S2	30.4'	30.0'	205. 1A2	20.2'	20.0'
145. 1C1	30.4'	30.0'	206. 1A2+(2A2)	20.2'	20.0'
146. 1C2	30.4'	30.0'	207. 1A2+(1A2)	20.2'	20.0'
147. 1A1	30.4'	30.0'	208. 1A2+(1A2+1A3)	20.2'	20.0'
148. 4A2	30.4'	30.0'	209. 1A3+(1A3)	20.2'	20.0'
149. 2A3	30.4'	30.0'	210. 1A3+(2A3)	20.2'	20.0'
150. 1C1	23.3'	23.0'	211. 1C3	20.2'	20.0'
151. 1C2	23.3'	23.0'	212. 1C3+(2C3)	20.2'	20.0'
152. 2C3	23.3'	23.0'	213. 1C3+(1C3)	20.2'	20.0'
153. 1C3	23.3'	23.0'	214. 3C3	20.2'	20.0'
154. 1C3+(1C3)	23.3'	23.0'	215. 2C3	20.2'	20.0'
155. 1C1	23.2'	23.0'	216. 2C3+(1C3)	20.2'	20.0'
156. 1C2	23.2'	23.0'	217. 1A1+(1A1)	20.2'	20.0'
157. 1C3+(1C3)	23.2'	23.0'	218. 4C3	20.2'	20.0'
158. 2C3	23.2'	23.0'	219. 3C3+(1C3)	20.2'	20.0'
159. 1C3	23.2'	23.0'	220. 4A3+(2A3)	20.2'	20.0'
160. 4A1	23.2'	23.0'	221. 4A3	20.2'	20.0'
161. 3A1+(1A1)	23.2'	23.0'			
162. 3A1	23.2'	23.0'			
163. 2A1+(1A1)	23.2'	23.0'			
164. 2A1	23.2'	23.0'			

Note: (*) Wires 2S2 means the test wires consist of two steel wires S2 and no superimposed loads. The steel wires are continuous to the supports.

(**) Composite wire 1S2+(1C2) means the test wires consist of one steel wire S2 and one copper wire C2. The steel wire is continuous to the support. The copper wire is continuous but is cut near the support, and then is served as a superimposed load.

APPENDIX B: JUSTIFICATION OF EXCITEMENT MECHANISM

It will be shown that a single-span wire line under base motion is equivalent to a simply-supported system under uniform external load of a particular magnitude along the wire. In this Appendix, single and two degree-of-freedom (DOF) models would be first investigated. The results will be applied to a multiple DOF model by induction and then to a continuous system which is the particular case with infinite DOF.

(i) Single DOF:

Consider a simple spring-mass-dashpot model as shown in Fig. B-1 in which a mass m_1 free to move in the horizontal direction is excited by a simple harmonic base motion $z(t) = Z \cos(\Omega t)$. The spring constant with the unit of force/length is k_1 and the coefficient of viscous damping with the unit of force/length/time is c_1 . Then, by selecting $u_1(t)$ being the displacement of the mass in the horizontal direction, the equation of motion in terms of displacement relative to the base, i.e., $u_1(t) - z(t)$, or $w_1(t)$, is found to be [28]

$$m_1 \ddot{w}_1(t) + c_1 \dot{w}_1(t) + k_1 w_1 = m_1 \Omega^2 Z \cos(\Omega t) \quad (B1)$$

It could be verified [28] that Equation B1 is also the equation of motion of a simply-supported single DOF system under external load $m_1 \Omega^2 Z \cos(\Omega t)$ as shown in Fig. B-2. Note that the coordinate $w_1(t)$ there is the absolute displacement in the horizontal direction. Therefore, the system of the

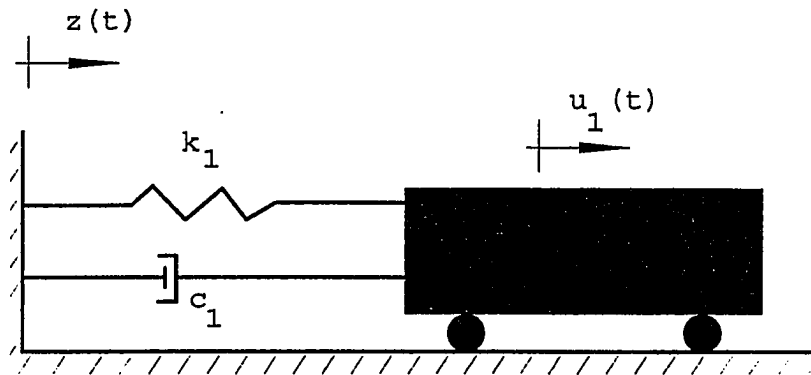


Fig. B-1: A simple spring-mass-dashpot system under base motion $z(t) = Z \cos(\Omega t)$.

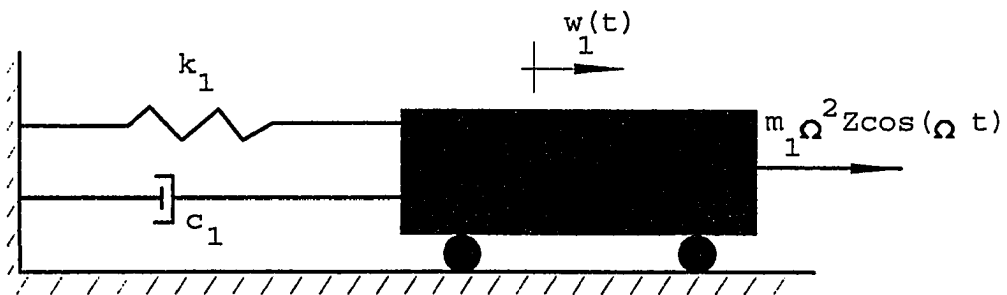


Fig. B-2: A simple spring-mass-dashpot system under external load $m_1 \Omega^2 Z \cos(\Omega t)$.

relative motion in Fig. B-1 is equivalent to that of the absolute motion in Fig. B-2.

(ii) Two DOF:

Consider now a two DOF model as shown in Fig. B-3 which is under a simple harmonic base motion $\mathbf{z}(t) = Z \cos(\Omega t)$. The masses, spring constants, coefficient of viscous damping, and displacement coordinates, respectively, are also shown in that figure. Then the equations of motion in terms of displacement relative to the base are found to be [28]

$$\begin{bmatrix} m_1 & 0 \\ 0 & m_2 \end{bmatrix} \begin{Bmatrix} \ddot{w}_1 \\ \ddot{w}_2 \end{Bmatrix} + \begin{bmatrix} c_1 + c_2 & -c_2 \\ -c_2 & c_2 \end{bmatrix} \begin{Bmatrix} \dot{w}_1 \\ \dot{w}_2 \end{Bmatrix} + \begin{bmatrix} k_1 + k_2 & -k_2 \\ -k_2 & k_2 \end{bmatrix} \begin{Bmatrix} w_1 \\ w_2 \end{Bmatrix} = \begin{Bmatrix} m_1 \Omega^2 Z \cos(\Omega t) \\ m_2 \Omega^2 Z \cos(\Omega t) \end{Bmatrix} \quad (B2)$$

, where $w_1(t) = u_1(t) - z(t)$ and $w_2(t) = u_2(t) - z(t)$, are the relative displacements of masses m_1 and m_2 with respect to the base, respectively. It could be verified [28] that Equation B2 are also the equations of motion of a simply-supported two DOF system under external loads $m_1 \Omega^2 Z \cos(\Omega t)$ and $m_2 \Omega^2 Z \cos(\Omega t)$ on the masses m_1 and m_2 , respectively, as shown in Fig. B-4. Note that the coordinates $w_1(t)$ and $w_2(t)$ there are the absolute displacements of the masses m_1 and m_2 , respectively, in the horizontal direction. Therefore, the system of the relative motion in Fig. B-3 is equivalent to that of the absolute motion in Fig. B-4.

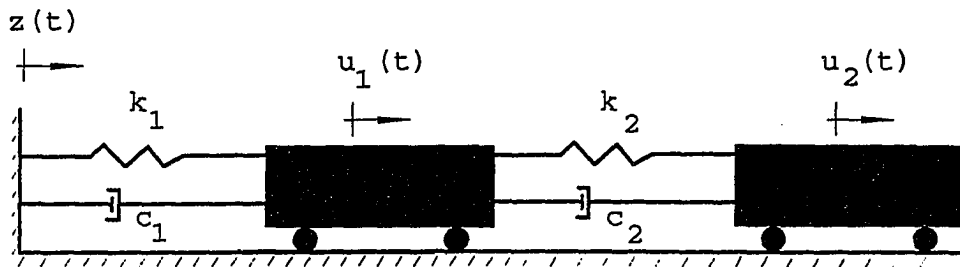


Fig. B-3: A two degree-of-freedom model under base motion $z(t) = Z \cos(\Omega t)$.

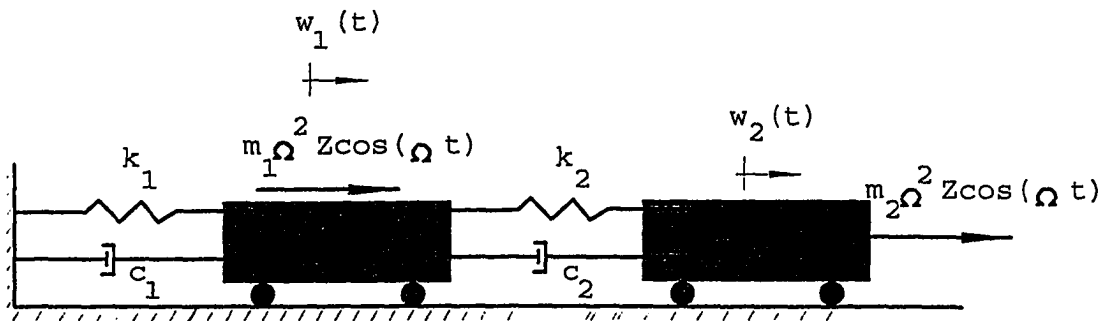


Fig. B-4: A two degree-of-freedom model under external loads $m_1 \Omega^2 Z \cos(\Omega t)$ and $m_2 \Omega^2 Z \cos(\Omega t)$ on masses m_1 and m_2 , respectively.

(iii) Multiple DOF:

By induction, the relative motion of an n DOF model under base motion $z(t) = Z \cos(\Omega t)$ as shown in Fig. B-5 is equivalent to the absolute motion of a simply-supported system under external load on the respective masses as shown in Fig. B-6. Similarly, since the vertical motion of the n DOF system in Fig. B-7 in which the masses formed in a shape of a catenary is essentially the same as that in Fig. B-5, the system of the relative motion in Fig. B-7 is equivalent to that of the absolute motion in Fig. B-8.

(iv) Continuous system:

As

- (1) in Fig. B-7, $m_1 = m_t / (2n)$, $m_2 = \dots = m_n = m_t / n$, where m_t is the total mass of the left half of wire in Fig. B-9, and
- (2) $n \rightarrow \infty$,

the system in Fig. B-7 is basically the same as the continuous system of a wire under base motion $z(t) = Z \cos(\Omega t)$ as shown in Fig. B-9. Also the system corresponding to the one in Fig. B-8 as $n \rightarrow \infty$ will be a simply-supported wire under uniform load $m \Omega^2 Z \cos(\Omega t)$, where m is the mass per unit length of the wire, as shown in Fig. B-10. Consequently, the relative motion of a wire under base motion $z(t) = Z \cos(\Omega t)$ as shown in Fig. B-9 is equivalent to the absolute motion of a simply-supported wire under uniform load $m \Omega^2 Z \cos(\Omega t)$ as shown in Fig. B-10.

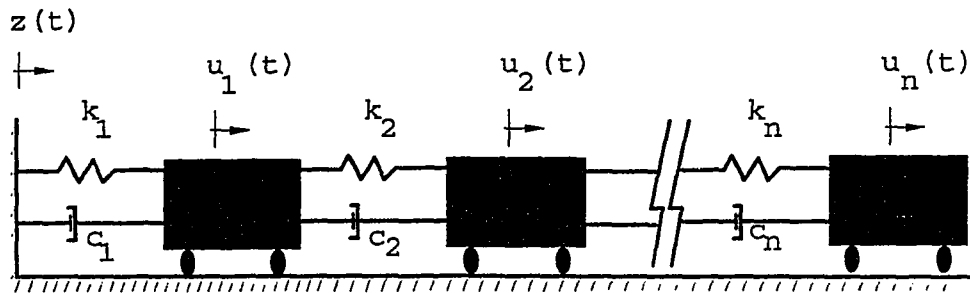


Fig. B-5: An n degree-of-freedom model under base motion $z(t) = Z \cos(\Omega t)$.

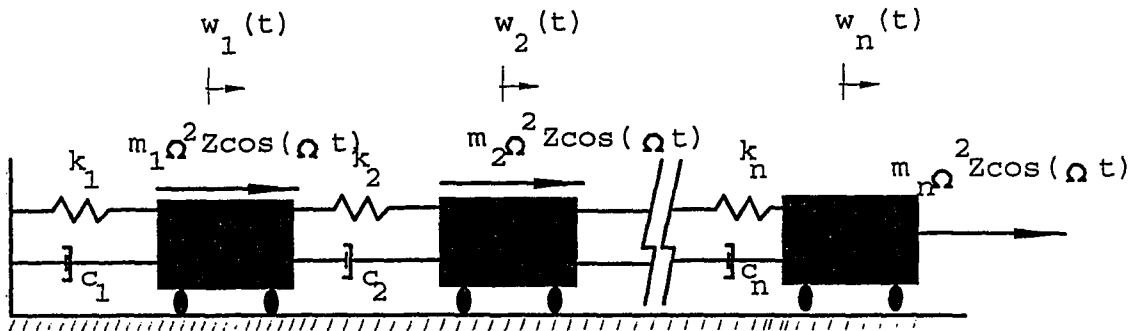


Fig. B-6: An n degree-of-freedom model under external loads $m_1 \Omega^2 Z \cos(\Omega t)$, $m_2 \Omega^2 Z \cos(\Omega t)$, ..., and $m_n \Omega^2 Z \cos(\Omega t)$ on masses m_1 , m_2 , ..., and m_n , respectively.

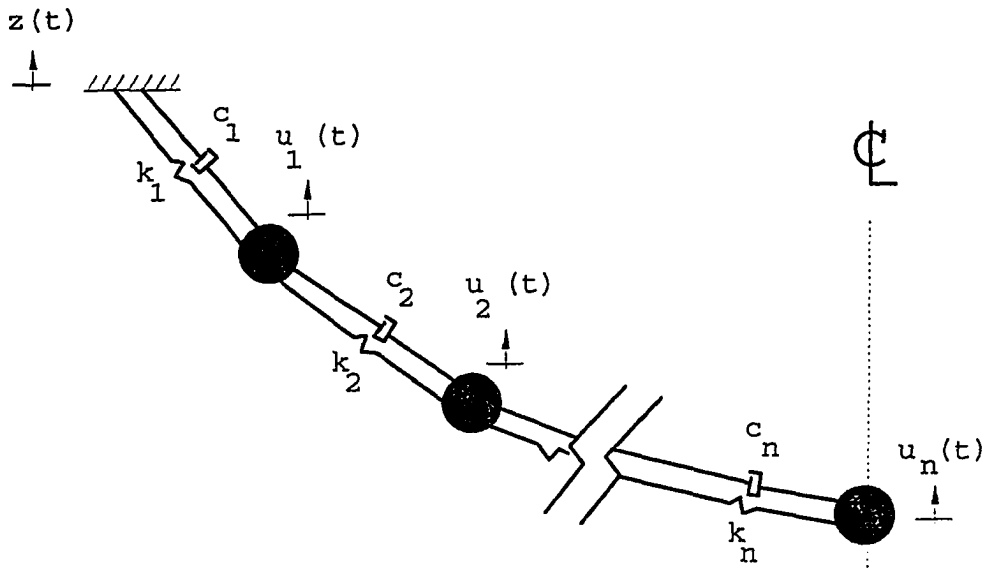


Fig. B-7: An n degree-of-freedom model formed in a catenary shape is under base motion $z(t) = Z\cos(\Omega t)$.

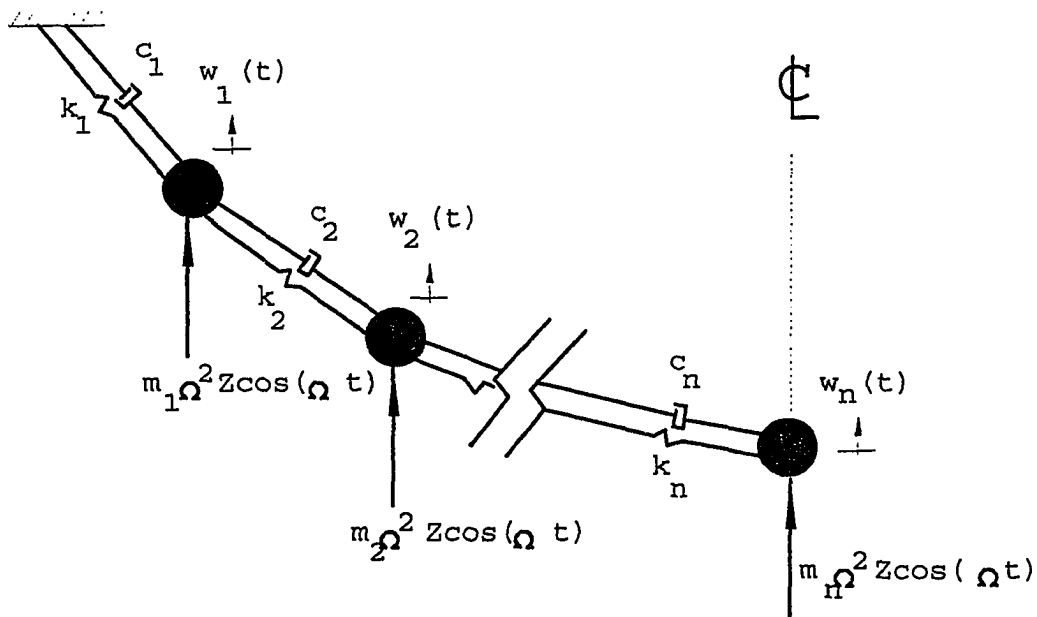


Fig. B-8: An n degree-of-freedom model formed in a catenary shape is under external loads $m_1\Omega^2 Z\cos(\Omega t)$, $m_2\Omega^2 Z\cos(\Omega t)$, ..., and $m_n\Omega^2 Z\cos(\Omega t)$.

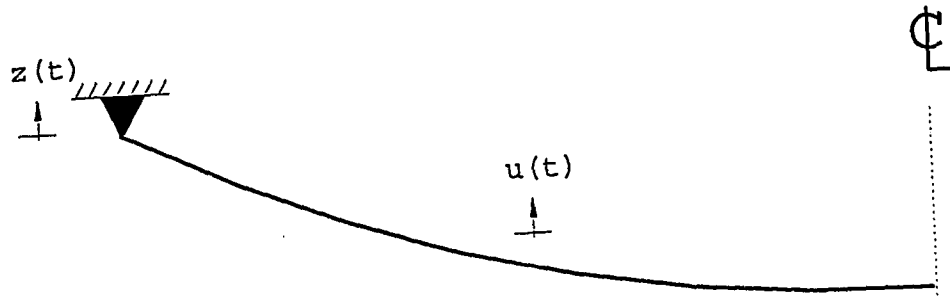


Fig. B-9: A single-span wire under base motion $z(t) = Z \cos(\Omega t)$.

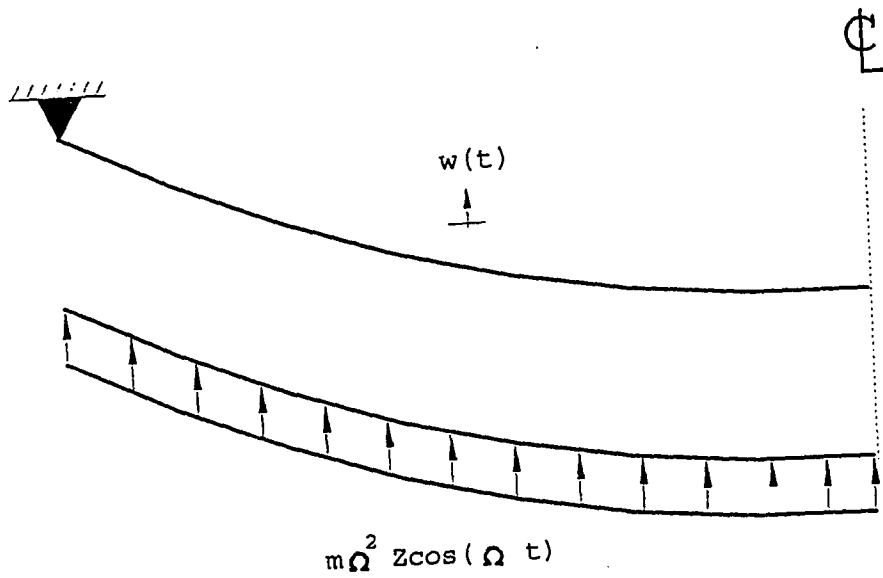


Fig. B-10: A simply-supported single-span wire under uniform load $m\Omega^2 Z \cos(\Omega t)$.

APPENDIX C: SCALES OF THE PARAMETERS OF THE SIMILARITY PAIRS

The 17 pairs of wires along with their unit mass scale n_m , area scale n_A , modulus of elasticity scale n_E , wire length scales n_l , and span length scale n_s are listed below. The 17 pairs of wires satisfy the similarity requirements in Equation 3-5.

Pair #	Prototype	Model	n_m	n_A	n_E	n_l	n_s
1	4A2+(2A2)	1A2+(2A2)	2	4	1	2	2
2	4A2	1A2+(1A2)	2	4	1	2	2
3	4A2+(2A3)	1A2+(1A2+1A3)	2	4	1	2	2
4	4A3+(2A3)	1A3+(2A3)	2	4	1	2	2
5	4A3	1A3+(1A3)	2	4	1	2	2
6	4A2+(2A3)	1A2+(1A2+1A3)	2	4	1	2	2
7	4A2	1A2+(1A2)	2	4	1	2	2
8	4A2+(2A2)	1A2+(2A2)	2	4	1	2	2
9	4A3+(2A3)	1A3+(2A3)	2	4	1	2	2
10	4A3	1A3+(1A3)	2	4	1	2	2
11	4A2+(2A2)	1A2+(2A2)	2	4	1	2	2
12	4A2	1A2+(1A2)	2	4	1	2	2
13	4A2+(2A3)	1A2+(1A2+1A3)	2	4	1	2	2
14	4A3+(2A3)	1A3+(2A3)	2	4	1	2	2
15	4A3	1A3+(1A3)	2	4	1	2	2
16	4C3	1C3+(1C3)	2	4	1	2	2
17	4A1	1A1+(1A1)	2	4	1	2	2

APPENDIX D: STATISTICAL METHOD

In this appendix, several commonly used statistical methods will be briefly introduced as follows:

D.1 Estimation about the Population Mean, μ

With n measurements y_1, y_2, \dots, y_n , the $100(1-\alpha)\%$ confidence interval of μ , the unknown population mean, is [24]

$$\bar{y} \pm t_{\frac{\alpha}{2}, n-1} SE \quad (D-1)$$

$$\text{, where } \bar{y} \text{ is the sample mean, i.e. } \bar{y} = (\sum y_i) / n \quad (D-1a)$$

, SE is the sample standard error of the mean, i.e.,

$$SE = \left[\frac{\sum y_i^2 - \frac{(\sum y_i)^2}{n}}{n(n-1)} \right]^{1/2} \quad (D-1b)$$

, and $t_{\alpha/2, n-1}$ is the value beyond which the area under the t -distribution curve equals $\alpha/2$ for $n-1$ degrees of freedom (DOFs).

D.2 Mean and Standard Error of the Combination of Measurements

It may happen that the physical quantity of interest is not measured directly, but is a function of two or more different measurements made in an experiment. For instance, in order to compute the modulus of elasticity of a wire, the diameter of the wire, the tensile load, as well as the corresponding strain should be first measured. The modulus of elasticity is then obtained under a series of division and multiplication of those three separated measurements.

Suppose there were n measurements x_1, x_2, \dots, x_n of \mathbf{x} and m measurements Y_1, Y_2, \dots, Y_m of \mathbf{y} . The means and standard errors of \mathbf{x} and \mathbf{y} , denoted as

\bar{x} and SE_x for x , and \bar{y} and SE_y for y , respectively,

can be obtained from Equation D-1a and Equation D-1b. Then for $z = \alpha x^a y^b \dots$, where α, a, b, \dots are constants, the mean and standard error of z are found to be [29]

$$\bar{z} = \alpha \bar{x}^a \bar{y}^b \dots$$

$$\text{and } SE_z = \left\{ \frac{a^2}{\bar{x}^2} SE_x^2 + \frac{b^2}{\bar{y}^2} SE_y^2 + \dots \right\}^{1/2} \bar{z} \quad (D-2)$$

, respectively. On the other hand, if $z = a + bx + cy + \dots$, where a, b, c, \dots are constants, the mean and standard error of z will be [29]

$$\bar{z} = a + b\bar{x} + c\bar{y} \dots$$

$$\text{and } SE_z = \left\{ (bSE_x)^2 + (cSE_y)^2 + \dots \right\}^{1/2} \bar{z}, \text{ respectively.} \quad (D-3)$$

In either of the above two cases, the $100(1-\alpha)\%$ confidence interval for the mean of z is

$$\bar{z} \pm t_{\frac{\alpha}{2}, n+m-2} SE_z$$

, where $t_{\alpha/2, n+m-2}$ has the same meaning as that in Equation D-1 except for $(n+m-2)$ DOFs.

D.3 Inference Related to Linear Regression

Suppose there were n measurements x_1, x_2, \dots, x_n of \mathbf{x} and the same amounts of measurements Y_1, Y_2, \dots, Y_n of \mathbf{y} . Also the relation of the two quantities \mathbf{x} and \mathbf{y} is linear, denoted as

$y = \beta_0 + \beta_1 x$. Then the $100(1-\alpha)\%$ confidence interval for the slope, β_1 , in linear regression is [24]

$$\bar{\beta}_1 \pm t_{\frac{\alpha}{2}, n-2} SE_{\bar{\beta}_1}$$

, where $\bar{\beta}_1 = \frac{S_{xy}}{S_{xx}}$

$$SE_{\bar{\beta}_1} = \sqrt{\frac{SSE}{(n-2)S_{xx}}}$$

$$SSE = S_{yy} - \bar{\beta}_1 S_{xy}$$

$$S_{xy} = \Sigma xy - \frac{\Sigma x \Sigma y}{n}$$

$$S_{xx} = \Sigma x^2 - \frac{(\Sigma x)^2}{n}$$

$$S_{yy} = \Sigma y^2 - \frac{(\Sigma y)^2}{n}$$

(D-4)

and $t_{\alpha/2, n-2}$ has the same meaning as that in Equation D-1 except for $(n-2)$ DOFs.

D.4 Best Estimate of the Results of the Combined Experiment

Suppose $\bar{x}_1 \pm SE_1, \bar{x}_2 \pm SE_2, \dots, \text{ and } \bar{x}_n \pm SE_n$

were the results from n experiments, respectively, where the same parameter x was measured and the materials of the same qualities were used in each of the experiments. Also assume the numbers of measurements were $m_1, m_2, \dots, \text{ and } m_n$, respectively. Then the best combined estimate of x will be [29]

$$\bar{x} \pm SE_x$$

$$, \text{ where } \bar{x} = \frac{\bar{X}_1 + \bar{X}_2 + \dots + \bar{X}_n}{n}$$

$$\text{ and } SE_x = \sqrt{\frac{\sum (SE_i)^2}{n}} \quad (D-5)$$

Therefore, the $100(1-\alpha)\%$ confidence interval for the mean of x is

$$\bar{x} \pm t_{\frac{\alpha}{2}, m_1 + m_2 + \dots + m_n - n} SE_x \quad (D-6)$$

, where $t_{\alpha/2, m_1 + m_2 + \dots + m_n - n}$ has the same meaning as that in Equation D-1 except for $(m_1 + m_2 + \dots + m_n - n)$ DOFs.

D.5 Significant figure

As far as the numbers of decimals to be used in the statistical results are concerned, Truman L. Kelley [30] suggested that the mean and standard error should be rounded to the places indicated by one third of the standard error. As an illustration, suppose the result of a series of measurements were calculated as $64.342159 \dots \pm 0.634432 \dots$, where $0.634432 \dots$ is the standard error. Then Kelley's rule would say that the number should be recorded to the first place after decimal point, i.e., 64.3 ± 0.6 . This is because one-third of standard error, or $0.634432/3$, is 0.211477 where the first non-zero number, i.e. 2, is at the first place after decimal point.

When a physical quantity is the combination of several different measurements as described in Section D.2, the

significant figure will only be considered at the step in which that quantity is obtained. For instance, if there are n measurements a_1, a_2, \dots, a_n and D , the quantity of interest, is obtained by

$$D = B^2 \pm BC$$

, where

$$B = \frac{\sum a_i}{n} \quad \text{and} \quad C = \left[\frac{\sum a_i^2 - \frac{(\sum a_i)^2}{n}}{n-1} \right]^{1/2},$$

then the quantities B and C can keep as many numbers of decimal places as one likes and when the quantity D is found, Kelley's rule will be used to determine its precision of numbers to be displayed. This is because, if C is calculated as $0.634432\dots$, to use $C=0.63$ is equivalent to use $C=0.630000\dots$. Therefore, it is not convincing to say $0.630000\dots$ is better than $0.634432\dots$ which is obtained from statistical formula, to represent the value of C . However, if D is calculated as $64.342159\dots \pm 0.634432\dots$, it would be recorded as 64.3 ± 0.6 when Kelley's rule is applied. This does not mean that 64.3 or $64.300000\dots$ is better than $64.342159\dots$ for the mean of D . Rather, it means that, with a particular percentage of confidence from statistical point of view, 64.3 is accurate up to the first place after decimal point for the true mean of the variable D . The digits after the first decimal point are inaccurate due to the limitation in the accuracy of the measuring instrument.

APPENDIX E: SPRING CONSTANT OF THE LOAD CELL LC1

In this appendix, the detailed calculations for the mean and standard error of the spring constant of load cell LC1 will be performed. Those for the load cells LC2 and LC3 can be obtained in the same manner.

Referring to Table 3-2, the values of the parameters listed in Equation D-4 for load cell LC1 can be found as follows:

n	=60
$\Sigma x = 0+42+\dots+1375$	$=37967*10^{-5}$
$\Sigma y = 0+783+\dots+25443$	=699508
$\Sigma x^2 = 0^2+42^2+\dots+1375^2$	$=36210499*10^{-10}$
$\Sigma y^2 = 0^2+783^2+\dots+25443^2$	=12307648272
$\Sigma xy = 0*0+42*783+\dots+1375*25443$	$=667578644*10^{-5}$
$S_{xy} = 667578644*10^{-5} - 37967*10^{-5}*699508/60 = 224941640*10^{-5}$	
$S_{xx} = 36210499*10^{-10} - (37967*10^{-5})^2/60$	$= 12185614.18*10^{-10}$
$S_{yy} = 12307648272 - 699508^2/60$	=4152457570

Then the mean and standard error of the spring constant, respectively, are

$$\bar{k} = \frac{S_{xy}}{S_{xx}} = \frac{224941640*10^{-5}}{12185614.18*10^{-10}} = 18.460*10^5 \text{ gram/volt}$$

$$= 4069.7 \text{ lb/volt}$$

$$\text{and } SE_{\bar{k}} = \sqrt{\frac{SSE}{(n-2)S_{xx}}} = \sqrt{\frac{123460.0202}{(60-2)(12185614.18*10^{-10})}} = 0.013*10^5 \text{ gram/v}$$

$$= 2.9 \text{ lb/volt,}$$

$$\text{where } SSE = S_{yy} - \bar{k}S_{xy} = 4152457570 - 18.460*10^5*224941640*10^{-5}$$

$$= 123460.0202$$

APPENDIX F: MEASUREMENT ERROR

In this appendix, the detailed calculations of the measurement error for unit weight, cross-sectional area of the wire, wire length, modulus of elasticity of the wire, span length, frequency of excitation, magnitude of external load, amplitude, and support force will be presented. The calculations are based on the statistical methods introduced in Appendix D.

F.1 Unit weight, Cross-sectional area, and Wire Length

To find the measurement errors for the wire's unit weight, cross-sectional area, and length, nine typical wires, each from one of the nine groups of wires mentioned in Section 3.1.1.1, were selected. The lengths were measured by the Stanley tape measurer in the same manner as that discussed in Section 3.2.2. The first of the nine wires was measured five times by pulling and releasing the wire at the right end while holding the other end unmoved under the weight. Because of no differences among the measured results, only one value was recorded. Similarly, the lengths of the other eight wires were measured. On the other hand, the Ohaus' top-loading electronic scale of model Galaxy 4000D as shown in Fig. F-1 was used to measure the weight. The scale could measure up to the accuracy of 0.00002 lb. Again, one measurement for each wire was made since there were no differences among multiple measurements. The results are listed in Table F-1.

Table F-1

Measured lengths and weights for the nine typical wires.

Wire Type	Measured Length ($\pm 1/16''$ or $\pm 0.005'$)	Measured Weight (± 0.00002 lb)
S1	23'5-4/8" or 23.458'	0.59924
S2	29'6" or 29.500'	0.43932
S3	20'0" or 20.000'	0.20348
C1	18'6" or 18.500'	0.57626
C2	19'10-7/8" or 19.906'	0.38330
C3	26'6-7/8" or 26.573'	0.32818
A1	20'0" or 20.000'	0.20888
A2	26'1-6/8" or 26.146'	0.15963
A3	21'7" or 21.583'	0.07561

Next, ten segments of 1 to 2 inches in length were cut from each wire. To ensure the inclusion of possible non-uniformity of the material, those wires were cut randomly along the lengths as shown in Fig. F-2. Then all segments were weighed once by the Ohaus' top-loading electronic scale and their diameters were measured twenty times in which the Mitutoyo's micrometer as shown in Fig. F-3 was used for the first ten measurements while the others were performed by Vernier scale as shown in Fig. F-4. Note that even though the former could measure the diameter more accurately, i.e., up to 0.0001 inch vs. 0.001 inch, the errors during the measurement from the former might lead to the results not so accurate as those obtained from the latter. The measurement errors resulted from inconsistent instrument usage relating to the contact pressure when clamping the wire as shown in Fig. F-3. Therefore, it was decided to consider all measurements from both instruments. Finally, the length for each segment of the wires was measured ten times by Vernier scale. The results are listed in Table F-

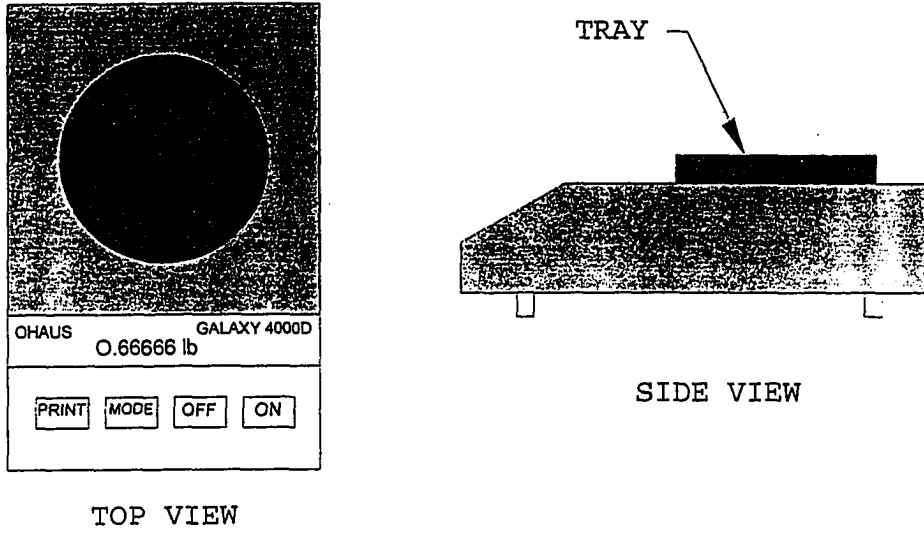


Fig. F-1: Ohaus' top-loading electronic scale used to measure the weight.

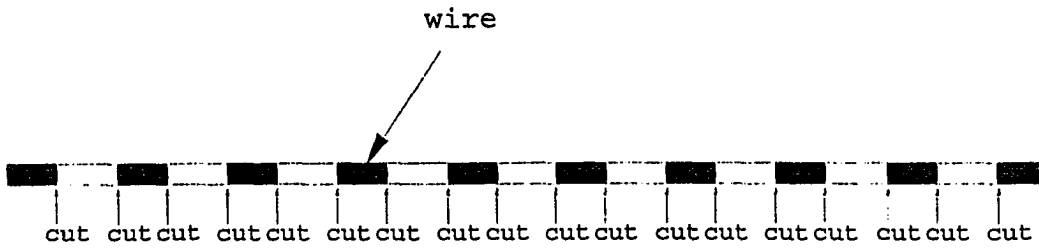


Fig. F-2: Ten segments ranging from 1 to 2 inches in length were cut from each of the nine wires.

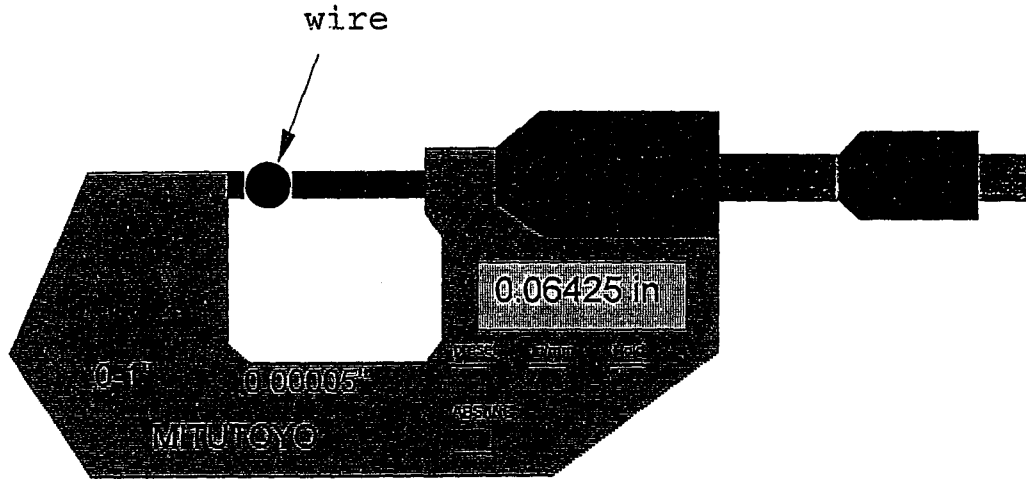


Fig. F-3: Mitutoyo's micrometer used to measure the diameter.

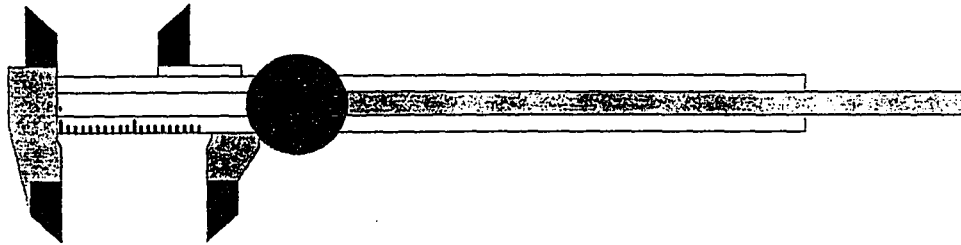


Fig. F-4: Vernier scale used to measure the length and diameter.

2.

Table F-2

Measured weights, diameters, and lengths of the ten segments of wires S1, S2, S3, C1, C2, C3, A1, A2, and A3.

Wire S1:

WEIGHT(lb)										
	SEG.1	SEG.2	SEG.3	SEG.4	SEG.5	SEG.6	SEG.7	SEG.8	SEG.9	SEG.10
	0.00314	0.00288	0.00336	0.00310	0.00306	0.00322	0.00308	0.00328	0.00342	0.00322
DIAMETER(in)										
MEA.NO	SEG.1	SEG.2	SEG.3	SEG.4	SEG.5	SEG.6	SEG.7	SEG.8	SEG.9	SEG.10
1	0.09775	0.09785	0.09795	0.09815	0.09740	0.09790	0.09785	0.09795	0.09805	0.09820
2	0.09780	0.09820	0.09710	0.09765	0.09875	0.09785	0.09810	0.09820	0.09785	0.09750
3	0.09810	0.09805	0.09740	0.09750	0.09835	0.09750	0.09805	0.09800	0.09780	0.09760
4	0.09755	0.09800	0.09785	0.09795	0.09725	0.09805	0.09810	0.09765	0.09825	0.09795
5	0.09810	0.09795	0.09810	0.09820	0.09765	0.09770	0.09805	0.09740	0.09820	0.09740
6	0.09755	0.09765	0.09765	0.09770	0.09840	0.09780	0.09785	0.09770	0.09805	0.09830
7	0.09775	0.09830	0.09815	0.09765	0.09835	0.09745	0.09750	0.09770	0.09790	0.09765
8	0.09820	0.09775	0.09805	0.09805	0.09750	0.09820	0.09820	0.09775	0.09820	0.09765
9	0.09770	0.09780	0.09765	0.09790	0.09770	0.09785	0.09730	0.09785	0.09805	0.09835
10	0.09815	0.09840	0.09810	0.09795	0.09770	0.09810	0.09840	0.09805	0.09815	0.09750
11	0.0981	0.0985	0.0991	0.0985	0.0983	0.0988	0.0990	0.0982	0.0988	0.0988
12	0.0981	0.0979	0.0989	0.0989	0.0981	0.0992	0.0987	0.0981	0.0989	0.0992
13	0.0985	0.0979	0.0988	0.0982	0.0973	0.0982	0.0989	0.0987	0.0987	0.0984
14	0.0980	0.0996	0.0984	0.0989	0.0987	0.0988	0.0983	0.0978	0.0979	0.0988
15	0.0978	0.0989	0.0988	0.0972	0.0992	0.0982	0.0988	0.0980	0.0982	0.0990
16	0.0993	0.0984	0.0979	0.0985	0.0988	0.0983	0.0989	0.0981	0.0983	0.0988
17	0.0978	0.0990	0.0996	0.0975	0.0992	0.0980	0.0976	0.0985	0.0986	0.0990
18	0.0988	0.0980	0.0979	0.0987	0.0995	0.0978	0.0985	0.0983	0.0992	0.0990
19	0.0978	0.0989	0.0982	0.0984	0.0985	0.0988	0.0982	0.0980	0.0988	0.0988
20	0.0985	0.0982	0.0982	0.0984	0.0991	0.0993	0.0981	0.0991	0.0987	0.0982
LENGTH(in)										
MEA.NO	SEG.1	SEG.2	SEG.3	SEG.4	SEG.5	SEG.6	SEG.7	SEG.8	SEG.9	SEG.10
1	1.4772	1.3549	1.5887	1.4562	1.4415	1.5090	1.4554	1.5411	1.5978	1.5071
2	1.4791	1.3551	1.5881	1.4562	1.4422	1.5098	1.4548	1.5401	1.5999	1.5052
3	1.4795	1.3547	1.5865	1.4562	1.4412	1.5089	1.4546	1.5413	1.6018	1.5078
4	1.4797	1.3559	1.5885	1.4532	1.4422	1.5090	1.4548	1.5449	1.5988	1.5050
5	1.4798	1.3552	1.5876	1.4558	1.4415	1.5098	1.4548	1.5441	1.6012	1.5070
6	1.4791	1.3559	1.5874	1.4542	1.4418	1.5102	1.4552	1.5462	1.6009	1.5061
7	1.4765	1.3555	1.5885	1.4562	1.4419	1.5108	1.4549	1.5437	1.6005	1.5079
8	1.4800	1.3552	1.5879	1.4568	1.4428	1.5102	1.4553	1.5402	1.6020	1.5067
9	1.4800	1.3562	1.5887	1.4539	1.4422	1.5102	1.4552	1.5412	1.6008	1.5080
10	1.4768	1.3572	1.5885	1.4542	1.4420	1.5095	1.4551	1.5402	1.5991	1.5088

Wire S2:

WEIGHT(lb)										
	SEG.1	SEG.2	SEG.3	SEG.4	SEG.5	SEG.6	SEG.7	SEG.8	SEG.9	SEG.10
	0.00198	0.00184	0.00186	0.00180	0.00172	0.00194	0.00192	0.00208	0.00174	0.00202
DIAMETER(in)										
MEA.NO	SEG.1	SEG.2	SEG.3	SEG.4	SEG.5	SEG.6	SEG.7	SEG.8	SEG.9	SEG.10
1	0.07475	0.07460	0.07475	0.07470	0.07450	0.07430	0.07510	0.07455	0.07465	0.07495
2	0.07475	0.07450	0.07480	0.07430	0.07490	0.07440	0.07515	0.07485	0.07475	0.07490
3	0.07465	0.07450	0.07445	0.07435	0.07495	0.07470	0.07485	0.07470	0.07465	0.07490
4	0.07480	0.07455	0.07455	0.07410	0.07500	0.07470	0.07525	0.07485	0.07455	0.07475
5	0.07475	0.07445	0.07470	0.07435	0.07505	0.07445	0.07510	0.07495	0.07470	0.07510
6	0.07470	0.07485	0.07470	0.07460	0.07505	0.07425	0.07505	0.07505	0.07455	0.07455
7	0.07470	0.07440	0.07450	0.07435	0.07475	0.07435	0.07495	0.07485	0.07470	0.07485
8	0.07495	0.07450	0.07445	0.07450	0.07490	0.07420	0.07505	0.07490	0.07465	0.07480
9	0.07475	0.07460	0.07470	0.07450	0.07480	0.07445	0.07510	0.07475	0.07450	0.07495
10	0.07465	0.07465	0.07460	0.07450	0.07505	0.07430	0.07505	0.07490	0.07470	0.07490
11	0.0755	0.0758	0.0756	0.0750	0.0755	0.0752	0.0757	0.0754	0.0751	0.0757
12	0.0765	0.0751	0.0753	0.0750	0.0755	0.0749	0.0758	0.0753	0.0752	0.0751
13	0.0750	0.0753	0.0750	0.0751	0.0757	0.0750	0.0753	0.0751	0.0751	0.0755
14	0.0754	0.0752	0.0752	0.0750	0.0758	0.0750	0.0760	0.0754	0.0752	0.0749
15	0.0752	0.0753	0.0753	0.0749	0.0758	0.0753	0.0752	0.0755	0.0756	0.0759
16	0.0759	0.0754	0.0756	0.0749	0.0760	0.0750	0.0754	0.0755	0.0758	0.0753
17	0.0758	0.0757	0.0755	0.0750	0.0756	0.0750	0.0758	0.0750	0.0752	0.0755
18	0.0750	0.0754	0.0756	0.0750	0.0757	0.0748	0.0751	0.0752	0.0753	0.0757
19	0.0755	0.0757	0.0754	0.0749	0.0761	0.0748	0.0761	0.0752	0.0754	0.0752
20	0.0753	0.0755	0.0755	0.0750	0.0750	0.0749	0.0757	0.0750	0.0750	0.0755
LENGTH(in)										
MEA.NO	SEG.1	SEG.2	SEG.3	SEG.4	SEG.5	SEG.6	SEG.7	SEG.8	SEG.9	SEG.10
1	1.5995	1.4841	1.5089	1.4679	1.3810	1.5799	1.5311	1.6709	1.4062	1.6121
2	1.5997	1.4836	1.5078	1.4658	1.3810	1.5791	1.5313	1.6719	1.4049	1.6119
3	1.5989	1.4841	1.5070	1.4649	1.3812	1.5792	1.5303	1.6719	1.4050	1.6121
4	1.5995	1.4838	1.5071	1.4676	1.3813	1.5798	1.5300	1.6715	1.4045	1.6120
5	1.5987	1.4836	1.5080	1.4665	1.3804	1.5791	1.5313	1.6725	1.4048	1.6111
6	1.5997	1.4830	1.5068	1.4679	1.3820	1.5788	1.5310	1.6720	1.4031	1.6118
7	1.5995	1.4830	1.5067	1.4676	1.3800	1.5782	1.5308	1.6714	1.4030	1.6125
8	1.5993	1.4840	1.5059	1.4675	1.3800	1.5778	1.5307	1.6711	1.4049	1.6122
9	1.5998	1.4838	1.5058	1.4680	1.3813	1.5780	1.5300	1.6720	1.4045	1.6128
10	1.5999	1.4831	1.5072	1.4673	1.3796	1.5779	1.5308	1.6729	1.4041	1.6119

Wire S3:

WEIGHT(lb)										
	SEG.1	SEG.2	SEG.3	SEG.4	SEG.5	SEG.6	SEG.7	SEG.8	SEG.9	SEG.10
	0.00130	0.00128	0.00136	0.00124	0.00118	0.00116	0.00124	0.00128	0.00130	0.00126
DIAMETER(in)										
MEA.NO	SEG.1	SEG.2	SEG.3	SEG.4	SEG.5	SEG.6	SEG.7	SEG.8	SEG.9	SEG.10
1	0.06160	0.06145	0.06165	0.06135	0.06125	0.06170	0.06155	0.06190	0.06165	0.06135
2	0.06155	0.06145	0.06140	0.06160	0.06140	0.06160	0.06140	0.06145	0.06145	0.06155
3	0.06130	0.06140	0.06170	0.06135	0.06150	0.06120	0.06155	0.06160	0.06175	0.06160
4	0.06160	0.06145	0.06130	0.06170	0.06120	0.06140	0.06160	0.06135	0.06145	0.06150
5	0.06135	0.06155	0.06150	0.06170	0.06145	0.06105	0.06135	0.06175	0.06195	0.06135
6	0.06185	0.06155	0.06180	0.06140	0.06130	0.06120	0.06145	0.06175	0.06150	0.06155
7	0.06160	0.06165	0.06155	0.06160	0.06160	0.06120	0.06150	0.06165	0.06155	0.06170
8	0.06140	0.06150	0.06155	0.06140	0.06145	0.06170	0.06160	0.06165	0.06165	0.06190
9	0.06135	0.06165	0.06160	0.06180	0.06155	0.06165	0.06185	0.06175	0.06135	0.06140
10	0.06160	0.06160	0.06140	0.06155	0.06125	0.06130	0.06155	0.06170	0.06185	0.06160
11	0.0619	0.0624	0.0613	0.0617	0.0613	0.0619	0.0618	0.0623	0.0619	0.0612
12	0.0612	0.0626	0.0617	0.0633	0.0609	0.0609	0.0608	0.0615	0.0613	0.0617
13	0.0619	0.0624	0.0615	0.0618	0.0621	0.0621	0.0612	0.0616	0.0618	0.0617
14	0.0625	0.0619	0.0617	0.0617	0.0617	0.0613	0.0607	0.0608	0.0614	0.0619
15	0.0629	0.0618	0.0616	0.0621	0.0601	0.0612	0.0616	0.0618	0.0615	0.0617
16	0.0614	0.0615	0.0613	0.0619	0.0608	0.0616	0.0613	0.0621	0.0617	0.0614
17	0.0613	0.0613	0.0616	0.0612	0.0613	0.0616	0.0612	0.0619	0.0616	0.0611
18	0.0612	0.0609	0.0615	0.0619	0.0617	0.0613	0.0615	0.0617	0.0612	0.0616
19	0.0613	0.0613	0.0615	0.0612	0.0613	0.0614	0.0615	0.0617	0.0619	0.0614
20	0.0613	0.0614	0.0613	0.0615	0.0610	0.0616	0.0613	0.0615	0.0615	0.0619
LENGTH(in)										
MEA.NO	SEG.1	SEG.2	SEG.3	SEG.4	SEG.5	SEG.6	SEG.7	SEG.8	SEG.9	SEG.10
1	1.5396	1.5277	1.6268	1.4781	1.4109	1.3939	1.4684	1.5240	1.5375	1.5019
2	1.5381	1.5278	1.6272	1.4765	1.4096	1.3934	1.4675	1.5239	1.5371	1.5037
3	1.5400	1.5263	1.6274	1.4782	1.4097	1.3940	1.4681	1.5239	1.5375	1.5039
4	1.5369	1.5264	1.6263	1.4779	1.4114	1.3931	1.4689	1.5241	1.5369	1.5018
5	1.5374	1.5260	1.6264	1.4769	1.4119	1.3932	1.4673	1.5240	1.5370	1.5032
6	1.5392	1.5282	1.6260	1.4770	1.4118	1.3939	1.4680	1.5229	1.5365	1.5032
7	1.5400	1.5261	1.6281	1.4774	1.4112	1.3919	1.4682	1.5240	1.5370	1.5009
8	1.5382	1.5263	1.6279	1.4788	1.4096	1.3929	1.4691	1.5229	1.5360	1.5019
9	1.5382	1.5263	1.6271	1.4778	1.4117	1.3920	1.4669	1.5237	1.5358	1.5019
10	1.5373	1.5282	1.6269	1.4782	1.4099	1.3913	1.4681	1.5241	1.5361	1.5035

Wire C1:

WEIGHT(lb)										
	SEG.1	SEG.2	SEG.3	SEG.4	SEG.5	SEG.6	SEG.7	SEG.8	SEG.9	SEG.10
	0.00376	0.00424	0.00388	0.00414	0.00378	0.00398	0.00410	0.00394	0.00416	0.00396
DIAMETER(in)										
MEA.NO	SEG.1	SEG.2	SEG.3	SEG.4	SEG.5	SEG.6	SEG.7	SEG.8	SEG.9	SEG.10
1	0.10110	0.10100	0.10085	0.10145	0.10140	0.10095	0.10120	0.10180	0.10095	0.10185
2	0.10155	0.10160	0.10110	0.10135	0.10210	0.10150	0.10140	0.10100	0.10160	0.10165
3	0.10125	0.10105	0.10125	0.10120	0.10150	0.10115	0.10085	0.10180	0.10105	0.10145
4	0.10120	0.10100	0.10115	0.10145	0.10120	0.10140	0.10160	0.10095	0.10130	0.10095
5	0.10120	0.10115	0.10150	0.10155	0.10150	0.10095	0.10150	0.10170	0.10080	0.10120
6	0.10120	0.10135	0.10100	0.10125	0.10175	0.10175	0.10155	0.10110	0.10095	0.10120
7	0.10120	0.10150	0.10125	0.10125	0.10170	0.10095	0.10135	0.10155	0.10100	0.10100
8	0.10100	0.10120	0.10130	0.10135	0.10095	0.10135	0.10110	0.10135	0.10175	0.10175
9	0.10155	0.10105	0.10155	0.10120	0.10110	0.10120	0.10150	0.10110	0.10135	0.10115
10	0.10120	0.10115	0.10105	0.10095	0.10135	0.10135	0.10135	0.10155	0.10095	0.10170
11	0.1016	0.1019	0.1028	0.1033	0.1032	0.1020	0.1022	0.1035	0.1028	0.1015
12	0.1030	0.1019	0.1018	0.1021	0.1019	0.1025	0.1022	0.1028	0.1018	0.1032
13	0.1021	0.1022	0.1022	0.1019	0.1011	0.1018	0.1019	0.1023	0.1022	0.1032
14	0.1021	0.1019	0.1015	0.1021	0.1027	0.1028	0.1019	0.1018	0.1029	0.1028
15	0.1032	0.1019	0.1026	0.1022	0.1022	0.1022	0.1022	0.1023	0.1015	0.1030
16	0.1022	0.1019	0.1019	0.1025	0.1018	0.1018	0.1026	0.1017	0.1017	0.1030
17	0.1022	0.1021	0.1031	0.1022	0.1029	0.1034	0.1031	0.1026	0.1015	0.1031
18	0.1016	0.1019	0.1015	0.1015	0.1017	0.1019	0.1015	0.1012	0.1019	0.1019
19	0.1016	0.1018	0.1019	0.1013	0.1022	0.1022	0.1019	0.1022	0.1013	0.1019
20	0.1020	0.1019	0.1015	0.1030	0.1023	0.1029	0.1032	0.1030	0.1031	0.1031
LENGTH(in)										
MEA.NO	SEG.1	SEG.2	SEG.3	SEG.4	SEG.5	SEG.6	SEG.7	SEG.8	SEG.9	SEG.10
1	1.4650	1.6487	1.5178	1.6106	1.4768	1.5489	1.5918	1.5260	1.6225	1.5460
2	1.4654	1.6485	1.5149	1.6098	1.4755	1.5472	1.5927	1.5250	1.6222	1.5458
3	1.4649	1.6482	1.5150	1.6117	1.4755	1.5482	1.5919	1.5251	1.6229	1.5452
4	1.4649	1.6473	1.5158	1.6119	1.4747	1.5493	1.5909	1.5239	1.6207	1.5480
5	1.4659	1.6481	1.5167	1.6109	1.4750	1.5461	1.5938	1.5262	1.6231	1.5467
6	1.4658	1.6469	1.5149	1.6113	1.4748	1.5479	1.5921	1.5263	1.6229	1.5481
7	1.4643	1.6485	1.5155	1.6111	1.4748	1.5469	1.5921	1.5259	1.6220	1.5475
8	1.4658	1.6482	1.5155	1.6111	1.4748	1.5475	1.5929	1.5238	1.6209	1.5459
9	1.4650	1.6467	1.5139	1.6110	1.4751	1.5468	1.5929	1.5251	1.6210	1.5459
10	1.4641	1.6469	1.5154	1.6109	1.4761	1.5479	1.5922	1.5242	1.6205	1.5468

Wire C2:

WEIGHT(lb)										
	SEG.1	SEG.2	SEG.3	SEG.4	SEG.5	SEG.6	SEG.7	SEG.8	SEG.9	SEG.10
	0.00254	0.00242	0.00264	0.00238	0.00240	0.00278	0.00240	0.00264	0.00254	0.00236
DIAMETER(in)										
MEA.NO	SEG.1	SEG.2	SEG.3	SEG.4	SEG.5	SEG.6	SEG.7	SEG.8	SEG.9	SEG.10
1	0.07930	0.08015	0.07970	0.07970	0.08000	0.08035	0.08040	0.07955	0.07940	0.08035
2	0.07950	0.07950	0.08005	0.07955	0.07980	0.08055	0.07975	0.07985	0.07970	0.07985
3	0.07925	0.07990	0.07970	0.07980	0.07990	0.08055	0.07970	0.08030	0.07930	0.07995
4	0.07950	0.07965	0.07980	0.07940	0.07960	0.08035	0.07935	0.08025	0.07965	0.07920
5	0.07925	0.08005	0.07970	0.07970	0.07945	0.08020	0.07970	0.08005	0.07940	0.08010
6	0.07915	0.07970	0.07995	0.08010	0.07995	0.08025	0.08020	0.07995	0.07925	0.08010
7	0.07990	0.08015	0.07975	0.08000	0.07990	0.08005	0.07965	0.08020	0.07950	0.07975
8	0.07995	0.07945	0.07970	0.07975	0.07980	0.08010	0.07950	0.08040	0.07970	0.07970
9	0.07950	0.07970	0.07970	0.07960	0.07990	0.08030	0.07970	0.08035	0.07955	0.07965
10	0.07935	0.08000	0.07985	0.07990	0.07965	0.07990	0.08010	0.08070	0.07950	0.08005
11	0.0812	0.0810	0.0818	0.0806	0.0808	0.0812	0.0804	0.0798	0.0803	0.0804
12	0.0809	0.0818	0.0805	0.0810	0.0802	0.0810	0.0801	0.0799	0.0800	0.0802
13	0.0817	0.0803	0.0805	0.0817	0.0809	0.0813	0.0806	0.0798	0.0799	0.0806
14	0.0810	0.0811	0.0805	0.0809	0.0801	0.0805	0.0800	0.0812	0.0801	0.0801
15	0.0800	0.0804	0.0806	0.0803	0.0806	0.0805	0.0805	0.0811	0.0800	0.0803
16	0.0800	0.0803	0.0797	0.0808	0.0804	0.0805	0.0806	0.0817	0.0800	0.0805
17	0.0802	0.0805	0.0806	0.0800	0.0805	0.0807	0.0802	0.0800	0.0800	0.0802
18	0.0799	0.0800	0.0802	0.0802	0.0798	0.0805	0.0805	0.0804	0.0801	0.0800
19	0.0799	0.0803	0.0802	0.0810	0.0803	0.0805	0.0808	0.0798	0.0799	0.0802
20	0.0802	0.0802	0.0807	0.0809	0.0802	0.0810	0.0808	0.0805	0.0802	0.0808
LENGTH(in)										
MEA.NO	SEG.1	SEG.2	SEG.3	SEG.4	SEG.5	SEG.6	SEG.7	SEG.8	SEG.9	SEG.10
1	1.5999	1.5151	1.6503	1.5004	1.4984	1.7362	1.5182	1.6633	1.6091	1.4823
2	1.5991	1.5170	1.6497	1.5009	1.4973	1.7348	1.5169	1.6608	1.6112	1.4822
3	1.5988	1.5158	1.6498	1.5009	1.4972	1.7356	1.5169	1.6602	1.6111	1.4830
4	1.5999	1.5158	1.6499	1.4997	1.4978	1.7355	1.5180	1.6602	1.6089	1.4829
5	1.6000	1.5172	1.6502	1.4996	1.4969	1.7359	1.5185	1.6629	1.6096	1.4825
6	1.6005	1.5160	1.6503	1.4997	1.4971	1.7363	1.5169	1.6631	1.6095	1.4825
7	1.6009	1.5168	1.6496	1.4998	1.4974	1.7363	1.5165	1.6619	1.6077	1.4811
8	1.6011	1.5159	1.6491	1.5001	1.4982	1.7367	1.5177	1.6628	1.6077	1.4837
9	1.6004	1.5168	1.6509	1.5002	1.4992	1.7356	1.5173	1.6624	1.6065	1.4830
10	1.5999	1.5152	1.6502	1.5003	1.4976	1.7359	1.5173	1.6623	1.6094	1.4812

Wire C3:

WEIGHT(lb)										
	SEG.1	SEG.2	SEG.3	SEG.4	SEG.5	SEG.6	SEG.7	SEG.8	SEG.9	SEG.10
	0.00166	0.00158	0.00150	0.00156	0.00154	0.00164	0.00146	0.00158	0.00164	0.00156
DIAMETER(in)										
MEA.NO	SEG.1	SEG.2	SEG.3	SEG.4	SEG.5	SEG.6	SEG.7	SEG.8	SEG.9	SEG.10
1	0.06390	0.06385	0.06360	0.06405	0.06375	0.06360	0.06410	0.06425	0.06365	0.06350
2	0.06410	0.06345	0.06345	0.06375	0.06350	0.06375	0.06420	0.06405	0.06375	0.06375
3	0.06405	0.06280	0.06385	0.06395	0.06365	0.06360	0.06410	0.06445	0.06390	0.06415
4	0.06400	0.06325	0.06380	0.06375	0.06400	0.06395	0.06415	0.06435	0.06385	0.06420
5	0.06390	0.06320	0.06375	0.06420	0.06395	0.06380	0.06400	0.06390	0.06365	0.06405
6	0.06375	0.06385	0.06335	0.06400	0.06395	0.06400	0.06405	0.06435	0.06390	0.06385
7	0.06370	0.06365	0.06345	0.06420	0.06370	0.06395	0.06435	0.06405	0.06395	0.06410
8	0.06365	0.06335	0.06350	0.06415	0.06375	0.06365	0.06390	0.06390	0.06370	0.06415
9	0.06385	0.06395	0.06390	0.06390	0.06380	0.06395	0.06390	0.06415	0.06400	0.06375
10	0.06405	0.06395	0.06375	0.06375	0.06365	0.06395	0.06395	0.06405	0.06410	0.06400
11	0.0639	0.0639	0.0649	0.0639	0.0639	0.0641	0.0638	0.0650	0.0640	0.0640
12	0.0640	0.0638	0.0639	0.0641	0.0638	0.0640	0.0645	0.0645	0.0639	0.0635
13	0.0635	0.0631	0.0639	0.0640	0.0640	0.0638	0.0642	0.0641	0.0628	0.0640
14	0.0641	0.0632	0.0635	0.0628	0.0638	0.0634	0.0638	0.0644	0.0620	0.0635
15	0.0631	0.0632	0.0649	0.0639	0.0638	0.0641	0.0639	0.0643	0.0640	0.0640
16	0.0646	0.0631	0.0641	0.0630	0.0638	0.0640	0.0642	0.0648	0.0640	0.0638
17	0.0639	0.0638	0.0633	0.0639	0.0639	0.0642	0.0642	0.0635	0.0640	0.0643
18	0.0645	0.0639	0.0633	0.0640	0.0641	0.0641	0.0644	0.0641	0.0641	0.0640
19	0.0639	0.0635	0.0639	0.0630	0.0639	0.0643	0.0642	0.0635	0.0641	0.0633
20	0.0638	0.0638	0.0650	0.0632	0.0636	0.0638	0.0638	0.0642	0.0639	0.0638
LENGTH(in)										
MEA.NO	SEG.1	SEG.2	SEG.3	SEG.4	SEG.5	SEG.6	SEG.7	SEG.8	SEG.9	SEG.10
1	1.6251	1.4699	1.5330	1.5001	1.5501	1.5909	1.4259	1.5368	1.5968	1.5126
2	1.6248	1.4680	1.5320	1.5001	1.5496	1.5925	1.4262	1.5359	1.5961	1.5119
3	1.6240	1.4679	1.5320	1.4992	1.5492	1.5937	1.4269	1.5349	1.5962	1.5111
4	1.6236	1.4672	1.5322	1.4989	1.5511	1.5919	1.4283	1.5358	1.5962	1.5116
5	1.6239	1.4681	1.5331	1.4991	1.5509	1.5910	1.4258	1.5363	1.5967	1.5110
6	1.6239	1.4698	1.5330	1.4989	1.5509	1.5918	1.4250	1.5366	1.5963	1.5120
7	1.6235	1.4681	1.5320	1.5001	1.5505	1.5913	1.4254	1.5352	1.5958	1.5111
8	1.6255	1.4674	1.5313	1.5001	1.5498	1.5916	1.4250	1.5369	1.5966	1.5121
9	1.6242	1.4683	1.5324	1.4988	1.5513	1.5917	1.4258	1.5357	1.5959	1.5119
10	1.6235	1.4689	1.5327	1.4988	1.5513	1.5909	1.4252	1.5358	1.5967	1.5119

Wire A1:

WEIGHT(lb)										
	SEG.1	SEG.2	SEG.3	SEG.4	SEG.5	SEG.6	SEG.7	SEG.8	SEG.9	SEG.10
	0.00136	0.00138	0.00142	0.00142	0.00144	0.00134	0.00138	0.00140	0.00146	0.00138
DIAMETER(in)										
MEA.NO	SEG.1	SEG.2	SEG.3	SEG.4	SEG.5	SEG.6	SEG.7	SEG.8	SEG.9	SEG.10
1	0.10690	0.10915	0.10830	0.10815	0.10650	0.10595	0.10650	0.10730	0.10875	0.10950
2	0.10675	0.10800	0.10840	0.10600	0.10735	0.10625	0.10805	0.10580	0.10920	0.10600
3	0.10875	0.10725	0.10920	0.10730	0.10490	0.10555	0.10855	0.10920	0.10765	0.10990
4	0.10635	0.10870	0.10655	0.10420	0.10735	0.10885	0.10735	0.10710	0.10885	0.10635
5	0.10730	0.10850	0.10760	0.10750	0.10690	0.10805	0.10705	0.10725	0.10815	0.10710
6	0.10710	0.10495	0.10910	0.10765	0.10765	0.10495	0.10845	0.10920	0.10665	0.10600
7	0.10780	0.10755	0.10645	0.10770	0.10845	0.10710	0.10765	0.10675	0.10860	0.10875
8	0.10860	0.10850	0.10690	0.10860	0.10560	0.10700	0.10560	0.10635	0.10720	0.10795
9	0.10660	0.10545	0.10765	0.10810	0.10730	0.10785	0.10690	0.10820	0.10815	0.10780
10	0.10770	0.10855	0.10765	0.10825	0.10785	0.10715	0.10725	0.10670	0.10715	0.10820
11	0.1085	0.1042	0.1079	0.1089	0.1082	0.1057	0.1072	0.1059	0.1082	0.1050
12	0.1089	0.1072	0.1080	0.1051	0.1091	0.1078	0.1092	0.1090	0.1075	0.1091
13	0.1085	0.1061	0.1055	0.1040	0.1091	0.1080	0.1085	0.1075	0.1085	0.1059
14	0.1089	0.1053	0.1075	0.1089	0.1080	0.1079	0.1069	0.1089	0.1071	0.1085
15	0.1081	0.1070	0.1089	0.1081	0.1095	0.1089	0.1082	0.1090	0.1077	0.1079
16	0.1090	0.1089	0.1080	0.1090	0.1081	0.1098	0.1091	0.1091	0.1070	0.1063
17	0.1050	0.1065	0.1075	0.1085	0.1092	0.1082	0.1085	0.1085	0.1082	0.1082
18	0.1087	0.1087	0.1072	0.1051	0.1072	0.1078	0.1069	0.1061	0.1091	0.1085
19	0.1075	0.1061	0.1060	0.1081	0.1082	0.1083	0.1085	0.1082	0.1081	0.1077
20	0.1070	0.1079	0.1090	0.1072	0.1075	0.1082	0.1090	0.1062	0.1091	0.1076
LENGTH(in)										
MEA.NO	SEG.1	SEG.2	SEG.3	SEG.4	SEG.5	SEG.6	SEG.7	SEG.8	SEG.9	SEG.10
1	1.5666	1.5900	1.6372	1.6210	1.6614	1.5431	1.5901	1.6180	1.6752	1.5844
2	1.5662	1.5898	1.6378	1.6202	1.6607	1.5433	1.5908	1.6179	1.6749	1.5856
3	1.5659	1.5899	1.6371	1.6205	1.6585	1.5439	1.5919	1.6190	1.6757	1.5860
4	1.5658	1.5896	1.6370	1.6201	1.6581	1.5437	1.5908	1.6171	1.6760	1.5865
5	1.5661	1.5887	1.6382	1.6215	1.6590	1.5432	1.5906	1.6179	1.6750	1.5855
6	1.5663	1.5894	1.6372	1.6212	1.6589	1.5440	1.5907	1.6172	1.6744	1.5861
7	1.5684	1.5887	1.6382	1.6209	1.6585	1.5434	1.5913	1.6181	1.6761	1.5860
8	1.5669	1.5887	1.6382	1.6211	1.6610	1.5430	1.5906	1.6191	1.6741	1.5852
9	1.5685	1.5889	1.6362	1.6209	1.6581	1.5435	1.5914	1.6174	1.6750	1.5854
10	1.5664	1.5881	1.6362	1.6205	1.6578	1.5428	1.5903	1.6181	1.6742	1.5848

Wire A2:

WEIGHT(lb)										
	SEG.1	SEG.2	SEG.3	SEG.4	SEG.5	SEG.6	SEG.7	SEG.8	SEG.9	SEG.10
	0.00084	0.00080	0.00074	0.00076	0.00078	0.00080	0.00080	0.00078	0.00080	0.00078
DIAMETER(in)										
MEA.NO	SEG.1	SEG.2	SEG.3	SEG.4	SEG.5	SEG.6	SEG.7	SEG.8	SEG.9	SEG.10
1	0.08140	0.08175	0.08265	0.08250	0.08220	0.08190	0.08120	0.08120	0.08115	0.08250
2	0.08175	0.08300	0.08270	0.08270	0.08255	0.08145	0.08170	0.08250	0.08135	0.08105
3	0.08220	0.08130	0.08225	0.08225	0.08290	0.08155	0.08215	0.08160	0.08270	0.08195
4	0.08210	0.08120	0.08250	0.08225	0.08120	0.08170	0.08100	0.08265	0.08265	0.08175
5	0.08150	0.08145	0.08225	0.08190	0.08265	0.08125	0.08145	0.08170	0.08265	0.08185
6	0.08270	0.08215	0.08220	0.08220	0.08080	0.08085	0.08225	0.08130	0.08115	0.08215
7	0.08300	0.08240	0.08295	0.08235	0.08190	0.08170	0.08225	0.08245	0.08230	0.08200
8	0.08250	0.08270	0.08195	0.08135	0.08140	0.08135	0.08120	0.08155	0.08280	0.08165
9	0.08155	0.08220	0.08175	0.08165	0.08285	0.08205	0.08230	0.08195	0.08165	0.08175
10	0.08135	0.08195	0.08135	0.08165	0.08250	0.08120	0.08220	0.08155	0.08145	0.08175
11	0.0827	0.0822	0.0829	0.0811	0.0818	0.0819	0.0822	0.0828	0.0822	0.0822
12	0.0831	0.0830	0.0811	0.0829	0.0829	0.0821	0.0819	0.0830	0.0827	0.0825
13	0.0816	0.0823	0.0827	0.0824	0.0808	0.0825	0.0829	0.0833	0.0831	0.0821
14	0.0821	0.0819	0.0820	0.0831	0.0808	0.0820	0.0810	0.0819	0.0817	0.0830
15	0.0812	0.0821	0.0821	0.0831	0.0805	0.0819	0.0831	0.0829	0.0829	0.0828
16	0.0819	0.0821	0.0822	0.0825	0.0812	0.0827	0.0827	0.0822	0.0821	0.0809
17	0.0816	0.0820	0.0819	0.0820	0.0812	0.0830	0.0822	0.0816	0.0815	0.0826
18	0.0811	0.0825	0.0821	0.0831	0.0811	0.0805	0.0825	0.0827	0.0823	0.0830
19	0.0819	0.0830	0.0831	0.0821	0.0811	0.0813	0.0827	0.0822	0.0825	0.0817
20	0.0822	0.0819	0.0829	0.0811	0.0820	0.0809	0.0818	0.0826	0.0825	0.0829
LENGTH(in)										
MEA.NO	SEG.1	SEG.2	SEG.3	SEG.4	SEG.5	SEG.6	SEG.7	SEG.8	SEG.9	SEG.10
1	1.6922	1.6151	1.4548	1.5287	1.5348	1.5962	1.5859	1.5502	1.6089	1.5831
2	1.6912	1.6147	1.4552	1.5261	1.5348	1.5959	1.5856	1.5501	1.6092	1.5831
3	1.6915	1.6129	1.4551	1.5281	1.5343	1.5969	1.5849	1.5504	1.6095	1.5819
4	1.6918	1.6158	1.4549	1.5273	1.5330	1.5951	1.5849	1.5502	1.6091	1.5801
5	1.6903	1.6148	1.4551	1.5288	1.5352	1.5955	1.5848	1.5495	1.6095	1.5822
6	1.6897	1.6150	1.4545	1.5290	1.5352	1.5949	1.5829	1.5496	1.6091	1.5830
7	1.6897	1.6161	1.4545	1.5289	1.5343	1.5960	1.5839	1.5495	1.6096	1.5835
8	1.6919	1.6142	1.4558	1.5288	1.5355	1.5931	1.5828	1.5496	1.6089	1.5812
9	1.6912	1.6133	1.4545	1.5268	1.5351	1.5934	1.5821	1.5496	1.6096	1.5826
10	1.6911	1.6150	1.4548	1.5273	1.5339	1.5943	1.5829	1.5496	1.6094	1.5821

Wire A3:

WEIGHT(lb)										
	SEG.1	SEG.2	SEG.3	SEG.4	SEG.5	SEG.6	SEG.7	SEG.8	SEG.9	SEG.10
	0.00074	0.00086	0.00076	0.00074	0.00080	0.00074	0.00086	0.00078	0.00066	0.00078
DIAMETER(inch)										
MEA.NO	SEG.1	SEG.2	SEG.3	SEG.4	SEG.5	SEG.6	SEG.7	SEG.8	SEG.9	SEG.10
1	0.06290	0.06250	0.06305	0.06265	0.06280	0.06250	0.06275	0.06305	0.06275	0.06260
2	0.06275	0.06210	0.06265	0.06220	0.06255	0.06225	0.06260	0.06210	0.06210	0.06270
3	0.06115	0.06250	0.06210	0.06265	0.06270	0.06210	0.06175	0.06230	0.06250	0.06275
4	0.06235	0.06225	0.06255	0.06250	0.06265	0.06200	0.06200	0.06215	0.06285	0.06240
5	0.06375	0.06285	0.06265	0.06245	0.06260	0.06210	0.06195	0.06230	0.06275	0.06210
6	0.06355	0.06230	0.06175	0.06235	0.06230	0.06130	0.06155	0.06230	0.06275	0.06265
7	0.06165	0.06210	0.06225	0.06245	0.06230	0.06220	0.06185	0.06200	0.06230	0.06265
8	0.06265	0.06265	0.06150	0.06200	0.06235	0.06230	0.06255	0.06240	0.06255	0.06285
9	0.06295	0.06175	0.06130	0.06205	0.06250	0.06240	0.06255	0.06255	0.06250	0.06295
10	0.06265	0.06255	0.06175	0.06175	0.06235	0.06200	0.06250	0.06250	0.06225	0.06280
11	0.0607	0.0636	0.0636	0.0629	0.0625	0.0612	0.0622	0.0637	0.0639	0.0627
12	0.0616	0.0632	0.0639	0.0635	0.0614	0.0634	0.0615	0.0617	0.0624	0.0639
13	0.0601	0.0639	0.0621	0.0631	0.0628	0.0631	0.0635	0.0630	0.0621	0.0635
14	0.0621	0.0634	0.0632	0.0638	0.0634	0.0624	0.0641	0.0635	0.0641	0.0624
15	0.0605	0.0622	0.0636	0.0622	0.0627	0.0607	0.0641	0.0635	0.0635	0.0611
16	0.0602	0.0615	0.0632	0.0617	0.0632	0.0606	0.0645	0.0632	0.0632	0.0621
17	0.0609	0.0622	0.0630	0.0639	0.0635	0.0625	0.0625	0.0621	0.0634	0.0609
18	0.0619	0.0628	0.0630	0.0629	0.0620	0.0631	0.0631	0.0623	0.0623	0.0631
19	0.0630	0.0632	0.0631	0.0634	0.0639	0.0635	0.0629	0.0616	0.0613	0.0632
20	0.0620	0.0635	0.0629	0.0625	0.0626	0.0625	0.0635	0.0625	0.0636	0.0629
LENGTH(inch)										
MEA.NO	SEG.1	SEG.2	SEG.3	SEG.4	SEG.5	SEG.6	SEG.7	SEG.8	SEG.9	SEG.10
1	2.5235	2.9067	2.6268	2.5499	2.7210	2.5411	2.9518	2.7076	2.2865	2.6623
2	2.5250	2.9090	2.6261	2.5482	2.7209	2.5413	2.9513	2.7072	2.2882	2.6609
3	2.5250	2.9075	2.6232	2.5482	2.7205	2.5419	2.9493	2.7059	2.2864	2.6604
4	2.5237	2.9071	2.6253	2.5492	2.7204	2.5418	2.9493	2.7051	2.2856	2.6605
5	2.5248	2.9089	2.6252	2.5495	2.7202	2.5412	2.9485	2.7059	2.2877	2.6615
6	2.5240	2.9075	2.6265	2.5482	2.7205	2.5408	2.9513	2.7075	2.2872	2.6621
7	2.5230	2.9069	2.6250	2.5488	2.7202	2.5408	2.9511	2.7051	2.2869	2.6608
8	2.5233	2.9043	2.6265	2.5492	2.7202	2.5409	2.9501	2.7052	2.2870	2.6615
9	2.5235	2.9050	2.6251	2.5491	2.7200	2.5412	2.9510	2.7066	2.2875	2.6619
10	2.5231	2.9058	2.6257	2.5480	2.7201	2.5409	2.9515	2.7061	2.2881	2.6615

F.1.1 Unit Weight

The unit weight and the corresponding maximum percentage measurement error of the nine wires can be obtained by applying Equation D-1 and Equation D-2 in Appendix D. For instance, from Equation D-1 and the first block of Table F-2, the mean and standard error of length 1 for the first segment of steel wire S1 are

$$\bar{l} = \frac{1.4772 + \dots + 1.4768}{10} = 1.4788 \text{ in}$$

$$\text{and } SE_l = \sqrt{\frac{(1.4772^2 + \dots + 1.4768^2) - \frac{(1.4772 + \dots + 1.4768)^2}{10}}{10(10-1)}} = 0.0004 \text{ in}^2$$

, respectively. Then, from Equation D-2, the corresponding mean and standard error for the unit weight γ which is defined as the weight w divided by the length l , become

$$\bar{\gamma} = \frac{w}{l} = \frac{0.00314}{1.4788} = 0.0021233 \text{ lb/in}$$

$$\text{and } SE_{\gamma} = \left\{ \left(\frac{-1}{l} SE_l \right)^2 \right\}^{1/2} \bar{\gamma} = \frac{1}{l} SE_l \bar{\gamma}$$

$$= \frac{0.0004 \times 0.0021233}{1.4788} = 0.0000006 \text{ lb/in, respectively.}$$

The means and standard errors of the unit weights for the other segments of steel wire S1 can be obtained in the same manner. The results are listed in the fourth columns of Table F-3.

The unit weights for the ten segments of steel wire S1 can be combined, according to Equation D-5, to give the best estimate. For instance, from Equation D-5 and the fourth column Table F-3, the best estimate for the mean and standard error of the unit weight for steel wire S1 are

$$\bar{\gamma} = \frac{0.0021233 + \dots + 0.0021367}{10} = 0.0021266 \text{ lb/in}$$

$$\text{and } SE_{\gamma} = \sqrt{\frac{0.0000006^2 + \dots + 0.0000005^2}{10}} = 0.0000005 \text{ lb/in}$$

, respectively. The degrees of freedom (DOFs) in this case are $9+9+\dots+9$, or 90, and the corresponding $t_{2.5\%,90}$ is 1.99. Then,

from Equation D-6, the 95% confidence interval for the mean of the unit weight of steel wire S1 becomes

$$\bar{Y} \pm t_{2.5\%, 90} SE_Y = 0.0021266 \pm 1.99 * 0.0000005 = 0.0021266 \pm 0.0000010 \text{ lb/in}$$

Note that the numbers of significant figures shown above are determined by Kelley's one-third rule as discussed in Section D.5 of Appendix D.

Define the maximum percentage measurement error as the maximum possible error divided by the corresponding mean in terms of percentage. Then the maximum percentage error in the measurement of the unit weight of steel wire S1 is

$$0.0000010 / 0.0021266 = 0.05\%$$

Table F-3

The 95% confidence interval for the best estimates of the unit weights and the corresponding maximum percentage measurement errors (MPME) of the nine wires.

Wire	Segment	Length (in)	Unit weight (lb/in)		Best estimate of unit weight (lb/in)		
			Mean ± SE	DOF	Mean ± $t_{\alpha/2, 90}$ SE	DOF	MPME
S1	1	1.4788±0.0004	0.0021233±0.0000006	9	0.0021266±0.0000010	90	0.05%
	2	1.3556±0.0002	0.0021245±0.0000003	9			
	3	1.5880±0.0002	0.0021158±0.0000002	9			
	4	1.4553±0.0004	0.0021301±0.0000005	9			
	5	1.4419±0.0001	0.0021221±0.0000002	9			
	6	1.5097±0.0002	0.0021328±0.0000002	9			
	7	1.4550±0.0001	0.0021168±0.0000001	9			
	8	1.5423±0.0007	0.0021266±0.0000009	9			
	9	1.6003±0.0004	0.0021371±0.0000005	9			
	10	1.5070±0.0004	0.0021367±0.0000005	9			
S2	1	1.5995±0.0001	0.0012379±0.0000000	9	0.0012404±0.0000004	90	0.03%
	2	1.4836±0.0001	0.0012402±0.0000001	9			
	3	1.5071±0.0003	0.0012341±0.0000002	9			
	4	1.4671±0.0003	0.0012269±0.0000002	9			
	5	1.3808±0.0002	0.0012456±0.0000002	9			
	6	1.5788±0.0002	0.0012287±0.0000001	9			
	7	1.5307±0.0002	0.0012543±0.0000001	9			
	8	1.6718±0.0002	0.0012441±0.0000001	9			
	9	1.4045±0.0003	0.0012388±0.0000002	9			
	10	1.6120±0.0001	0.0012530±0.0000001	9			

Wire	Segment	Length (in)	Unit weight (lb/in)		Best estimate of unit weight (lb/in)		
			Mean \pm SE	DOF	Mean \pm $t_{\alpha/2, DOF}$ SE	DOF	MPME
S3	1	1.5385 \pm 0.0004	0.0008449 \pm 0.0000001	9	0.0008397 \pm 0.0000003	90	0.03%
	2	1.5269 \pm 0.0003	0.0008382 \pm 0.0000001	9			
	3	1.6270 \pm 0.0002	0.0008358 \pm 0.0000001	9			
	4	1.4777 \pm 0.0002	0.0008391 \pm 0.0000001	9			
	5	1.4108 \pm 0.0003	0.0008364 \pm 0.0000001	9			
	6	1.3930 \pm 0.0003	0.0008327 \pm 0.0000001	9			
	7	1.4681 \pm 0.0002	0.0008446 \pm 0.0000001	9			
	8	1.5238 \pm 0.0001	0.0008400 \pm 0.0000000	9			
	9	1.5367 \pm 0.0002	0.0008459 \pm 0.0000001	9			
	10	1.5026 \pm 0.0003	0.0008385 \pm 0.0000001	9			
C1	1	1.4651 \pm 0.0002	0.0025663 \pm 0.0000003	9	0.0025687 \pm 0.0000009	90	0.03%
	2	1.6478 \pm 0.0002	0.0025731 \pm 0.0000003	9			
	3	1.5155 \pm 0.0003	0.0025601 \pm 0.0000005	9			
	4	1.6110 \pm 0.0002	0.0025697 \pm 0.0000002	9			
	5	1.4753 \pm 0.0002	0.0025621 \pm 0.0000003	9			
	6	1.5477 \pm 0.0003	0.0025716 \pm 0.0000005	9			
	7	1.5923 \pm 0.0002	0.0025748 \pm 0.0000004	9			
	8	1.5252 \pm 0.0003	0.0025833 \pm 0.0000005	9			
	9	1.6219 \pm 0.0003	0.0025649 \pm 0.0000005	9			
	10	1.5466 \pm 0.0003	0.0025604 \pm 0.0000005	9			
C2	1	1.6001 \pm 0.0002	0.0015874 \pm 0.0000002	9	0.0015915 \pm 0.0000005	90	0.03%
	2	1.5162 \pm 0.0002	0.0015961 \pm 0.0000002	9			
	3	1.6500 \pm 0.0002	0.0016000 \pm 0.0000001	9			
	4	1.5002 \pm 0.0002	0.0015864 \pm 0.0000001	9			
	5	1.4977 \pm 0.0002	0.0016024 \pm 0.0000002	9			
	6	1.7359 \pm 0.0002	0.0016014 \pm 0.0000001	9			
	7	1.5174 \pm 0.0002	0.0015816 \pm 0.0000002	9			
	8	1.6620 \pm 0.0004	0.0015884 \pm 0.0000003	9			
	9	1.6091 \pm 0.0005	0.0015785 \pm 0.0000004	9			
	10	1.4824 \pm 0.0003	0.0015919 \pm 0.0000002	9			
C3	1	1.6242 \pm 0.0002	0.0010220 \pm 0.0000001	9	0.0010250 \pm 0.0000003	90	0.03%
	2	1.5505 \pm 0.0002	0.0010190 \pm 0.0000001	9			
	3	1.4684 \pm 0.0003	0.0010215 \pm 0.0000002	9			
	4	1.5324 \pm 0.0002	0.0010180 \pm 0.0000001	9			
	5	1.4994 \pm 0.0002	0.0010270 \pm 0.0000001	9			
	6	1.5917 \pm 0.0003	0.0010303 \pm 0.0000001	9			
	7	1.4260 \pm 0.0003	0.0010238 \pm 0.0000002	9			
	8	1.5360 \pm 0.0002	0.0010286 \pm 0.0000001	9			
	9	1.5963 \pm 0.0001	0.0010273 \pm 0.0000000	9			
	10	1.5117 \pm 0.0002	0.0010319 \pm 0.0000001	9			
A1	1	1.5667 \pm 0.0003	0.0008680 \pm 0.0000001	9	0.0008691 \pm 0.0000003	90	0.03%
	2	1.5892 \pm 0.0002	0.0008683 \pm 0.0000001	9			
	3	1.6373 \pm 0.0002	0.0008672 \pm 0.0000001	9			
	4	1.6208 \pm 0.0001	0.0008761 \pm 0.0000000	9			
	5	1.6592 \pm 0.0004	0.0008678 \pm 0.0000002	9			
	6	1.5434 \pm 0.0001	0.0008682 \pm 0.0000000	9			
	7	1.5909 \pm 0.0002	0.0008674 \pm 0.0000000	9			
	8	1.6180 \pm 0.0002	0.0008652 \pm 0.0000001	9			
	9	1.6751 \pm 0.0002	0.0008716 \pm 0.0000001	9			
	10	1.5856 \pm 0.0002	0.0008703 \pm 0.0000001	9			
A2	1	1.6911 \pm 0.0003	0.0004967 \pm 0.0000000	9	0.0005006 \pm 0.0000002	90	0.04%
	2	1.6147 \pm 0.0003	0.0004954 \pm 0.0000000	9			
	3	1.4549 \pm 0.0001	0.0005086 \pm 0.0000000	9			
	4	1.5280 \pm 0.0003	0.0004973 \pm 0.0000001	9			
	5	1.5346 \pm 0.0002	0.0005082 \pm 0.0000000	9			
	6	1.5951 \pm 0.0004	0.0005015 \pm 0.0000001	9			
	7	1.5841 \pm 0.0004	0.0005050 \pm 0.0000001	9			
	8	1.5498 \pm 0.0001	0.0005032 \pm 0.0000000	9			
	9	1.6093 \pm 0.0001	0.0004971 \pm 0.0000000	9			
	10	1.5823 \pm 0.0003	0.0004929 \pm 0.0000001	9			

Wire	Segment	Length (in)	Unit weight (lb/in)		Best estimate of unit weight (lb/in)		
			Mean \pm SE	DOF	Mean \pm $t_{\alpha/2,90}$ SE	DOF	MPME
A3	1	2.5239 \pm 0.0002	0.0002931 \pm 0.0000000	9	0.0002915 \pm 0.0000001	90	0.02%
	2	2.9069 \pm 0.0005	0.0002958 \pm 0.0000000	9			
	3	2.6255 \pm 0.0003	0.0002894 \pm 0.0000000	9			
	4	2.5488 \pm 0.0002	0.0002903 \pm 0.0000000	9			
	5	2.7204 \pm 0.0001	0.0002940 \pm 0.0000000	9			
	6	2.5412 \pm 0.0001	0.0002912 \pm 0.0000000	9			
	7	2.9505 \pm 0.0004	0.0002914 \pm 0.0000000	9			
	8	2.7062 \pm 0.0003	0.0002882 \pm 0.0000000	9			
	9	2.2871 \pm 0.0003	0.0002885 \pm 0.0000000	9			
	10	2.6613 \pm 0.0002	0.0002930 \pm 0.0000000	9			
Average of maximum percentage measurement error							0.03%

In the same manner, the unit weights and the corresponding maximum percentage measurement errors for the rest of wires are obtained. The results are listed in the sixth and last columns of Table F-3.

Two phenomena are observed from the last column of Table F-3. They are: (i) the maximum percentage measurement errors are small, and (ii) those errors are close to one another. The first phenomenon is due to the fact that the unit weight is obtained by dividing the weight, which is a constant in this case, by the length. Therefore, the variances among the ten measurements of the length are narrowed down because of the division operation. The second phenomenon is consistent with the expectation since the nine wires are measured by the same person and by the same instrument. Consequently, those errors are expected to be close to one another.

Therefore, the average of the maximum percentage measurement error is

$$(0.05+0.03+\dots+0.02)/9=0.03\%$$

as listed in the last row of Table F-3.

F.1.2 Cross-sectional Area

The cross-sectional area and the corresponding maximum percentage measurement error of the nine wires can be obtained by applying Equation D-1 and Equation D-2 in Appendix D. For instance, from Equation D-1 and the first block of Table F-2, the mean and standard error of the diameter for the first segment of steel wire S1 are

$$\bar{d} = \frac{0.09775 + \dots + 0.0985}{20} = 0.0981 \text{ in}$$

$$\text{and } SE_d = \sqrt{\frac{(0.09775^2 + \dots + 0.0985^2) - \frac{(0.09775 + \dots + 0.0985)^2}{20}}{20(20-1)}} = 0.0001 \text{ in}^2, \text{ respectively.}$$

, respectively. Then, since $A = \pi d^2/4$, where d and A are, respectively, the diameter and the cross-sectional area of the wire, the corresponding mean and standard error of the cross-sectional area can be found from Equation D-2, i.e.

$$\text{mean } \bar{A} = \frac{\pi}{4} \bar{d}^2 = \frac{\pi}{4} (0.0981)^2 = 0.00755 \text{ in}^2$$

$$\text{standard error } SE_A = \left\{ \left(\frac{2}{\bar{d}} SE_d \right)^2 \right\}^{1/2} \bar{A} = \frac{2}{\bar{d}} SE_d \bar{A}$$

$$= \frac{2 \times 0.0001 \times 0.00755}{0.0981} = 0.00002 \text{ in}^2$$

In the same manner, the means and standard errors of the cross-sectional areas for the other segments of steel wire S1 can be obtained. The results are listed in the third and fourth columns of Table F-4. The DOFs in the fifth column are nineteen since twenty measurements are made for the cross-sectional area of each segment and one DOF is used when

calculating its mean.

The cross-sectional areas for the ten segments of steel wire S1 can be combined, according to Equation D-5, to give the best estimate. For instance, from Equation D-5 and the fourth column of Table F-4, the best estimate for the mean and standard error of the cross-sectional area steel wire S1 are

$$\bar{A} = \frac{0.00755 + \dots + 0.00759}{10} = 0.00757 \text{ in}^2$$

$$\text{and } SE_A = \sqrt{\frac{0.00002^2 + \dots + 0.00002^2}{10}} = 0.00002 \text{ in}^2$$

, respectively. The DOFs in this case are 19+19+...+19, or 190, and the corresponding $t_{2.5\%,190}$ is 1.96. Then, from Equation D-6, the 95% confidence interval for the mean of the cross-sectional area will be

$$\bar{A} \pm t_{2.5\%,190} SE_A = 0.00757 \pm 1.96 * 0.00002 = 0.00757 \pm 0.00004 \text{ in}^2$$

Therefore, the maximum percentage error in the measurement of the cross-sectional area measurement of steel wire S1 becomes

$$0.00004/0.00757 = 0.46\%.$$

In the same manner, the cross-sectional areas and the corresponding maximum percentage measurement errors for the other eight wires are obtained. The results are listed in the sixth and last columns of Table F-4.

Table F-4

The 95% confidence interval for the best estimates of the cross-sectional areas and the corresponding maximum percentage measurement errors (MPME) of the nine wires.

Wire	Segment	Diameter(in)	Cross-sectional area(in ²)		Best estimate of cross-sectional area (in ²)		
			Mean ± SE	DOF	Mean ± $t_{\alpha/2, 190}$ SE	DOF	MPME
S1	1	0.0981±0.0001	0.00755±0.00002	19	0.00757±0.00004	190	0.46%
	2	0.0983±0.0001	0.00758±0.00002	19			
	3	0.0982±0.0001	0.00757±0.00002	19			
	4	0.0981±0.0001	0.00756±0.00002	19			
	5	0.0983±0.0002	0.00759±0.00002	19			
	6	0.0982±0.0001	0.00757±0.00002	19			
	7	0.0982±0.0001	0.00758±0.00002	19			
	8	0.0981±0.0001	0.00755±0.00001	19			
	9	0.0983±0.0001	0.00759±0.00001	19			
	10	0.0983±0.0001	0.00759±0.00002	19			
S2	1	0.0751±0.0001	0.00443±0.00001	19	0.00442±0.00002	190	0.47%
	2	0.0750±0.0001	0.00442±0.00001	19			
	3	0.0750±0.0001	0.00442±0.00001	19			
	4	0.0747±0.0001	0.00438±0.00001	19			
	5	0.0753±0.0001	0.00445±0.00001	19			
	6	0.0747±0.0001	0.00438±0.00001	19			
	7	0.0753±0.0001	0.00446±0.00001	19			
	8	0.0750±0.0001	0.00442±0.00001	19			
	9	0.0750±0.0001	0.00441±0.00001	19			
	10	0.0751±0.0001	0.00444±0.00001	19			
S3	1	0.0616±0.0001	0.00298±0.00001	19	0.00298±0.00001	190	0.47%
	2	0.0616±0.0001	0.00298±0.00001	19			
	3	0.0615±0.0000	0.00297±0.00000	19			
	4	0.0617±0.0001	0.00299±0.00001	19			
	5	0.0613±0.0001	0.00295±0.00001	19			
	6	0.0614±0.0001	0.00297±0.00001	19			
	7	0.0614±0.0001	0.00296±0.00001	19			
	8	0.0617±0.0001	0.00299±0.00001	19			
	9	0.0616±0.0000	0.00298±0.00000	19			
	10	0.0616±0.0000	0.00298±0.00000	19			
C1	1	0.1017±0.0001	0.00812±0.00002	19	0.00813±0.00005	190	0.56%
	2	0.1016±0.0001	0.00810±0.00001	19			
	3	0.1016±0.0001	0.00811±0.00002	19			
	4	0.1018±0.0001	0.00813±0.00002	19			
	5	0.1018±0.0001	0.00814±0.00002	19			
	6	0.1018±0.0002	0.00814±0.00002	19			
	7	0.1018±0.0001	0.00814±0.00002	19			
	8	0.1019±0.0002	0.00815±0.00003	19			
	9	0.1016±0.0002	0.00811±0.00002	19			
	10	0.1020±0.0002	0.00818±0.00003	19			
C2	1	0.0800±0.0002	0.00502±0.00002	19	0.00505±0.00003	190	0.55%
	2	0.0802±0.0001	0.00505±0.00002	19			
	3	0.0802±0.0001	0.00505±0.00002	19			
	4	0.0802±0.0001	0.00506±0.00002	19			
	5	0.0801±0.0001	0.00504±0.00001	19			
	6	0.0805±0.0001	0.00509±0.00001	19			
	7	0.0801±0.0001	0.00504±0.00001	19			
	8	0.0803±0.0001	0.00506±0.00002	19			
	9	0.0798±0.0001	0.00500±0.00001	19			
	10	0.0801±0.0001	0.00504±0.00001	19			

Wire	Segment	Diameter(in)	Cross-sectional area(in ²)		Best estimate of cross-sectional area (in ²)		
C3	1	0.0639±0.0001	0.00321±0.00001	19	0.00320±0.00002	190	0.48%
	2	0.0635±0.0001	0.00317±0.00001	19			
	3	0.0639±0.0001	0.00320±0.00001	19			
	4	0.0638±0.0001	0.00319±0.00001	19			
	5	0.0638±0.0000	0.00320±0.00000	19			
	6	0.0639±0.0001	0.00321±0.00001	19			
	7	0.0641±0.0000	0.00323±0.00000	19			
	8	0.0642±0.0001	0.00324±0.00001	19			
	9	0.0638±0.0001	0.00319±0.00001	19			
	10	0.0639±0.0001	0.00321±0.00001	19			
A1	1	0.1077±0.0002	0.00911±0.00004	19	0.00910±0.00009	190	0.98%
	2	0.1072±0.0003	0.00903±0.00006	19			
	3	0.1077±0.0002	0.00910±0.00004	19			
	4	0.1073±0.0004	0.00905±0.00006	19			
	5	0.1077±0.0003	0.00911±0.00004	19			
	6	0.1075±0.0003	0.00907±0.00005	19			
	7	0.1078±0.0002	0.00912±0.00004	19			
	8	0.1076±0.0003	0.00910±0.00005	19			
	9	0.1080±0.0002	0.00917±0.00003	19			
	10	0.1076±0.0003	0.00910±0.00005	19			
A2	1	0.0820±0.0001	0.00528±0.00002	19	0.00529±0.00004	190	0.66%
	2	0.0822±0.0001	0.00530±0.00002	19			
	3	0.0823±0.0001	0.00532±0.00002	19			
	4	0.0822±0.0001	0.00531±0.00002	19			
	5	0.0817±0.0002	0.00524±0.00002	19			
	6	0.0817±0.0001	0.00524±0.00002	19			
	7	0.0820±0.0001	0.00529±0.00002	19			
	8	0.0822±0.0001	0.00530±0.00002	19			
	9	0.0822±0.0001	0.00530±0.00002	19			
	10	0.0821±0.0001	0.00529±0.00002	19			
A3	1	0.0620±0.0002	0.00302±0.00002	19	0.00307±0.00003	190	1.04%
	2	0.0627±0.0001	0.00308±0.00001	19			
	3	0.0627±0.0002	0.00308±0.00002	19			
	4	0.0626±0.0001	0.00308±0.00001	19			
	5	0.0627±0.0001	0.00308±0.00001	19			
	6	0.0622±0.0002	0.00304±0.00002	19			
	7	0.0627±0.0002	0.00309±0.00002	19			
	8	0.0625±0.0001	0.00307±0.00001	19			
	9	0.0628±0.0002	0.00309±0.00002	19			
	10	0.0626±0.0002	0.00308±0.00002	19			
Average of maximum percentage measurement error							0.63%

Two phenomena are observed from the last column of Table F-4. They are: (i) the maximum percentage measurement errors of cross-sectional areas are relatively larger than those of unit weights in Table F-3, and (ii) the maximum percentage measurement errors are close to one another. The first phenomenon is due to the fact that the cross-sectional area is obtained by multiplying the square of the diameter with a

constant. Therefore, the variances among the twenty measurements of the diameter are enlarged because of the multiplication operation. The second phenomenon is consistent with the expectation since the nine wires were measured by the same person and by the same instrument. Consequently, those errors are expected to be close to one another.

Finally, the average of the maximum percentage measurement error of cross-sectional area is

$$(0.46+0.47+\dots+1.04)/9=0.63\%$$

as listed in the last row of Table F-4.

F.1.3 Wire Length

The actual lengths of the nine wires can be obtained by dividing the weights by the corresponding unit weights. For instance, since the weight and the mean of unit weight of the steel wire S1 are 0.59924 lb (Table F-1) and 0.0021266 lb/in (Table F-3), respectively, the actual length will be

$$0.59924/0.0021266/12=23.482 \text{ feet.}$$

Define the percentage error in the measurement of the wire length as the differences between the actual and measured lengths divided by the measured one in terms of percentage. Then, since the measured length of steel wire S1 is 23.458 feet from Table F-1, the percentage length measurement error will be

$$(23.482-23.458)/23.458, \text{ or } 0.10\%.$$

The percentage length measurement errors for the other

eight wires can be obtained in the same manner. The results are listed in the last column of Table F-5.

Table F-5

Percentage length measurement error for the nine wires.

WIRE TYPE	MEASURED LENGTH (feet)	ACTUAL LENGTH (feet)	% error
S1	23.458	23.482	0.10%
S2	29.500	29.515	0.05%
S3	20.000	20.194	0.97%
C1	18.500	18.695	1.05%
C2	19.906	20.070	0.82%
C3	26.573	26.681	0.41%
A1	20.000	20.028	0.14%
A2	26.146	26.573	1.63%
A3	21.583	21.615	0.15%
95% confidence interval for the % length measurement error			(0.59±0.43)%

By applying Equation D-1 in Appendix D, the 95% confidence interval for the mean of the percentage length measurement error is calculated as $0.59\% \pm 0.43\%$, where 0.43% is obtained by using $t_{2.5\%,8} = 2.306$.

F.2 Modulus of Elasticity:

Select the wires from the nine groups of wires mentioned in Section 3.1.1.1 which have been used in the test. Cut the parts which were as uniform in cross section and straight in length as possible into 3' long segments for test. The quantities selected were 7, 7, 8, 7, 9, 8, 7, 7, and 8 for steel wires S1, S2, and S3, copper wires C1, C2, and C3, and

aluminum wires A1, A2, and A3, respectively. The diameter for each segment of the wire was then measured ten times by Mitutoyo's micrometer at different locations along its length. The results are listed in Table F-6.

Table F-6

Measured diameters in inches for wires S1, S2, S3, C1, C2, C3, A1, A2, and A3, respectively, which will be used to calculate the modulus of elasticity.

Wire	MEAS NO	Wire 1	Wire 2	Wire 3	Wire 4	Wire 5	Wire 6	Wire 7	Wire 8	Wire 9
S1	1	0.09970	0.10000	0.09965	0.09995	0.09985	0.09635	0.09650		
	2	0.09975	0.09990	0.10015	0.09975	0.09975	0.09605	0.09635		
	3	0.09935	0.10035	0.09990	0.09995	0.09970	0.09595	0.09650		
	4	0.10005	0.09995	0.09955	0.10005	0.09950	0.09605	0.09660		
	5	0.09965	0.09960	0.09990	0.09990	0.09985	0.09610	0.09665		
	6	0.09930	0.09960	0.09950	0.10005	0.09990	0.09640	0.09680		
	7	0.09965	0.09990	0.09980	0.09955	0.10055	0.09650	0.09690		
	8	0.09945	0.09995	0.09975	0.09970	0.09995	0.09705	0.09685		
	9	0.09940	0.09980	0.09995	0.09965	0.10000	0.09625	0.09690		
	10	0.09910	0.09980	0.09975	0.10000	0.09980	0.09605	0.09690		
S2	1	0.07490	0.07450	0.07465	0.07475	0.07485	0.07480	0.07505		
	2	0.07485	0.07450	0.07450	0.07455	0.07490	0.07475	0.07470		
	3	0.07420	0.07435	0.07465	0.07435	0.07490	0.07440	0.07485		
	4	0.07450	0.07415	0.07495	0.07440	0.07505	0.07470	0.07435		
	5	0.07440	0.07415	0.07475	0.07490	0.07465	0.07455	0.07450		
	6	0.07470	0.07390	0.07475	0.07450	0.07500	0.07490	0.07435		
	7	0.07470	0.07435	0.07450	0.07480	0.07475	0.07500	0.07440		
	8	0.07440	0.07470	0.07495	0.07430	0.07495	0.07415	0.07450		
	9	0.07490	0.07425	0.07445	0.07435	0.07470	0.07460	0.07470		
	10	0.07500	0.07390	0.07455	0.07415	0.07440	0.07435	0.07480		
S3	1	0.06210	0.06190	0.06190	0.06225	0.06210	0.06190	0.06210	0.06175	
	2	0.06210	0.06180	0.06195	0.06230	0.06230	0.06175	0.06230	0.06225	
	3	0.06195	0.06205	0.06185	0.06205	0.06230	0.06185	0.06185	0.06190	
	4	0.06240	0.06175	0.06155	0.06210	0.06225	0.06150	0.06190	0.06135	
	5	0.06225	0.06155	0.06175	0.06210	0.06195	0.06180	0.06190	0.06170	
	6	0.06195	0.06155	0.06190	0.06205	0.06170	0.06215	0.06190	0.06225	
	7	0.06205	0.06155	0.06175	0.06220	0.06175	0.06160	0.06170	0.06250	
	8	0.06185	0.06170	0.06210	0.06180	0.06190	0.06210	0.06175	0.06210	
	9	0.06180	0.06210	0.06210	0.06155	0.06180	0.06175	0.06175	0.06155	
	10	0.06170	0.06195	0.06195	0.06155	0.06165	0.06135	0.06160	0.06140	
C1	1	0.10065	0.10120	0.10135	0.10065	0.10100	0.10155	0.10135		
	2	0.10100	0.10050	0.10135	0.10095	0.10080	0.10100	0.10115		
	3	0.10040	0.10060	0.10110	0.10080	0.10105	0.10100	0.10100		
	4	0.10125	0.10055	0.10150	0.10065	0.10090	0.10060	0.10100		
	5	0.10080	0.10100	0.10065	0.10100	0.10115	0.10045	0.10045		
	6	0.10090	0.10075	0.10080	0.10075	0.10120	0.10100	0.10135		
	7	0.10050	0.10080	0.10100	0.10120	0.10100	0.10105	0.10085		
	8	0.10055	0.10080	0.10080	0.10130	0.10065	0.10050	0.10110		
	9	0.10060	0.10070	0.10140	0.10135	0.10085	0.10135	0.10135		
	10	0.10065	0.10075	0.10120	0.10100	0.10045	0.10070	0.10100		

Wire	MEA NO	Wire 1	Wire 2	Wire 3	Wire 4	Wire 5	Wire 6	Wire 7	Wire 8	Wire 9
C2	1	0.07930	0.07990	0.07990	0.07905	0.07990	0.07980	0.07960	0.07945	0.07935
	2	0.07955	0.07950	0.08020	0.07875	0.07915	0.07930	0.07955	0.07925	0.07925
	3	0.07950	0.07960	0.08050	0.07915	0.07920	0.07940	0.07960	0.07915	0.07940
	4	0.07930	0.07980	0.07985	0.07935	0.07930	0.07940	0.07935	0.07960	0.07955
	5	0.07905	0.07970	0.07955	0.07935	0.07945	0.07950	0.07945	0.07950	0.07980
	6	0.07915	0.07970	0.08000	0.07915	0.07930	0.07915	0.07940	0.07935	0.07960
	7	0.07935	0.07970	0.07955	0.07940	0.07970	0.07925	0.07950	0.07915	0.08010
	8	0.07920	0.07945	0.07970	0.07925	0.07965	0.07960	0.07950	0.07935	0.07980
	9	0.07945	0.07990	0.07985	0.07910	0.07970	0.07935	0.07960	0.07905	0.08000
	10	0.07950	0.07875	0.07940	0.07945	0.07970	0.08005	0.07925	0.07915	0.07970
C3	1	0.06370	0.06305	0.06415	0.06300	0.06390	0.06360	0.06340	0.06360	
	2	0.06340	0.06390	0.06400	0.06280	0.06315	0.06320	0.06385	0.06320	
	3	0.06360	0.06335	0.06385	0.06350	0.06400	0.06360	0.06375	0.06390	
	4	0.06340	0.06360	0.06375	0.06340	0.06305	0.06300	0.06325	0.06400	
	5	0.06355	0.06365	0.06355	0.06350	0.06415	0.06365	0.06360	0.06320	
	6	0.06340	0.06340	0.06410	0.06360	0.06415	0.06350	0.06385	0.06335	
	7	0.06370	0.06345	0.06390	0.06310	0.06375	0.06315	0.06370	0.06395	
	8	0.06345	0.06335	0.06370	0.06315	0.06380	0.06325	0.06380	0.06395	
	9	0.06320	0.06350	0.06340	0.06310	0.06380	0.06325	0.06340	0.06360	
	10	0.06370	0.06360	0.06340	0.06320	0.06350	0.06360	0.06435	0.06350	
A1	1	0.10765	0.10750	0.10595	0.10740	0.10720	0.10750	0.10760		
	2	0.10610	0.10660	0.10700	0.10785	0.10675	0.10695	0.10770		
	3	0.10765	0.10825	0.10580	0.10815	0.10350	0.10730	0.10320		
	4	0.10755	0.10635	0.10710	0.10775	0.10675	0.10635	0.10660		
	5	0.10770	0.10685	0.10755	0.10795	0.10710	0.10750	0.10730		
	6	0.10690	0.10805	0.10785	0.10545	0.10695	0.10620	0.10605		
	7	0.10810	0.10715	0.10760	0.10765	0.10710	0.10740	0.10750		
	8	0.10655	0.10795	0.10435	0.10340	0.10670	0.10300	0.10680		
	9	0.10745	0.10800	0.10690	0.10765	0.10705	0.10535	0.10730		
	10	0.10860	0.10785	0.10530	0.10750	0.10560	0.10755	0.10545		
A2	1	0.07985	0.08110	0.08175	0.08125	0.08145	0.08125	0.08030		
	2	0.08090	0.08070	0.08120	0.08120	0.08125	0.08110	0.08030		
	3	0.08010	0.08080	0.08160	0.08115	0.08175	0.08115	0.08045		
	4	0.08120	0.08130	0.08195	0.08120	0.08130	0.08060	0.08140		
	5	0.08030	0.08090	0.08150	0.08130	0.08110	0.08130	0.08080		
	6	0.08045	0.08050	0.08160	0.08120	0.08155	0.08130	0.08175		
	7	0.08095	0.08070	0.08150	0.08065	0.08135	0.08075	0.08180		
	8	0.08025	0.08095	0.08140	0.08085	0.08150	0.08100	0.08165		
	9	0.08150	0.08055	0.08135	0.08095	0.08160	0.08040	0.08060		
	10	0.07975	0.08110	0.08105	0.08085	0.08100	0.08060	0.08075		
A3	1	0.06080	0.06195	0.05975	0.05940	0.05930	0.05865	0.06110	0.05885	
	2	0.05915	0.05995	0.06000	0.06150	0.06100	0.05875	0.05935	0.05960	
	3	0.05895	0.06175	0.06210	0.06080	0.06115	0.05910	0.06115	0.06165	
	4	0.05850	0.06100	0.06200	0.06135	0.06135	0.05920	0.06135	0.06085	
	5	0.06120	0.06095	0.05955	0.06230	0.06075	0.05905	0.05940	0.06070	
	6	0.06100	0.06155	0.06180	0.06100	0.06160	0.05965	0.06120	0.06080	
	7	0.06120	0.06145	0.05980	0.06145	0.06040	0.05940	0.06120	0.06120	
	8	0.06155	0.06180	0.06170	0.06095	0.06140	0.05935	0.06015	0.06080	
	9	0.06160	0.06030	0.05955	0.06135	0.06025	0.06105	0.06010	0.06085	
	10	0.06135	0.06100	0.06180	0.05985	0.05935	0.05870	0.06170	0.05935	

Next, an MTS 2" gauge length extensometer of model 632.25B-20 as shown in Fig. F-5 which could measure with the accuracy of 0.15% of the measured value was bound to the center of the wire by rubber band. The top of the wire was

mounted to a load cell while the other end was clamped to the dynamic grip of the MTS dynamic system as shown in Fig. F-6. Since the wire would bend slightly due to the clamping it was then pulled straight by the MTS system in the beginning of the test. In the meantime, the wire was under tension of a small magnitude (5-10 lbs). The load-reading in the MTS system was then reset to zero and the pin of the extensometer was pulled out to start test. The test continued until the wire yielded which could be seen from the plotting in the monitor. The data relating to the load at both ends of the wire and the corresponding strain in the center were recorded. A representative sample of the first of seven steel wires S1 is listed in Table F-7.

Table F-7

The load and strain for the first of seven steel wire S1.

Load (lb)	strain (in/in)	Load (lb)	strain (in/in)	Load (lb)	strain (in/in)	Load (lb)	strain (in/in)	Load (lb)	strain (in/in)
0.0	0.000000	21.8	0.000147	44.2	0.000268	66.0	0.000386	87.3	0.000524
1.0	0.000013	22.8	0.000156	45.2	0.000278	67.0	0.000414	88.5	0.000539
1.9	0.000012	23.8	0.000149	46.3	0.000272	67.9	0.000416	89.4	0.000548
2.9	0.000024	24.8	0.000144	47.3	0.000280	68.8	0.000428	90.5	0.000545
3.9	0.000020	25.9	0.000162	48.3	0.000291	69.6	0.000419	91.4	0.000542
4.8	0.000040	26.9	0.000132	49.3	0.000325	70.5	0.000425	92.4	0.000558
5.8	0.000030	27.9	0.000161	50.3	0.000302	71.4	0.000422	93.4	0.000563
6.8	0.000031	28.9	0.000176	51.3	0.000314	73.0	0.000459	94.4	0.000570
7.8	0.000050	30.0	0.000173	52.3	0.000332	73.8	0.000453	95.4	0.000589
8.7	0.000073	31.0	0.000201	53.3	0.000328	74.6	0.000460	96.4	0.000594
9.7	0.000074	32.0	0.000216	54.4	0.000312	76.0	0.000469	97.4	0.000590
10.7	0.000057	33.0	0.000198	55.4	0.000359	76.7	0.000467	98.4	0.000573
11.7	0.000066	34.0	0.000205	56.4	0.000348	77.4	0.000464	99.4	0.000591
12.8	0.000066	35.0	0.000222	57.4	0.000344	78.7	0.000475	100.4	0.000619
13.8	0.000077	36.1	0.000231	58.4	0.000359	79.8	0.000502	101.4	0.000604
14.8	0.000099	37.1	0.000225	59.4	0.000352	80.4	0.000481	102.3	0.000614
15.8	0.000099	38.1	0.000227	60.3	0.000355	81.7	0.000505	103.3	0.000611
16.8	0.000113	39.1	0.000243	61.3	0.000377	82.5	0.000502	104.4	0.000606
17.8	0.000121	40.1	0.000245	62.3	0.000369	83.4	0.000514	105.4	0.000626
18.8	0.000115	41.2	0.000248	63.2	0.000379	84.5	0.000514	106.3	0.000638
19.8	0.000135	42.2	0.000255	64.2	0.000388	85.6	0.000525	107.4	0.000637
20.8	0.000113	43.2	0.000256	65.1	0.000402	86.5	0.000526	108.4	0.000647

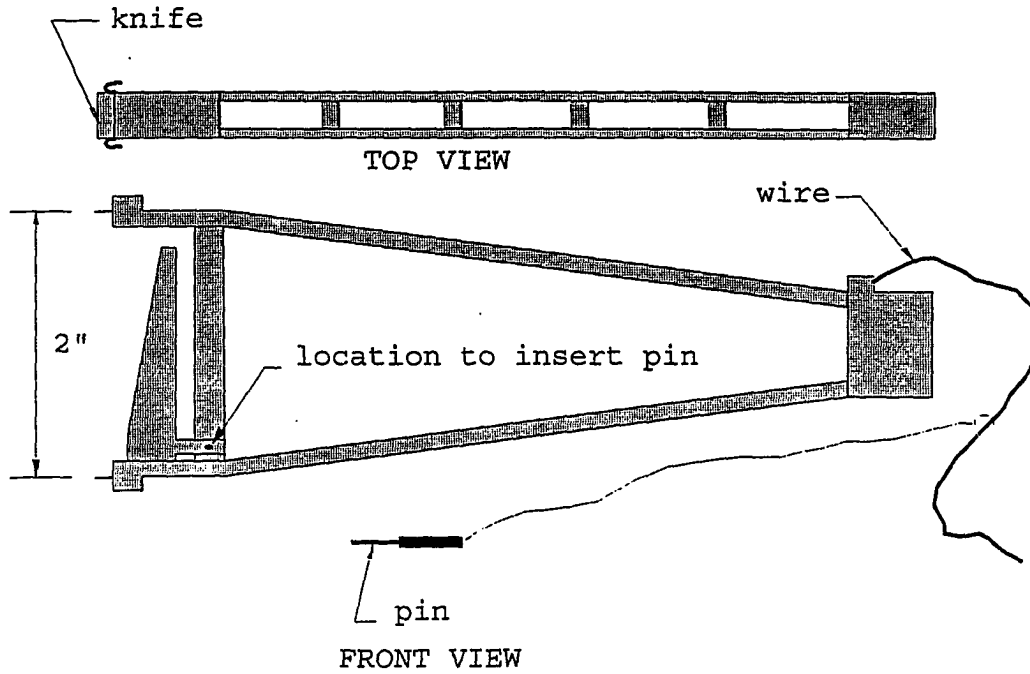


Fig. F-5: Two-inch gauge length extensometer used to measure the strain of the wire.

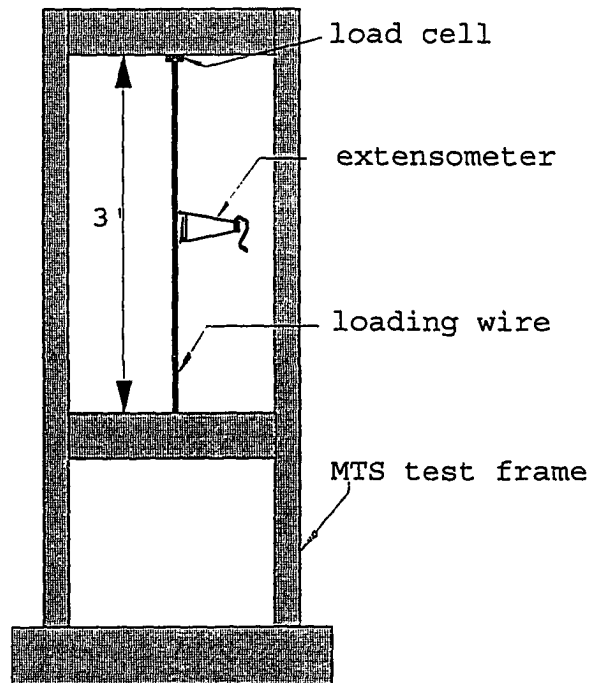


Fig. F-6: Configuration of the test wire and equipment to determine the modulus of elasticity.

As a result, the slope of the load-strain relation can be obtained from Equation D-4 and Table F-7, i.e. since

$$\begin{aligned}
 n &= 110 \\
 \Sigma x &= 0.000000 + 0.000013 + \dots + 0.000647 = 0.036286 \\
 \Sigma y &= 0.0 + 1.0 + \dots + 108.4 = 5976.8 \\
 \Sigma x^2 &= 0.000000^2 + 0.000013^2 + \dots + 0.000647^2 = 0.000015 \\
 \Sigma y^2 &= 0.0^2 + 1.0^2 + \dots + 108.4^2 = 434524.2 \\
 \Sigma xy &= 0.000000 * 0.0 + 0.000013 * 1.0 + \dots + 0.000647 * 108.4 = 2.629111 \\
 S_{xy} &= \frac{2.629111 - 0.036286 * 5976.8}{110} = 0.657524 \\
 S_{xx} &= \frac{0.000015 - 0.036286^2}{110} = 0.000003 \\
 S_{yy} &= \frac{434524.2 - 5976.8^2}{110} = 109780.4
 \end{aligned}$$

, then

$$\text{mean of slope: } \bar{\beta}_1 = \frac{S_{xy}}{S_{xx}} = \frac{0.657524}{0.000003} = 166495$$

$$\begin{aligned}
 \text{and standard error } SE &= \sqrt{\frac{SSE}{(n-2)S_{xx}}} \\
 &= \sqrt{\frac{306.1291}{(110-2)(0.000003)}} = 847, \text{ respectively,}
 \end{aligned}$$

$$\begin{aligned}
 \text{where } SSE &= S_{yy} - \bar{\beta}_1 S_{xy} \\
 &= 109780.4 - 166495 * 0.657524 = 306.1291
 \end{aligned}$$

On the other hand, the mean and standard error of the diameter can be obtained by applying Equation D-1a, i.e.

$$\begin{aligned}
 \bar{d} &= \frac{0.09770 + \dots + 0.09910}{10} = 0.09954 \text{ in} \\
 \text{and } SE_d &= \sqrt{\frac{(0.09970^2 + \dots + 0.09910^2) - \frac{(0.09970 + \dots + 0.09910)^2}{10}}{10(10-1)}} \\
 &= 0.00009 \text{ in}^2
 \end{aligned}$$

, respectively. Then, since $A = \pi d^2 / 4$ where d and A are,

respectively, the diameter and the cross-sectional area of the wire, the corresponding mean and standard error of the area, as from Equation D-2, becomes

$$\begin{aligned} \text{mean } \bar{A} &= \frac{\pi}{4} \bar{d}^2 = \frac{\pi}{4} (0.09954)^2 = 0.007782 \text{ in}^2 \\ \text{standard error } SE_A &= \left\{ \left(\frac{2}{d} SE_d \right)^2 \right\}^{1/2} \bar{A} = \frac{2}{d} SE_d * \frac{\pi}{4} \bar{d}^2 = \frac{\pi}{2} \bar{d} SE_d \\ &= \frac{\pi}{2} (0.09954) (0.00009) = 0.000013 \text{ in}^2 \end{aligned}$$

Note that the DOFs are nine because ten measurements were made for the cross-sectional area of the wire and one DOF is used when calculating its mean.

Finally, the modulus of elasticity, E , equals β_1/A by definition, where β_1 and A are, respectively, the slope of the load-strain relation and the cross-sectional area of the wire. Then, from Equation D-2, the mean and standard error of the modulus of elasticity for the first of seven steel wire S1 are

$$\begin{aligned} \bar{E} &= \frac{\bar{\beta}_1}{\bar{A}} = \frac{166495}{0.007782} = 21394837 \text{ psi} \\ \text{and } SE_E &= \left\{ \left(\frac{1}{\bar{\beta}_1} SE_{\bar{\beta}_1} \right)^2 + \left(\frac{-1}{\bar{A}} SE_{\bar{A}} \right)^2 \right\}^{1/2} \bar{E} \\ &= \left\{ \left(\frac{1}{166495} * 847 \right)^2 + \left(\frac{-1}{0.007782} * 0.000013 \right)^2 \right\}^{1/2} * 21394837 \\ &= 114583 \text{ psi, respectively.} \end{aligned}$$

Similarly, the means and standard errors of the moduli of elasticity for other segments of steel wire S1 are obtained. The results are listed in the seventh column of Table F-8.

Table F-8

Best estimates for the moduli of elasticity of wires S1, S2, S3, C1, C2, C3, A1, A2, and A3, respectively. Also listed are the corresponding maximum percentage measurement errors (MPME).

Wire	Wire #	Load/strain(lb)		Cross-sectional area(in ²)		Modulus of elasticity (psi)	Best estimate of modulus of elasticity (*10 ⁷ psi)		
		Mean ± SE	DOF	Mean ± SE	DOF		Mean ± t*SE	DOF	MPME
S1	1	166495± 847	108	0.007782±0.000013	9	21394837±114583	2.201±0.027	808	1.23 %
	2	155578± 757	107	0.007836±0.000011	9	19854227±100582			
	3	149996± 699	117	0.007821±0.000010	9	19178621± 92634			
	4	155115± 762	114	0.007831±0.000009	9	19807790± 99920			
	5	156905± 795	90	0.007836±0.000014	9	20023633±107616			
	6	237304±1807	124	0.007280±0.000016	9	32596661±258308			
	7	155651± 922	85	0.007343±0.000010	9	21197221±128810			
S2	1	126494± 397	120	0.004377±0.000010	9	28899660±112184	2.482±0.021	786	0.85 %
	2	110832± 355	117	0.004333±0.000010	9	25578656±101019			
	3	114855± 461	107	0.004379±0.000007	9	26228666±113299			
	4	90466± 401	81	0.004360±0.000009	9	20749151±101535			
	5	94358± 412	78	0.004396±0.000007	9	21464609± 99713			
	6	113059± 449	93	0.004373±0.000010	9	25853780±118438			
	7	109122± 353	127	0.004373±0.000009	9	24953582± 95647			
S3	1	67985± 396	69	0.003021±0.000006	9	22504288±138588	2.395±0.043	903	1.80 %
	2	72511± 914	103	0.002999±0.000006	9	24178511±308547			
	3	61161± 765	106	0.003007±0.000005	9	20339559±256586			
	4	77707±1121	110	0.003019±0.000008	9	25739445±377642			
	5	91388± 566	104	0.003016±0.000008	9	30301054±204132			
	6	62440± 178	125	0.002997±0.000008	9	20834138± 81456			
	7	74295± 286	80	0.003007±0.000006	9	24707503±107082			
	8	69059± 146	134	0.003007±0.000012	9	22966021±103764			
C1	1	95941± 347	103	0.007969±0.000013	9	12039315± 47716	1.395±0.015	734	1.08 %
	2	109485± 471	99	0.007975±0.000010	9	13728529± 61462			
	3	105402± 605	89	0.008030±0.000015	9	13126017± 79176			
	4	165517±1031	106	0.008006±0.000013	9	20674100±133084			
	5	113807± 499	102	0.007997±0.000011	9	14231268± 65397			
	6	106879± 519	96	0.007999±0.000018	9	13361598± 71500			
	7	84228± 431	76	0.008021±0.000014	9	10500966± 56757			
C2	1	71884± 804	54	0.004943±0.000007	9	14542684±164013	1.401±0.039	645	2.78 %
	2	66938± 299	62	0.004976±0.000013	9	13452082± 69621			
	3	75204±1017	44	0.005008±0.000013	9	15016770±206880			
	4	79294±1412	76	0.004927±0.000008	9	16093781±287714			
	5	57659± 354	49	0.004965±0.000010	9	11613034± 75088			
	6	76713±1249	80	0.004961±0.000011	9	15463163±253989			
	7	69618±1055	44	0.004961±0.000005	9	14032978±213103			
	8	75598±1404	80	0.004939±0.000007	9	15306281±285175			
	9	52802± 280	75	0.004983±0.000011	9	10596408± 60791			
C3	1	33071± 159	42	0.003168±0.000005	9	10438937± 52952	1.416±0.053	384	3.74 %
	2	52826±1416	47	0.003165±0.000007	9	16690636±448943			
	3	33736± 335	34	0.003195±0.000009	9	10558974±108935			
	4	49382± 980	36	0.003141±0.000008	9	15721779±314502			
	5	46306± 963	21	0.003182±0.000011	9	14552613±306760			
	6	51227± 377	55	0.003154±0.000007	9	16241804±124821			
	7	50947±1195	42	0.003186±0.000010	9	15990928±378327			
	8	41485± 279	35	0.003179±0.000010	9	13049590± 96812			

Wire	Wire #	Load/strain(lb)		Cross-sectional area(in ²)		Modulus of elasticity (psi)	Best estimate of modulus of elasticity (*10 ⁷ psi)		
		Mean ± SE	DOF	Mean ± SE	DOF		Mean ± t*SE	DOF	MPME
A1	1	59548± 588	42	0.009064±0.000039	9	6569780± 70792	0.782±0.036	402	4.60 %
	2	99330±3950	60	0.009069±0.000036	9	10952745±437696			
	3	64030± 532	54	0.008915±0.000060	9	7182264± 76780			
	4	56468± 423	51	0.009005±0.000079	9	6270766± 72314			
	5	80483± 926	43	0.008903±0.000060	9	9040019±120562			
	6	76256± 790	43	0.008910±0.000076	9	8558517±114833			
	7	54868± 348	46	0.008917±0.000073	9	6153180± 63739			
A2	1	32629± 111	70	0.005093±0.000023	9	6406573± 36195	1.051±0.028	470	2.66 %
	2	50163± 240	70	0.005135±0.000010	9	9768745± 50538			
	3	71563±1200	55	0.005216±0.000011	9	13719896±231942			
	4	32371± 127	78	0.005161±0.000009	9	6272209± 27002			
	5	60096± 463	46	0.005202±0.000009	9	11552412± 91219			
	6	69845± 995	46	0.005146±0.000013	9	13572710±196460			
	7	63178± 911	42	0.005150±0.000024	9	12267512±185908			
A3	1	31284± 398	33	0.002878±0.000036	9	10869914±194015	1.045±0.031	336	2.97 %
	2	34970± 424	27	0.002939±0.000020	9	11898630±165474			
	3	27126± 199	34	0.002904±0.000035	9	9340841±131801			
	4	28586± 248	28	0.002906±0.000028	9	9836835±127502			
	5	38299± 448	30	0.002890±0.000025	9	13252294±192761			
	6	37048± 525	29	0.002761±0.000021	9	13418248±215863			
	7	22616± 136	37	0.002891±0.000026	9	7822887± 84719			
	8	20625± 116	46	0.002871±0.000027	9	7183847± 78635			
Average of maximum percentage measurement error									2.41 %

The moduli of elasticity of the seven steel wires S1 could be combined, according to Equation D-5, to give the best estimate. For instance, from Equation D-5 and the seventh column of Table F-8, the best estimate for the mean and standard error of the modulus of elasticity for steel wire S1 are

$$\bar{E} = \frac{21394837 + \dots + 21197221}{7} = 22007570 \text{ psi}$$

$$\text{and } SE_E = \sqrt{\frac{114583^2 + \dots + 128810^2}{7}} = 139748 \text{ psi, respectively.}$$

The DOFs in this case are $(108+107+\dots+85)+(9+9+\dots+9)$, or 808, and the corresponding $t_{2.5\%,808}$ is 1.96. Therefore, the 95% confidence interval for the mean of modulus of elasticity of

steel wire S1 is

$$\bar{E} \pm t_{2.5\%, 808} SE_E = 22007570 \pm 1.96 * 139748 = 22007570 \pm 273907$$

Since $SE_E/3 = 46583$, by Kelley's rule, the modulus of elasticity should be $(2.201 \pm 0.027) * 10^7$ psi. Then the maximum percentage measurement error of the modulus of elasticity of steel wire S1 is

$$0.027/2.201 = 1.23\%$$

as shown in the last column of Table F-8.

Similarly, the moduli of elasticity as well as the best estimates and the corresponding maximum percentage measurement errors for the other wires are obtained as listed in Table F-8. The average of the maximum percentage error is calculated as 2.41% as shown in the last row of Table F-8.

The theoretical moduli of elasticity for steel, copper, and aluminum wires are $29 * 10^6$ psi, $15 * 10^6$ psi, $10 * 10^6$ psi, respectively. It is found from Table F-8 that the experimental results for the first two wires are close to the theoretical values and, therefore, are reliable. As for the steel wires, the experimental results are 17% to 24% smaller than the theoretical one. However, they are still reliable since, in one respect, they are close to one another which should be so because steel wires S1, S2, and S3 are made of the same material.

F.3 Span Length

The support equipments of the single-span wire line were mounted on two giant steel frames, one at one end as shown in Fig. F-7. The frame at the right end was unmovable while the other at the left end could be moved by a crane to the desired location. A Stanley tape measurer taped down to the ground right below the wire was used along with a plumb to check the span length between the two ends of the wire.

Due to the practical difficulty to move the steel frame to the desired location, the actual span lengths under which the wires were tested were slightly different from the ones listed in Appendix A. The differences were believed to be within $1/8$ ". Therefore, $1/8$ " would be used as the maximum measurement error of the span length.

Eight span lengths have been tested during the galloping experiment as listed in the first column of Table F-9. The corresponding maximum percentage error can be obtained by dividing $1/8$ " by the span length. The results are listed in the second column of Table F-9. The average of the maximum percentage error in the measurement of span length is then calculated as 0.035%.

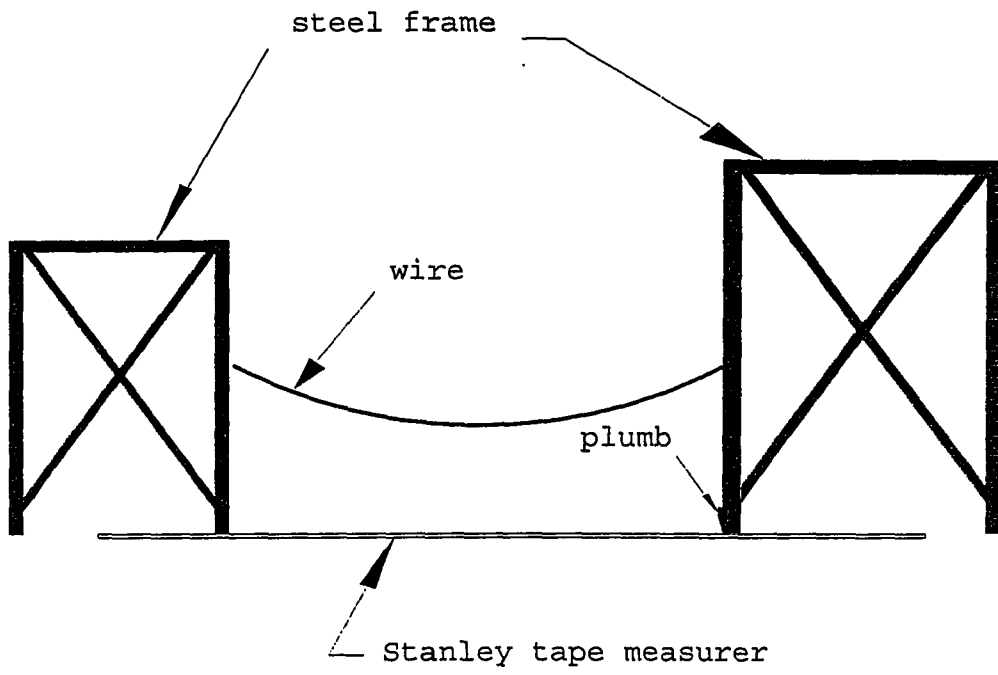


Fig.F-7: The arrangement to measure the span length.

Table F-9

Maximum percentage errors in the measurement of span lengths.

Span	Max % error of span length measurement
46'	0.023%
43'	0.024%
40'	0.026%
35'	0.029%
30'	0.035%
23'	0.045%
21.5'	0.048%
20'	0.052%
Average= 0.035%	

F.4 Frequency

The exciting frequency of the hydraulic actuator was set by turning manually the knob of the frequency dial in the MTS dynamic system. The one set in the dial is thus called the nominal frequency. On the other hand, the actual frequency under which the hydraulic actuator exerted on the wires can be obtained from the output in the stripchart. For instance, the output of the vertical and horizontal tensions of the 46.6' steel wire S1 hanging on 46' span and vibrating at 1.05 Hz of nominal frequency (Test No.1 in Appendix A) are shown in the top and middle of Fig. 3-12 while the support movement is shown in the bottom. Then from left to right and from top to bottom of in that figure, the distances, d , between two consecutive cycles are

23.0, 23.4, 23.4, 23.4, 23.8, 22.7, 23.2, 23.3, 23.2, 23.2, 23.1, 23.3, 23.4, 23.2, and 23.1 units

, respectively. Note that it is intended to measure more cycles to increase the accuracy. Also it is easier to

distinguish the lowest point ,the equilibrium position and the highest peak from the output of support motion than the other two. Therefore, the former is measured two more times than the latter two. As a result, by using Equation D-1 of Appendix D, the mean and standard error of \bar{d} are

$$\bar{d} = \frac{23.0+23.4+\dots+23.1}{15} = 23.25 \text{ units}$$

$$\text{and } SE_d = \sqrt{\frac{(23.0^2+23.4^2+\dots+23.1^2) - \frac{(23.0+23.4+\dots+23.1)^2}{15}}{15(15-1)}} = 0.06 \text{ units}$$

, respectively. Since, from calibration, 1 unit=0.04 seconds, the period is then found to be 0.04 \bar{d} seconds or the frequency is 1/(0.04 \bar{d}) Hz. Therefore, the mean and standard error of the frequency, as from Equation D-2, become

$$\text{mean } \bar{f} = \frac{1}{0.04\bar{d}} = \frac{1}{0.04(23.25)} = 1.075 \text{ Hz}$$

$$\text{standard error } SE_f = \left\{ \left(\frac{-1}{\bar{d}} SE_d \right)^2 \right\}^{1/2} \bar{f} = \frac{1}{\bar{d}} SE_d * \frac{1}{0.04\bar{d}} = \frac{SE_d}{0.04\bar{d}^2}$$

$$= \frac{0.06}{0.04(23.25)^2} = 0.003 \text{ Hz}$$

As a result, the 95% confidence interval for the mean of the frequency is

$$\bar{f} \pm t_{2.5\%,14} SE_f = 1.075 \pm 2.145 * 0.003 = 1.075 \pm 0.006 \text{ Hz}$$

where $t_{2.5\%,14}$ for 14 DOFs is 2.145. The maximum percentage error of steel wire S1 in Test No.1 at 1.05 Hz of nominal frequency is, therefore,

$$0.006/1.075 = 0.56\%$$

Similarly, the 95% confidence intervals for the means of

the exciting frequencies of the other tests and the corresponding maximum percentage measurement errors are obtained. The results are listed in Table F-10. The average of the maximum percentage error in the measurement of the frequencies is calculated as 0.56%.

Table F-10: Nominal frequencies (NF) in Hz, 95% confidence intervals of the mean of actual frequencies (Hz), and the maximum percentage measurement error for the 221 tests listed in Appendix A.

NO.	NF	ACT.FREQ.	%ERR	NO.	NF	ACT.FREQ.	%ERR	NO.	NF	ACT.FREQ.	%ERR	NO.	NF	ACT.FREQ.	%ERR
1.1.05	1.08±0.01	0.56		10.1.05	1.08±0.01	0.69		19.1.10	1.14±0.00	0.44		29.1.10	1.13±0.02	1.43	
1.1.10	1.13±0.01	1.12		1.1.10	1.14±0.01	0.80		1.15	1.19±0.01	0.47		1.15	1.18±0.01	0.62	
1.1.15	1.19±0.01	1.21		1.15	1.19±0.00	0.03		1.20	1.25±0.00	0.35		1.20	1.24±0.01	0.48	
1.2.0	1.24±0.01	0.80		1.20	1.24±0.00	0.22		1.25	1.30±0.01	0.60		1.25	1.30±0.01	0.48	
1.25	1.30±0.00	0.32		1.25	1.30±0.01	0.66		1.30	1.36±0.01	0.57		1.30	1.35±0.00	0.17	
1.30	1.36±0.00	0.31		1.30	1.35±0.00	0.22		20.1.10	1.14±0.00	0.34		1.35	1.41±0.01	0.54	
2.1.05	1.08±0.01	0.67		1.35	1.41±0.00	0.28		1.15	1.16±0.02	1.48		1.40	1.46±0.00	0.21	
1.10	1.14±0.01	0.59		11.1.05	1.08±0.00	0.37		1.20	1.24±0.00	0.30		30.1.15	1.19±0.01	0.42	
1.15	1.20±0.01	0.70		1.10	1.14±0.00	0.20		1.25	1.30±0.01	0.48		1.20	1.24±0.01	0.67	
1.20	1.24±0.01	0.81		1.15	1.19±0.00	0.24		1.30	1.35±0.00	0.27		1.25	1.29±0.01	0.40	
1.25	1.30±0.00	0.31		1.20	1.24±0.00	0.29		1.35	1.41±0.00	0.26		1.30	1.36±0.00	0.23	
1.30	1.35±0.01	0.56		1.25	1.30±0.00	0.26		21.1.10	1.13±0.00	0.21		1.35	1.41±0.00	0.28	
3.1.05	1.07±0.01	0.89		1.30	1.36±0.00	0.31		1.15	1.19±0.01	0.75		31.1.10	1.13±0.01	0.67	
1.10	1.11±0.00	0.41		12.1.05	1.08±0.00	0.31		1.20	1.24±0.01	1.19		1.15	1.19±0.00	0.25	
1.15	1.19±0.00	0.17		1.10	1.13±0.00	0.42		1.25	1.30±0.01	0.40		1.20	1.24±0.01	0.46	
1.20	1.24±0.00	0.23		1.15	1.19±0.00	0.13		1.30	1.35±0.00	0.21		1.25	1.30±0.00	0.25	
1.25	1.30±0.00	0.37		1.20	1.24±0.00	0.21		1.35	1.41±0.00	0.28		1.30	1.35±0.00	0.10	
1.30	1.36±0.01	0.81		1.25	1.30±0.00	0.13		22.1.10	1.15±0.01	0.56		1.35	1.42±0.01	0.49	
1.35	1.41±0.01	0.41		1.30	1.35±0.01	0.45		1.15	1.20±0.01	0.49		32.1.10	1.13±0.00	0.40	
4.1.05	1.07±0.01	0.62		1.35	1.41±0.00	0.30		1.20	1.25±0.01	0.80		1.15	1.19±0.01	0.82	
1.10	1.13±0.01	0.61		13.1.05	1.08±0.00	0.18		1.25	1.31±0.00	0.20		1.20	1.25±0.00	0.25	
1.15	1.20±0.01	1.03		1.10	1.13±0.00	0.30		1.30	1.36±0.00	0.31		1.25	1.30±0.01	0.39	
1.20	1.24±0.00	0.17		1.15	1.19±0.00	0.11		1.35	1.41±0.00	0.32		1.30	1.35±0.01	0.42	
1.25	1.29±0.00	0.22		1.20	1.24±0.00	0.07		23.1.10	1.16±0.02	1.51		1.35	1.41±0.00	0.33	
1.30	1.35±0.00	0.31		1.25	1.30±0.00	0.26		1.15	1.19±0.00	0.41		33.1.10	1.13±0.00	0.14	
5.1.05	1.07±0.01	0.83		1.30	1.35±0.00	0.34		1.20	1.25±0.01	0.48		1.15	1.19±0.01	1.01	
1.10	1.13±0.00	0.29		1.35	1.40±0.00	0.26		1.25	1.30±0.01	0.61		1.20	1.25±0.01	0.44	
1.15	1.19±0.00	0.22		14.1.05	1.08±0.00	0.46		1.30	1.35±0.00	0.29		1.25	1.30±0.00	0.27	
1.20	1.24±0.01	0.54		1.10	1.14±0.00	0.44		1.35	1.41±0.01	0.41		1.30	1.35±0.00	0.13	
1.25	1.30±0.02	1.18		1.15	1.19±0.00	0.29		24.1.10	1.13±0.00	0.28		1.35	1.41±0.00	0.30	
1.30	1.35±0.01	0.43		1.20	1.25±0.00	0.24		1.15	1.19±0.00	0.36		34.1.10	1.14±0.00	0.20	
1.35	1.42±0.02	1.25		1.25	1.30±0.01	0.46		1.20	1.24±0.01	0.58		1.15	1.19±0.00	0.31	
6.1.05	1.07±0.01	0.93		1.30	1.35±0.00	0.21		1.25	1.30±0.00	0.31		1.20	1.26±0.01	0.52	
1.10	1.12±0.01	0.46		15.1.05	1.08±0.00	0.30		1.30	1.35±0.01	0.47		1.25	1.30±0.00	0.22	
1.15	1.19±0.00	0.41		1.10	1.14±0.00	0.43		1.35	1.42±0.02	1.09		1.30	1.35±0.00	0.22	
1.20	1.26±0.00	0.31		1.15	1.20±0.00	0.35		25.1.10	1.14±0.02	1.57		35.1.15	1.19±0.00	0.22	
1.25	1.30±0.01	0.41		1.20	1.25±0.01	0.42		1.15	1.19±0.01	0.86		1.20	1.24±0.00	0.19	
1.30	1.35±0.01	0.78		1.25	1.31±0.00	0.25		1.20	1.24±0.01	0.85		1.25	1.29±0.00	0.26	
1.35	1.41±0.01	0.63		1.30	1.35±0.00	0.34		1.25	1.30±0.00	0.36		1.30	1.36±0.00	0.15	
7.1.05	1.08±0.01	1.22		16.1.05	1.08±0.00	0.28		1.30	1.36±0.01	0.64		1.35	1.41±0.00	0.22	
1.10	1.14±0.01	0.89		1.10	1.14±0.00	0.16		1.35	1.42±0.01	0.78		1.40	1.46±0.00	0.18	
1.15	1.19±0.02	1.49		1.15	1.19±0.00	0.25		1.40	1.47±0.00	0.15		1.45	1.52±0.01	0.45	
1.20	1.24±0.01	1.02		1.20	1.25±0.00	0.36		26.1.10	1.13±0.01	0.89		36.1.15	1.19±0.00	0.17	
1.25	1.30±0.00	0.32		1.25	1.30±0.00	0.32		1.15	1.19±0.01	0.87		1.20	1.25±0.00	0.36	
1.30	1.35±0.00	0.21		1.30	1.36±0.00	0.21		1.20	1.24±0.01	0.41		1.25	1.30±0.00	0.21	
1.35	1.41±0.01	0.45		17.1.05	1.08±0.00	0.21		1.25	1.30±0.01	0.57		1.30	1.37±0.01	0.92	
1.40	1.47±0.01	0.67		1.10	1.13±0.00	0.21		1.30	1.36±0.01	0.58		1.35	1.41±0.00	0.33	
8.1.05	1.07±0.01	0.55		1.15	1.19±0.00	0.16		1.35	1.41±0.01	0.53		1.40	1.47±0.00	0.16	
1.10	1.13±0.01	0.91		1.20	1.24±0.00	0.20		1.40	1.46±0.00	0.30		1.45	1.54±0.01	0.52	
1.15	1.19±0.00	0.23		1.25	1.30±0.00	0.22		27.1.10	1.13±0.00	0.37		37.1.15	1.19±0.00	0.12	
1.20	1.24±0.00	0.26		1.30	1.35±0.01	0.45		1.15	1.19±0.01	0.45		1.20	1.24±0.00	0.27	
1.25	1.29±0.00	0.31		18.1.05	1.06±0.01	0.95		1.20	1.24±0.00	0.27		1.25	1.30±0.00	0.25	
1.30	1.36±0.00	0.14		1.10	1.13±0.00	0.15		1.25	1.30±0.00	0.17		1.30	1.36±0.00	0.26	
1.35	1.41±0.00	0.29		1.15	1.19±0.01	0.58		1.30	1.35±0.01	0.41		1.35	1.41±0.00	0.32	
9.1.05	1.07±0.01	0.48		1.20	1.24±0.00	0.28		1.35	1.41±0.00	0.32		1.40	1.47±0.00	0.20	
1.10	1.13±0.02	1.71		1.25	1.30±0.00	0.18		28.1.10	1.13±0.00	0.18		1.45	1.52±0.00	0.29	
1.15	1.20±0.02	1.34		1.30	1.35±0.00	0.30		1.15	1.18±0.01	0.63		38.1.15	1.20±0.01	1.16	
1.20	1.24±0.02	1.23						1.20	1.25±0.00	0.30		1.20	1.24±0.01	1.04	
1.25	1.31±0.02	1.34						1.25	1.30±0.00	0.36		1.25	1.30±0.00	0.36	
1.30	1.35±0.01	0.61						1.30	1.36±0.01	0.51		1.30	1.36±0.01	0.40	
1.35	1.41±0.01	0.82						1.35	1.42±0.00	0.35		1.35	1.41±0.01	0.38	
								1.40	1.46±0.01	0.40		1.40	1.47±0.00	0.34	
												1.45	1.52±0.01	0.44	
												1.50	1.57±0.00	0.28	

NO.	NF	ACT.FREQ.	%ERR	NO.	NF	ACT.FREQ.	%ERR	NO.	NF	ACT.FREQ.	%ERR	NO.	NF	ACT.FREQ.	%ERR
67.1	1.15	1.20±0.02	1.44	72.1	1.15	1.21±0.02	1.42	78.1	1.15	1.19±0.01	0.49	84.1	1.15	1.19±0.00	0.41
	1.20	1.25±0.00	0.27		1.20	1.25±0.00	0.26		1.20	1.24±0.00	0.17		1.20	1.25±0.00	0.37
	1.25	1.30±0.00	0.19		1.25	1.31±0.00	0.37		1.25	1.30±0.00	0.28		1.25	1.31±0.00	0.30
	1.30	1.35±0.00	0.25		1.30	1.36±0.01	0.67		1.30	1.36±0.01	0.49		1.30	1.36±0.00	0.32
	1.35	1.41±0.00	0.32		1.35	1.42±0.01	0.61		1.35	1.41±0.00	0.25		1.35	1.41±0.01	0.80
	1.40	1.47±0.00	0.09		1.40	1.47±0.00	0.26		1.40	1.47±0.00	0.20		1.40	1.47±0.00	0.32
	1.45	1.53±0.00	0.28		1.45	1.53±0.01	0.37		1.45	1.52±0.01	0.41		1.45	1.53±0.01	0.42
	1.50	1.59±0.01	0.35		1.50	1.58±0.01	0.36		1.50	1.58±0.00	0.22		1.50	1.58±0.00	0.31
	1.55	1.64±0.00	0.23		1.55	1.64±0.01	0.42		1.55	1.63±0.00	0.30		1.55	1.64±0.00	0.19
	1.60	1.69±0.00	0.30	73.1	1.15	1.19±0.02	1.45		1.60	1.69±0.01	0.32		1.60	1.66±0.02	1.29
	1.65	1.76±0.01	0.49		1.20	1.25±0.01	1.20	79.1	1.15	1.20±0.00	0.21		1.65	1.76±0.01	0.31
	1.70	1.81±0.00	0.24		1.25	1.31±0.01	1.04		1.20	1.25±0.01	0.76	85.1	1.15	1.20±0.00	0.42
68.1	1.15	1.20±0.00	0.18		1.30	1.36±0.01	0.57		1.25	1.31±0.01	0.69		1.20	1.25±0.00	0.17
	1.20	1.25±0.01	0.88		1.35	1.41±0.00	0.31		1.30	1.36±0.00	0.30		1.25	1.30±0.02	1.30
	1.25	1.30±0.00	0.23		1.40	1.47±0.00	0.12		1.35	1.41±0.00	0.30		1.30	1.35±0.00	0.25
	1.30	1.36±0.00	0.21		1.45	1.52±0.01	0.41		1.40	1.47±0.00	0.13		1.35	1.41±0.01	0.37
	1.35	1.41±0.00	0.19		1.50	1.58±0.01	0.46		1.45	1.53±0.00	0.29		1.40	1.47±0.01	0.38
	1.40	1.47±0.00	0.10	74.1	1.15	1.20±0.01	0.60		1.50	1.59±0.01	0.70		1.45	1.53±0.01	0.44
	1.45	1.52±0.00	0.26		1.20	1.25±0.01	0.56		1.55	1.64±0.00	0.25		1.50	1.58±0.00	0.20
	1.50	1.58±0.00	0.18		1.25	1.31±0.01	1.01		1.60	1.71±0.01	0.78		1.55	1.64±0.01	0.40
	1.55	1.63±0.00	0.27		1.30	1.36±0.01	0.85		1.65	1.76±0.01	0.52		1.60	1.70±0.01	0.31
	1.60	1.69±0.01	0.34		1.35	1.41±0.01	0.47		1.70	1.81±0.01	0.52		1.65	1.75±0.01	0.39
	1.65	1.75±0.00	0.28		1.40	1.47±0.01	0.65		1.75	1.86±0.01	0.53	86.1	1.15	1.19±0.00	0.17
	1.70	1.80±0.01	0.29		1.45	1.54±0.02	1.19	80.1	1.15	1.20±0.01	0.43		1.20	1.25±0.01	0.41
	1.75	1.86±0.01	0.29		1.50	1.58±0.01	0.49		1.20	1.24±0.01	0.45		1.25	1.31±0.01	0.70
69.1	1.15	1.20±0.01	0.61		1.55	1.64±0.01	0.33		1.25	1.31±0.01	0.50		1.30	1.37±0.02	1.14
	1.20	1.25±0.00	0.26		1.60	1.70±0.01	0.45		1.30	1.36±0.01	0.45		1.35	1.41±0.00	0.22
	1.25	1.30±0.00	0.25		1.65	1.75±0.01	0.45		1.35	1.41±0.01	0.37		1.40	1.47±0.00	0.22
	1.30	1.36±0.00	0.17		1.70	1.81±0.01	0.58		1.40	1.47±0.00	0.28		1.45	1.52±0.01	0.34
	1.35	1.41±0.01	0.38	75.1	1.10	1.14±0.00	0.43		1.45	1.53±0.00	0.23		1.50	1.59±0.00	0.25
	1.40	1.47±0.00	0.09		1.15	1.20±0.00	0.36		1.50	1.58±0.00	0.20		1.55	1.64±0.01	0.56
	1.45	1.52±0.00	0.25		1.20	1.25±0.00	0.11		1.55	1.64±0.01	0.34		1.60	1.69±0.01	0.34
	1.50	1.58±0.00	0.28		1.25	1.31±0.00	0.36		1.60	1.69±0.00	0.28		1.65	1.75±0.01	0.30
	1.55	1.63±0.00	0.23		1.30	1.35±0.01	0.39		1.65	1.75±0.01	0.29		1.70	1.80±0.01	0.30
	1.60	1.69±0.00	0.19		1.35	1.41±0.00	0.22		1.70	1.81±0.01	0.33	87.1	1.15	1.20±0.01	0.56
	1.65	1.76±0.01	0.35		1.40	1.47±0.00	0.11		1.75	1.86±0.01	0.49		1.20	1.26±0.00	0.16
	1.70	1.81±0.01	0.42		1.45	1.52±0.00	0.28		1.80	1.92±0.03	1.35		1.25	1.30±0.00	0.27
	1.75	1.86±0.01	0.45		1.50	1.59±0.01	0.61	81.1	1.15	1.20±0.00	0.22		1.30	1.35±0.00	0.24
	1.80	1.92±0.01	0.28		1.55	1.64±0.01	0.39		1.20	1.25±0.00	0.33		1.35	1.42±0.01	0.37
70.1	1.15	1.19±0.00	0.41		1.60	1.69±0.00	0.21		1.25	1.31±0.00	0.28		1.40	1.47±0.00	0.23
	1.20	1.24±0.00	0.11	76.1	1.15	1.19±0.00	0.34		1.30	1.36±0.00	0.32		1.45	1.53±0.01	0.72
	1.25	1.30±0.00	0.22		1.20	1.24±0.01	0.95		1.35	1.41±0.01	0.40		1.50	1.59±0.01	0.61
	1.30	1.36±0.00	0.21		1.25	1.30±0.00	0.23		1.40	1.48±0.02	1.12		1.55	1.64±0.01	0.41
	1.35	1.41±0.00	0.25		1.30	1.37±0.01	0.56		1.45	1.53±0.01	0.44		1.60	1.69±0.02	1.04
	1.40	1.47±0.00	0.19		1.35	1.41±0.00	0.20		1.50	1.57±0.00	0.29	88.1	1.15	1.20±0.00	0.19
	1.45	1.53±0.01	0.55		1.40	1.47±0.00	0.10	82.1	1.15	1.19±0.00	0.26		1.20	1.25±0.00	0.10
	1.50	1.57±0.00	0.28		1.45	1.52±0.01	0.35		1.20	1.25±0.02	1.25		1.25	1.31±0.00	0.25
	1.55	1.63±0.01	0.55		1.50	1.59±0.00	0.21		1.25	1.30±0.01	0.44		1.30	1.36±0.00	0.34
	1.60	1.69±0.01	0.75		1.55	1.64±0.01	0.56		1.30	1.35±0.01	0.51		1.35	1.41±0.00	0.21
	1.65	1.75±0.01	0.40		1.60	1.70±0.00	0.25		1.35	1.41±0.00	0.32		1.40	1.47±0.00	0.16
	1.70	1.80±0.00	0.23		1.65	1.75±0.01	0.42		1.40	1.47±0.01	0.40		1.45	1.54±0.01	0.69
	1.75	1.87±0.01	0.64		1.70	1.81±0.01	0.63		1.45	1.52±0.01	0.44		1.50	1.58±0.01	0.33
71.1	1.15	1.20±0.00	0.39	77.1	1.15	1.19±0.01	0.43		1.50	1.58±0.00	0.25		1.55	1.65±0.02	1.01
	1.20	1.25±0.00	0.33		1.20	1.25±0.00	0.15	83.1	1.15	1.19±0.00	0.22	89.1	1.15	1.20±0.00	0.31
	1.25	1.31±0.00	0.26		1.25	1.30±0.00	0.26		1.20	1.24±0.01	0.49		1.20	1.25±0.00	0.09
	1.30	1.36±0.00	0.31		1.30	1.36±0.00	0.17		1.25	1.30±0.00	0.17		1.25	1.31±0.01	0.88
	1.35	1.42±0.00	0.27		1.35	1.41±0.00	0.26		1.30	1.36±0.00	0.27		1.30	1.37±0.01	1.00
	1.40	1.47±0.00	0.20		1.40	1.46±0.00	0.18		1.35	1.41±0.00	0.32		1.35	1.41±0.00	0.31
	1.45	1.53±0.02	1.44		1.45	1.52±0.01	0.38		1.40	1.46±0.01	0.54		1.40	1.47±0.01	0.94
	1.50	1.58±0.00	0.15		1.50	1.58±0.00	0.19		1.45	1.52±0.01	0.53		1.45	1.54±0.01	0.69
	1.55	1.63±0.01	0.38						1.50	1.58±0.01	0.34		1.50	1.60±0.01	0.86
									1.55	1.63±0.01	0.35		1.55	1.63±0.00	0.28
									1.60	1.69±0.01	0.39		1.60	1.70±0.00	0.26
													1.65	1.75±0.01	0.42
													1.70	1.79±0.01	0.49

NO.	NF	ACT.FREQ.	%ERR	NO.	NF	ACT.FREQ.	%ERR	NO.	NF	ACT.FREQ.	%ERR	NO.	NF	ACT.FREQ.	%ERR
90.	1.15	1.20±0.00	0.20	99.	1.15	1.20±0.01	0.72	111.	1.15	1.20±0.01	0.79	124.	1.25	1.31±0.00	0.16
	1.20	1.25±0.01	0.82		1.20	1.24±0.02	1.23		1.20	1.24±0.01	0.76		1.30	1.36±0.00	0.26
	1.25	1.30±0.00	0.30		1.25	1.30±0.01	0.57		1.25	1.30±0.01	0.40		1.35	1.41±0.01	0.85
	1.30	1.35±0.01	0.42		1.30	1.35±0.01	0.40		1.30	1.36±0.00	0.20		1.40	1.47±0.00	0.17
	1.35	1.41±0.00	0.19		1.35	1.42±0.01	0.40		1.35	1.41±0.01	0.58		1.45	1.52±0.00	0.29
	1.40	1.47±0.00	0.24		1.40	1.47±0.00	0.09		1.35	1.41±0.01	0.44	125.	1.25	1.30±0.01	0.58
	1.45	1.53±0.01	0.49	100.	1.15	1.20±0.01	0.49	112.	1.15	1.19±0.01	0.77		1.30	1.37±0.01	1.06
	1.50	1.58±0.00	0.27		1.20	1.25±0.01	0.77		1.20	1.24±0.00	0.27		1.35	1.41±0.00	0.26
	1.55	1.64±0.01	0.37		1.25	1.31±0.00	0.35		1.25	1.31±0.01	0.60		1.40	1.46±0.00	0.27
	1.60	1.69±0.00	0.26		1.30	1.36±0.02	1.19		1.30	1.36±0.01	0.55		1.45	1.52±0.01	0.33
	1.65	1.75±0.01	0.38		1.35	1.41±0.01	1.06	113.	1.15	1.19±0.00	0.35	126.	1.25	1.30±0.01	0.46
	1.70	1.81±0.01	0.32		1.40	1.47±0.00	0.31		1.20	1.24±0.00	0.23		1.30	1.35±0.00	0.37
91.	1.15	1.19±0.00	0.13	101.	1.15	1.19±0.00	0.33		1.25	1.30±0.01	0.67		1.35	1.41±0.01	0.38
	1.20	1.25±0.01	0.77		1.20	1.24±0.00	0.38		1.30	1.36±0.01	0.99		1.40	1.48±0.01	0.67
	1.25	1.31±0.01	0.54		1.25	1.30±0.01	0.48		1.35	1.41±0.00	0.31	127.	1.25	1.30±0.00	0.21
	1.30	1.36±0.01	0.66		1.30	1.35±0.01	0.44	114.	1.15	1.20±0.00	0.30		1.30	1.35±0.00	0.18
	1.35	1.42±0.01	0.39		1.35	1.42±0.01	0.39		1.20	1.25±0.00	0.17		1.35	1.43±0.01	0.70
	1.40	1.47±0.00	0.14		1.40	1.46±0.01	0.57		1.25	1.32±0.01	0.92		1.40	1.46±0.00	0.16
	1.45	1.52±0.02	1.15		1.45	1.52±0.01	0.56		1.30	1.35±0.01	0.48	128.	1.25	1.30±0.00	0.24
	1.50	1.57±0.00	0.16	102.	1.10	1.14±0.00	0.13		1.35	1.41±0.00	0.27		1.30	1.35±0.00	0.37
	1.55	1.64±0.01	0.47		1.15	1.19±0.00	0.16	115.	1.15	1.20±0.00	0.39		1.35	1.41±0.01	0.40
	1.60	1.69±0.00	0.26		1.20	1.25±0.00	0.20		1.20	1.25±0.00	0.19	129.	1.25	1.30±0.01	0.45
92.	1.15	1.19±0.00	0.40		1.25	1.31±0.00	0.32		1.25	1.30±0.00	0.32		1.30	1.36±0.01	0.58
	1.20	1.24±0.00	0.30		1.30	1.36±0.01	0.49		1.30	1.35±0.01	0.76		1.35	1.41±0.01	0.89
	1.25	1.30±0.01	0.45		1.35	1.41±0.01	0.47		1.35	1.41±0.00	0.31		1.40	1.46±0.02	1.06
	1.30	1.36±0.01	0.71	103.	1.10	1.14±0.00	0.15	116.	1.15	1.19±0.01	0.64		1.45	1.54±0.02	1.22
	1.35	1.42±0.01	0.45		1.15	1.19±0.00	0.07		1.20	1.24±0.01	0.41	130.	1.25	1.30±0.01	0.59
	1.40	1.47±0.01	0.54		1.20	1.24±0.00	0.17		1.25	1.30±0.00	0.22		1.30	1.35±0.01	0.43
	1.45	1.53±0.01	0.44		1.25	1.30±0.00	0.32		1.30	1.35±0.01	0.65		1.35	1.41±0.00	0.33
	1.50	1.58±0.00	0.31		1.30	1.36±0.01	0.37		1.35	1.41±0.01	0.37		1.40	1.46±0.02	1.26
	1.55	1.63±0.01	0.34		1.35	1.41±0.01	0.64	117.	1.15	1.19±0.00	0.33		1.45	1.53±0.02	1.13
	1.60	1.70±0.01	0.41	104.	1.15	1.20±0.00	0.20		1.20	1.24±0.00	0.28	131.	1.25	1.30±0.01	0.48
	1.65	1.76±0.01	0.38		1.20	1.25±0.00	0.19		1.25	1.29±0.00	0.29		1.30	1.35±0.01	1.02
93.	1.15	1.20±0.01	0.63		1.25	1.31±0.01	0.47		1.30	1.35±0.01	0.40		1.35	1.39±0.02	1.39
	1.20	1.25±0.01	0.52		1.30	1.35±0.01	0.79		1.35	1.42±0.01	0.67		1.40	1.47±0.01	0.73
	1.25	1.30±0.01	0.56		1.35	1.41±0.01	1.03		1.40	1.47±0.00	0.28		1.45	1.52±0.01	0.46
	1.30	1.36±0.01	0.94	105.	1.10	1.13±0.01	0.73	118.	1.25	1.30±0.00	0.28	132.	1.25	1.30±0.01	0.54
	1.35	1.41±0.01	0.85		1.15	1.19±0.01	0.46		1.30	1.35±0.01	0.79		1.30	1.36±0.01	0.57
94.	1.10	1.13±0.00	0.39		1.20	1.24±0.01	0.44		1.35	1.41±0.01	0.42		1.35	1.41±0.00	0.23
	1.15	1.19±0.02	1.47		1.25	1.30±0.01	0.41		1.40	1.46±0.01	0.54		1.40	1.46±0.00	0.23
	1.20	1.25±0.01	0.99		1.30	1.35±0.01	0.41		1.45	1.53±0.00	0.21		1.45	1.52±0.01	0.64
	1.25	1.31±0.01	0.51		1.35	1.41±0.00	0.29	119.	1.25	1.30±0.01	1.07		1.50	1.58±0.01	0.40
	1.30	1.36±0.01	1.02	106.	1.10	1.14±0.00	0.18		1.30	1.36±0.01	0.56	133.	1.25	1.30±0.01	0.69
	1.35	1.41±0.02	1.27		1.15	1.20±0.00	0.16		1.35	1.41±0.01	0.36		1.30	1.36±0.01	0.41
95.	1.10	1.14±0.01	0.61		1.20	1.25±0.00	0.05		1.40	1.46±0.00	0.31		1.35	1.41±0.00	0.32
	1.15	1.20±0.01	0.90		1.25	1.31±0.01	0.43		1.45	1.52±0.01	0.56		1.40	1.46±0.00	0.24
	1.20	1.25±0.01	0.41		1.30	1.36±0.02	1.12	120.	1.25	1.30±0.01	0.91		1.45	1.52±0.01	0.42
	1.25	1.31±0.01	1.06		1.35	1.42±0.01	0.87		1.30	1.35±0.02	1.18	134.	1.25	1.30±0.01	0.46
	1.30	1.36±0.01	0.87	107.	1.15	1.18±0.00	0.18		1.35	1.41±0.00	0.23		1.30	1.36±0.00	0.23
	1.35	1.41±0.01	0.60		1.20	1.25±0.00	0.17		1.40	1.46±0.01	0.46		1.35	1.41±0.01	0.39
	1.40	1.46±0.01	0.67		1.25	1.30±0.01	0.80		1.45	1.55±0.03	1.90		1.40	1.46±0.01	1.01
96.	1.15	1.19±0.01	0.98		1.30	1.35±0.00	0.25	121.	1.25	1.30±0.00	0.30		1.45	1.52±0.00	0.22
	1.20	1.24±0.01	0.70		1.35	1.42±0.01	0.37		1.30	1.36±0.01	0.74	135.	1.25	1.31±0.01	0.60
	1.25	1.30±0.01	0.72	108.	1.15	1.20±0.01	0.91		1.35	1.40±0.01	0.68		1.30	1.35±0.01	0.56
	1.30	1.35±0.01	0.57		1.20	1.25±0.00	0.24		1.40	1.46±0.00	0.23		1.35	1.42±0.01	0.83
	1.35	1.41±0.00	0.28		1.25	1.30±0.01	0.53		1.45	1.52±0.01	0.51		1.40	1.47±0.01	0.66
97.	1.15	1.19±0.01	0.86		1.30	1.36±0.01	0.96	122.	1.25	1.29±0.01	0.63		1.45	1.52±0.01	0.66
	1.20	1.25±0.01	0.54		1.35	1.41±0.02	1.08		1.30	1.35±0.01	0.42	136.	1.25	1.30±0.00	0.30
	1.25	1.30±0.01	0.42	109.	1.15	1.19±0.01	0.74		1.35	1.41±0.01	0.45		1.30	1.35±0.01	0.58
	1.30	1.36±0.01	0.70		1.20	1.25±0.01	0.95		1.40	1.46±0.01	0.38		1.35	1.41±0.01	0.96
	1.35	1.41±0.01	0.59	110.	1.15	1.19±0.00	0.38		1.45	1.52±0.01	0.50		1.40	1.46±0.02	1.28
	1.40	1.47±0.01	0.92		1.20	1.25±0.01	0.84		1.50	1.58±0.00	0.28		1.45	1.52±0.01	0.46
98.	1.15	1.19±0.01	0.43		1.25	1.30±0.01	0.62	123.	1.25	1.30±0.00	0.33	137.	1.20	1.24±0.00	0.22
	1.20	1.24±0.01	0.60		1.30	1.36±0.01	0.52		1.30	1.33±0.02	1.27		1.25	1.30±0.00	0.21
	1.25	1.31±0.01	1.07		1.35	1.41±0.00	0.27		1.35	1.41±0.01	0.44		1.30	1.36±0.00	0.21
	1.30	1.36±0.01	1.10						1.40	1.47±0.01	0.36		1.35	1.41±0.01	0.45
	1.35	1.41±0.01	0.55						1.45	1.52±0.01	0.43		1.40	1.47±0.01	0.38
	1.40	1.47±0.00	0.24						1.50	1.57±0.00	0.30		1.45	1.53±0.01	0.51

NO.	NF	ACT.FREQ.	XERR	NO.	NF	ACT.FREQ.	XERR	NO.	NF	ACT.FREQ.	XERR	NO.	NF	ACT.FREQ.	XERR
193.	1.60	1.69±0.01	0.59	198.	1.60	1.68±0.02	1.04	203.	1.55	1.64±0.01	0.50	209.	1.65	1.75±0.01	0.39
	1.65	1.75±0.02	1.41		1.65	1.75±0.01	0.61		1.60	1.69±0.01	0.77		1.70	1.80±0.01	0.42
	1.70	1.81±0.01	0.40		1.70	1.80±0.02	1.19		1.65	1.74±0.02	1.37		1.75	1.86±0.01	0.57
	1.75	1.86±0.01	0.79		1.75	1.86±0.01	0.62		1.70	1.79±0.02	1.02		1.80	1.92±0.02	1.00
	1.80	1.92±0.02	0.97		1.80	1.92±0.01	0.45		1.75	1.86±0.02	1.01		1.85	2.00±0.03	1.28
	1.85	1.98±0.02	0.79		1.85	1.99±0.02	0.85		1.80	1.92±0.01	0.57		1.90	2.03±0.02	0.75
	1.90	2.03±0.02	0.99		1.90	2.03±0.01	0.73		1.85	1.97±0.01	0.72		1.95	2.09±0.01	0.49
	1.95	2.09±0.03	1.47		1.95	2.09±0.01	0.30		1.90	2.05±0.03	1.32		2.00	2.18±0.03	1.48
	2.00	2.15±0.02	1.00		2.00	2.15±0.01	0.43		1.95	2.10±0.03	1.23		2.05	2.20±0.01	0.42
	2.05	2.20±0.03	1.26		2.05	2.20±0.01	0.44		2.00	2.15±0.02	0.88		2.10	2.29±0.02	0.89
	2.10	2.26±0.02	0.89		2.10	2.26±0.00	0.16		2.05	2.21±0.01	0.65		2.15	2.31±0.02	1.08
	2.15	2.32±0.03	1.10		2.15	2.32±0.01	0.26	204.	1.55	1.63±0.01	0.42	210.	1.65	1.75±0.01	0.69
	2.20	2.37±0.01	0.63		2.20	2.37±0.01	0.46		1.60	1.72±0.02	1.36		1.70	1.81±0.01	0.46
194.	1.60	1.69±0.01	0.63	199.	1.60	1.69±0.01	0.76		1.65	1.74±0.02	0.87		1.75	1.87±0.02	0.88
	1.65	1.75±0.01	0.56		1.65	1.75±0.01	0.77		1.70	1.80±0.01	0.61		1.80	1.91±0.02	0.83
	1.70	1.80±0.01	0.50		1.70	1.81±0.02	0.91		1.75	1.86±0.01	0.35		1.85	1.97±0.02	0.99
	1.75	1.88±0.02	0.85		1.75	1.86±0.01	0.80		1.80	1.92±0.01	0.45		1.90	2.02±0.02	1.17
	1.80	1.92±0.01	0.67		1.80	1.92±0.02	0.96		1.85	1.98±0.01	0.62		1.95	2.09±0.01	0.31
	1.85	1.97±0.02	0.96		1.85	1.97±0.02	0.99		1.90	2.04±0.01	0.57		2.00	2.15±0.02	0.75
	1.90	2.03±0.02	1.17		1.90	2.03±0.02	1.05		1.95	2.09±0.01	0.68		2.05	2.29±0.01	0.67
	1.95	2.09±0.03	1.67		1.95	2.10±0.03	1.38		2.00	2.14±0.01	0.58		2.10	2.26±0.01	0.42
	2.00	2.15±0.03	1.24		2.00	2.14±0.03	1.35		2.05	2.20±0.01	0.57		2.15	2.31±0.02	0.73
	2.05	2.20±0.03	1.20		2.05	2.21±0.03	1.46		2.10	2.30±0.02	1.06	211.	1.65	1.75±0.01	0.41
	2.10	2.26±0.02	0.99		2.10	2.26±0.02	0.96	205.	1.70	1.81±0.01	0.82		1.70	1.81±0.01	0.28
195.	1.60	1.70±0.02	0.92		2.15	2.30±0.04	1.87		1.75	1.87±0.02	1.33		1.75	1.89±0.02	1.10
	1.65	1.75±0.01	0.57		2.20	2.39±0.01	0.60		1.80	1.92±0.00	0.18		1.80	1.92±0.01	0.29
	1.70	1.80±0.01	0.48		2.25	2.42±0.01	0.39		1.85	2.00±0.02	0.83		1.85	1.98±0.01	0.44
	1.75	1.86±0.01	0.47	200.	1.60	1.70±0.01	0.79		1.90	2.03±0.02	1.06		1.90	2.03±0.01	0.55
	1.80	1.92±0.01	0.44		1.65	1.75±0.01	0.73		1.95	2.09±0.01	0.59		1.95	2.09±0.00	0.11
	1.85	1.97±0.01	0.30		1.70	1.84±0.03	1.52		2.00	2.14±0.02	0.87		2.00	2.17±0.03	1.24
	1.90	2.03±0.02	1.15		1.75	1.86±0.02	0.81		2.05	2.25±0.03	1.37		2.05	2.21±0.01	0.37
	1.95	2.10±0.01	0.60		1.80	1.93±0.02	0.95		2.10	2.26±0.01	0.49	212.	1.60	1.69±0.01	0.34
	2.00	2.15±0.04	1.66		1.85	1.99±0.02	0.95		2.15	2.31±0.02	0.86		1.65	1.75±0.01	0.37
	2.05	2.20±0.02	0.75		1.90	2.03±0.02	0.78		2.20	2.40±0.03	1.31		1.70	1.80±0.00	0.16
	2.10	2.26±0.01	0.24		1.95	2.08±0.01	0.29		2.25	2.42±0.01	0.58		1.75	1.86±0.01	0.29
	2.15	2.32±0.01	0.27		2.00	2.15±0.01	0.32	206.	1.70	1.82±0.02	1.07		1.80	1.92±0.00	0.17
196.	1.60	1.70±0.01	0.77		2.05	2.25±0.04	1.95		1.75	1.87±0.01	0.74		1.85	1.97±0.01	0.36
	1.65	1.77±0.03	1.84		2.10	2.25±0.01	0.36		1.80	1.92±0.02	1.27		1.90	2.03±0.01	0.40
	1.70	1.80±0.02	1.34		2.15	2.33±0.02	1.04		1.85	1.98±0.02	0.99	213.	1.60	1.71±0.02	1.19
	1.75	1.86±0.02	1.21		2.20	2.36±0.01	0.60		1.90	2.03±0.02	0.85		1.65	1.75±0.01	0.30
	1.80	1.92±0.02	0.98		2.25	2.42±0.01	0.59		1.95	2.11±0.02	0.96		1.70	1.81±0.01	0.39
	1.85	2.01±0.02	0.90	201.	1.60	1.71±0.01	0.77		2.00	2.16±0.01	0.53		1.75	1.86±0.01	0.74
	1.90	2.03±0.02	1.07		1.65	1.74±0.01	0.73		2.05	2.21±0.01	0.57		1.80	1.91±0.02	0.86
	1.95	2.09±0.03	1.31		1.70	1.80±0.02	1.29		2.10	2.26±0.01	0.57		1.85	1.97±0.01	0.47
	2.00	2.14±0.02	1.09		1.75	1.86±0.02	0.84	207.	1.70	1.81±0.01	0.65		1.90	2.03±0.02	0.91
	2.05	2.20±0.01	0.50		1.80	1.92±0.02	1.15		1.75	1.85±0.02	1.17		1.95	2.09±0.02	1.17
	2.10	2.26±0.01	0.31		1.85	1.98±0.01	0.66		1.80	1.92±0.02	1.09		2.00	2.15±0.02	0.81
197.	1.60	1.70±0.01	0.56		1.85	1.98±0.01	0.66		1.85	1.97±0.02	1.25		2.05	2.21±0.01	0.58
	1.65	1.77±0.03	1.73		1.90	2.03±0.02	0.83		1.90	2.03±0.03	1.44		2.10	2.25±0.03	1.14
	1.70	1.80±0.01	0.79		1.95	2.09±0.02	1.05		1.95	2.09±0.02	1.17		2.15	2.32±0.02	0.72
	1.75	1.86±0.01	0.52		2.00	2.15±0.01	0.51		2.00	2.15±0.02	0.81		2.20	2.29±0.02	0.89
	1.80	1.92±0.00	0.13		2.05	2.23±0.01	0.64		2.05	2.21±0.01	0.58		2.25	2.34±0.01	0.67
	1.85	1.98±0.01	0.41		2.10	2.26±0.00	0.20		2.10	2.25±0.03	1.14		1.90	2.03±0.01	0.45
	1.90	2.03±0.01	0.43	202.	1.55	1.64±0.01	0.48		2.15	2.32±0.02	0.72		1.95	2.08±0.02	1.06
	1.95	2.09±0.01	0.28		1.60	1.69±0.01	0.43		2.20	2.37±0.01	0.65	215.	1.60	1.69±0.01	0.60
	2.00	2.15±0.01	0.50		1.65	1.75±0.01	0.40	208.	1.70	1.82±0.03	1.44		1.65	1.75±0.01	0.46
	2.05	2.19±0.01	0.51		1.70	1.80±0.01	0.35		1.75	1.87±0.01	0.73		1.70	1.81±0.00	0.27
	2.10	2.26±0.01	0.25		1.75	1.86±0.01	0.30		1.80	1.92±0.03	1.33		1.75	1.86±0.01	0.53
					1.80	1.92±0.00	0.12		1.85	1.99±0.03	1.31		1.80	1.92±0.00	0.11
					1.85	1.97±0.02	1.20		1.90	2.04±0.02	1.06		1.85	1.98±0.01	0.29
					1.90	2.04±0.01	0.36		1.95	2.09±0.03	1.25		2.00	2.17±0.04	1.63
					1.95	2.09±0.00	0.14		2.00	2.17±0.04	1.63	216.	1.70	1.81±0.01	0.37
					2.00	2.15±0.01	0.38		2.05	2.21±0.02	1.02		1.75	1.87±0.01	0.52
					2.05	2.20±0.01	0.42		2.10	2.27±0.01	0.60		1.80	1.95±0.03	1.58
									2.15	2.32±0.02	0.85		1.85	1.98±0.01	0.26
													1.90	2.03±0.01	0.53
													1.95	2.09±0.01	0.51
													2.00	2.14±0.02	1.16

NO.	NF	ACT.FREQ.	%ERR	NO.	NF	ACT.FREQ.	%ERR	NO.	NF	ACT.FREQ.	%ERR	NO.	NF	ACT.FREQ.	%ERR
217.	1.65	1.75±0.00	0.19												
	1.70	1.80±0.01	0.28												
	1.75	1.86±0.01	0.49												
	1.80	1.92±0.01	0.48												
	1.85	1.97±0.01	0.54												
	1.90	2.04±0.01	0.36												
	1.95	2.09±0.01	0.25												
	2.00	2.16±0.02	0.80												
	2.05	2.21±0.01	0.41												
218.	1.65	1.75±0.02	1.08												
	1.70	1.81±0.01	0.62												
	1.75	1.87±0.02	1.26												
	1.80	1.92±0.00	0.25												
	1.85	1.98±0.02	1.03												
219.	1.70	1.81±0.02	1.08												
	1.75	1.87±0.03	1.43												
	1.80	1.92±0.01	0.55												
	1.85	1.97±0.01	0.30												
	1.90	2.04±0.01	0.44												
	1.95	2.10±0.03	1.53												
220.	1.65	1.75±0.02	1.31												
	1.70	1.81±0.01	0.32												
	1.75	1.86±0.01	0.44												
	1.80	1.92±0.01	0.41												
	1.85	1.99±0.02	0.82												
	1.90	2.03±0.01	0.59												
	1.95	2.09±0.01	0.37												
	2.00	2.15±0.01	0.55												
	2.05	2.19±0.01	0.64												
	2.10	2.26±0.01	0.28												
	2.15	2.34±0.02	1.00												
221.	1.60	1.69±0.01	0.50												
	1.65	1.75±0.01	0.77												
	1.70	1.81±0.01	0.82												
	1.75	1.87±0.01	0.74												
	1.80	1.92±0.00	0.23												
	1.85	1.98±0.01	0.33												
	1.90	2.03±0.01	0.32												
	1.95	2.09±0.01	0.42												
	2.00	2.14±0.01	0.57												
	2.05	2.21±0.01	0.66												

F.5 Magnitude of External Load

It is verified in Appendix B that the system of a wire excited into galloping motion by the moving hydraulic actuators as shown in Fig. 3-3 is equivalent to that of a simply-supported wire under uniform external load of the magnitude $m\Omega^2 Z$, where

m =unit mass of the wire,

Ω =frequency of the base motion, and

Z =amplitude of the base motion.

From Equation D-2, Table F-3, and Table F-10, the 95% confidence interval for the mean of the magnitudes of the external loads for all tests listed in Appendix A can be obtained. For instance, consider the 46.6' steel wire S1 hanging on 46' span and vibrating at 1.05 Hz of nominal frequency (Test No.1 in Appendix A). The 95% confidence interval for the mean of the unit weight is 0.0021266 ± 0.0000010 lb/in from Table F-3. Since the t-value is 1.99 and the acceleration of gravity equals 32.2 ft/sec^2 , the mean and standard error of the unit mass become

$$\begin{aligned} \bar{m} &= 0.00079252 \text{ lb-sec}^2/\text{ft}^2 \\ \text{and } SE_m &= 0.00000019 \text{ lb-sec}^2/\text{ft}^2 \end{aligned}$$

, respectively. On the other hand, the mean and standard error of the actual frequency corresponding to 1.05 Hz of nominal frequency are ,as referring to Table F-10,

$$\begin{aligned} \bar{\Omega} &= 1.075 \text{ Hz} \\ \text{and } SE_{\Omega} &= 0.003 \text{ Hz} \end{aligned}$$

, respectively. Since Z was measured as $3-11/16''$ or $0.3073'$, the mean and standard error of the magnitude of the external load, P, which equals $m\Omega^2 Z$, are calculated from Equation D-2 as

$$\begin{aligned}\bar{P} &= \bar{m}\bar{\Omega}^2 Z = (0.00079252)(1.075 * 2\pi)(0.3073) = 0.01111 \text{ lb/ft} \\ SE_P &= \left\{ \left(\frac{1}{\bar{m}} SE_m \right)^2 + \left(\frac{2}{\bar{\Omega}} SE_{\Omega} \right)^2 \right\}^{1/2} \bar{P} \\ &= \left\{ \left(\frac{1}{0.00079252} * 0.00000019 \right)^2 + \left(\frac{2}{1.075} * 0.003 \right)^2 \right\}^{1/2} * 0.01111 \\ &= 0.00006 \text{ lb/ft, respectively.}\end{aligned}$$

Then the 95% confidence interval for the mean of the magnitude of the external load is

$$\bar{P} \pm t_{2.5\%, 104} SE_P = 0.01111 \pm 1.985 * 0.00006 = 0.0111 \pm 0.0001 \text{ lb/ft}$$

, where the t-value for 104 DOFs is 1.985. The 104 DOFs are calculated from 90+14, where

- (a) 90 is the total DOFs for the length measurements as shown in Table F-3, and
- (b) 14 is the total DOFs for the frequency measurements as mentioned in Section F-4.

Then the maximum percentage measurement error of the magnitude of the external load for steel wire S1 at Test No.1 under 1.05 Hz of nominal frequency is

$$0.0001/0.0111, \text{ or } 0.90\%.$$

Similarly, the 95% confidence intervals for the means of the magnitudes of the external loads and the corresponding maximum percentage measurement errors for other tests are obtained. The results are listed in Table F-11. The average of the maximum percentage measurement error is calculated as **1.06%**.

Table F-11: The 95% confidence intervals of the mean of magnitude of external load (lb/ft) and the corresponding max. % measurement error at each nominal frequency (Hz) for the 221 tests listed in Appendix A.

NO.	NF	LOAD(*E-2)	%ERR	NO.	NF	LOAD(*E-2)	%ERR	NO.	NF	LOAD(*E-2)	%ERR	NO.	NF	LOAD(*E-2)	%ERR
1.1.05	1.11±0.01	0.90		10.1.05	0.44±0.01	1.47		19.1.10	1.44±0.01	0.70		29.1.10	0.49±0.01	2.80	
1.1.10	1.23±0.03	2.10		1.1.10	0.49±0.01	1.39		1.15	1.59±0.02	1.00		1.15	0.53±0.01	1.01	
1.1.15	1.37±0.03	2.32		1.15	0.54±0.00	0.04		1.20	1.74±0.01	0.64		1.20	0.59±0.01	0.96	
1.2.0	1.48±0.02	1.59		1.2.0	0.58±0.00	0.32		1.25	1.89±0.02	1.22		1.25	0.64±0.01	0.92	
1.25	1.62±0.01	0.61		1.25	0.64±0.01	1.22		1.30	2.06±0.02	1.17		1.30	0.69±0.00	0.29	
1.30	1.77±0.01	0.59		1.30	0.70±0.00	0.29		20.1.10	1.45±0.01	0.70		1.35	0.76±0.01	1.12	
2.1.05	1.31±0.01	1.10		1.35	0.75±0.00	0.56		1.15	1.50±0.04	2.74		1.40	0.81±0.00	0.27	
1.10	1.47±0.02	1.04		11.1.05	0.98±0.01	0.73		1.20	1.72±0.01	0.64		30.1.15	1.31±0.01	0.67	
1.15	1.60±0.02	1.32		1.10	1.09±0.00	0.35		1.25	1.90±0.02	0.91		1.20	1.43±0.02	1.28	
1.20	1.74±0.03	1.59		1.15	1.20±0.00	0.33		1.30	2.06±0.01	0.59		1.25	1.55±0.01	0.61	
1.25	1.88±0.01	0.61		1.20	1.30±0.01	0.64		1.35	2.24±0.01	0.56		1.30	1.70±0.01	0.29	
1.30	2.04±0.02	1.17		1.25	1.42±0.01	0.61		21.1.10	0.72±0.00	0.35		1.35	1.84±0.01	0.56	
3.1.05	1.29±0.02	1.48		1.30	1.55±0.01	0.59		1.15	0.79±0.01	1.33		31.1.10	1.19±0.02	1.40	
1.10	1.38±0.01	0.71		12.1.05	0.99±0.01	0.73		1.20	0.86±0.02	2.24		1.15	1.31±0.00	0.33	
1.15	1.58±0.01	0.33		1.10	1.08±0.01	0.70		1.25	0.94±0.01	0.61		1.20	1.43±0.01	0.96	
1.20	1.73±0.01	0.32		1.15	1.19±0.00	0.34		1.30	1.02±0.00	0.29		1.25	1.56±0.01	0.61	
1.25	1.90±0.01	0.61		1.20	1.30±0.00	0.32		1.35	1.11±0.01	0.56		1.30	1.69±0.00	0.29	
1.30	2.07±0.03	1.46		1.25	1.42±0.00	0.31		22.1.10	1.68±0.02	1.04		1.35	1.87±0.02	0.84	
1.35	2.24±0.02	0.84		1.30	1.55±0.01	0.88		1.15	1.83±0.02	0.99		32.1.10	0.59±0.00	0.70	
4.1.05	0.65±0.01	1.11		1.35	1.68±0.01	0.56		1.20	2.00±0.03	1.59		1.15	0.66±0.01	1.66	
1.10	0.72±0.01	1.05		13.1.05	0.54±0.00	0.37		1.25	2.18±0.01	0.31		1.20	0.72±0.00	0.32	
1.15	0.81±0.02	1.98		1.10	0.59±0.00	0.70		1.30	2.35±0.01	0.58		1.25	0.78±0.00	0.61	
1.20	0.86±0.00	0.32		1.15	0.65±0.00	0.33		1.35	2.55±0.01	0.56		1.30	0.84±0.01	0.88	
1.25	0.94±0.00	0.31		1.20	0.71±0.00	0.03		23.1.10	1.72±0.05	2.73		1.35	0.92±0.01	0.56	
1.30	1.02±0.01	0.59		1.25	0.78±0.00	0.61		1.15	1.82±0.01	0.67		33.1.10	1.08±0.00	0.35	
5.1.05	1.48±0.02	1.48		1.30	0.85±0.00	0.59		1.20	1.99±0.02	0.95		1.15	1.20±0.02	1.99	
1.10	1.63±0.01	0.70		1.35	0.91±0.01	0.56		1.25	2.15±0.03	1.22		1.20	1.31±0.01	0.95	
1.15	1.81±0.01	0.33		14.1.05	1.35±0.01	0.74		1.30	2.34±0.01	0.59		1.25	1.42±0.01	0.61	
1.20	1.97±0.02	0.96		1.10	1.50±0.01	0.70		1.35	2.56±0.02	0.84		1.30	1.54±0.00	0.29	
1.25	2.17±0.05	2.13		1.15	1.65±0.01	0.66		24.1.10	0.92±0.00	0.35		1.35	1.67±0.01	0.56	
1.30	2.34±0.02	0.88		1.20	1.80±0.01	0.32		1.15	1.02±0.01	0.67		34.1.10	1.51±0.01	0.35	
1.35	2.57±0.06	2.23		1.25	1.96±0.02	0.92		1.20	1.11±0.01	0.96		1.15	1.66±0.01	0.66	
6.1.05	1.31±0.02	1.84		1.30	2.13±0.01	0.29		1.25	1.21±0.01	0.61		1.20	1.83±0.02	0.95	
1.10	1.44±0.01	0.70		15.1.05	1.51±0.01	0.73		1.30	1.32±0.01	0.88		1.25	1.97±0.01	0.31	
1.15	1.61±0.01	0.67		1.10	1.67±0.01	0.69		1.35	1.46±0.03	1.95		1.30	2.13±0.01	0.29	
1.20	1.79±0.01	0.63		1.15	1.85±0.01	0.66		25.1.10	1.49±0.05	3.12		35.1.15	1.66±0.01	0.34	
1.25	1.93±0.02	0.91		1.20	2.01±0.01	0.63		1.15	1.62±0.03	1.66		1.20	1.82±0.01	0.32	
1.30	2.09±0.03	1.46		1.25	2.19±0.01	0.61		1.20	1.76±0.03	1.59		1.25	1.98±0.01	0.61	
1.35	2.26±0.03	1.12		1.30	2.34±0.01	0.59		1.25	1.94±0.01	0.61		1.30	2.16±0.01	0.29	
7.1.05	1.32±0.03	2.20		16.1.05	0.83±0.00	0.37		1.30	2.12±0.02	1.16		1.35	2.34±0.01	0.28	
1.10	1.47±0.03	1.74		1.10	0.93±0.00	0.35		1.35	2.31±0.03	1.39		1.40	2.52±0.01	0.27	
1.15	1.60±0.04	2.67		1.15	1.02±0.00	0.33		1.40	2.46±0.01	0.27		1.45	2.72±0.02	0.78	
1.20	1.76±0.03	1.91		1.20	1.12±0.01	0.64		26.1.10	1.46±0.03	1.75		36.1.15	1.67±0.01	0.33	
1.25	1.92±0.01	0.61		1.25	1.22±0.01	0.61		1.15	1.60±0.03	1.67		1.20	1.84±0.01	0.64	
1.30	2.09±0.01	0.29		1.30	1.32±0.00	0.29		1.20	1.76±0.01	0.64		1.25	2.00±0.01	0.31	
1.35	2.26±0.02	0.84		17.1.05	1.08±0.00	0.37		1.25	1.92±0.02	0.91		1.30	2.21±0.04	1.74	
1.40	2.46±0.03	1.35		1.10	1.19±0.00	0.35		1.30	2.09±0.02	1.17		1.35	2.34±0.01	0.56	
8.1.05	0.88±0.01	1.11		1.15	1.31±0.00	0.33		1.35	2.26±0.03	1.12		1.40	2.55±0.01	0.27	
1.10	0.97±0.02	1.75		1.20	1.43±0.00	0.32		1.40	2.44±0.01	0.54		1.45	2.79±0.03	1.03	
1.15	1.07±0.00	0.34		1.25	1.57±0.00	0.31		27.1.10	0.98±0.01	0.70		37.1.15	1.11±0.00	0.33	
1.20	1.17±0.01	0.64		1.30	1.70±0.01	0.88		1.15	1.07±0.01	1.00		1.20	1.21±0.01	0.64	
1.25	1.27±0.01	0.61		18.1.05	1.05±0.02	1.86		1.20	1.17±0.01	0.64		1.25	1.33±0.01	0.61	
1.30	1.40±0.00	0.29		1.10	1.19±0.00	0.35		1.25	1.29±0.00	0.31		1.30	1.44±0.01	0.58	
1.35	1.51±0.01	0.56		1.15	1.32±0.01	1.00		1.30	1.39±0.01	0.88		1.35	1.57±0.01	0.56	
9.1.05	0.87±0.01	0.74		1.20	1.43±0.01	0.64		1.35	1.51±0.01	0.56		1.40	1.69±0.00	0.27	
1.10	0.96±0.03	3.16		1.25	1.56±0.00	0.31		28.1.10	0.98±0.00	0.35		1.45	1.83±0.01	0.52	
1.15	1.08±0.03	2.65		1.30	1.70±0.01	0.59		1.15	1.06±0.01	1.34		38.1.15	1.13±0.03	2.32	
1.20	1.17±0.03	2.23						1.20	1.18±0.01	0.64		1.20	1.20±0.02	1.92	
1.25	1.30±0.03	2.42						1.25	1.28±0.01	0.61		1.25	1.33±0.01	0.61	
1.30	1.38±0.02	1.17						1.30	1.40±0.01	0.88		1.30	1.44±0.01	0.88	
1.35	1.50±0.02	1.41						1.35	1.52±0.01	0.56		1.35	1.56±0.01	0.84	
								1.40	1.63±0.01	0.81		1.40	1.70±0.01	0.54	
												1.45	1.81±0.01	0.78	
												1.50	1.95±0.01	0.50	

NO.	NF	LOAD(*E-2)	%ERR	NO.	NF	LOAD(*E-2)	%ERR	NO.	NF	LOAD(*E-2)	%ERR	NO.	NF	LOAD(*E-2)	%ERR	
67.	1.15	0.38±0.01	2.64	72.	1.15	1.33±0.03	2.62	78.	1.15	0.75±0.01	1.00	84.	1.15	0.96±0.01	0.67	
	1.20	0.41±0.00	0.64		1.20	1.42±0.01	0.63		1.20	0.81±0.00	0.32		1.20	1.06±0.01	0.64	
	1.25	0.44±0.00	0.31		1.25	1.55±0.01	0.61		1.25	0.89±0.01	0.61		1.25	1.16±0.01	0.61	
	1.30	0.48±0.00	0.58		1.30	1.69±0.02	1.16		1.30	0.98±0.01	0.87		1.30	1.25±0.01	0.58	
	1.35	0.52±0.00	0.56		1.35	1.83±0.02	1.12		1.35	1.05±0.01	0.56		1.35	1.36±0.02	1.40	
	1.40	0.57±0.00	0.27		1.40	1.95±0.01	0.54		1.40	1.13±0.00	0.27		1.40	1.46±0.01	0.54	
	1.45	0.61±0.00	0.52		1.45	2.11±0.02	0.78		1.45	1.22±0.01	0.78		1.45	1.59±0.01	0.78	
	1.50	0.67±0.00	0.75		1.50	2.26±0.02	0.75		1.50	1.31±0.01	0.50		1.50	1.69±0.01	0.50	
	1.55	0.71±0.00	0.48		1.55	2.45±0.02	0.72		1.55	1.40±0.01	0.49		1.55	1.83±0.01	0.48	
	1.60	0.76±0.00	0.47	73.	1.15	1.91±0.05	2.67		1.60	1.50±0.01	0.70		1.60	1.87±0.04	2.39	
	1.65	0.82±0.01	0.90		1.20	2.12±0.05	2.22		79.	1.15	0.57±0.00	0.33		1.65	2.10±0.01	0.68
	1.70	0.86±0.00	0.44		1.25	2.33±0.04	1.81			1.20	0.62±0.01	1.58	85.	1.15	0.65±0.00	0.66
68.	1.15	0.38±0.00	0.33		1.30	2.53±0.03	1.16			1.25	0.68±0.01	1.21		1.20	0.71±0.00	0.32
	1.20	0.41±0.01	1.58		1.35	2.70±0.02	0.56			1.30	0.73±0.00	0.58		1.25	0.77±0.02	2.44
	1.25	0.45±0.00	0.30		1.40	2.94±0.01	0.27			1.35	0.79±0.00	0.56		1.30	0.83±0.00	0.59
	1.30	0.48±0.00	0.29		1.45	3.13±0.02	0.78			1.40	0.85±0.00	0.27		1.35	0.91±0.01	0.56
	1.35	0.53±0.00	0.28		1.50	3.38±0.03	0.75			1.45	0.92±0.00	0.52		1.40	0.98±0.01	0.81
	1.40	0.57±0.00	0.27	74.	1.15	0.98±0.01	0.99			1.50	1.00±0.01	1.24		1.45	1.06±0.01	0.78
	1.45	0.61±0.00	0.52		1.20	1.05±0.01	0.95			1.55	1.06±0.01	0.48		1.50	1.13±0.00	0.25
	1.50	0.66±0.00	0.25		1.25	1.16±0.02	1.82			1.60	1.16±0.02	1.39		1.55	1.22±0.01	0.73
	1.55	0.70±0.00	0.49		1.30	1.25±0.02	1.46			1.65	1.22±0.01	0.90		1.60	1.30±0.01	0.70
	1.60	0.75±0.01	0.70		1.35	1.36±0.01	0.84			1.70	1.29±0.01	0.88		1.65	1.38±0.01	0.68
	1.65	0.81±0.00	0.45		1.40	1.46±0.02	1.35			1.75	1.37±0.01	1.06	86.	1.15	0.83±0.00	0.33
	1.70	0.86±0.00	0.44		1.45	1.62±0.04	2.31		80.	1.15	0.38±0.00	0.66		1.20	0.91±0.01	0.63
	1.75	0.91±0.01	0.64		1.50	1.70±0.02	1.00			1.20	0.41±0.00	0.96		1.25	1.00±0.01	1.21
69.	1.15	0.57±0.01	1.31		1.55	1.82±0.01	0.73			1.25	0.45±0.00	0.91		1.30	1.09±0.02	2.03
	1.20	0.61±0.00	0.64		1.60	1.95±0.03	1.63			1.30	0.49±0.00	0.87		1.35	1.17±0.01	0.56
	1.25	0.67±0.00	0.61		1.65	2.08±0.02	0.91			1.35	0.53±0.00	0.56		1.40	1.26±0.01	0.54
	1.30	0.73±0.00	0.29		1.70	2.23±0.02	1.09			1.40	0.57±0.00	0.54		1.45	1.36±0.01	0.78
	1.35	0.79±0.01	0.84	75.	1.10	0.59±0.00	0.70			1.45	0.61±0.00	0.52		1.50	1.47±0.01	0.50
	1.40	0.85±0.00	0.27		1.15	0.65±0.00	0.66			1.50	0.66±0.00	0.50		1.55	1.58±0.02	0.96
	1.45	0.92±0.00	0.52		1.20	0.71±0.00	0.32			1.55	0.71±0.01	0.72		1.60	1.68±0.01	0.70
	1.50	0.98±0.00	0.50		1.25	0.77±0.00	0.61			1.60	0.76±0.00	0.47		1.65	1.80±0.01	0.68
	1.55	1.05±0.01	0.49		1.30	0.83±0.01	0.88			1.65	0.81±0.00	0.45		1.70	1.90±0.01	0.66
	1.60	1.13±0.01	0.47		1.35	0.90±0.00	0.28			1.70	0.86±0.01	0.66	87.	1.15	1.13±0.01	0.99
	1.65	1.22±0.01	0.68		1.40	0.97±0.00	0.27			1.75	0.92±0.01	0.85		1.20	1.25±0.00	0.32
	1.70	1.29±0.01	0.88		1.45	1.05±0.01	0.52			1.80	0.98±0.03	2.67		1.25	1.34±0.01	0.61
	1.75	1.37±0.01	0.85		1.50	1.14±0.01	1.25		81.	1.15	1.94±0.01	0.33		1.30	1.45±0.01	0.59
	1.80	1.45±0.01	0.62		1.55	1.22±0.01	0.73			1.20	2.13±0.01	0.63		1.35	1.59±0.01	0.84
70.	1.15	0.19±0.00	0.66		1.60	1.30±0.01	0.47			1.25	2.33±0.01	0.61		1.40	1.70±0.01	0.54
	1.20	0.20±0.00	0.32	76.	1.15	0.83±0.01	0.67			1.30	2.51±0.01	0.58		1.45	1.86±0.02	1.29
	1.25	0.22±0.00	0.31		1.20	0.91±0.02	1.91			1.35	2.70±0.02	0.84		1.50	1.99±0.02	1.25
	1.30	0.24±0.00	0.29		1.25	0.99±0.00	0.31			1.40	2.96±0.06	2.15		1.55	2.12±0.02	0.73
	1.35	0.26±0.00	0.56		1.30	1.09±0.01	1.16			1.45	3.18±0.02	0.78		1.60	2.26±0.04	1.87
	1.40	0.28±0.00	0.27		1.35	1.17±0.00	0.28			1.50	3.36±0.02	0.50	88.	1.15	0.76±0.00	0.33
	1.45	0.31±0.00	1.04		1.40	1.26±0.00	0.27		82.	1.15	1.29±0.00	0.33		1.20	0.83±0.00	0.32
	1.50	0.32±0.00	0.51		1.45	1.35±0.01	0.52			1.20	1.41±0.03	2.23		1.25	0.90±0.01	0.61
	1.55	0.35±0.00	0.97		1.50	1.47±0.01	0.50			1.25	1.53±0.01	0.91		1.30	0.98±0.01	0.58
	1.60	0.38±0.01	1.41		1.55	1.58±0.02	0.96			1.30	1.66±0.01	0.88		1.35	1.05±0.00	0.28
	1.65	0.40±0.00	0.68		1.60	1.68±0.01	0.47			1.35	1.80±0.01	0.56		1.40	1.14±0.00	0.27
	1.70	0.43±0.00	0.44		1.65	1.79±0.02	0.91			1.40	1.95±0.02	0.81		1.45	1.25±0.02	1.28
	1.75	0.46±0.01	1.27		1.70	1.91±0.02	1.10			1.45	2.10±0.02	0.78		1.50	1.32±0.01	0.50
71.	1.15	1.68±0.01	0.66	77.	1.15	1.12±0.01	0.67			1.50	2.25±0.01	0.50		1.55	1.43±0.03	1.92
	1.20	1.84±0.01	0.63		1.20	1.23±0.00	0.32		83.	1.15	1.65±0.01	0.33	89.	1.15	0.57±0.00	0.66
	1.25	2.00±0.01	0.61		1.25	1.34±0.01	0.61			1.20	1.81±0.02	0.96		1.20	0.62±0.00	0.32
	1.30	2.16±0.01	0.58		1.30	1.46±0.00	0.29			1.25	1.98±0.01	0.31		1.25	0.67±0.01	1.82
	1.35	2.34±0.01	0.56		1.35	1.57±0.01	0.56			1.30	2.15±0.01	0.58		1.30	0.74±0.02	2.02
	1.40	2.53±0.01	0.27		1.40	1.69±0.00	0.27			1.35	2.33±0.01	0.56		1.35	0.79±0.00	0.56
	1.45	2.74±0.07	2.59		1.45	1.83±0.01	0.78			1.40	2.51±0.03	1.08		1.40	0.86±0.02	1.88
	1.50	2.92±0.01	0.25		1.50	1.96±0.00	0.25			1.45	2.70±0.03	1.04		1.45	0.94±0.01	1.28
	1.55	3.10±0.02	0.73							1.50	2.93±0.02	0.75		1.50	1.02±0.02	1.73
										1.55	3.12±0.02	0.73		1.55	1.05±0.01	0.49
										1.60	3.35±0.02	0.70		1.60	1.14±0.01	0.47
														1.65	1.21±0.01	0.90
														1.70	1.27±0.01	0.88

NO.	NF LOAD(*E-2)	%ERR	NO.	NF LOAD(*E-2)	%ERR	NO.	NF LOAD(*E-2)	%ERR	NO.	NF LOAD(*E-2)	%ERR				
90.1	1.15	0.38±0.00	0.33	99.1	1.15	1.10±0.01	1.32	111.1	1.15	1.62±0.03	1.65	124.1	1.25	1.35±0.00	0.30
1.20	0.42±0.01	1.58	1.20	1.16±0.03	2.24	1.20	1.73±0.03	1.59	1.30	1.46±0.01	0.58	1.30	1.46±0.01	0.58	
1.25	0.45±0.00	0.61	1.25	1.28±0.02	1.22	1.25	1.90±0.01	0.61	1.35	1.58±0.03	1.68	1.35	1.58±0.03	1.68	
1.30	0.48±0.00	0.88	1.30	1.39±0.01	0.88	1.30	2.06±0.01	0.29	1.40	1.70±0.00	0.27	1.40	1.70±0.00	0.27	
1.35	0.53±0.00	0.28	1.35	1.52±0.01	0.84	1.35	2.25±0.03	1.12	1.45	1.83±0.01	0.52	1.45	1.83±0.01	0.52	
1.40	0.57±0.00	0.54	1.40	1.64±0.00	0.27	112.1	1.15	0.79±0.01	1.33	125.1	1.25	0.89±0.01	1.22		
1.45	0.62±0.01	1.04	100.1	1.15	1.09±0.01	0.99	1.20	0.87±0.01	0.64	1.30	0.99±0.02	2.03			
1.50	0.66±0.00	0.50	1.20	1.19±0.02	1.58	1.25	0.96±0.01	1.21	1.35	1.05±0.01	0.56				
1.55	0.71±0.01	0.73	1.25	1.30±0.01	0.61	1.30	1.04±0.01	1.16	1.40	1.13±0.01	0.54				
1.60	0.75±0.00	0.47	1.30	1.40±0.03	2.33	1.35	1.12±0.01	0.84	1.45	1.22±0.01	0.52				
1.65	0.81±0.01	0.68	1.35	1.51±0.03	1.97	113.1	1.15	1.64±0.01	0.67	126.1	1.25	0.67±0.01	0.91		
1.70	0.86±0.01	0.66	1.40	1.63±0.01	0.54	1.20	1.80±0.01	0.32	1.30	0.72±0.00	0.59				
91.1	1.15	0.19±0.00	0.33	101.1	1.15	0.54±0.00	0.67	1.25	1.96±0.02	1.22	1.35	0.78±0.01	0.84		
1.20	0.21±0.00	1.59	1.20	0.59±0.00	0.64	1.30	2.14±0.04	1.75	1.40	0.86±0.01	1.34				
1.25	0.23±0.00	0.91	1.25	0.64±0.01	0.92	1.35	2.33±0.01	0.56	127.1	1.25	0.44±0.00	0.31			
1.30	0.24±0.00	1.16	1.30	0.69±0.01	0.88	114.1	1.15	2.08±0.01	0.66	1.30	0.48±0.00	0.29			
1.35	0.27±0.00	0.84	1.35	0.76±0.01	0.84	1.20	2.24±0.01	0.32	1.35	0.54±0.01	1.39				
1.40	0.28±0.00	0.27	1.40	0.81±0.01	1.08	1.25	2.50±0.05	1.80	1.40	0.56±0.00	0.27				
1.45	0.31±0.01	2.08	1.45	0.88±0.01	1.04	1.30	2.63±0.02	0.88	128.1	1.25	0.22±0.00	0.30			
1.50	0.33±0.00	0.25	102.1	1.10	2.39±0.01	0.35	1.35	2.86±0.02	0.56	1.30	0.24±0.00	0.59			
1.55	0.35±0.00	0.97	1.15	2.63±0.01	0.33	115.1	1.15	2.07±0.01	0.66	1.35	0.26±0.00	0.84			
1.60	0.38±0.00	0.47	1.20	2.88±0.01	0.32	1.20	2.24±0.01	0.32	129.1	1.25	2.55±0.02	0.92			
92.1	1.15	0.32±0.00	0.66	1.25	3.16±0.02	0.61	1.25	2.45±0.01	0.61	1.30	2.79±0.03	1.17			
1.20	0.35±0.00	0.64	1.30	3.42±0.03	0.88	1.30	2.63±0.04	1.47	1.35	3.03±0.05	1.68				
1.25	0.38±0.00	0.91	1.35	3.69±0.03	0.84	1.35	2.87±0.02	0.56	1.40	3.24±0.06	1.90				
1.30	0.42±0.01	1.46	103.1	1.10	2.40±0.01	0.35	116.1	1.15	1.02±0.01	1.33	1.45	3.62±0.08	2.31		
1.35	0.46±0.00	0.84	1.15	2.62±0.00	0.03	1.20	1.11±0.01	0.64	130.1	1.25	2.66±0.03	1.22			
1.40	0.49±0.01	1.08	1.20	2.86±0.01	0.32	1.25	1.21±0.00	0.31	1.30	2.86±0.03	0.88				
1.45	0.53±0.00	0.78	1.25	3.14±0.02	0.61	1.30	1.32±0.02	1.17	1.35	3.11±0.02	0.56				
1.50	0.57±0.00	0.50	1.30	3.41±0.02	0.58	1.35	1.43±0.01	0.56	1.40	3.35±0.08	2.44				
1.55	0.60±0.00	0.73	1.35	3.68±0.04	1.12	117.1	1.15	2.22±0.01	0.67	1.45	3.68±0.08	2.07			
1.60	0.65±0.00	0.70	104.1	1.15	1.99±0.01	0.33	1.20	2.42±0.02	0.64	131.1	1.25	2.65±0.02	0.92		
1.65	0.70±0.00	0.68	1.20	2.18±0.01	0.32	1.25	2.63±0.02	0.61	1.30	2.87±0.06	2.05				
93.1	1.15	2.19±0.03	1.32	1.25	2.37±0.02	0.91	1.30	2.88±0.03	0.88	1.35	3.05±0.08	2.56			
1.20	2.38±0.02	0.95	1.30	2.55±0.04	1.46	1.35	3.16±0.04	1.40	1.40	3.39±0.05	1.35				
1.25	2.56±0.02	0.92	1.35	2.77±0.05	1.96	1.40	3.41±0.02	0.54	1.45	3.65±0.03	0.78				
1.30	2.81±0.05	1.75	105.1	1.10	1.79±0.02	1.40	118.1	1.25	0.98±0.01	0.61	132.1	1.25	1.99±0.02	0.92	
1.35	3.04±0.05	1.68	1.15	1.96±0.02	1.00	1.30	1.07±0.02	1.46	1.30	2.17±0.03	1.17				
94.1	1.10	1.94±0.01	0.70	1.20	2.14±0.02	0.96	1.35	1.16±0.01	0.84	1.35	2.34±0.01	0.56			
1.15	2.13±0.06	2.67	1.25	2.35±0.02	0.92	1.40	1.25±0.01	1.08	1.40	2.53±0.01	0.54				
1.20	2.37±0.05	1.90	1.30	2.54±0.02	0.88	1.45	1.36±0.01	0.52	1.45	2.73±0.04	1.30				
1.25	2.59±0.02	0.91	1.35	2.76±0.02	0.56	119.1	1.25	0.77±0.02	2.13	1.50	2.93±0.02	0.75			
1.30	2.80±0.06	2.04	106.1	1.10	1.21±0.00	0.35	1.30	0.83±0.01	1.17	133.1	1.25	2.00±0.02	1.22		
1.35	3.03±0.08	2.52	1.15	1.33±0.00	0.33	1.35	0.90±0.01	0.56	1.30	2.17±0.02	0.88				
95.1	1.10	1.98±0.02	1.04	1.20	1.45±0.00	0.03	1.40	0.97±0.01	0.54	1.35	2.34±0.01	0.56			
1.15	2.18±0.04	1.65	1.25	1.58±0.01	0.91	1.45	1.05±0.01	1.04	1.40	2.53±0.01	0.54				
1.20	2.37±0.02	0.63	1.30	1.71±0.03	2.04	120.1	1.25	1.15±0.02	1.83	1.45	2.72±0.02	0.78			
1.25	2.62±0.06	2.11	1.35	1.86±0.03	1.68	1.30	1.24±0.03	2.34	134.1	1.25	1.33±0.01	0.92			
1.30	2.82±0.05	1.74	107.1	1.15	1.29±0.00	0.34	1.35	1.35±0.01	0.56	1.30	1.45±0.01	0.58			
1.35	3.02±0.03	1.12	1.20	1.44±0.00	0.32	1.40	1.45±0.01	0.81	1.35	1.55±0.01	0.85				
1.40	3.25±0.04	1.35	1.25	1.57±0.02	1.52	1.45	1.64±0.06	3.57	1.40	1.68±0.03	1.90				
96.1	1.15	1.62±0.03	1.99	1.30	1.69±0.01	0.59	121.1	1.25	1.53±0.01	0.61	1.45	1.82±0.01	0.52		
1.20	1.76±0.02	1.27	1.35	1.87±0.01	0.56	1.30	1.68±0.02	1.45	135.1	1.25	1.35±0.02	1.21			
1.25	1.92±0.02	1.22	108.1	1.15	0.66±0.01	1.66	1.35	1.78±0.03	1.41	1.30	1.44±0.02	1.17			
1.30	2.08±0.02	1.17	1.20	0.73±0.00	0.32	1.40	1.94±0.01	0.54	1.35	1.58±0.03	1.68				
1.35	2.26±0.01	0.56	1.25	0.79±0.01	0.91	1.45	2.09±0.02	1.04	1.40	1.70±0.02	1.35				
97.1	1.15	1.62±0.03	1.66	1.30	0.85±0.01	1.75	122.1	1.25	2.28±0.03	1.22	1.45	1.82±0.02	1.30		
1.20	1.77±0.02	0.95	1.35	0.92±0.02	1.96	1.30	2.49±0.02	0.88	136.1	1.25	0.66±0.00	0.61			
1.25	1.92±0.02	0.92	109.1	1.15	1.37±0.02	1.33	1.35	2.71±0.02	0.84	1.30	0.72±0.01	1.17			
1.30	2.10±0.03	1.46	1.20	1.50±0.03	1.90	1.40	2.91±0.02	0.81	1.35	0.79±0.01	1.68				
1.35	2.26±0.03	1.12	110.1	1.15	1.58±0.01	0.67	1.45	3.15±0.03	1.04	1.40	0.84±0.02	2.44			
1.40	2.46±0.04	1.62	1.20	1.75±0.03	1.59	1.50	3.39±0.02	0.50	1.45	0.90±0.01	0.78				
98.1	1.15	1.61±0.01	0.67	1.25	1.90±0.02	1.22	123.1	1.25	1.98±0.01	0.61	137.1	1.20	1.80±0.01	0.32	
1.20	1.76±0.02	1.28	1.30	2.07±0.02	0.87	1.30	2.08±0.05	2.37	1.25	1.98±0.01	0.31				
1.25	1.94±0.04	2.12	1.35	2.24±0.01	0.56	1.35	2.32±0.02	0.84	1.30	2.15±0.01	0.29				
1.30	2.11±0.04	2.04				1.40	2.51±0.02	0.81	1.35	2.33±0.02	0.84				
1.35	2.27±0.03	1.12				1.45	2.71±0.02	0.78	1.40	2.52±0.02	0.81				
1.40	2.46±0.01	0.54				1.50	2.90±0.01	0.50	1.45	2.75±0.03	1.03				

NO.	NF	LOAD(*E-2)	%ERR	NO.	NF	LOAD(*E-2)	%ERR	NO.	NF	LOAD(*E-2)	%ERR	NO.	NF	LOAD(*E-2)	%ERR	
193.	1.60	0.94±0.01	1.17	198.	1.60	0.93±0.02	1.88	203.	1.55	0.34±0.00	0.97	209.	1.65	0.39±0.00	0.68	
	1.65	1.00±0.03	2.72		1.65	1.00±0.01	1.13		1.60	0.36±0.01	1.40		1.70	0.41±0.00	0.88	
	1.70	1.07±0.01	0.66		1.70	1.07±0.02	2.20		1.65	0.39±0.01	2.50		1.75	0.44±0.00	1.06	
	1.75	1.13±0.02	1.49		1.75	1.14±0.01	1.06		1.70	0.41±0.01	1.99		1.80	0.47±0.01	1.86	
	1.80	1.21±0.02	1.86		1.80	1.21±0.01	0.83		1.75	0.44±0.01	1.92		1.85	0.51±0.01	2.37	
	1.85	1.28±0.02	1.60		1.85	1.30±0.02	1.59		1.80	0.47±0.00	1.03		1.90	0.53±0.01	1.36	
	1.90	1.35±0.03	1.95		1.90	1.35±0.02	1.37		1.85	0.49±0.01	1.41		1.95	0.56±0.01	0.95	
	1.95	1.43±0.04	2.84		1.95	1.44±0.01	0.57		1.90	0.53±0.01	2.51		2.00	0.60±0.02	2.73	
	2.00	1.52±0.03	1.84		2.00	1.51±0.01	0.74		1.95	0.56±0.01	2.27		2.05	0.62±0.00	0.72	
	2.05	1.59±0.04	2.34		2.05	1.59±0.01	0.90		2.00	0.59±0.01	1.66		2.10	0.67±0.01	1.73	
	2.10	1.68±0.03	1.75		2.10	1.67±0.01	0.35		2.05	0.62±0.01	1.26		2.15	0.68±0.01	2.06	
	2.15	1.76±0.04	2.05		2.15	1.76±0.01	0.51		204.	1.55	0.17±0.00	0.73	210.	1.65	0.59±0.01	1.36
194.	1.60	0.80±0.01	1.18		2.20	1.84±0.02	0.84		1.60	0.19±0.00	2.53		1.70	0.62±0.01	0.88	
	1.65	0.86±0.01	1.13	199.	1.60	0.62±0.01	1.41		1.65	0.19±0.00	1.59		1.75	0.67±0.01	1.70	
	1.70	0.92±0.01	0.88		1.65	0.67±0.01	1.36		1.70	0.21±0.00	1.10		1.80	0.69±0.01	1.45	
	1.75	1.00±0.02	1.68		1.70	0.72±0.01	1.75		1.75	0.22±0.00	0.64		1.85	0.74±0.01	1.81	
	1.80	1.04±0.01	1.24		1.75	0.76±0.01	1.49		1.80	0.23±0.00	0.83		1.90	0.78±0.02	2.16	
	1.85	1.10±0.02	1.81		1.80	0.80±0.01	1.86		1.85	0.25±0.00	1.20		1.95	0.84±0.00	0.57	
	1.90	1.16±0.02	2.15		1.85	0.85±0.02	1.80		1.90	0.26±0.00	1.17		2.00	0.88±0.01	1.48	
	1.95	1.23±0.04	3.23		1.90	0.90±0.02	1.95		1.95	0.28±0.00	1.33		2.05	0.92±0.01	1.26	
	2.00	1.31±0.03	2.39		1.95	0.97±0.03	2.64		2.00	0.29±0.00	1.11		2.10	0.97±0.01	0.88	
	2.05	1.37±0.03	2.34		2.00	1.00±0.03	2.59		2.05	0.31±0.00	1.08		2.15	1.02±0.01	1.37	
	2.10	1.44±0.03	1.93		2.05	1.07±0.03	2.87		2.10	0.34±0.01	2.07	211.	1.65	0.68±0.00	0.68	
195.	1.60	1.26±0.02	1.63		2.10	1.11±0.02	1.76		205.	1.70	0.36±0.01	1.54		1.70	0.73±0.00	0.44
	1.65	1.34±0.02	1.13		2.15	1.16±0.04	3.44		1.75	0.38±0.01	2.54		1.75	0.80±0.02	2.10	
	1.70	1.41±0.01	0.88		2.20	1.25±0.01	1.16		1.80	0.40±0.00	0.41		1.80	0.82±0.01	0.62	
	1.75	1.52±0.01	0.85		2.25	1.28±0.01	0.82		1.85	0.44±0.01	1.59		1.85	0.88±0.01	0.80	
	1.80	1.62±0.01	0.82	200.	1.60	0.81±0.01	1.40		1.90	0.45±0.01	1.95		1.90	0.92±0.01	0.98	
	1.85	1.70±0.01	0.60		1.65	0.86±0.01	1.36		1.95	0.48±0.01	1.14		1.95	0.98±0.00	0.19	
	1.90	1.81±0.04	2.14		1.70	0.96±0.03	2.79		2.00	0.50±0.01	1.66		2.00	1.06±0.03	2.37	
	1.95	1.92±0.02	1.13		1.75	0.98±0.01	1.49		2.05	0.55±0.01	2.64		2.05	1.09±0.01	0.72	
	2.00	2.02±0.06	3.14		1.80	1.05±0.02	1.85		2.10	0.56±0.00	0.88	212.	1.60	1.92±0.01	0.70	
	2.05	2.12±0.03	1.44		1.85	1.11±0.02	1.40		2.15	0.58±0.01	1.54		1.65	2.05±0.01	0.68	
	2.10	2.23±0.01	0.53		1.90	1.17±0.02	1.36		2.20	0.63±0.02	2.47		1.70	2.19±0.00	0.22	
	2.15	2.35±0.01	0.51		1.95	1.22±0.01	0.57		2.25	0.64±0.01	1.15		1.75	2.32±0.01	0.64	
196.	1.60	1.89±0.03	1.40		2.00	1.31±0.01	0.55		206.	1.70	1.09±0.02	1.96		1.80	2.47±0.01	0.41
	1.65	2.06±0.07	3.58		2.05	1.43±0.05	3.70		1.75	1.14±0.02	1.49		1.85	2.60±0.02	0.60	
	1.70	2.13±0.06	2.64		2.10	1.43±0.01	0.71		1.80	1.21±0.03	2.47		1.90	2.76±0.02	0.78	
	1.75	2.28±0.05	2.34		2.15	1.54±0.03	2.04		1.85	1.28±0.02	1.80	213.	1.60	1.30±0.03	2.32	
	1.80	2.42±0.04	1.86		2.20	1.58±0.02	1.17		1.90	1.35±0.02	1.56		1.65	1.36±0.01	0.45	
	1.85	2.64±0.05	1.78		2.25	1.66±0.02	1.14		1.95	1.47±0.03	1.87		1.70	1.47±0.01	0.66	
	1.90	2.70±0.05	1.95	201.	1.60	0.32±0.00	1.39		2.00	1.53±0.01	0.92		1.75	1.56±0.02	1.49	
	1.95	2.87±0.07	2.46		1.65	0.33±0.00	1.37		2.05	1.60±0.02	1.08		1.80	1.64±0.03	1.66	
	2.00	3.01±0.06	2.03		1.70	0.35±0.01	2.42		207.	1.70	0.72±0.01	1.31		1.85	1.74±0.01	0.80
	2.05	3.18±0.03	0.90		1.75	0.38±0.01	1.49		1.75	0.75±0.02	2.14		1.90	1.85±0.03	1.75	
	2.10	3.36±0.02	0.53		1.80	0.40±0.01	2.27		1.80	0.81±0.02	2.06	214.	1.60	1.91±0.01	0.47	
197.	1.60	1.63±0.02	0.93		1.85	0.43±0.01	1.20		1.85	0.85±0.02	2.41		1.65	2.05±0.01	0.45	
	1.65	1.76±0.06	3.14		1.90	0.45±0.01	1.56		1.90	0.90±0.02	2.74		1.70	2.18±0.01	0.44	
	1.70	1.84±0.03	1.54		1.95	0.48±0.01	1.90		1.95	0.96±0.02	2.27		1.75	2.32±0.02	0.85	
	1.75	1.95±0.02	1.07		2.00	0.51±0.00	0.92		2.00	1.01±0.01	1.47		1.80	2.48±0.02	0.82	
	1.80	2.09±0.00	0.21		2.05	0.54±0.01	1.24		2.05	1.07±0.01	1.08		1.85	2.62±0.03	1.20	
	1.85	2.20±0.02	0.80		2.10	0.56±0.00	0.35		2.10	1.11±0.02	2.11		1.90	2.77±0.02	0.78	
	1.90	2.32±0.02	0.78	202.	1.55	0.51±0.00	0.97		2.15	1.17±0.02	1.37		1.95	2.90±0.06	2.10	
	1.95	2.48±0.01	0.57		1.60	0.55±0.00	0.70		208.	1.70	0.93±0.03	2.83	215.	1.60	1.28±0.02	1.17
	2.00	2.60±0.02	0.92		1.65	0.58±0.00	0.68		1.75	0.98±0.01	1.49		1.65	1.37±0.01	0.91	
	2.05	2.71±0.02	0.90		1.70	0.62±0.00	0.66		1.80	1.04±0.03	2.48		1.70	1.46±0.01	0.44	
	2.10	2.88±0.02	0.53		1.75	0.66±0.00	0.64		1.85	1.12±0.03	2.59		1.75	1.55±0.02	1.06	
					1.80	0.70±0.00	0.21		1.90	1.17±0.02	1.94		1.80	1.65±0.00	0.21	
					1.85	0.74±0.02	2.21		1.95	1.23±0.03	2.28		1.85	1.75±0.01	0.60	
					1.90	0.79±0.00	0.58		2.00	1.34±0.04	3.10	216.	1.70	2.19±0.01	0.66	
					1.95	0.84±0.00	0.19		2.05	1.38±0.03	1.97		1.75	2.34±0.02	1.06	
					2.00	0.88±0.01	0.74		2.10	1.45±0.02	1.22		1.80	2.55±0.08	3.05	
					2.05	0.92±0.01	0.72		2.15	1.52±0.02	1.54		1.85	2.64±0.01	0.40	
													1.90	2.76±0.03	0.98	
													1.95	2.93±0.03	0.95	
													2.00	3.07±0.07	2.22	

NO.	NF	LOAD(*E-2)	%ERR	NO.	NF	LOAD(*E-2)	%ERR	NO.	NF	LOAD(*E-2)	%ERR	NO.	NF	LOAD(*E-2)	%ERR
217.	1.65	1.17±0.01	0.45												
	1.70	1.23±0.01	0.44												
	1.75	1.31±0.01	0.85												
	1.80	1.40±0.01	0.83												
	1.85	1.48±0.01	1.00												
	1.90	1.57±0.01	0.78												
	1.95	1.66±0.01	0.57												
	2.00	1.78±0.03	1.46												
	2.05	1.85±0.01	0.72												
218.	1.65	2.73±0.06	2.04												
	1.70	2.94±0.03	1.09												
	1.75	3.14±0.07	2.33												
	1.80	3.30±0.01	0.41												
	1.85	3.49±0.07	2.01												
219.	1.70	2.95±0.06	1.96												
	1.75	3.13±0.09	2.75												
	1.80	3.30±0.03	1.03												
	1.85	3.47±0.02	0.60												
	1.90	3.71±0.03	0.78												
	1.95	3.94±0.12	3.02												
220.	1.65	1.17±0.03	2.48												
	1.70	1.25±0.01	0.66												
	1.75	1.32±0.01	0.85												
	1.80	1.40±0.01	0.83												
	1.85	1.51±0.02	1.60												
	1.90	1.58±0.02	1.17												
	1.95	1.67±0.01	0.76												
	2.00	1.76±0.02	1.11												
	2.05	1.84±0.02	1.26												
	2.10	1.95±0.01	0.53												
	2.15	2.09±0.04	1.86												
221.	1.60	0.73±0.01	0.94												
	1.65	0.78±0.01	1.36												
	1.70	0.83±0.01	1.54												
	1.75	0.89±0.01	1.49												
	1.80	0.94±0.00	0.41												
	1.85	1.00±0.01	0.60												
	1.90	1.05±0.01	0.59												
	1.95	1.11±0.01	0.76												
	2.00	1.17±0.01	1.11												
	2.05	1.25±0.02	1.25												

F.6 Amplitude

The VHS cassettes which recorded the amplitude in the center of the wire are replayed frame by frame in the video cassette recorder. Approximately 10 to 15 readings when the wire reaches the peaks are recorded at each nominal frequency. Note that those readings are the wire's center elevations projected on the scale by viewing from the position of the video camera. Since the elevation of the camera and the elevation of the wire when it reaches the peak are not always

the same, those readings should be revised by the triangular relation to obtain the elevation in the center of the wire. Also, because the wire was excited by the moving hydraulic actuators, the elevation of the support when the wire reached the peak should be taken into account to calculate the relative displacement between them. As an example, consider the 46.6' steel wire S1 hanging on 46' span (Test No. 1 in Appendix A). The consecutive readings at the stick scale when the wire reaches the lowest point at 1.05 Hz of nominal frequency are listed in Table F-12. Note that those readings in Table F-12 may not be the true one when the wire reaches the lowest point. This is because the wire moved faster than what the video camera could record. Therefore, the latter might miss to record the moment when the former arrived the lowest extreme.

Table F-12

The consecutive readings at the stick scale for the 46.6' steel wire S1 in Test No.1 at 1.05 Hz of nominal frequency.

Reading(ft)	3.87	3.77	3.85	3.70	3.80	3.89	3.90	3.82	3.93	4.00	3.97	3.78	3.99	3.84
-------------	------	------	------	------	------	------	------	------	------	------	------	------	------	------

From Equation D-1 and Table F-12, the mean and standard error of the readings, y_s , are

$$\bar{y}_s = \frac{3.87 + 3.77 + \dots + 3.84}{14} = 3.87 \text{ ft}$$

$$\text{and } SE_{y_s} = \sqrt{\frac{(3.87^2 + 3.77^2 + \dots + 3.84^2) - \frac{(3.87 + 3.77 + \dots + 3.84)^2}{14}}{14(14-1)}} = 0.02 \text{ ft}$$

, respectively. Fig. F-8 shows the relative positions and elevations of the steel wire S1, the scale, and the camera when the wire reaches the lowest point. By triangular relation, the elevation in the center of the wire, y_w , measured from the ground, is found to be

$$y_w = (30.5/160.5) * 4.224 + (130/160.5) * (y_s + 0.38)$$

$$= 1.1105 + 0.81y_s \text{ (ft)}$$

, where 0.38 ft is the elevation from ground to the zero mark of the stick scale. Then, from Equation D-3, the mean and standard error of y_w are

$$\bar{y}_w = 1.1105 + 0.81\bar{y}_s = 1.1105 + 0.81 * 3.87 = 4.24 \text{ ft}$$

$$\text{and } SE_{y_w} = \sqrt{(0.81SE_{y_s})^2} = 0.81SE_{y_s} = 0.81(0.02) = 0.02 \text{ ft}$$

, respectively. Next, the position of the support can be obtained by examining the output of the vertical tension, horizontal tension, and the support motion as shown in Fig. 3-12. The points A, B, C, and D which correspond to the relative maximum vertical tension represent the locations of the support when the wire reaches the highest point. The points E, F, G, and H which correspond to the relative maximum horizontal tension represent the locations of the support when the wire reaches the lowest point. Also the points I, J, and K

represent the locations of the support when it reaches the highest point, the equilibrium position, and the lowest point, respectively. Therefore, the locations of the support when the wire reaches the lowest point are read as 8.4, 8.2, 7.2, and 8.1 units, i.e., points L, M, N, and O, respectively, below the equilibrium position as shown in Fig. 3-12. Since, after measured, 10 units=3-11/16"=0.3073', those readings would, therefore, represent the locations 0.2581', 0.2520', 0.2213', and 0.2489', respectively, below the equilibrium position of the support. Then, from Equation D-1, the mean and standard error of the support position, y_p , are

$$\bar{y}_p = \frac{0.2581 + 0.2520 + \dots + 0.2489}{4} = 0.245 \text{ ft}$$

$$\text{and } SE_{y_p} = \sqrt{\frac{(0.2581^2 + 0.2520^2 + \dots + 0.2489^2) - \frac{(0.2581 + \dots + 0.2489)^2}{4}}{4(4-1)}} = 0.008 \text{ ft}$$

, respectively, below the equilibrium position of the support. Define the lower portion of the peak-to-peak, y_l , as the relative vertical distance between the support and the center of the wire when it reaches the lowest point. Then, since the elevation of the support in equilibrium position was measured as 94-3/8" from the ground, y_l is found from Fig. F-9 to be

$$y_l = 94.375/12 - y_p - y_w.$$

Therefore, from Equation D-3, the mean and standard error of y_l are

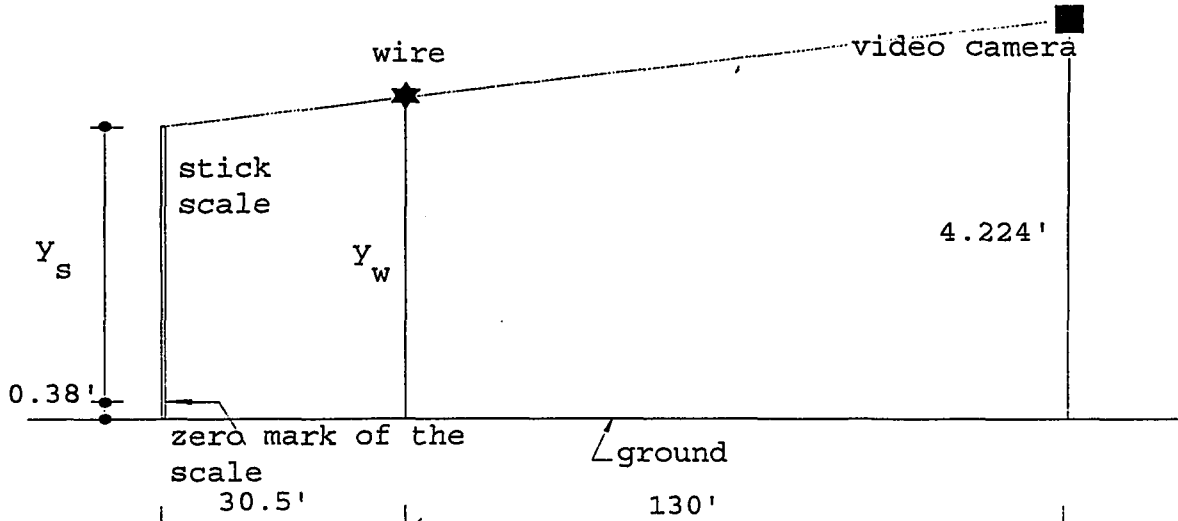


Fig. F-8: The relative positions of the steel wire S1, the stick scale, and the video camera when the wire reaches the lowest point.

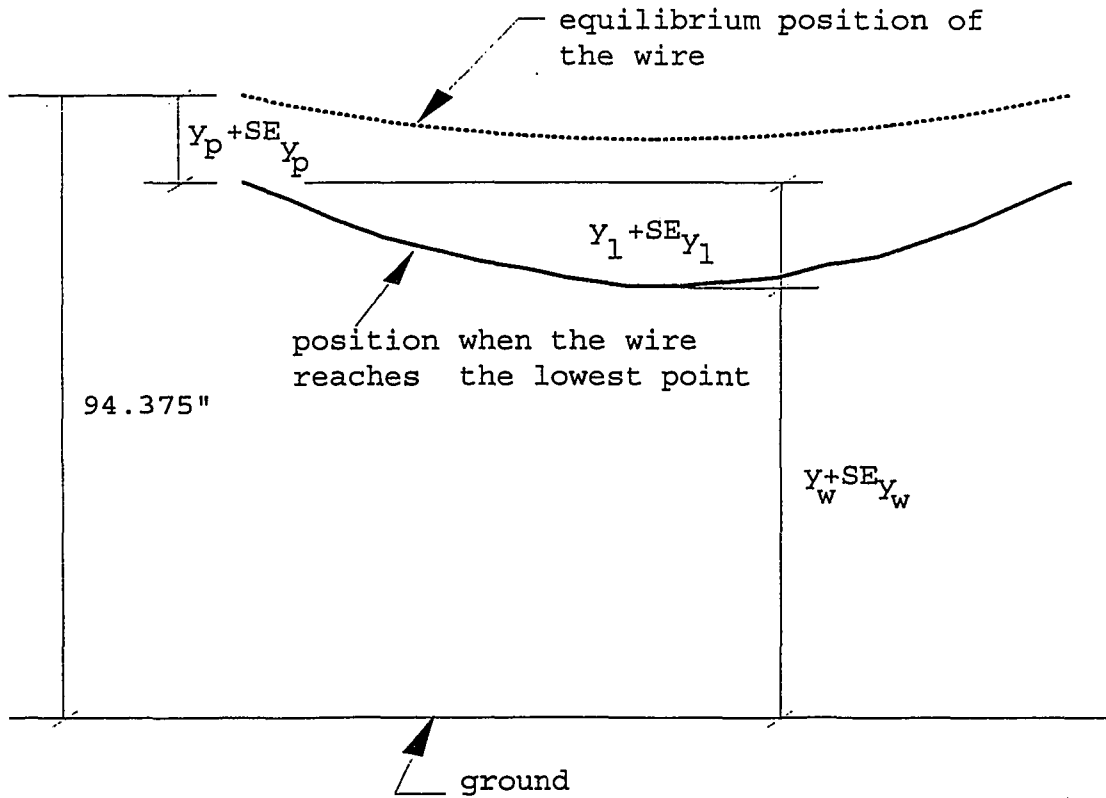


Fig. F-9: Relative position of the support and steel wire S1 when the wire reaches the lowest point.

$$\bar{y}_l = 94.375/12 - \bar{y}_p - \bar{y}_w = 94.375/12 - 0.245 - 4.24 = 3.38 \text{ ft}$$

$$\text{and } SE_{y_l} = \sqrt{(SE_{y_p})^2 + (SE_{y_w})^2} = \sqrt{0.008^2 + 0.02^2} = 0.02 \text{ ft, respectively}$$

On the other hand, define the higher portion of the peak-to-peak amplitude, y_h , as the relative vertical distance between the support and the center of the wire when it reaches the highest point. Then the mean and standard error of y_h can be obtained as 2.15 ft and 0.06 ft, respectively, in the same manner. The amplitude, y_a , defined as the average of y_l and y_h are found from Equation D-3 to be

$$\bar{y}_a = \frac{\bar{y}_l + \bar{y}_h}{2} = \frac{3.38 + 2.15}{2} = 2.77 \text{ ft}$$

$$\text{and } SE_{y_a} = \sqrt{\left(\frac{SE_{y_l}}{2}\right)^2 + \left(\frac{SE_{y_h}}{2}\right)^2} = \frac{\sqrt{0.02^2 + 0.06^2}}{2} = 0.03 \text{ ft, respectively}$$

Consequently, the 95% confidence interval for the mean of the amplitude is

$$\bar{y}_a \pm t_{2.5\%, 30} SE_{y_a} = 2.77 \pm 2.041 * 0.03 = 2.77 \pm 0.07 \text{ Hz}$$

, where t-value for 30 DOFs is 2.042. The 30 DOFs are obtained by $14+12+4+4-4$, where

- (a) 14 and 12 are the measurement numbers of the readings at the stick scale when the wire reaches the the lowest and highest points, respectively,
- (b) the two 4 in the middle of the expression are the measurement numbers of the support locations when the support reaches the lowest and highest points, respectively, and
- (c) the last 4 in the expression is the DOFs used to calculate

the mean of the four quantities mentioned previously.

Therefore, the maximum percentage error of the amplitude for steel wire S1 in Test No.1 at 1.05 Hz of nominal frequency becomes

$$0.07/2.77=2.39\%$$

Similarly, the 95% confidence intervals for the means of the amplitudes of other wires and the corresponding maximum percentage measurement errors were obtained. The results are listed in Table F-13. The average of the maximum percentage error in the measurement of the amplitudes was calculated as 0.84%.

Table F-13: The 95% confidence intervals of the amplitude (ft) and the corresponding maximum percentage measurement error at each nominal frequency (NF) in Hz for the 221 tests listed in Appendix A.

NO.	NF	AMPLITUDE	%ERR	NO.	NF	AMPLITUDE	%ERR	NO.	NF	AMPLITUDE	%ERR	NO.	NF	AMPLITUDE	%ERR
1.1	0.05	2.77±0.07	2.39	10.1	0.05	2.96±0.05	1.85	19.1	1.10	2.55±0.03	1.10	29.1	1.10	2.09±0.03	1.44
1.1	1.10	2.92±0.06	2.18	1.1	1.10	3.02±0.02	0.68	1.1	1.15	2.65±0.02	0.85	1.1	1.15	2.27±0.02	0.96
1.1	1.15	3.07±0.05	1.52	1.1	1.15	3.12±0.01	0.30	1.2	1.20	2.72±0.02	0.64	1.2	1.20	2.41±0.02	1.03
1.2	1.20	3.13±0.02	0.66	1.2	1.20	3.14±0.01	0.32	1.2	1.25	2.73±0.02	0.88	1.2	1.25	2.45±0.02	0.71
1.2	1.25	3.15±0.02	0.54	1.2	1.25	3.15±0.01	0.45	1.3	1.30	2.74±0.02	0.90	1.3	1.30	2.50±0.02	0.67
1.3	1.30	3.13±0.01	0.43	1.3	1.30	3.17±0.01	0.23	20.1	1.10	2.43±0.01	0.28	1.3	1.35	2.52±0.02	0.60
2.1	1.05	2.98±0.04	1.21	1.3	1.35	3.09±0.01	0.28	1.1	1.15	2.50±0.01	0.56	1.4	1.40	2.53±0.02	0.76
1.1	1.10	3.10±0.03	1.10	11.1	1.05	3.26±0.10	3.01	1.2	1.20	2.56±0.01	0.54	30.1	1.15	2.39±0.02	0.72
1.1	1.15	3.15±0.03	0.82	1.1	1.10	3.12±0.01	0.33	1.2	1.25	2.61±0.01	0.34	1.2	1.20	2.47±0.01	0.54
1.2	1.20	3.18±0.02	0.69	1.1	1.15	3.16±0.01	0.31	1.3	1.30	2.61±0.01	0.29	1.2	1.25	2.49±0.01	0.55
1.2	1.25	3.21±0.02	0.67	1.2	1.20	3.20±0.01	0.31	1.3	1.35	2.54±0.03	1.10	1.3	1.30	2.53±0.01	0.34
1.3	1.30	3.14±0.02	0.61	1.2	1.25	3.22±0.01	0.26	21.1	1.10	2.26±0.02	0.85	1.3	1.35	2.55±0.01	0.52
3.1	1.05	3.11±0.03	1.11	1.3	1.30	3.22±0.01	0.28	1.1	1.15	2.39±0.02	0.66	31.1	1.10	2.46±0.02	0.78
1.1	1.10	3.14±0.01	0.31	12.1	1.05	2.91±0.01	0.29	1.2	1.20	2.45±0.02	0.98	1.1	1.15	2.55±0.01	0.37
1.1	1.15	3.19±0.01	0.24	1.1	1.10	3.03±0.01	0.39	1.2	1.25	2.48±0.02	0.72	1.2	1.20	2.61±0.01	0.57
1.2	1.20	3.33±0.01	0.29	1.1	1.15	3.11±0.01	0.23	1.3	1.30	2.51±0.01	0.49	1.2	1.25	2.65±0.01	0.45
1.2	1.25	3.31±0.01	0.26	1.2	1.20	3.14±0.01	0.34	1.3	1.35	2.48±0.01	0.45	1.3	1.30	2.70±0.01	0.30
1.3	1.30	3.28±0.02	0.61	1.2	1.25	3.18±0.01	0.16	22.1	1.10	2.52±0.01	0.41	1.3	1.35	2.70±0.01	0.25
1.3	1.35	3.22±0.02	0.73	1.3	1.30	3.22±0.01	0.46	1.1	1.15	2.57±0.01	0.37	32.1	1.10	2.45±0.01	0.31
4.1	1.05	3.09±0.05	1.71	1.3	1.35	3.20±0.01	0.29	1.2	1.20	2.60±0.01	0.33	1.1	1.15	2.52±0.02	0.70
1.1	1.10	3.19±0.03	0.97	13.1	1.05	2.99±0.01	0.30	1.2	1.25	2.63±0.01	0.30	1.2	1.20	2.59±0.01	0.41
1.1	1.15	3.27±0.03	1.01	1.1	1.10	3.08±0.01	0.34	1.3	1.30	2.63±0.01	0.41	1.2	1.25	2.63±0.01	0.42
1.2	1.20	3.26±0.02	0.52	1.1	1.15	3.12±0.01	0.23	1.3	1.35	2.59±0.01	0.42	1.3	1.30	2.63±0.01	0.55
1.2	1.25	3.27±0.02	0.51	1.2	1.20	3.14±0.01	0.20	23.1	1.10	2.43±0.02	0.80	1.3	1.35	2.67±0.01	0.50
1.3	1.30	3.25±0.02	0.50	1.2	1.25	3.18±0.01	0.22	1.1	1.15	2.53±0.01	0.55	33.1	1.10	2.30±0.01	0.30
5.1	1.05	3.25±0.02	0.65	1.3	1.30	3.21±0.01	0.25	1.2	1.20	2.60±0.02	0.91	1.1	1.15	2.43±0.01	0.57
1.1	1.10	3.29±0.01	0.42	1.3	1.35	3.20±0.01	0.29	1.2	1.25	2.76±0.03	1.11	1.2	1.20	2.48±0.01	0.44
1.1	1.15	3.32±0.01	0.43	14.1	1.05	3.18±0.02	0.57	1.3	1.30	2.79±0.01	0.40	1.2	1.25	2.54±0.01	0.35
1.2	1.20	3.36±0.02	0.47	1.1	1.10	3.25±0.02	0.63	1.3	1.35	2.80±0.01	0.33	1.3	1.30	2.56±0.01	0.36
1.2	1.25	3.34±0.02	0.51	1.1	1.15	3.29±0.01	0.26	24.1	1.10	2.52±0.01	0.28	1.3	1.35	2.57±0.01	0.33
1.3	1.30	3.29±0.01	0.35	1.2	1.20	3.32±0.01	0.18	1.1	1.15	2.59±0.01	0.35	34.1	1.10	2.60±0.01	0.31
1.3	1.35	3.21±0.02	0.50	1.2	1.25	3.33±0.01	0.28	1.2	1.20	2.65±0.01	0.43	1.1	1.15	2.66±0.01	0.51
6.1	1.05	2.94±0.10	3.43	1.3	1.30	3.28±0.01	0.30	1.2	1.25	2.67±0.01	0.34	1.2	1.20	2.71±0.01	0.54
1.1	1.10	3.02±0.08	2.78	15.1	1.05	3.03±0.01	0.38	1.3	1.30	2.71±0.01	0.32	1.2	1.25	2.76±0.01	0.39
1.1	1.15	2.98±0.04	1.18	1.1	1.10	3.11±0.01	0.39	1.3	1.35	2.75±0.01	0.33	1.3	1.30	2.79±0.01	0.34
1.2	1.20	3.01±0.02	0.66	1.1	1.15	3.17±0.02	0.59	25.1	1.10	2.18±0.05	2.08	35.1	1.15	2.35±0.01	0.41
1.2	1.25	3.03±0.04	1.28	1.2	1.20	3.20±0.01	0.44	1.1	1.15	2.34±0.03	1.27	1.2	1.20	2.41±0.01	0.29
1.3	1.30	3.06±0.03	0.91	1.2	1.25	3.27±0.01	0.44	1.2	1.20	2.44±0.03	1.19	1.2	1.25	2.47±0.01	0.33
1.3	1.35	2.98±0.02	0.78	1.3	1.30	3.31±0.01	0.25	1.2	1.25	2.49±0.02	0.61	1.3	1.30	2.52±0.01	0.26
7.1	1.05	2.99±0.09	3.05	16.1	1.05	3.14±0.01	0.27	1.3	1.30	2.50±0.02	0.92	1.3	1.35	2.54±0.01	0.29
1.1	1.10	3.09±0.08	2.47	1.1	1.10	3.20±0.01	0.27	1.3	1.35	2.57±0.01	0.40	1.4	1.40	2.58±0.01	0.27
1.1	1.15	3.12±0.05	1.63	1.1	1.15	3.24±0.01	0.41	1.4	1.40	2.53±0.01	0.52	1.4	1.45	2.58±0.01	0.32
1.2	1.20	3.24±0.02	0.73	1.2	1.20	3.22±0.01	0.43	26.1	1.10	2.18±0.03	1.27	36.1	1.15	2.55±0.01	0.34
1.2	1.25	3.21±0.01	0.31	1.2	1.25	3.27±0.01	0.33	1.1	1.15	2.35±0.02	0.94	1.2	1.20	2.57±0.01	0.32
1.3	1.30	3.22±0.01	0.38	1.3	1.30	3.29±0.01	0.23	1.2	1.20	2.45±0.02	0.75	1.2	1.25	2.63±0.01	0.38
1.3	1.35	3.21±0.02	0.60	17.1	1.05	2.99±0.01	0.32	1.2	1.25	2.53±0.02	0.73	1.3	1.30	2.66±0.02	0.64
1.4	1.40	2.87±0.03	1.08	1.1	1.10	3.10±0.01	0.26	1.3	1.30	2.53±0.02	0.88	1.3	1.35	2.65±0.01	0.35
8.1	1.05	3.05±0.04	1.35	1.1	1.15	3.17±0.01	0.27	1.3	1.35	2.59±0.01	0.50	1.4	1.40	2.67±0.01	0.32
1.1	1.10	2.99±0.03	0.98	1.2	1.20	3.22±0.01	0.16	1.4	1.40	2.59±0.01	0.46	1.4	1.45	2.67±0.01	0.46
1.1	1.15	3.09±0.01	0.35	1.2	1.25	3.24±0.01	0.27	27.1	1.10	2.15±0.02	1.03	37.1	1.15	2.39±0.01	0.34
1.2	1.20	3.13±0.01	0.33	1.3	1.30	3.31±0.01	0.29	1.1	1.15	2.29±0.01	0.54	1.2	1.20	2.49±0.01	0.38
1.2	1.25	3.13±0.01	0.33	18.1	1.05	2.85±0.01	0.42	1.2	1.20	2.36±0.01	0.59	1.2	1.25	2.51±0.01	0.41
1.3	1.30	3.17±0.01	0.18	1.1	1.10	2.98±0.01	0.24	1.2	1.25	2.39±0.01	0.29	1.3	1.30	2.57±0.01	0.35
1.3	1.35	3.12±0.01	0.35	1.1	1.15	3.03±0.01	0.31	1.3	1.30	2.43±0.01	0.29	1.3	1.35	2.58±0.01	0.32
9.1	1.05	3.10±0.05	1.48	1.2	1.20	3.07±0.01	0.26	1.3	1.35	2.40±0.01	0.29	1.4	1.40	2.61±0.01	0.36
1.1	1.10	3.12±0.06	1.95	1.2	1.25	3.12±0.00	0.15	28.1	1.10	2.11±0.01	0.45	1.4	1.45	2.60±0.01	0.38
1.1	1.15	3.26±0.05	1.58	1.3	1.30	3.13±0.01	0.23	1.1	1.15	2.30±0.03	1.09	38.1	1.15	2.87±0.07	2.31
1.2	1.20	3.27±0.07	2.13					1.2	1.20	2.47±0.02	0.79	1.2	1.20	2.88±0.05	1.70
1.2	1.25	3.31±0.05	1.62					1.2	1.25	2.55±0.01	0.55	1.2	1.25	2.89±0.03	0.91
1.3	1.30	3.22±0.04	1.19					1.3	1.30	2.57±0.01	0.50	1.3	1.30	2.80±0.01	0.35
1.3	1.35	3.16±0.01	0.47					1.3	1.35	2.54±0.01	0.46	1.3	1.35	2.83±0.01	0.37
								1.4	1.40	2.58±0.01	0.39	1.4	1.40	2.85±0.01	0.33
												1.4	1.45	2.87±0.01	0.38
												1.5	1.50	2.59±0.02	0.68

NO.	NF	AMPLITUDE	%ERR	NO.	NF	AMPLITUDE	%ERR	NO.	NF	AMPLITUDE	%ERR	NO.	NF	AMPLITUDE	%ERR	
67.	1.15	2.36±0.04	1.51	72.	1.15	2.44±0.04	1.66	78.	1.15	2.03±0.01	0.72	84.	1.15	2.64±0.04	1.42	
	1.20	2.43±0.01	0.40		1.20	2.49±0.02	0.69		1.20	2.18±0.01	0.30		1.20	2.72±0.02	0.91	
	1.25	2.47±0.01	0.28		1.25	2.50±0.03	1.11		1.25	2.26±0.01	0.46		1.25	2.68±0.01	0.41	
	1.30	2.51±0.01	0.32		1.30	2.53±0.03	1.02		1.30	2.34±0.01	0.51		1.30	2.76±0.01	0.34	
	1.35	2.54±0.01	0.41		1.35	2.55±0.02	0.90		1.35	2.39±0.01	0.39		1.35	2.76±0.03	0.98	
	1.40	2.56±0.01	0.23		1.40	2.58±0.02	0.74		1.40	2.43±0.01	0.31		1.40	2.78±0.02	0.73	
	1.45	2.61±0.01	0.30		1.45	2.61±0.02	0.61		1.45	2.43±0.01	0.39		1.45	2.86±0.01	0.44	
	1.50	2.61±0.01	0.44		1.50	2.61±0.02	0.58		1.50	2.46±0.01	0.37		1.50	2.81±0.01	0.36	
	1.55	2.64±0.01	0.28		1.55	2.60±0.02	0.66		1.55	2.35±0.01	0.46		1.55	2.79±0.01	0.25	
	1.60	2.64±0.01	0.36	73.	1.15	2.53±0.06	2.40		1.60	2.29±0.07	3.19		1.60	2.73±0.02	0.88	
	1.65	2.47±0.02	0.76		1.20	2.69±0.06	2.30	79.	1.15	2.25±0.01	0.29		1.65	2.72±0.05	1.79	
	1.70	2.30±0.02	1.08		1.25	2.62±0.02	0.89		1.20	2.33±0.02	0.88	85.	1.15	2.62±0.02	0.79	
68.	1.15	2.32±0.01	0.23		1.30	2.66±0.02	0.62		1.25	2.42±0.02	0.77		1.20	2.66±0.02	0.87	
	1.20	2.41±0.03	1.08		1.35	2.64±0.01	0.29		1.30	2.47±0.01	0.39		1.25	2.66±0.03	1.30	
	1.25	2.48±0.01	0.38		1.40	2.66±0.01	0.24		1.35	2.52±0.02	0.80		1.30	2.65±0.01	0.30	
	1.30	2.50±0.01	0.32		1.45	2.71±0.01	0.35		1.40	2.55±0.01	0.27		1.35	2.68±0.01	0.41	
	1.35	2.55±0.01	0.32		1.50	2.79±0.02	0.68		1.45	2.59±0.01	0.36		1.40	2.74±0.01	0.49	
	1.40	2.57±0.01	0.34	74.	1.15	2.62±0.04	1.36		1.50	2.54±0.02	0.68		1.45	2.73±0.01	0.43	
	1.45	2.60±0.01	0.33		1.20	2.76±0.03	1.12		1.55	2.62±0.01	0.31		1.50	2.73±0.01	0.36	
	1.50	2.61±0.01	0.27		1.25	2.79±0.04	1.35		1.60	2.61±0.02	0.79		1.55	2.75±0.01	0.44	
	1.55	2.64±0.01	0.31		1.30	2.78±0.04	1.54		1.65	2.43±0.02	0.82		1.60	2.72±0.01	0.36	
	1.60	2.66±0.01	0.38		1.35	2.79±0.04	1.53		1.70	2.38±0.08	3.41		1.65	2.77±0.01	0.37	
	1.65	2.57±0.01	0.43		1.40	2.84±0.02	0.82		1.75	2.44±0.03	1.29	86.	1.15	2.68±0.01	0.52	
	1.70	2.40±0.01	0.45		1.45	2.88±0.07	2.48		80.	1.15	2.35±0.05	1.98		1.20	2.60±0.02	0.64
	1.75	2.37±0.07	2.83		1.50	2.83±0.02	0.63		1.20	2.45±0.04	1.62		1.25	2.64±0.01	0.39	
69.	1.15	2.42±0.02	0.73		1.55	2.85±0.01	0.37		1.25	2.50±0.02	0.99		1.30	2.65±0.02	0.59	
	1.20	2.49±0.01	0.35		1.60	2.88±0.02	0.72		1.30	2.53±0.02	0.82		1.35	2.72±0.01	0.25	
	1.25	2.56±0.01	0.39		1.65	2.89±0.01	0.45		1.35	2.57±0.01	0.44		1.40	2.74±0.01	0.33	
	1.30	2.61±0.01	0.23		1.70	2.88±0.02	0.68		1.40	2.61±0.01	0.40		1.45	2.75±0.01	0.42	
	1.35	2.63±0.01	0.47	75.	1.10	2.54±0.05	2.17		1.45	2.62±0.01	0.29		1.50	2.75±0.01	0.35	
	1.40	2.66±0.01	0.25		1.15	2.55±0.01	0.43		1.50	2.64±0.01	0.42		1.55	2.70±0.02	0.58	
	1.45	2.67±0.01	0.33		1.20	2.59±0.01	0.22		1.55	2.63±0.01	0.48		1.60	2.78±0.01	0.42	
	1.50	2.71±0.01	0.37		1.25	2.67±0.01	0.41		1.60	2.64±0.01	0.40		1.65	2.77±0.01	0.38	
	1.55	2.75±0.01	0.30		1.30	2.66±0.01	0.44		1.65	2.67±0.01	0.43		1.70	2.50±0.03	1.13	
	1.60	2.74±0.01	0.25		1.35	2.72±0.01	0.43		1.70	2.67±0.01	0.48	87.	1.15	1.97±0.01	0.50	
	1.65	2.77±0.01	0.44		1.40	2.72±0.01	0.35		1.75	2.53±0.02	0.77		1.20	2.07±0.01	0.37	
	1.70	2.78±0.01	0.44		1.45	2.76±0.01	0.29		1.80	2.54±0.07	2.69		1.25	2.17±0.01	0.30	
	1.75	2.71±0.01	0.46		1.50	2.77±0.02	0.57	81.	1.15	2.06±0.01	0.25		1.30	2.23±0.01	0.36	
	1.80	2.50±0.03	1.18		1.55	2.81±0.01	0.30		1.20	2.18±0.01	0.36		1.35	2.29±0.01	0.41	
70.	1.15	1.99±0.01	0.51		1.60	2.54±0.04	1.67		1.25	2.22±0.01	0.37		1.40	2.33±0.01	0.34	
	1.20	2.16±0.00	0.23	76.	1.15	2.70±0.05	1.78		1.30	2.25±0.01	0.47		1.45	2.33±0.01	0.63	
	1.25	2.29±0.01	0.31		1.20	2.71±0.05	1.93		1.35	2.28±0.01	0.50		1.50	2.40±0.01	0.47	
	1.30	2.34±0.01	0.24		1.25	2.65±0.01	0.26		1.40	2.36±0.01	0.58		1.55	2.39±0.01	0.43	
	1.35	2.40±0.01	0.33		1.30	2.70±0.01	0.49		1.45	2.33±0.01	0.46		1.60	2.13±0.07	3.32	
	1.40	2.43±0.01	0.30		1.35	2.75±0.01	0.22		1.50	2.30±0.01	0.42	88.	1.15	1.91±0.01	0.31	
	1.45	2.45±0.01	0.48		1.40	2.76±0.01	0.24		82.	1.15	1.94±0.01	0.33		1.20	2.07±0.01	0.34
	1.50	2.50±0.01	0.37		1.45	2.79±0.01	0.28		1.20	2.08±0.02	1.14		1.25	2.14±0.01	0.52	
	1.55	2.51±0.02	0.86		1.50	2.82±0.01	0.29		1.25	2.18±0.01	0.56		1.30	2.20±0.01	0.35	
	1.60	2.54±0.02	0.91		1.55	2.83±0.01	0.48		1.30	2.19±0.01	0.54		1.35	2.26±0.01	0.29	
	1.65	2.54±0.02	0.77		1.60	2.79±0.01	0.30		1.35	2.27±0.01	0.39		1.40	2.29±0.01	0.31	
	1.70	2.47±0.01	0.60		1.65	2.74±0.04	1.39		1.40	2.27±0.01	0.49		1.45	2.29±0.02	0.73	
	1.75	2.37±0.07	2.88		1.70	2.63±0.06	2.33		1.45	2.29±0.01	0.41		1.50	2.29±0.01	0.45	
71.	1.15	2.53±0.01	0.46	77.	1.15	2.06±0.01	0.52		1.50	2.22±0.01	0.52		1.55	2.04±0.01	0.56	
	1.20	2.53±0.01	0.43		1.20	2.17±0.00	0.19	83.	1.15	2.20±0.01	0.35	89.	1.15	2.09±0.01	0.31	
	1.25	2.61±0.01	0.46		1.25	2.24±0.01	0.24		1.20	2.32±0.01	0.32		1.20	2.23±0.00	0.21	
	1.30	2.62±0.01	0.32		1.30	2.32±0.00	0.21		1.25	2.38±0.01	0.31		1.25	2.33±0.01	0.44	
	1.35	2.66±0.01	0.29		1.35	2.39±0.01	0.32		1.30	2.42±0.01	0.37		1.30	2.37±0.01	0.51	
	1.40	2.71±0.01	0.30		1.40	2.43±0.01	0.40		1.35	2.45±0.01	0.41		1.35	2.43±0.01	0.36	
	1.45	2.69±0.01	0.49		1.45	2.41±0.01	0.42		1.40	2.46±0.01	0.43		1.40	2.48±0.02	0.79	
	1.50	2.68±0.01	0.23		1.50	2.43±0.01	0.43		1.45	2.46±0.01	0.50		1.45	2.54±0.02	0.74	
	1.55	2.76±0.02	0.87						1.50	2.47±0.01	0.42		1.50	2.58±0.02	0.67	
									1.55	2.50±0.01	0.34		1.55	2.68±0.01	0.34	
									1.60	2.47±0.01	0.42		1.60	2.68±0.01	0.37	
													1.65	2.41±0.02	0.73	
													1.70	2.80±0.02	0.58	

NO.	NF	AMPLITUDE	%ERR	NO.	NF	AMPLITUDE	%ERR	NO.	NF	AMPLITUDE	%ERR	NO.	NF	AMPLITUDE	%ERR
193.	1.60	1.07±0.04	3.69	198.	1.60	0.98±0.04	3.83	203.	1.55	0.92±0.00	0.50	209.	1.65	0.66±0.00	0.56
	1.65	1.19±0.01	0.93		1.65	1.17±0.05	3.98		1.60	0.99±0.01	0.89		1.70	0.78±0.00	0.47
	1.70	1.23±0.01	0.54		1.70	1.25±0.02	1.90		1.65	0.99±0.02	2.00		1.75	0.84±0.03	3.22
	1.75	1.27±0.01	0.88		1.75	1.25±0.02	1.66		1.70	1.08±0.02	1.67		1.80	0.90±0.04	4.13
	1.80	1.28±0.01	1.00		1.80	1.27±0.02	1.33		1.75	1.14±0.02	1.33		1.85	0.94±0.05	5.27
	1.85	1.30±0.02	1.84		1.85	1.31±0.03	1.92		1.80	1.18±0.01	1.23		1.90	0.97±0.05	5.25
	1.90	1.31±0.02	1.78		1.90	1.30±0.03	2.08		1.85	1.17±0.02	1.66		1.95	0.98±0.04	4.22
	1.95	1.32±0.03	2.11		1.95	1.30±0.01	0.51		1.90	1.15±0.01	0.88		2.00	0.98±0.03	3.33
	2.00	1.33±0.03	2.38		2.00	1.29±0.01	0.51		1.95	1.22±0.03	2.10		2.05	1.00±0.02	1.64
	2.05	1.33±0.04	2.90		2.05	1.30±0.02	1.78		2.00	1.25±0.02	1.81		2.10	1.01±0.01	1.01
	2.10	1.33±0.04	2.87		2.10	1.29±0.01	0.59		2.05	1.27±0.02	1.94		2.15	1.05±0.02	2.26
	2.15	1.33±0.04	2.69		2.15	1.28±0.01	0.70	204.	1.55	0.71±0.00	0.13	210.	1.65	0.77±0.02	3.18
194.	1.60	1.14±0.02	1.57		2.20	1.28±0.01	0.60		1.60	0.82±0.00	0.21		1.70	0.91±0.00	0.49
	1.65	1.21±0.01	0.84	199.	1.60	1.18±0.01	1.02		1.65	0.92±0.00	0.27		1.75	0.98±0.02	2.49
	1.70	1.25±0.01	1.07		1.65	1.26±0.01	0.86		1.70	0.98±0.00	0.34		1.80	1.00±0.01	0.74
	1.75	1.24±0.02	1.55		1.70	1.30±0.01	0.81		1.75	1.04±0.00	0.35		1.85	1.06±0.02	1.66
	1.80	1.27±0.02	1.78		1.75	1.31±0.01	0.96		1.80	1.09±0.00	0.38		1.90	1.07±0.01	1.18
	1.85	1.31±0.03	1.96		1.80	1.31±0.02	1.72		1.85	1.14±0.00	0.41		1.95	1.09±0.01	0.95
	1.90	1.32±0.03	2.04		1.85	1.32±0.04	2.69		1.90	1.17±0.00	0.40		2.00	1.09±0.01	1.07
	1.95	1.32±0.04	3.20		1.90	1.35±0.03	2.52		1.95	1.18±0.00	0.38		2.05	1.11±0.01	1.11
	2.00	1.33±0.04	3.30		1.95	1.34±0.04	2.88		2.00	1.21±0.01	0.45		2.10	1.12±0.01	0.84
	2.05	1.34±0.04	3.19		2.00	1.34±0.03	2.09		2.05	1.23±0.02	1.30		2.15	1.12±0.02	1.41
	2.10	1.34±0.02	1.58		2.05	1.38±0.02	1.52		2.10	1.25±0.02	1.29	211.	1.65	0.95±0.01	0.60
195.	1.60	1.10±0.02	1.47		2.10	1.35±0.02	1.59	205.	1.70	0.45±0.00	0.10		1.70	0.99±0.01	0.68
	1.65	1.17±0.01	1.00		2.15	1.38±0.02	1.61		1.75	0.86±0.01	1.14		1.75	1.01±0.01	0.60
	1.70	1.22±0.01	0.50		2.20	1.37±0.01	0.67		1.80	0.93±0.01	0.61		1.80	1.03±0.01	0.54
	1.75	1.25±0.01	0.67		2.25	1.37±0.01	0.82		1.85	1.01±0.01	1.06		1.85	1.06±0.01	0.61
	1.80	1.27±0.01	0.76	200.	1.60	1.13±0.03	2.79		1.90	1.02±0.02	1.47		1.90	1.06±0.01	0.61
	1.85	1.28±0.01	0.76		1.65	1.13±0.03	2.73		1.95	1.06±0.01	0.83		1.95	1.07±0.01	0.66
	1.90	1.29±0.02	1.59		1.70	1.24±0.02	1.59		2.00	1.08±0.01	0.82		2.00	1.09±0.01	0.79
	1.95	1.30±0.03	2.37		1.75	1.29±0.02	1.86		2.05	1.09±0.01	0.64		2.05	1.08±0.01	0.62
	2.00	1.30±0.02	1.87		1.80	1.34±0.02	1.67		2.10	1.10±0.00	0.41	212.	1.60	1.02±0.01	0.91
	2.05	1.29±0.04	3.23		1.85	1.35±0.03	1.99		2.15	1.10±0.01	0.51		1.65	1.04±0.01	0.76
	2.10	1.28±0.01	0.67		1.90	1.34±0.03	2.17		2.20	1.10±0.01	0.53		1.70	1.06±0.00	0.39
	2.15	1.28±0.01	0.47		1.95	1.37±0.02	1.56		2.25	1.12±0.01	0.53		1.75	1.07±0.01	0.61
196.	1.60	1.08±0.04	3.91		2.00	1.37±0.01	0.40	206.	1.70	0.84±0.03	4.09		1.80	1.08±0.01	0.76
	1.65	1.18±0.04	3.01		2.05	1.37±0.01	0.40		1.75	0.92±0.03	2.94		1.85	1.09±0.01	0.58
	1.70	1.10±0.05	4.70		2.10	1.36±0.01	0.42		1.80	0.99±0.02	1.70		1.90	1.08±0.01	0.89
	1.75	1.29±0.02	1.90		2.15	1.36±0.01	0.57		1.85	1.05±0.02	2.30		1.90	1.01±0.01	0.96
	1.80	1.26±0.02	1.74		2.20	1.39±0.01	0.86		1.90	1.04±0.02	2.18	213.	1.60	1.01±0.01	0.96
	1.85	1.26±0.03	2.16		2.25	1.42±0.01	0.70		1.95	1.07±0.02	2.07		1.65	1.05±0.01	0.59
	1.90	1.29±0.02	1.65	201.	1.60	0.97±0.02	2.27		2.00	1.07±0.01	1.04		1.70	1.07±0.01	0.69
	1.95	1.31±0.02	1.32		1.65	1.14±0.01	0.74		2.05	1.13±0.01	1.12		1.75	1.08±0.01	1.17
	2.00	1.32±0.02	1.73		1.70	1.18±0.02	1.73		2.05	1.13±0.01	1.12		1.80	1.09±0.01	1.18
	2.05	1.32±0.02	1.28		1.75	1.22±0.02	1.32	207.	1.70	0.87±0.01	1.58		1.85	1.10±0.01	1.06
	2.10	1.31±0.01	0.49		1.80	1.24±0.02	1.47		1.75	0.96±0.02	1.57		1.90	1.10±0.01	1.05
197.	1.60	1.11±0.04	3.52		1.85	1.28±0.02	1.89		1.80	1.01±0.01	1.24	214.	1.60	0.97±0.01	0.52
	1.65	1.23±0.03	2.52		1.90	1.30±0.02	1.39		1.85	1.03±0.02	1.67		1.65	1.01±0.00	0.47
	1.70	1.25±0.01	0.71		1.95	1.30±0.02	1.39		1.90	1.01±0.02	1.95		1.70	1.04±0.01	0.81
	1.75	1.26±0.01	0.54		2.00	1.29±0.02	1.83		1.95	1.04±0.04	3.75		1.75	1.05±0.01	0.89
	1.80	1.28±0.01	0.46		2.05	1.32±0.02	1.62		2.00	1.07±0.01	1.35		1.80	1.06±0.01	0.51
	1.85	1.30±0.01	0.40		2.05	1.28±0.02	1.85		2.05	1.08±0.02	1.40		1.85	1.07±0.01	0.89
	1.90	1.32±0.01	0.43		2.10	1.30±0.01	0.60		2.10	1.05±0.02	2.26		1.90	1.07±0.01	0.83
	1.95	1.31±0.01	0.52	202.	1.55	0.98±0.01	0.70		2.15	1.09±0.01	1.17		1.95	1.08±0.01	1.11
	2.00	1.33±0.01	0.55		1.60	1.13±0.01	0.90	208.	1.70	0.86±0.02	1.85	215.	1.60	0.99±0.01	1.07
	2.05	1.33±0.01	0.46		1.65	1.18±0.01	0.52		1.75	0.99±0.01	1.25		1.65	1.02±0.01	0.64
	2.10	1.33±0.01	0.51		1.70	1.21±0.01	0.51		1.80	1.04±0.02	2.23		1.70	1.05±0.00	0.48
					1.75	1.23±0.01	0.51		1.85	1.00±0.05	4.58		1.75	1.06±0.01	0.55
					1.80	1.25±0.01	0.43		1.90	1.09±0.01	0.98		1.80	1.07±0.00	0.33
					1.85	1.26±0.01	0.72		1.95	1.09±0.02	2.12		1.85	1.07±0.01	0.70
					1.90	1.29±0.00	0.38		2.00	1.09±0.02	1.78	216.	1.70	1.08±0.01	0.61
					1.95	1.30±0.01	0.50		2.05	1.12±0.01	1.10		1.75	1.09±0.01	0.89
					2.00	1.31±0.01	0.52		2.10	1.14±0.01	1.24		1.80	1.11±0.01	0.75
					2.05	1.30±0.01	0.56		2.15	1.14±0.02	1.36		1.85	1.12±0.01	0.87
													1.90	1.13±0.01	0.98
													1.95	1.14±0.01	1.21
													2.00	1.16±0.02	1.41

NO.	NF	AMPLITUDE	%ERR	NO.	NF	AMPLITUDE	%ERR	NO.	NF	AMPLITUDE	%ERR	NO.	NF	AMPLITUDE	%ERR
217.	1.65	0.99±0.01	0.51												
	1.70	1.02±0.01	0.60												
	1.75	1.05±0.00	0.21												
	1.80	1.07±0.01	0.86												
	1.85	1.08±0.01	0.49												
	1.90	1.10±0.01	0.48												
	1.95	1.10±0.01	0.52												
	2.00	1.10±0.01	0.62												
	2.05	1.09±0.01	0.58												
218.	1.65	1.01±0.01	0.80												
	1.70	1.05±0.01	0.98												
	1.75	1.06±0.02	1.65												
	1.80	1.07±0.01	0.96												
	1.85	1.11±0.02	1.38												
219.	1.70	1.07±0.01	1.19												
	1.75	1.09±0.02	1.46												
	1.80	1.11±0.01	0.62												
	1.85	1.11±0.01	0.72												
	1.90	1.12±0.01	0.91												
	1.95	1.13±0.01	1.00												
220.	1.65	0.87±0.01	0.83												
	1.70	0.97±0.00	0.45												
	1.75	1.01±0.01	0.52												
	1.80	1.02±0.02	2.05												
	1.85	1.04±0.01	1.24												
	1.90	1.06±0.01	0.70												
	1.95	1.08±0.01	0.82												
	2.00	1.08±0.01	1.06												
	2.05	1.09±0.01	0.90												
	2.10	1.09±0.01	0.74												
	2.15	1.11±0.01	0.70												
221.	1.60	0.69±0.01	0.90												
	1.65	0.87±0.03	3.36												
	1.70	0.93±0.02	2.48												
	1.75	0.97±0.01	1.27												
	1.80	1.00±0.01	1.12												
	1.85	1.04±0.00	0.26												
	1.90	1.07±0.00	0.41												
	1.95	1.07±0.02	1.75												
	2.00	1.08±0.01	1.37												
	2.05	1.07±0.02	1.68												

F.7 Support Force

The vertical and horizontal tensions at the left end of the wire and the tension force at the right end were plotted in the stripchart. The plotting is read manually and then analyzed statistically. Taking the 46.6' steel wire S1 hanging on 46' span and vibrating at 1.05 Hz of nominal frequency (Test No.1 in Appendix A) for instance, the plotting in the stripchart for the horizontal tension is read consecutively as

18.1 20.0 20.1 19.0 19.0 19.5 18.2 18.0 18.0 units.

Then from Equation D-1, the mean and standard error of the readings, R , are

$$\bar{R} = \frac{18.1+20.0+\dots+18.0}{9} = 18.88 \text{ units}$$

$$\text{and } SE_R = \sqrt{\frac{(18.1^2+20.0^2+\dots+18.0^2) - \frac{(18.1+20.0+\dots+18.0)^2}{9}}{9(9-1)}} = 0.28 \text{ units, respectively.}$$

The additional horizontal tension h_d , i.e., the force in addition to static horizontal tension, will be **0.0005 volt*R units/1.5 amplification factors *k lb/volt, or 0.000333Rk lb, where**

- (a) 0.0005 is the chart unit voltage value based on the full scale setting of the recorder,
- (b) 1.5 is the amplification factor of the signals from the load cell (so that the output is more readable), and
- (c) k is the spring constant for the load cell.

Since $k=(4097.2\pm 0.8)$ lb/volt for load cell LC2 which measures the horizontal tension as mentioned in Section 3.2.1, the mean and standard error of h_d , after applying Equation D-2, become

$$\bar{h}_d = 0.000333\bar{R}k = 0.000333(18.88)(4097.2) = 25.8 \text{ lb}$$

$$\text{and } SE_{h_d} = \sqrt{\left(\frac{SE_R}{R}\right)^2 + \left(\frac{SE_k}{k}\right)^2} \bar{h}_d = \sqrt{\left(\frac{0.28}{18.88}\right)^2 + \left(\frac{0.8}{4097.2}\right)^2} (25.8) = 0.4 \text{ lb, respectively.}$$

Then the horizontal tension in dynamic case, H_d , i.e., the sum of static horizontal tension and h_d , will be

$$H_d = \text{static horizontal tension} + h_d$$

$$=2.1+(25.8\pm 0.4)=(27.9\pm 0.4) \text{ lbs}$$

, where the static horizontal tension was measured as 2.1 lbs.

Consequently, the 95% confidence interval for the mean of horizontal tension is

$$\bar{H}_d \pm t_{2.5\%, 66} SE_{H_d} = 27.9 \pm 2 * 0.4 = 27.9 \pm 0.8 \text{ lb}$$

, where t-value for 66 DOFs is 2. The 66 is obtained by 58+8, where 58 is the DOFs for spring constant and 8 is the DOFs for the readings of horizontal tension.

Then the maximum percentage error of the support horizontal tension in dynamic case for steel wire S1 in Test No.1 at 1.05 Hz of nominal frequency is

$$0.8/27.9=2.77\%$$

Similarly, the 95% confidence intervals for the means of the vertical and horizontal tensions of other tests in Appendix A and the corresponding maximum percentage measurement errors are obtained. The results are listed in Table F-14. The average of the maximum percentage error in the measurement of the support forces is calculated as 0.82%.

Table F-14: The 95% confidence intervals of the support dynamic vertical tension V_d , horizontal tension H_d and the corresponding maximum percentage measurement error at each nominal frequency (NF) in Hz for the 221 tests listed in Appendix A.

NO.	NF	V_d (lb) %ERR	H_d (lb) %ERR	NO.	NF	V_d (lb) %ERR	H_d (lb) %ERR	NO.	NF	V_d (lb) %ERR	H_d (lb) %ERR
1.1.05	3.8±0.4	9.52	27.9±0.8 2.77	10.1.05	1.8±0.1	3.21	11.0±0.4 3.37	19.1.10	3.1±0.2	7.06	32.5±1.0 3.00
1.1.10	3.8±0.2	4.86	30.1±0.7 2.47	1.1.10	1.4±0.0	1.83	11.9±0.1 0.89	1.1.15	3.4±0.2	6.20	34.6±1.1 3.10
1.1.15	4.0±0.3	8.13	26.4±1.0 3.70	1.1.15	1.4±0.0	0.57	12.8±0.1 0.44	1.2.0	3.5±0.2	6.01	37.4±0.8 2.05
1.2.0	5.0±0.3	5.84	33.8±0.4 1.21	1.2.0	1.5±0.0	0.12	13.3±0.0 0.04	1.25	3.2±0.2	5.47	38.6±0.8 2.14
1.25	4.9±0.1	2.48	34.9±0.0 0.13	1.25	1.6±0.0	0.12	14.0±0.0 0.04	1.30	4.5±0.5	10.2	41.2±0.8 1.88
1.30	4.8±0.1	1.14	36.3±0.0 0.13	1.30	1.6±0.0	0.12	14.6±0.0 0.04	20.1.10	3.0±0.1	2.35	40.7±0.3 0.67
2.1.05	3.8±0.4	9.77	28.8±1.0 3.56	1.35	1.6±0.0	0.12	14.8±0.0 0.04	1.15	3.1±0.0	0.11	43.6±0.0 0.04
1.1.10	4.0±0.2	4.34	29.6±0.4 1.48	11.1.05	4.6±0.2	4.10	25.2±1.2 4.58	1.20	3.1±0.1	2.12	45.6±0.0 0.04
1.1.15	4.0±0.1	2.10	31.4±0.6 1.82	1.1.10	3.3±0.2	4.74	27.7±0.5 1.71	1.25	3.2±0.0	0.11	47.2±0.0 0.04
1.2.0	4.2±0.1	3.19	32.6±0.8 2.37	1.15	3.8±0.0	0.82	29.0±0.0 0.04	1.30	3.3±0.0	0.11	48.5±0.0 0.04
1.25	4.3±0.2	5.44	34.0±0.6 1.62	1.20	3.6±0.2	4.99	30.2±0.0 0.04	1.35	3.9±0.1	1.93	48.9±0.5 1.00
1.30	4.4±0.2	4.07	35.6±0.7 2.03	1.25	3.7±0.2	5.22	31.3±0.0 0.04	21.1.10	1.5±0.1	4.04	19.4±0.3 1.62
3.1.05	4.7±0.1	2.53	33.0±0.6 1.88	1.30	3.6±0.0	0.12	32.1±0.0 0.04	1.15	1.6±0.1	3.18	21.0±0.2 1.00
1.1.10	4.5±0.0	0.59	34.4±0.1 0.37	12.1.05	2.6±0.1	2.61	26.0±0.3 1.26	1.20	1.7±0.0	2.36	22.1±0.0 0.04
1.1.15	5.4±0.0	0.74	36.8±0.1 0.16	1.1.10	2.8±0.0	1.37	27.1±0.0 0.04	1.25	1.8±0.0	1.97	23.1±0.0 0.04
1.2.0	5.9±0.1	1.47	38.7±0.3 0.76	1.15	2.8±0.1	2.13	29.0±0.0 0.04	1.30	1.9±0.0	2.24	24.0±0.1 0.46
1.25	6.1±0.1	1.16	40.7±0.0 0.08	1.20	2.9±0.0	1.04	29.9±0.0 0.04	1.35	1.9±0.0	1.37	24.7±0.2 0.66
1.30	5.9±0.2	3.90	42.1±0.1 0.17	1.25	2.9±0.0	1.30	30.8±0.0 0.04	22.1.10	3.2±0.0	0.11	37.6±0.5 1.33
1.35	5.5±0.1	1.29	42.7±0.3 0.60	1.30	3.2±0.0	1.37	32.0±0.0 0.04	1.15	3.3±0.0	0.11	40.3±0.0 0.04
4.1.05	1.7±0.1	4.50	13.8±0.3 2.52	1.35	3.1±0.1	1.71	32.3±0.0 0.04	1.20	3.5±0.0	0.11	42.3±0.0 0.04
1.1.0	2.0±0.1	2.88	14.9±0.4 2.58	13.1.05	1.6±0.0	0.98	14.7±0.0 0.04	1.25	3.7±0.0	0.11	44.0±0.0 0.04
1.1.15	2.1±0.1	3.39	15.3±0.2 1.10	1.1.10	1.6±0.0	0.12	15.4±0.0 0.04	1.30	3.9±0.0	0.11	46.2±0.0 0.04
1.2.0	2.1±0.1	2.65	16.1±0.2 1.48	1.15	1.7±0.0	0.68	16.1±0.0 0.04	1.35	4.0±0.2	4.25	46.8±0.0 0.04
1.25	2.2±0.1	3.54	16.9±0.2 1.08	1.20	1.8±0.0	1.04	16.2±0.0 0.04	23.1.10	3.8±0.1	1.84	45.8±0.0 0.04
1.30	2.2±0.1	3.43	17.7±0.2 1.04	1.25	1.8±0.0	1.53	17.2±0.1 0.49	1.15	4.0±0.1	3.52	48.7±0.0 0.04
5.1.05	3.5±0.2	4.79	30.8±0.8 2.62	1.30	1.8±0.0	0.12	17.8±0.0 0.04	1.20	4.4±0.1	1.57	50.7±0.0 0.04
1.1.0	3.7±0.1	2.09	32.4±0.3 1.05	1.35	1.9±0.0	2.23	18.3±0.0 0.04	1.25	4.4±0.1	1.89	52.2±0.0 0.04
1.1.15	3.9±0.1	2.38	34.5±0.4 1.14	14.1.05	3.5±0.2	6.25	29.3±0.5 1.81	1.30	4.7±0.1	1.30	53.6±0.0 0.04
1.2.0	4.0±0.2	4.57	36.1±0.4 1.06	1.1.0	3.7±0.1	3.22	31.0±0.0 0.04	1.35	4.8±0.1	1.37	55.0±0.0 0.04
1.25	4.3±0.2	4.06	37.0±0.7 4.60	1.15	3.9±0.1	3.32	32.2±0.0 0.04	24.1.10	2.0±0.0	2.22	26.2±0.0 0.04
1.30	4.7±0.1	2.26	40.8±0.3 0.62	1.20	4.2±0.1	1.73	33.4±0.0 0.04	1.15	2.1±0.0	2.10	27.3±0.0 0.04
1.35	5.0±0.2	3.31	43.4±0.5 1.12	1.25	4.4±0.1	2.35	35.5±0.0 0.04	1.20	2.2±0.0	1.90	28.1±0.0 0.04
6.1.05	5.8±0.4	6.09	35.7±1.3 3.64	1.30	4.6±0.1	1.58	46.1±0.0 0.04	1.25	2.3±0.1	2.37	29.2±0.0 0.04
1.1.0	6.2±0.3	4.49	35.9±1.6 4.56	15.1.05	3.4±0.2	4.57	32.5±0.6 1.76	1.30	2.4±0.0	1.66	30.3±0.0 0.04
1.1.15	4.0±0.2	6.09	32.3±1.2 3.63	1.1.0	3.7±0.0	1.32	35.2±0.2 0.60	1.35	2.4±0.0	1.83	31.0±0.0 0.04
1.2.0	4.1±0.4	8.85	34.7±1.0 2.87	1.15	4.1±0.0	0.11	36.3±0.4 1.22	25.1.10	3.9±0.1	3.24	37.4±0.4 1.00
1.25	4.2±0.2	5.66	36.2±0.9 2.59	1.20	4.4±0.1	1.89	38.0±0.4 0.96	1.15	4.5±0.1	1.99	43.2±0.5 1.13
1.30	4.5±0.4	8.70	37.9±1.2 3.12	1.25	4.8±0.2	5.06	40.4±0.0 0.04	1.20	4.7±0.1	3.15	46.6±0.0 0.04
1.35	4.8±0.4	8.60	40.6±0.9 2.20	1.30	4.9±0.1	1.85	41.9±0.3 0.73	1.25	5.0±0.1	1.53	48.6±0.6 1.13
7.1.05	6.2±0.2	3.66	33.2±1.7 5.25	16.1.05	1.8±0.0	1.33	18.0±0.2 1.38	1.30	4.8±0.1	1.80	50.1±0.0 0.04
1.1.0	5.9±0.4	6.09	35.2±1.6 4.52	1.1.0	2.0±0.1	2.84	19.4±0.2 1.06	1.35	4.8±0.0	0.12	51.1±0.0 0.04
1.1.15	6.9±0.3	4.76	37.7±1.1 2.95	1.15	2.2±0.1	4.21	20.5±0.2 1.09	1.40	4.7±0.0	0.12	52.4±0.0 0.04
1.2.0	5.5±0.3	5.02	41.0±1.0 2.39	1.20	2.4±0.1	5.60	21.4±0.3 1.36	26.1.10	4.1±0.1	2.66	36.9±0.6 1.65
1.25	5.5±0.1	1.55	43.3±0.1 0.34	1.25	2.5±0.2	6.60	22.4±0.3 1.24	1.15	4.3±0.1	2.63	42.6±0.5 1.19
1.30	5.7±0.1	1.30	44.5±0.2 0.40	1.30	2.7±0.2	5.77	23.6±0.3 1.14	1.20	4.6±0.1	2.57	45.2±0.0 0.04
1.35	5.8±0.1	2.32	46.0±0.2 0.47	17.1.05	3.1±0.0	0.11	29.3±0.0 0.04	1.25	4.6±0.0	0.12	47.7±0.0 0.04
1.40	5.3±0.1	2.62	45.9±0.5 1.17	1.1.0	3.2±0.0	0.12	30.8±0.0 0.04	1.30	5.0±0.1	2.07	49.9±0.0 0.04
8.1.05	3.6±0.2	5.29	23.0±1.1 4.68	1.15	3.4±0.0	0.12	32.7±0.0 0.04	1.35	5.2±0.1	1.66	50.5±0.0 0.04
1.1.0	3.8±0.2	4.51	24.2±0.6 2.63	1.20	3.6±0.0	0.12	33.7±0.0 0.04	1.40	5.3±0.0	0.12	52.0±0.0 0.04
1.1.15	2.9±0.0	0.83	25.2±0.1 0.37	1.25	3.8±0.0	0.12	34.8±0.0 0.04	27.1.10	2.9±0.1	3.11	26.1±0.2 0.74
1.2.0	3.0±0.0	0.67	26.8±0.0 0.04	1.30	4.0±0.0	0.12	36.0±0.0 0.04	1.15	3.0±0.1	1.94	29.0±0.0 0.04
1.25	3.0±0.0	1.59	28.1±0.0 0.04	18.1.05	4.0±0.0	0.12	29.2±0.0 0.04	1.20	3.2±0.0	0.12	30.7±0.0 0.04
1.30	3.1±0.0	0.12	29.2±0.0 0.04	1.1.0	4.3±0.0	0.12	30.8±0.0 0.04	1.25	3.3±0.0	0.12	32.0±0.0 0.04
1.35	3.2±0.0	0.99	30.2±0.0 0.04	1.15	4.5±0.0	0.12	32.2±0.0 0.04	1.30	3.5±0.0	0.12	33.1±0.0 0.04
9.1.05	3.7±0.2	6.47	21.4±0.9 4.03	1.20	4.7±0.0	0.12	33.4±0.0 0.04	1.35	3.5±0.0	0.12	34.0±0.0 0.04
1.1.0	4.1±0.2	5.14	24.6±1.1 4.39	1.25	4.9±0.0	0.12	34.8±0.0 0.04	28.1.10	2.5±0.0	0.11	23.9±0.0 0.04
1.1.15	4.4±0.2	4.32	25.1±1.1 4.58	1.30	5.2±0.0	0.13	36.1±0.0 0.04	1.15	3.0±0.1	1.99	26.7±0.0 0.04
1.2.0	4.7±0.2	4.01	25.9±0.9 3.42					1.20	3.3±0.1	2.29	29.5±0.0 0.04
1.25	4.9±0.2	3.55	27.4±1.0 3.49					1.25	3.4±0.0	0.12	31.8±0.0 0.04
1.30	4.8±0.0	0.00	27.1±0.0 0.00					1.30	3.3±0.0	0.12	33.0±0.0 0.04
1.35	5.1±0.1	2.78	28.9±0.7 2.52					1.35	3.5±0.0	0.12	33.7±0.0 0.04
								1.40	3.6±0.0	0.12	34.5±0.0 0.04

NO.	NF	V _g (lb)	%ERR	H _g (lb)	%ERR	NO.	NF	V _g (lb)	%ERR	H _g (lb)	%ERR	NO.	NF	V _g (lb)	%ERR	H _g (lb)	%ERR
29.	1.10	1.3±0.0	2.57	11.7±0.1	1.28	39.	1.10	2.3±0.1	3.53	12.4±0.4	2.97	47.	1.15	4.1±0.0	0.12	32.2±0.0	0.04
	1.15	1.5±0.0	2.55	13.9±0.0	0.04		1.15	2.8±0.1	4.25	13.8±0.4	3.02		1.20	4.4±0.0	0.12	33.9±0.0	0.04
	1.20	1.7±0.0	1.70	14.9±0.0	0.04		1.20	1.8±0.0	0.13	14.7±0.0	0.04		1.25	4.6±0.0	0.12	35.6±0.0	0.04
	1.25	1.7±0.0	0.13	15.9±0.0	0.04		1.25	1.9±0.0	0.13	15.4±0.0	0.04		1.30	4.8±0.0	0.12	37.1±0.0	0.04
	1.30	1.9±0.0	0.13	16.5±0.0	0.04		1.30	2.0±0.0	0.13	16.1±0.0	0.04		1.35	4.9±0.0	0.12	38.6±0.0	0.04
	1.35	2.0±0.0	0.13	17.1±0.0	0.04		1.35	2.1±0.0	0.13	16.7±0.0	0.04		1.40	5.2±0.0	0.13	39.5±0.0	0.04
	1.40	2.1±0.0	0.13	17.5±0.0	0.04		1.40	2.2±0.0	0.13	17.2±0.0	0.04		1.45	5.2±0.0	0.13	40.6±0.0	0.04
30.	1.15	4.0±0.0	1.10	35.6±0.0	0.04		1.45	2.2±0.0	0.13	17.6±0.0	0.04		1.50	5.4±0.0	0.13	42.0±0.0	0.04
	1.20	4.2±0.1	1.30	36.9±0.0	0.04		1.50	2.3±0.0	0.13	18.2±0.0	0.04	48.	1.15	2.8±0.0	0.12	23.7±0.0	0.04
	1.25	4.4±0.0	0.12	38.1±0.0	0.04	40.	1.15	3.6±0.1	3.01	21.0±0.6	2.74		1.20	2.9±0.0	0.12	25.3±0.0	0.04
	1.30	4.2±0.0	0.12	39.4±0.0	0.04		1.20	3.6±0.2	5.31	23.2±0.5	2.01		1.25	3.2±0.0	0.12	26.7±0.0	0.04
	1.35	5.0±0.0	0.13	40.7±0.0	0.04		1.25	2.9±0.0	0.12	24.9±0.0	0.04		1.30	3.4±0.0	0.13	27.9±0.0	0.04
31.	1.10	3.9±0.0	0.12	32.8±0.0	0.04		1.30	3.0±0.0	0.12	26.0±0.0	0.04		1.35	3.5±0.0	0.13	29.1±0.0	0.04
	1.15	4.1±0.0	0.12	34.6±0.0	0.04		1.35	3.2±0.0	0.12	27.1±0.0	0.04		1.40	3.7±0.0	0.13	30.2±0.0	0.04
	1.20	4.4±0.0	0.12	36.4±0.0	0.04		1.40	3.2±0.0	0.12	27.8±0.0	0.04		1.45	3.7±0.0	0.13	30.7±0.1	0.37
	1.25	4.5±0.0	0.12	37.6±0.0	0.04		1.45	3.3±0.0	0.12	28.3±0.0	0.04		1.50	3.6±0.0	0.13	31.4±0.2	0.51
	1.30	4.7±0.0	0.12	38.3±0.0	0.04		1.50	3.0±0.0	0.12	28.7±0.0	0.04	49.	1.15	2.7±0.0	0.12	23.4±0.0	0.04
	1.35	4.9±0.0	0.12	39.4±0.0	0.04	41.	1.15	7.4±0.3	3.94	41.3±0.7	1.80		1.20	2.8±0.0	0.12	25.2±0.0	0.04
32.	1.10	2.0±0.0	0.12	16.5±0.0	0.04		1.20	7.2±0.3	4.78	43.8±0.6	1.31		1.25	3.0±0.0	0.12	26.5±0.0	0.04
	1.15	2.1±0.0	0.12	17.4±0.0	0.04		1.25	8.9±0.4	4.69	45.5±1.1	2.39		1.30	3.2±0.0	0.12	27.9±0.0	0.04
	1.20	2.2±0.0	1.56	18.0±0.0	0.04		1.30	6.9±0.0	0.13	49.0±0.0	0.04		1.35	3.3±0.0	0.12	29.0±0.0	0.04
	1.25	2.3±0.0	1.48	18.7±0.0	0.04		1.35	7.4±0.0	0.13	51.6±0.0	0.04		1.40	3.5±0.0	0.13	29.4±0.0	0.04
	1.30	2.4±0.0	1.14	19.4±0.0	0.04		1.40	8.0±0.0	0.13	52.7±0.0	0.04		1.45	3.5±0.0	0.13	30.3±0.0	0.04
	1.35	2.5±0.0	0.12	19.6±0.0	0.04		1.45	8.9±0.0	0.13	54.3±0.0	0.04		1.50	3.5±0.0	0.13	30.9±0.0	0.04
33.	1.10	3.3±0.0	0.12	29.9±0.0	0.04		1.50	8.8±0.0	0.13	54.7±0.0	0.04	50.	1.15	3.8±0.0	0.12	31.2±0.0	0.04
	1.15	3.6±0.0	0.12	32.4±0.0	0.04	42.	1.15	3.9±0.0	0.12	31.5±0.0	0.04		1.20	3.9±0.0	0.12	33.4±0.0	0.04
	1.20	3.7±0.0	0.12	33.9±0.0	0.04		1.20	4.1±0.0	0.12	33.5±0.0	0.04		1.25	4.1±0.0	0.12	35.2±0.0	0.04
	1.25	3.9±0.0	0.12	35.1±0.0	0.04		1.25	4.3±0.0	0.12	35.4±0.0	0.04		1.30	4.3±0.0	0.12	36.5±0.0	0.04
	1.30	4.0±0.0	0.12	36.3±0.0	0.04		1.30	4.4±0.0	0.12	36.2±0.0	0.04		1.35	4.5±0.0	0.12	38.0±0.0	0.04
	1.35	4.1±0.0	0.12	37.6±0.0	0.04		1.35	4.7±0.0	0.12	37.8±0.0	0.04		1.40	4.7±0.0	0.12	39.3±0.0	0.04
34.	1.10	4.5±0.0	0.12	41.6±0.0	0.04		1.40	4.9±0.0	0.12	39.5±0.0	0.04		1.45	4.7±0.0	0.12	40.4±0.0	0.04
	1.15	4.8±0.0	0.12	43.7±0.0	0.04		1.45	5.0±0.0	0.12	40.1±0.0	0.04		1.50	4.8±0.0	0.12	41.3±0.0	0.04
	1.20	5.2±0.0	0.12	44.7±0.0	0.04		1.50	5.2±0.0	0.13	41.3±0.0	0.04	51.	1.15	1.9±0.0	0.12	15.7±0.0	0.04
	1.25	5.3±0.0	0.12	46.5±0.0	0.04	43.	1.15	2.6±0.1	1.97	15.0±0.2	1.42		1.20	2.1±0.0	0.12	17.0±0.0	0.04
	1.30	5.5±0.0	0.12	48.2±0.0	0.04		1.20	2.0±0.0	0.12	16.5±0.0	0.04		1.25	2.2±0.0	0.12	18.2±0.0	0.04
35.	1.15	3.8±0.0	0.12	41.1±0.0	0.04		1.25	2.2±0.0	0.12	17.7±0.0	0.04		1.30	2.2±0.0	0.12	19.0±0.0	0.04
	1.20	4.1±0.0	0.12	44.2±0.0	0.04		1.30	2.3±0.0	0.12	18.4±0.0	0.04		1.35	2.4±0.0	0.12	19.7±0.0	0.04
	1.25	4.3±0.0	0.12	46.0±0.0	0.04		1.35	2.4±0.0	0.12	19.2±0.0	0.04		1.40	2.4±0.0	0.12	20.3±0.0	0.04
	1.30	4.5±0.0	0.12	47.9±0.0	0.04		1.40	2.5±0.0	0.13	19.9±0.0	0.04		1.45	2.5±0.0	0.12	20.7±0.0	0.04
	1.35	4.7±0.0	0.12	48.9±0.0	0.04		1.45	2.6±0.0	0.13	20.5±0.0	0.04		1.50	2.5±0.0	0.13	21.3±0.0	0.04
	1.40	5.0±0.0	0.12	50.5±0.0	0.04		1.50	2.7±0.0	0.13	21.1±0.0	0.04		1.55	2.6±0.0	0.13	21.9±0.0	0.04
	1.45	5.1±0.0	0.12	52.2±0.0	0.04	44.	1.15	5.3±0.0	0.64	46.6±0.0	0.04	52.	1.15	1.9±0.0	0.12	16.2±0.0	0.04
36.	1.15	4.2±0.0	0.12	42.1±0.0	0.04		1.20	5.6±0.1	1.51	49.1±0.0	0.04		1.20	2.0±0.0	0.12	17.2±0.0	0.04
	1.20	4.5±0.0	0.12	44.4±0.0	0.04		1.25	5.8±0.1	1.31	52.4±0.0	0.04		1.25	2.2±0.0	0.12	18.3±0.0	0.04
	1.25	4.8±0.0	0.12	46.4±0.0	0.04		1.30	6.1±0.0	0.12	54.8±0.0	0.04		1.30	2.2±0.0	0.12	19.0±0.0	0.04
	1.30	5.1±0.0	0.12	48.3±0.0	0.04		1.35	6.5±0.0	0.12	56.9±0.0	0.04		1.35	2.3±0.0	0.12	19.7±0.0	0.04
	1.35	5.4±0.0	0.12	50.1±0.0	0.04		1.40	6.7±0.0	0.13	58.9±0.0	0.04		1.40	2.4±0.0	1.24	20.4±0.0	0.04
	1.40	5.6±0.0	0.12	50.9±0.0	0.04		1.45	6.9±0.0	0.13	60.6±0.0	0.04		1.45	2.5±0.0	0.13	20.9±0.0	0.04
	1.45	5.8±0.0	0.12	52.2±0.0	0.04		1.50	6.9±0.0	0.13	61.2±0.0	0.04		1.50	2.6±0.0	0.13	21.5±0.0	0.04
37.	1.15	2.8±0.0	0.12	30.6±0.0	0.04	45.	1.15	4.0±0.0	0.12	38.0±0.0	0.04	53.	1.15	0.9±0.0	0.13	7.9±0.0	0.04
	1.20	3.1±0.0	0.12	30.9±0.0	0.04		1.20	4.4±0.0	0.12	41.2±0.3	0.64		1.20	1.0±0.0	0.13	8.4±0.0	0.04
	1.25	3.2±0.0	0.12	32.3±0.0	0.04		1.25	4.6±0.1	1.61	43.6±0.0	0.04		1.25	1.0±0.0	0.13	8.9±0.0	0.04
	1.30	3.3±0.0	0.12	33.6±0.0	0.04		1.30	4.9±0.0	0.12	44.6±0.0	0.04		1.30	1.1±0.0	0.13	9.3±0.0	0.04
	1.35	3.4±0.0	0.12	35.0±0.0	0.04		1.35	5.2±0.0	0.12	47.7±0.0	0.04		1.35	1.1±0.0	0.13	9.7±0.0	0.04
	1.40	3.5±0.0	0.12	36.2±0.0	0.04		1.40	5.4±0.0	0.12	48.7±0.0	0.04		1.40	1.2±0.0	0.13	10.1±0.0	0.04
	1.45	3.8±0.0	0.12	37.1±0.0	0.04		1.45	5.5±0.0	0.12	50.1±0.0	0.04		1.45	1.3±0.0	0.13	10.4±0.0	0.04
38.	1.15	5.3±0.2	3.18	27.5±0.7	2.59	46.	1.15	3.6±0.0	0.12	30.8±0.0	0.04		1.50	1.4±0.0	0.13	10.8±0.0	0.04
	1.20	5.6±0.2	3.59	28.1±0.7	2.41		1.20	3.9±0.0	0.12	33.4±0.0	0.04		1.55	1.1±0.0	0.13	10.7±0.0	0.04
	1.25	5.8±0.2	3.84	30.1±0.8	2.67		1.25	4.0±0.0	0.12	35.2±0.0	0.04	54.	1.15	2.9±0.0	0.12	23.8±0.0	0.04
	1.30	4.5±0.0	0.13	32.1±0.0	0.04		1.30	4.1±0.0	0.12	36.7±0.0	0.04		1.20	3.1±0.0	0.12	25.3±0.0	0.04
	1.35	4.7±0.0	0.13	33.5±0.0	0.04		1.35	4.4±0.0	0.12	38.2±0.0	0.04		1.25	3.3±0.0	0.12	26.5±0.0	0.04
	1.40	5.1±0.0	0.13	34.2±0.0	0.04		1.40	4.4±0.0	0.12	39.3±0.0	0.04		1.30	3.4±0.0	0.13	27.6±0.0	0.04
	1.45	5.4±0.0	0.13	35.0±0.0	0.04		1.45	4.6±0.0	0.12	40.4±0.0	0.04		1.35	3.5±0.0	0.13	29.0±0.0	0.04
	1.50	5.4±0.0	0.13	34.6±0.0	0.04		1.50	4.7±0.0	0.12	41.7±0.0	0.04		1.40	3.6±0.0	0.13	29.3±0.0	0.04
							1.55	5.1±0.0	0.13	43.1±0.0	0.04		1.45	3.7±0.0	0.13	29.8±0.0	0.04
													1.50	3.1±0.0	0.12	29.3±0.0	0.04

NO.	NF	$V_d(\text{lb})$	%ERR	$H_d(\text{lb})$	%ERR	NO.	NF	$V_d(\text{lb})$	%ERR	$H_d(\text{lb})$	%ERR	NO.	NF	$V_d(\text{lb})$	%ERR	$H_d(\text{lb})$	%ERR	
72.	1.15	3.7±0.2	4.05	24.7±0.0	0.04	78.	1.15	2.1±0.0	0.12	14.7±0.0	0.04	84.	1.15	3.4±0.0	0.13	16.9±0.0	0.04	
	1.20	2.9±0.3	9.08	25.4±0.0	0.04		1.20	2.3±0.0	0.12	16.8±0.0	0.04		1.20	4.0±0.0	0.13	17.9±0.0	0.04	
	1.25	3.0±0.2	5.75	26.8±0.0	0.04		1.25	2.4±0.0	0.12	18.4±0.0	0.04		1.25	3.0±0.0	0.12	18.9±0.0	0.04	
	1.30	3.1±0.2	5.31	28.1±0.0	0.04		1.30	2.6±0.0	0.13	19.5±0.0	0.04		1.30	3.6±0.0	0.13	19.8±0.0	0.04	
	1.35	3.4±0.2	5.21	29.5±0.0	0.04		1.35	2.7±0.0	0.13	19.9±0.0	0.04		1.35	4.6±0.0	0.13	20.1±0.0	0.04	
	1.40	3.5±0.2	6.57	30.9±0.0	0.04		1.40	2.9±0.0	0.13	21.0±0.0	0.04		1.40	4.0±0.0	0.13	21.6±0.0	0.04	
	1.45	3.9±0.2	5.09	32.2±0.0	0.04		1.45	3.0±0.0	0.13	21.8±0.0	0.04		1.45	4.1±0.0	0.13	21.9±0.0	0.04	
	1.50	3.9±0.2	4.55	33.6±0.0	0.04		1.50	3.1±0.0	0.13	22.0±0.0	0.04		1.50	4.4±0.0	0.13	23.1±0.0	0.04	
	1.55	4.1±0.1	3.05	35.7±0.0	0.04		1.55	3.1±0.0	0.13	22.1±0.0	0.04		1.55	4.7±0.0	0.13	24.0±0.0	0.04	
73.	1.15	5.7±0.0	0.12	37.9±0.0	0.04		1.60	2.9±0.0	0.13	22.3±0.0	0.04		1.60	4.8±0.0	0.13	25.2±0.0	0.04	
	1.20	6.7±0.0	0.13	40.2±0.0	0.04	79.	1.15	1.8±0.0	0.13	11.2±0.0	0.04		1.65	5.0±0.0	0.13	25.3±0.0	0.04	
	1.25	7.3±0.0	0.13	42.6±0.0	0.04		1.20	1.9±0.0	0.13	12.6±0.0	0.04	85.	1.15	2.2±0.0	0.13	10.5±0.0	0.04	
	1.30	5.8±0.0	0.12	44.5±0.0	0.04		1.25	2.0±0.0	0.13	13.4±0.0	0.04		1.20	2.3±0.0	0.13	11.9±0.0	0.04	
	1.35	6.3±0.0	0.12	46.9±0.0	0.04		1.30	2.1±0.0	0.13	14.3±0.0	0.04		1.25	1.8±0.0	0.13	12.6±0.0	0.04	
	1.40	6.8±0.0	0.13	49.4±0.0	0.04		1.35	2.2±0.0	0.13	14.8±0.0	0.04		1.30	1.9±0.0	0.13	13.3±0.0	0.04	
	1.45	6.9±0.0	0.13	51.0±0.0	0.04		1.40	2.3±0.0	0.13	15.4±0.0	0.04		1.35	2.0±0.0	0.13	13.9±0.0	0.04	
	1.50	7.3±0.0	0.13	52.5±0.0	0.04		1.45	2.4±0.0	0.13	16.0±0.0	0.04		1.40	2.1±0.0	0.13	14.6±0.0	0.04	
74.	1.15	3.5±0.0	0.13	20.0±0.0	0.04		1.50	2.5±0.0	0.13	16.3±0.0	0.04		1.45	2.2±0.0	0.13	15.1±0.0	0.04	
	1.20	3.7±0.0	0.13	21.1±0.0	0.04		1.55	2.6±0.0	0.13	16.8±0.0	0.04		1.50	2.3±0.0	0.13	15.4±0.0	0.04	
	1.25	3.9±0.0	0.13	22.1±0.0	0.04		1.60	2.7±0.0	0.13	17.3±0.0	0.04		1.55	2.4±0.0	0.13	16.0±0.0	0.04	
	1.30	4.1±0.0	0.13	23.1±0.0	0.04		1.65	2.5±0.0	0.13	17.1±0.0	0.04		1.60	2.5±0.0	0.13	16.5±0.0	0.04	
	1.35	4.4±0.0	0.13	23.9±0.0	0.04		1.70	2.7±0.0	0.13	17.3±0.0	0.04		1.65	2.8±0.0	0.13	16.7±0.0	0.04	
	1.40	4.5±0.0	0.13	24.2±0.0	0.04		1.75	2.6±0.0	0.13	17.9±0.0	0.04	86.	1.15	2.9±0.0	0.13	13.8±0.0	0.04	
	1.45	4.7±0.0	0.13	25.2±0.0	0.04	80.	1.15	1.4±0.0	0.12	8.3±0.0	0.04		1.20	3.0±0.0	0.13	14.4±0.0	0.04	
	1.50	4.9±0.0	0.13	27.2±0.0	0.04		1.20	1.5±0.0	0.12	8.3±0.0	0.04		1.25	2.6±0.0	0.13	16.2±0.0	0.04	
	1.55	5.1±0.0	0.13	28.2±0.0	0.04		1.25	1.6±0.0	0.12	8.5±0.0	0.04		1.30	2.7±0.0	0.13	17.0±0.0	0.04	
	1.60	5.3±0.0	0.13	29.3±0.0	0.04		1.30	1.7±0.0	0.13	8.8±0.0	0.04		1.35	2.8±0.0	0.13	17.7±0.0	0.04	
	1.65	5.5±0.0	0.13	30.1±0.0	0.04		1.35	1.5±0.0	0.12	9.6±0.0	0.04		1.40	2.9±0.0	0.13	18.5±0.0	0.04	
	1.70	5.7±0.0	0.13	30.3±0.0	0.04		1.40	1.6±0.0	0.12	10.2±0.0	0.04		1.45	3.1±0.0	0.13	19.3±0.0	0.04	
75.	1.10	1.7±0.0	0.12	11.3±0.0	0.04		1.45	1.7±0.0	0.13	10.6±0.0	0.04		1.50	3.2±0.0	0.13	20.0±0.0	0.04	
	1.15	2.1±0.0	0.12	12.0±0.0	0.04		1.50	1.8±0.0	0.13	10.8±0.0	0.04		1.55	3.4±0.0	0.13	20.3±0.0	0.04	
	1.20	2.1±0.0	0.12	14.0±0.0	0.04		1.55	1.8±0.0	0.13	11.3±0.0	0.04		1.60	3.6±0.0	0.13	21.0±0.0	0.04	
	1.25	2.2±0.0	0.12	15.0±0.0	0.04		1.60	1.9±0.0	0.13	11.6±0.0	0.04		1.65	3.7±0.0	0.13	21.7±0.0	0.04	
	1.30	2.3±0.0	0.12	15.8±0.0	0.04		1.65	2.0±0.0	0.13	12.0±0.0	0.04		1.70	3.4±0.0	0.13	21.7±0.0	0.04	
	1.35	2.5±0.0	0.12	16.3±0.0	0.04		1.70	2.2±0.0	0.13	12.4±0.0	0.04	87.	1.15	2.8±0.0	0.12	20.5±0.0	0.04	
	1.40	2.6±0.0	0.13	16.9±0.0	0.04		1.75	2.0±0.0	0.13	12.2±0.0	0.04		1.20	3.1±0.0	0.12	22.3±0.0	0.04	
	1.45	2.7±0.0	0.13	17.5±0.0	0.04		1.80	2.0±0.0	0.13	12.7±0.0	0.04		1.25	3.4±0.0	0.13	23.7±0.0	0.04	
	1.50	2.8±0.0	0.13	18.1±0.0	0.04		1.80	2.0±0.0	0.13	12.7±0.0	0.04		1.30	3.7±0.0	0.13	25.1±0.0	0.04	
	1.55	2.9±0.0	0.13	18.7±0.0	0.04	81.	1.15	4.8±0.0	0.12	35.5±0.0	0.04		1.35	3.9±0.0	0.13	26.4±0.0	0.04	
	1.60	2.7±0.0	0.13	18.3±0.0	0.04		1.20	5.5±0.0	0.12	39.2±0.0	0.04		1.40	4.1±0.0	0.13	27.5±0.0	0.04	
76.	1.15	2.9±0.0	0.13	15.5±0.0	0.04		1.25	5.7±0.0	0.12	41.6±0.0	0.04		1.45	4.2±0.0	0.13	28.6±0.0	0.04	
	1.20	3.0±0.0	0.13	16.1±0.0	0.04		1.30	6.0±0.0	0.13	42.8±0.0	0.04		1.50	4.3±0.0	0.13	29.2±0.0	0.04	
	1.25	2.9±0.0	0.13	18.5±0.0	0.04		1.35	6.4±0.0	0.13	44.3±0.0	0.04		1.55	4.5±0.0	0.13	30.4±0.0	0.04	
	1.30	3.0±0.0	0.13	19.4±0.0	0.04		1.40	6.4±0.0	0.13	46.1±0.0	0.04		1.60	4.2±0.0	0.13	30.2±0.0	0.04	
	1.35	3.2±0.0	0.13	20.3±0.0	0.04		1.45	6.5±0.0	0.13	47.1±0.0	0.04	88.	1.15	1.9±0.0	0.12	13.8±0.0	0.04	
	1.40	3.3±0.0	0.13	21.2±0.0	0.04		1.50	6.8±0.0	0.13	47.8±0.0	0.04		1.20	2.2±0.0	0.12	15.3±0.0	0.04	
	1.45	3.4±0.0	0.13	21.9±0.0	0.04		82.	1.15	3.0±0.0	0.12	22.5±0.0	0.04		1.25	2.5±0.0	0.13	16.4±0.0	0.04
	1.50	3.7±0.0	0.13	22.6±0.0	0.04		1.20	3.4±0.0	0.12	24.9±0.0	0.04		1.30	2.6±0.0	0.13	17.3±0.0	0.04	
	1.55	3.8±0.0	0.13	23.2±0.0	0.04		1.25	3.8±0.0	0.12	26.7±0.0	0.04		1.35	2.7±0.0	0.13	17.7±0.0	0.04	
	1.60	4.0±0.0	0.13	23.5±0.0	0.04		1.30	3.9±0.0	0.12	27.9±0.0	0.04		1.40	2.8±0.0	0.13	18.5±0.0	0.04	
	1.65	4.0±0.0	0.13	23.9±0.0	0.04		1.35	4.1±0.0	0.12	29.2±0.0	0.04		1.45	2.8±0.0	0.13	19.3±0.0	0.04	
	1.70	4.2±0.0	0.13	24.2±0.0	0.04		1.40	4.3±0.0	0.13	30.3±0.0	0.04		1.50	2.9±0.0	0.13	19.6±0.0	0.04	
77.	1.15	3.1±0.0	0.12	23.8±0.0	0.04		1.45	4.3±0.0	0.13	30.8±0.0	0.04		1.55	2.7±0.0	0.13	19.6±0.0	0.04	
	1.20	3.4±0.0	0.12	26.5±0.0	0.04		1.50	4.3±0.0	0.13	31.6±0.0	0.04	89.	1.15	1.7±0.0	0.13	10.4±0.0	0.04	
	1.25	3.8±0.0	0.12	28.4±0.0	0.04	83.	1.15	4.1±0.0	0.12	29.5±0.0	0.04		1.20	1.8±0.0	0.13	11.1±0.0	0.04	
	1.30	4.0±0.0	0.12	30.0±0.0	0.04		1.20	4.7±0.0	0.12	33.0±0.0	0.04		1.25	2.0±0.0	0.13	11.9±0.0	0.04	
	1.35	4.2±0.0	0.13	30.9±0.0	0.04		1.25	5.0±0.0	0.13	34.9±0.0	0.04		1.30	2.1±0.0	0.13	12.5±0.0	0.04	
	1.40	4.4±0.0	0.13	32.1±0.0	0.04		1.30	5.3±0.0	0.13	36.1±0.0	0.04		1.35	2.2±0.0	0.13	13.2±0.0	0.04	
	1.45	4.5±0.0	0.13	33.2±0.0	0.04		1.35	5.4±0.0	0.13	37.7±0.0	0.04		1.40	2.3±0.0	0.13	13.7±0.0	0.04	
	1.50	4.6±0.0	0.13	33.9±0.0	0.04		1.40	5.7±0.0	0.13	39.4±0.0	0.04		1.45	2.4±0.0	0.13	14.1±0.0	0.04	
							1.45	5.8±0.0	0.13	40.2±0.0	0.04		1.50	2.5±0.0	0.13	14.6±0.0	0.04	
							1.50	6.0±0.0	0.13	41.4±0.0	0.04		1.55	2.6±0.0	0.13	14.8±0.0	0.04	
							1.55	6.3±0.0	0.13	43.3±0.0	0.04		1.60	2.6±0.0	0.13	15.2±0.0	0.04	
							1.60	6.4±0.0	0.13	43.9±0.0	0.04		1.65	2.5±0.0	0.13	14.6±0.0	0.04	
												1.70	3.0±0.0	0.13	16.1±0.0	0.04		

NO.	NF	V _g (lb) %ERR	H _g (lb) %ERR	NO.	NF	V _g (lb) %ERR	H _g (lb) %ERR	NO.	NF	V _g (lb) %ERR	H _g (lb) %ERR						
156.	1.55	1.4±0.0	2.16	10.6±0.1	0.54	164.	1.55	1.5±0.0	0.12	12.0±0.0	0.04	171.	1.55	1.3±0.0	0.12	9.9±0.0	0.03
	1.60	1.5±0.0	1.60	11.1±0.1	0.49		1.60	1.6±0.0	0.12	12.5±0.0	0.04		1.60	1.5±0.0	0.12	11.0±0.1	0.53
	1.65	1.6±0.0	0.12	11.5±0.0	0.04		1.65	1.7±0.0	0.13	13.0±0.0	0.04		1.65	1.6±0.0	0.12	11.8±0.0	0.04
	1.70	1.6±0.0	0.12	11.8±0.0	0.04		1.70	1.8±0.0	0.13	13.4±0.0	0.04		1.70	1.7±0.0	0.54	12.3±0.0	0.04
	1.75	1.6±0.0	1.11	12.1±0.0	0.04		1.75	1.8±0.0	0.13	13.9±0.0	0.04		1.75	1.8±0.0	0.88	12.7±0.0	0.04
157.	1.50	1.7±0.0	0.85	13.0±0.0	0.04		1.80	1.9±0.0	0.13	14.2±0.0	0.04		1.80	1.8±0.0	0.13	13.0±0.0	0.04
	1.55	1.8±0.0	0.98	13.5±0.0	0.04		1.85	1.9±0.1	3.56	14.6±0.1	0.84		1.85	1.9±0.0	0.56	13.5±0.0	0.04
	1.60	1.9±0.0	0.84	14.0±0.0	0.04		1.90	2.0±0.1	2.98	14.7±0.1	0.59		1.90	2.1±0.0	0.43	13.9±0.0	0.04
	1.65	2.0±0.0	0.12	14.5±0.0	0.04		1.95	2.0±0.1	4.99	15.0±0.1	0.64		1.95	2.1±0.0	0.13	14.1±0.0	0.04
	1.70	2.0±0.0	0.12	14.9±0.0	0.04		2.00	2.1±0.1	2.97	15.3±0.1	0.54		2.00	2.1±0.0	0.13	14.5±0.0	0.04
	1.75	2.1±0.0	1.32	15.2±0.0	0.04	165.	1.55	1.7±0.0	0.80	11.9±0.0	0.04		2.05	2.1±0.0	0.13	14.9±0.0	0.04
	1.80	2.1±0.0	0.12	15.5±0.0	0.04		1.60	1.8±0.0	0.70	12.3±0.0	0.04		2.10	2.2±0.0	0.13	15.2±0.0	0.04
	1.85	2.2±0.0	1.61	16.0±0.0	0.04		1.65	1.8±0.0	0.13	12.8±0.0	0.04	172.	1.55	1.2±0.0	0.12	8.1±0.0	0.03
	1.90	2.2±0.0	1.30	16.2±0.1	0.46		1.70	1.9±0.0	0.58	13.0±0.0	0.04		1.60	1.4±0.0	2.27	9.2±0.0	0.04
158.	1.55	1.8±0.0	0.97	13.8±0.0	0.04		1.75	2.0±0.0	0.13	13.4±0.0	0.04		1.65	1.3±0.0	1.66	9.8±0.0	0.04
	1.60	1.8±0.0	1.28	14.1±0.0	0.04		1.80	2.0±0.0	0.50	13.9±0.0	0.04		1.70	1.4±0.0	0.12	10.3±0.0	0.04
	1.65	1.9±0.0	1.18	14.6±0.0	0.04		1.85	2.1±0.0	0.87	14.3±0.0	0.04		1.75	1.5±0.0	1.73	10.8±0.1	0.68
	1.70	2.0±0.0	0.65	15.0±0.0	0.04		1.90	2.1±0.0	0.13	14.4±0.0	0.04		1.80	1.5±0.0	2.58	11.2±0.0	0.04
	1.75	2.0±0.0	0.44	15.2±0.0	0.04		1.95	2.2±0.0	1.71	14.7±0.1	0.78		1.85	1.6±0.0	1.89	11.8±0.0	0.39
	1.80	2.1±0.0	0.62	15.8±0.0	0.04	166.	1.60	0.9±0.0	0.13	6.3±0.0	0.04		1.90	1.6±0.0	0.12	12.1±0.0	0.04
	1.85	2.1±0.0	0.71	16.1±0.0	0.04		1.65	0.9±0.0	0.13	6.4±0.0	0.04		1.95	1.7±0.0	0.13	12.2±0.0	0.04
159.	1.55	0.9±0.0	0.77	7.0±0.0	0.04		1.70	0.9±0.0	0.76	6.6±0.0	0.04		2.00	1.7±0.0	0.13	12.3±0.0	0.04
	1.60	0.9±0.0	0.38	7.2±0.0	0.04		1.75	1.0±0.0	0.13	6.9±0.0	0.04		2.05	1.7±0.0	0.13	12.7±0.0	0.04
	1.65	1.0±0.0	0.13	7.4±0.0	0.04		1.80	1.0±0.0	0.70	7.0±0.0	0.04		2.10	1.7±0.0	0.13	12.9±0.0	0.04
	1.70	1.0±0.0	1.02	7.6±0.0	0.04		1.85	1.1±0.0	0.13	7.2±0.0	0.04	173.	1.55	1.0±0.0	0.12	6.4±0.0	0.03
	1.75	1.1±0.0	0.93	7.8±0.0	0.04		1.90	1.1±0.0	2.26	7.2±0.1	0.91		1.60	1.1±0.0	0.12	6.6±0.0	0.03
	1.80	1.1±0.0	0.65	7.9±0.0	0.04		1.95	1.1±0.0	3.29	7.3±0.0	0.62		1.65	1.1±0.0	0.12	7.3±0.0	0.04
	1.85	1.1±0.0	0.82	8.1±0.0	0.04		2.00	1.1±0.0	2.18	7.4±0.0	0.04		1.70	1.1±0.0	0.12	7.8±0.0	0.04
	1.90	1.1±0.0	0.76	8.3±0.0	0.04	167.	1.60	2.5±0.0	0.12	16.4±0.0	0.03		1.75	1.1±0.0	0.12	8.2±0.0	0.04
160.	1.55	2.7±0.0	0.12	21.5±0.0	0.04		1.65	2.6±0.0	0.12	17.5±0.0	0.04		1.80	1.1±0.0	0.12	8.4±0.0	0.04
	1.60	2.8±0.0	0.12	22.4±0.0	0.04		1.70	2.8±0.0	0.12	18.2±0.0	0.04		1.85	1.2±0.0	2.58	8.9±0.0	0.04
	1.65	2.9±0.0	0.12	22.8±0.0	0.04		1.75	2.9±0.0	0.12	18.8±0.0	0.04		1.90	1.2±0.0	0.12	9.0±0.0	0.04
	1.70	3.0±0.0	0.12	23.6±0.0	0.04		1.80	3.0±0.0	0.12	19.5±0.0	0.04		1.95	1.3±0.0	0.12	9.3±0.0	0.04
	1.75	3.1±0.0	0.12	24.1±0.0	0.04		1.85	3.2±0.2	6.24	20.4±0.3	1.26		2.00	1.3±0.0	0.12	9.4±0.0	0.04
	1.80	3.2±0.0	0.12	24.6±0.0	0.04	168.	1.55	1.2±0.0	0.12	7.8±0.0	0.03		2.05	1.4±0.0	0.12	9.7±0.0	0.04
	1.85	3.2±0.0	0.12	25.4±0.0	0.04		1.60	1.3±0.0	0.12	8.5±0.0	0.04		2.10	1.4±0.0	0.12	9.8±0.0	0.04
	1.90	3.3±0.0	0.12	25.7±0.0	0.04		1.65	1.3±0.0	0.12	9.1±0.0	0.04	174.	1.60	1.1±0.0	0.12	6.6±0.0	0.03
	1.95	3.4±0.0	0.12	25.9±0.0	0.04		1.70	1.4±0.0	0.12	9.5±0.0	0.04		1.65	1.1±0.0	0.12	7.2±0.0	0.04
	2.00	3.4±0.0	0.72	26.6±0.0	0.04		1.75	1.4±0.0	1.85	9.8±0.0	0.04		1.70	1.1±0.0	0.12	7.7±0.0	0.04
161.	1.55	2.8±0.0	0.12	21.4±0.0	0.04		1.80	1.4±0.0	0.84	10.1±0.0	0.04		1.75	1.2±0.0	0.12	8.1±0.0	0.04
	1.60	3.0±0.0	0.39	22.3±0.0	0.04		1.85	1.5±0.0	1.36	10.6±0.0	0.04		1.80	1.2±0.0	0.12	8.4±0.0	0.04
	1.65	3.1±0.0	0.12	22.9±0.0	0.04		1.90	1.5±0.0	1.72	11.4±0.3	2.91		1.85	1.2±0.0	0.12	8.8±0.0	0.04
	1.70	3.2±0.0	0.12	23.7±0.0	0.04		1.95	1.5±0.0	0.12	11.9±0.0	0.04		1.90	1.3±0.0	0.12	9.1±0.0	0.04
	1.75	3.2±0.0	0.12	24.3±0.0	0.04		2.00	1.5±0.0	0.12	12.2±0.0	0.04		1.95	1.3±0.0	0.12	9.2±0.0	0.04
	1.80	3.3±0.0	0.12	24.7±0.0	0.04		2.05	1.5±0.0	0.12	12.3±0.0	0.04		2.00	1.4±0.0	0.12	9.5±0.0	0.04
	1.85	3.4±0.0	0.12	25.5±0.0	0.04		2.10	1.6±0.0	0.12	12.6±0.0	0.04		2.05	1.4±0.0	0.12	9.6±0.0	0.04
	1.90	3.4±0.0	0.37	25.7±0.0	0.04	169.	1.55	2.1±0.0	0.62	15.7±0.0	0.04	175.	1.55	0.6±0.0	0.12	4.6±0.0	0.03
	1.95	3.5±0.0	0.12	26.4±0.0	0.04		1.60	2.2±0.0	0.40	16.4±0.0	0.04		1.60	0.7±0.0	0.12	5.3±0.0	0.04
162.	1.55	2.1±0.0	0.12	16.8±0.0	0.04		1.65	2.3±0.0	0.30	16.9±0.0	0.04		1.65	0.8±0.0	0.12	5.1±0.0	0.04
	1.60	2.3±0.0	0.12	17.7±0.0	0.04		1.70	2.4±0.0	0.12	17.2±0.0	0.04		1.70	0.8±0.0	0.12	5.4±0.0	0.04
	1.65	2.4±0.0	0.12	18.3±0.0	0.04		1.75	2.4±0.0	0.37	17.8±0.0	0.04		1.75	0.9±0.0	0.13	5.8±0.0	0.04
	1.70	2.5±0.0	0.12	19.1±0.0	0.04		1.80	2.5±0.0	0.12	18.3±0.0	0.04		1.80	0.8±0.0	0.12	6.1±0.0	0.04
	1.75	2.6±0.0	0.77	19.4±0.0	0.04		1.85	2.6±0.0	0.13	18.6±0.0	0.04		1.85	0.9±0.0	0.13	6.4±0.0	0.04
	1.80	2.8±0.0	0.12	20.0±0.0	0.04		1.90	2.7±0.0	0.13	19.1±0.0	0.04		1.90	0.9±0.0	0.13	6.5±0.0	0.04
	1.85	2.7±0.0	0.79	20.2±0.0	0.04		1.95	2.7±0.0	0.13	19.2±0.0	0.04		1.95	1.0±0.0	0.13	6.7±0.0	0.04
	1.90	2.8±0.1	2.69	20.7±0.0	0.04		2.00	2.8±0.0	0.13	19.4±0.0	0.04		2.00	1.0±0.0	0.13	6.9±0.0	0.04
	1.95	2.8±0.1	2.70	21.2±0.0	0.04		2.05	2.8±0.0	0.13	19.8±0.0	0.04		2.05	1.0±0.0	0.13	7.1±0.0	0.04
163.	1.55	2.2±0.0	0.12	16.7±0.0	0.04	170.	1.55	1.1±0.0	0.12	7.7±0.0	0.04	176.	1.55	0.5±0.0	0.11	2.5±0.0	0.03
	1.60	2.3±0.0	0.12	17.5±0.0	0.04		1.60	1.1±0.0	1.27	8.0±0.0	0.62		1.60	0.7±0.0	0.12	4.4±0.0	0.03
	1.65	2.4±0.0	0.12	18.1±0.0	0.04		1.65	1.2±0.0	0.12	8.3±0.0	0.04		1.65	0.8±0.0	0.12	4.9±0.0	0.03
	1.70	2.6±0.0	0.12	18.7±0.0	0.04		1.70	1.3±0.0	0.36	8.7±0.0	0.04		1.70	0.8±0.0	0.12	5.3±0.0	0.04
	1.75	2.6±0.1	2.08	19.3±0.0	0.04		1.75	1.3±0.0	0.64	9.0±0.0	0.39		1.75	0.9±0.0	0.13	5.6±0.0	0.04
	1.80	2.7±0.1	2.31	19.5±0.2	1.12		1.80	1.3±0.0	0.52	9.3±0.0	0.04		1.80	0.9±0.0	0.13	5.9±0.0	0.04
							1.85	1.4±0.0	0.30	9.6±0.0	0.04		1.85	1.0±0.0	0.13	6.2±0.0	0.04
							1.90	1.4±0.0	0.74	9.7±0.0	0.04		1.90	1.0±0.0	0.13	6.4±0.0	0.04
							1.95	1.4±0.0	0.51	9.9±0.0	0.04		1.95	1.0±0.0	0.13	6.6±0.0	0.04
													2.00	1.0±0.0	0.13	6.8±0.0	0.04
													2.05	1.1±0.0	0.13	6.9±0.0	0.04

NO.	NF	V _d (lb)	%ERR	H _d (lb)	%ERR	NO.	NF	V _d (lb)	%ERR	H _d (lb)	%ERR	NO.	NF	V _d (lb)	%ERR	H _d (lb)	%ERR
193.	1.60	1.0±0.0	4.74	8.3±0.2	2.10	198.	1.60	1.0±0.2	19.9	7.4±0.1	1.85	203.	1.55	0.4±0.0	0.11	2.3±0.0	0.03
	1.65	1.1±0.1	7.93	9.4±0.1	1.34		1.65	1.2±0.2	17.1	7.9±0.2	2.62		1.60	0.5±0.0	1.20	2.7±0.0	1.18
	1.70	1.2±0.1	7.34	10.1±0.1	0.94		1.70	1.0±0.0	4.49	8.5±0.2	2.37		1.65	0.6±0.0	2.42	2.9±0.0	1.67
	1.75	1.3±0.1	6.41	10.5±0.1	0.96		1.75	1.0±0.1	6.12	8.8±0.2	2.10		1.70	0.6±0.0	0.12	3.2±0.0	0.04
	1.80	1.3±0.0	0.12	10.8±0.1	0.48		1.80	1.3±0.1	8.77	9.3±0.1	1.43		1.75	0.7±0.0	2.05	3.5±0.0	0.62
	1.85	1.4±0.0	0.12	11.2±0.0	0.04		1.85	1.3±0.1	11.0	9.9±0.2	1.53		1.80	0.7±0.0	2.35	3.7±0.1	1.51
	1.90	1.5±0.0	0.12	11.5±0.0	0.04		1.90	1.3±0.0	2.02	10.7±0.1	1.39		1.85	0.7±0.0	4.32	3.8±0.1	1.38
	1.95	1.5±0.0	0.12	11.8±0.0	0.04		1.95	1.4±0.0	0.12	11.1±0.0	0.04		1.90	0.7±0.0	2.26	3.9±0.0	0.04
	2.00	1.5±0.0	0.12	12.0±0.0	0.04		2.00	1.4±0.0	0.12	11.2±0.0	0.04		1.95	0.7±0.0	5.76	4.0±0.1	1.77
	2.05	1.6±0.0	0.12	12.2±0.0	0.04		2.05	1.4±0.0	0.12	11.5±0.0	0.04		2.00	0.8±0.0	4.82	4.1±0.1	1.80
	2.10	1.6±0.1	4.73	12.5±0.1	1.16		2.10	1.5±0.0	0.12	11.5±0.0	0.04		2.05	0.8±0.0	0.12	4.2±0.0	0.54
	2.15	1.7±0.1	4.32	12.8±0.2	1.84		2.15	1.5±0.0	0.12	11.9±0.0	0.04	204.	1.55	0.2±0.0	0.14	0.9±0.0	0.03
194.	1.60	0.9±0.1	6.95	7.4±0.2	2.15		2.20	1.6±0.0	0.12	12.1±0.0	0.04		1.60	0.2±0.0	0.14	1.1±0.0	0.03
	1.65	1.0±0.1	6.03	7.9±0.1	1.68	199.	1.60	0.6±0.0	0.12	4.6±0.0	0.03		1.65	0.2±0.0	1.53	1.3±0.0	0.45
	1.70	1.2±0.1	7.84	8.5±0.1	1.36		1.65	0.7±0.0	0.12	5.1±0.0	0.04		1.70	0.3±0.0	3.34	1.4±0.0	0.42
	1.75	1.1±0.0	0.12	9.0±0.0	0.04		1.70	0.7±0.0	0.12	5.5±0.0	0.04		1.75	0.3±0.0	2.62	1.5±0.0	0.03
	1.80	1.2±0.0	0.12	9.4±0.0	0.04		1.75	0.8±0.0	5.84	5.8±0.0	0.04		1.80	0.3±0.0	2.39	1.6±0.0	0.03
	1.85	1.2±0.0	0.12	9.7±0.0	0.04		1.80	0.7±0.0	5.40	6.2±0.1	0.82		1.85	0.3±0.0	2.18	1.7±0.0	0.03
	1.90	1.3±0.0	0.12	9.9±0.0	0.04		1.85	0.7±0.0	0.12	6.4±0.0	0.04		1.90	0.3±0.0	2.73	1.7±0.0	0.03
	1.95	1.3±0.0	0.12	10.0±0.0	0.04		1.90	0.9±0.0	0.13	6.6±0.0	0.04		1.95	0.3±0.0	3.90	1.8±0.0	0.03
	2.00	1.4±0.0	0.12	10.4±0.0	0.04		1.95	1.0±0.1	6.18	6.8±0.1	1.26		2.00	0.3±0.0	0.14	1.8±0.0	0.03
	2.05	1.4±0.0	0.12	10.6±0.0	0.04		2.00	1.0±0.1	5.16	6.9±0.1	2.07		2.05	0.4±0.0	0.14	2.0±0.0	0.04
	2.10	1.4±0.1	7.23	10.8±0.2	1.95		2.05	0.9±0.0	4.86	7.0±0.1	1.74		2.10	0.4±0.0	1.20	2.0±0.0	0.04
195.	1.60	1.3±0.1	9.51	9.8±0.3	2.83		2.10	1.0±0.1	6.97	7.2±0.2	3.44	205.	1.70	0.3±0.0	0.09	1.4±0.0	0.03
	1.65	1.5±0.1	7.33	10.6±0.1	1.29		2.15	1.1±0.1	6.74	7.3±0.2	2.60		1.75	0.4±0.0	3.77	2.4±0.0	1.22
	1.70	1.6±0.1	6.16	11.3±0.0	0.04		2.20	1.1±0.0	0.13	7.8±0.0	0.04		1.80	0.4±0.0	2.08	2.6±0.0	1.02
	1.75	1.7±0.1	6.48	12.0±0.1	0.80		2.25	1.2±0.0	0.85	8.0±0.0	0.04		1.85	0.4±0.0	0.11	2.9±0.0	0.04
	1.80	1.7±0.1	3.94	12.3±0.2	1.27	200.	1.60	0.8±0.0	5.62	6.1±0.2	3.54		1.90	0.4±0.0	0.11	3.0±0.0	0.04
	1.85	1.8±0.1	4.48	12.9±0.0	0.04		1.65	0.9±0.1	9.28	6.4±0.2	3.04		1.95	0.5±0.0	1.22	3.1±0.0	0.04
	1.90	1.8±0.0	0.12	13.2±0.0	0.04		1.70	1.0±0.1	7.04	7.4±0.2	2.76		2.00	0.5±0.0	0.11	3.2±0.0	0.04
	1.95	1.9±0.0	0.12	13.6±0.0	0.04		1.75	1.0±0.1	9.18	7.9±0.2	2.43		2.05	0.5±0.0	0.88	3.3±0.0	0.04
	2.00	2.2±0.1	5.73	13.7±0.1	0.73		1.80	1.1±0.1	5.16	8.2±0.2	2.40		2.10	0.5±0.0	0.12	3.5±0.0	0.04
	2.05	2.2±0.2	7.09	14.1±0.2	1.69		1.85	1.2±0.1	4.23	8.6±0.2	1.82		2.15	0.6±0.0	0.12	3.6±0.0	0.04
	2.10	2.1±0.0	0.12	15.8±0.0	0.04		1.90	1.3±0.0	3.36	9.4±0.2	1.74		2.20	0.7±0.0	0.12	3.8±0.0	0.04
	2.15	2.1±0.0	0.12	16.0±0.0	0.04		1.95	1.4±0.0	3.41	9.6±0.1	0.72		2.25	0.7±0.0	0.12	3.8±0.0	0.04
196.	1.60	2.0±0.5	24.0	13.3±0.2	1.49		2.00	1.4±0.0	0.12	9.9±0.0	0.04	206.	1.70	1.0±0.1	11.6	7.0±0.2	3.16
	1.65	2.3±0.1	5.66	16.9±0.5	2.82		2.05	1.4±0.0	0.12	10.1±0.0	0.04		1.75	1.0±0.1	6.30	7.7±0.2	2.59
	1.70	2.6±0.2	7.33	17.1±0.5	2.67		2.10	1.4±0.0	0.12	10.3±0.0	0.04		1.80	1.0±0.1	8.71	8.0±0.1	1.67
	1.75	2.7±0.1	4.90	19.1±0.4	2.03		2.15	1.4±0.0	0.12	10.5±0.0	0.04		1.85	1.1±0.1	4.68	8.5±0.2	2.24
	1.80	2.6±0.1	5.00	19.9±0.2	1.21		2.20	1.6±0.0	1.34	10.8±0.1	0.66		1.90	1.2±0.0	0.12	8.7±0.0	0.04
	1.85	2.7±0.2	6.87	19.3±0.5	2.82		2.25	1.7±0.0	0.13	11.0±0.0	0.04		1.95	1.3±0.1	7.79	9.0±0.1	1.26
	1.90	2.7±0.2	7.12	20.3±0.4	2.19	201.	1.60	0.4±0.0	7.41	2.1±0.1	3.13		2.00	1.3±0.1	9.12	9.2±0.1	0.99
	1.95	2.8±0.3	10.9	20.4±0.0	0.04		1.65	0.3±0.0	0.10	2.4±0.0	0.03		2.05	1.3±0.1	10.9	9.4±0.3	3.70
	2.00	3.0±0.1	3.24	21.8±0.2	1.03		1.70	0.3±0.0	7.43	2.6±0.0	0.03	207.	1.70	0.7±0.1	9.55	4.7±0.1	1.26
	2.05	3.1±0.1	2.88	22.1±0.2	0.78		1.75	0.4±0.0	0.11	2.9±0.0	0.03		1.75	0.7±0.0	2.03	5.2±0.1	1.96
	2.10	3.0±0.0	0.12	22.2±0.0	0.04		1.80	0.4±0.0	0.11	2.9±0.0	0.03		1.80	0.8±0.0	0.12	5.6±0.1	1.61
197.	1.60	2.0±0.1	3.63	14.9±0.2	1.45		1.85	0.4±0.0	0.11	3.0±0.0	0.04		1.85	0.8±0.1	10.4	5.9±0.1	2.19
	1.65	1.9±0.0	0.12	16.1±0.0	0.04		1.90	0.5±0.0	7.34	3.1±0.0	0.04		1.90	0.8±0.0	4.34	6.2±0.0	0.04
	1.70	2.0±0.0	0.12	17.0±0.0	0.04		1.95	0.5±0.0	6.54	3.2±0.0	0.04		1.95	0.8±0.0	4.82	6.5±0.0	0.04
	1.75	2.1±0.0	0.12	17.7±0.0	0.04		2.00	0.5±0.0	5.46	3.4±0.1	2.17		2.00	0.9±0.1	12.5	6.8±0.1	1.50
	1.80	2.2±0.0	0.12	18.0±0.0	0.04		2.05	0.6±0.0	4.34	3.5±0.1	2.13		2.05	1.0±0.0	1.80	7.0±0.0	0.64
	1.85	2.2±0.0	0.12	18.5±0.0	0.04		2.10	0.6±0.0	0.12	3.6±0.0	0.04		2.10	1.0±0.0	0.13	7.2±0.0	0.04
	1.90	2.2±0.0	0.12	18.9±0.0	0.04	202.	1.55	0.6±0.0	0.12	4.0±0.0	0.03		2.15	1.0±0.0	3.91	7.3±0.1	1.37
	1.95	2.3±0.0	0.12	19.2±0.0	0.04		1.60	0.7±0.0	0.12	4.7±0.0	0.03	208.	1.70	0.9±0.1	11.4	6.2±0.2	3.75
	2.00	2.3±0.0	0.12	19.6±0.0	0.04		1.65	0.8±0.0	0.12	5.0±0.0	0.04		1.75	0.9±0.1	6.00	7.0±0.1	2.00
	2.05	2.3±0.0	0.12	19.9±0.0	0.04		1.70	0.8±0.0	0.13	5.3±0.0	0.04		1.80	1.0±0.1	7.51	7.2±0.1	2.05
	2.10	2.3±0.0	0.12	20.0±0.0	0.04		1.75	0.9±0.0	0.13	5.6±0.0	0.04		1.85	1.0±0.0	0.11	7.4±0.0	0.04
							1.80	0.9±0.0	0.13	5.8±0.0	0.04		1.90	1.0±0.0	0.11	8.0±0.0	0.04
							1.85	1.0±0.0	0.13	6.0±0.0	0.04		1.95	1.1±0.0	0.12	8.3±0.0	0.04
							1.90	1.0±0.0	0.13	6.1±0.0	0.04		2.00	1.1±0.1	8.19	8.5±0.1	1.57
							1.95	1.0±0.0	0.13	6.2±0.0	0.04		2.05	1.2±0.1	6.99	8.7±0.1	0.89
							2.00	1.1±0.0	0.13	6.3±0.0	0.04		2.10	1.2±0.0	0.12	9.1±0.0	0.04
							2.05	1.3±0.0	0.40	6.4±0.0	0.04		2.15	1.3±0.0	0.12	9.2±0.0	0.04

APPENDIX G: SIMILARITY PAIRS

PART I: The wire type, wire length, and span length for each of the 108 wire pairs which only differ in unit weight between the two sets of wires in the same pair.

UNIT WEIGHT RATIO	PAIR NO.	WIRE TYPE	WIRE LENGTH(ft)	SPAN (ft)
1:3	1	1A2 vs. 1A2+(2A2)	46.6	46.0
	2	1A3 vs. 1A3+(2A3)	46.6	46.0
	3	1A2 vs. 1A2+(2A2)	40.4	40.0
	4	1A3 vs. 1A3+(2A3)	40.4	40.0
	5	1S3 vs. 1S3+(2S3)	40.4	40.0
	6	1A3 vs. 1A3+(2A3)	40.2	40.0
	7	1A3 vs. 1A3+(2A3)	23.2	23.0
	8	1A2 vs. 1A2+(2A2)	21.7	21.5
	9	1A3 vs. 1A3+(2A3)	21.7	21.5
	10	1A2 vs. 1A2+(2A2)	20.2	20.0
	11	1C3 vs. 1C3+(2C3)	20.2	20.0
1:2	12	1S2 vs. 1S2+(1S2)	46.6	46.0
	13	1S3 vs. 1S3+(1S3)	46.6	46.0
	14	1C3 vs. 1C3+(1C3)	46.6	46.0
	15	1S2 vs. 1S2+(1S2)	46.4	46.0
	16	1S3 vs. 1S3+(1S3)	46.4	46.0
	17	1C3 vs. 1C3+(1C3)	46.4	46.0
	18	1A1 vs. 1A1+(1A1)	46.4	46.0
	19	1A1+1A2 vs. 1A1+1A2+(1A1+1A2)	46.4	46.0
	20	1A1+1A3 vs. 1A1+1A3+(1A1+1A3)	46.4	46.0
	21	2A2 vs. 2A2+(2A2)	46.4	46.0
	22	1A2 vs. 1A2+(1A2)	46.4	46.0
	23	1A2+1A3 vs. 1A2+1A3+(1A2+1A3)	46.4	46.0
	24	2A3 vs. 2A3+(2A3)	46.4	46.0
	25	1A3 vs. 1A3+(1A3)	46.4	46.0
	26	1A3 vs. 1A3+(1A3)	40.4	40.0
	27	1A2 vs. 1A2+(1A2)	40.4	40.0
	28	2S3 vs. 2S3+(2S3)	40.4	40.0
	29	1S3 vs. 1S3+(1S3)	40.4	40.0
	30	1C3 vs. 1C3+(1C3)	40.4	40.0
	31	1S2 vs. 1S2+(1S2)	40.4	40.0
	32	1C2 vs. 1C2+(1C2)	40.4	40.0
	33	1A3 vs. 1A3+(1A3)	40.2	40.0
	34	1A1 vs. 1A1+(1A1)	40.2	40.0
	35	1C3 vs. 1C3+(1C3)	23.2	23.0
	36	1C3 vs. 1C3+(1C3)	23.2	23.0
	37	1A1 vs. 1A1+(1A1)	23.2	23.0
	38	1A1+1A2 vs. 1A1+1A2+(1A1+1A2)	23.2	23.0
	39	1A1+1A3 vs. 1A1+1A3+(1A1+1A3)	23.2	23.0
	40	2A3 vs. 2A3+(2A3)	23.2	23.0
	41	1A3 vs. 1A3+(1A3)	23.2	23.0
	42	2A2 vs. 2A2+(2A2)	23.2	23.0
	43	1A2 vs. 1A2+(1A2)	21.7	21.5
	44	1A3 vs. 1A3+(1A3)	21.7	21.5
	45	1A2 vs. 1A2+(1A2)	20.2	20.0
46	1C3 vs. 1C3+(1C3)	20.2	20.0	

UNIT WEIGHT RATIO	PAIR NO.	WIRE TYPE	WIRE LENGTH(ft)	SPAN (ft)
2:3	47	2S3 vs. 2S3+(1S3)	46.6	46.0
	48	2S3 vs. 2S3+(1S3)	46.4	46.0
	49	2A1 vs. 2A1+(1A1)	46.4	46.0
	50	4A2 vs. 4A2+(2A2)	46.4	46.0
	51	2A2 vs. 2A2+(1A2)	46.4	46.0
	52	4A3 vs. 4A3+(2A3)	46.4	46.0
	53	2A3 vs. 2A3+(1A3)	46.4	46.0
	54	4A2 vs. 4A2+(2A2)	43.4	43.0
	55	4A3 vs. 4A3+(2A3)	43.4	43.0
	56	4A2 vs. 4A2+(2A2)	40.4	40.0
	57	4A3 vs. 4A3+(2A3)	40.4	40.0
	58	2S3 vs. 2S3+(1S3)	40.4	40.0
	59	2C3 vs. 2C3+(1C3)	40.4	40.0
	60	4A2 vs. 4A2+(2A2)	40.2	40.0
	61	4A3 vs. 4A3+(2A3)	40.2	40.0
	62	2A1 vs. 2A1+(1A1)	40.2	40.0
	63	2A1 vs. 2A1+(1A1)	23.2	23.0
	64	4A3 vs. 4A3+(2A3)	23.2	23.0
	65	2A3 vs. 2A3+(1A3)	23.2	23.0
	66	4A2 vs. 4A2+(2A2)	23.2	23.0
	67	2A2 vs. 2A2+(1A2)	23.2	23.0
	68	4A2 vs. 4A2+(2A2)	21.7	21.5
	69	2C3 vs. 2C3+(1C3)	21.7	21.5
	70	4A3 vs. 4A3+(2A3)	21.7	21.5
	71	1A2+(1A2) vs. 1A2+(2A2)	46.4	46.0
	72	1A3+(1A3) vs. 1A3+(2A3)	46.4	46.0
	73	1A2+(1A2) vs. 1A2+(2A2)	43.4	43.0
	74	1A3+(1A3) vs. 1A3+(2A3)	43.4	43.0
	75	1A2+(1A2) vs. 1A2+(2A2)	40.4	40.0
	76	1A3+(1A3) vs. 1A3+(2A3)	40.4	40.0
	77	1S3+(1S3) vs. 1S3+(2S3)	40.4	40.0
	78	1A2+(1A2) vs. 1A2+(2A2)	40.2	40.0
	79	1A3+(1A3) vs. 1A3+(2A3)	40.2	40.0
	80	1A3+(1A3) vs. 1A3+(2A3)	23.2	23.0
	81	1A2+(1A2) vs. 1A2+(2A2)	23.2	23.0
	82	1A2+(1A2) vs. 1A2+(2A2)	21.7	21.5
83	1A3+(1A3) vs. 1A3+(2A3)	21.7	21.5	
84	1A2+(1A2) vs. 1A2+(2A2)	20.2	20.0	
85	1A3+(1A3) vs. 1A3+(2A3)	20.2	20.0	
86	1C3+(1C3) vs. 1C3+(2C3)	20.2	20.0	
3:4	87	3A2 vs. 3A2+(1A2)	46.4	46.0
	88	3A3 vs. 3A3+(1A3)	46.4	46.0
	89	3S3 vs. 3S3+(1S3)	40.4	40.0
	90	3C3 vs. 3C3+(1C3)	40.4	40.0
	91	3A1 vs. 3A1+(1A1)	40.2	40.0
	92	3A1 vs. 3A1+(1A1)	23.2	23.0
	93	3A3 vs. 3A3+(1A3)	23.2	23.0
	94	3A2 vs. 3A2+(1A2)	23.2	23.0
	95	3C3 vs. 3C3+(1C3)	20.2	20.0
	96	2A2+(1A2) vs. 2A2+(2A2)	46.4	46.0
	97	2A3+(1A3) vs. 2A3+(2A3)	46.4	46.0
	98	2S3+(1S3) vs. 2S3+(2S3)	40.4	40.0
	99	2A3+(1A3) vs. 2A3+(2A3)	23.2	23.0
	100	2A2+(1A2) vs. 2A2+(2A2)	23.2	23.0
4:5	101	4A2 vs. 4A2+(1A2)	46.4	46.0
	102	4A3 vs. 4A3+(1A3)	46.4	46.0
	103	4A3 vs. 4A3+(1A3)	23.2	23.0
	104	4A2 vs. 4A2+(1A2)	23.2	23.0
5:6	105	4A2+(1A2) vs. 4A2+(2A2)	46.4	46.0
	106	4A3+(1A3) vs. 4A3+(2A3)	46.4	46.0
	107	4A3+(1A3) vs. 4A3+(2A3)	23.2	23.0
	108	4A2+(1A2) vs. 4A2+(2A2)	23.2	23.0

PART II: The wire type, wire length, and span length for each of the 60 wire pairs which only differ in cross-sectional area between the two sets of wires in the same pair.

AREA RATIO	PAIR NO.	WIRE TYPE	WIRE LENGTH(ft)	SPAN (ft)
1:3	1	1A2+(2A2) vs. 3A2	46.4	46.0
	2	1A3+(2A3) vs. 3A3	46.4	46.0
	3	1S3+(2S3) vs. 3S3	40.4	40.0
	4	1A3+(2A3) vs. 3A3	23.2	23.0
	5	1A2+(2A2) vs. 3A2	23.2	23.0
	6	1C3+(2C3) vs. 3C3	20.2	20.0
1:2	7	1S2+(1S2) vs. 2S2	46.6	46.0
	8	1S3+(1S3) vs. 2S3	46.6	46.0
	9	1C3+(1C3) vs. 2C3	46.6	46.0
	10	1S2+(1S2) vs. 2S2	46.4	46.0
	11	1S3+(1S3) vs. 2S3	46.4	46.0
	12	1C3+(1C3) vs. 2C3	46.4	46.0
	13	1A1+(1A1) vs. 2A1	46.4	46.0
	14	2A2+(2A2) vs. 4A2	46.4	46.0
	15	1A2+(2A2) vs. 2A2+(1A2)	46.4	46.0
	16	2A3+(2A3) vs. 4A3	46.4	46.0
	17	1A3+(2A3) vs. 2A3+(1A3)	46.4	46.0
	18	1A3+(1A3) vs. 2A3	46.4	46.0
	19	2S3+(2S3) vs. 4S3	40.4	40.0
	20	1S3+(2S3) vs. 2S3+(1S3)	40.4	40.0
	21	1S3+(1S3) vs. 2S3	40.4	40.0
	22	1C3+(1C3) vs. 2C3	40.4	40.0
	23	1S2+(1S2) vs. 2S2	40.4	40.0
	24	1C2+(1C2) vs. 2C2	40.4	40.0
	25	1A1+(1A1) vs. 2A1	40.2	40.0
	26	1C3+(1C3) vs. 2C3	23.3	23.0
	27	1C3+(1C3) vs. 2C3	23.2	23.0
	28	1A1+(1A1) vs. 2A1	23.2	23.0
	29	2A3+(2A3) vs. 4A3	23.2	23.0
	30	1A3+(2A3) vs. 2A3+(1A3)	23.2	23.0
	31	1A3+(1A3) vs. 2A3	23.2	23.0
	32	2A2+(2A2) vs. 4A2	23.2	23.0
	33	1A2+(2A2) vs. 2A2+(1A2)	23.2	23.0
	34	1A2+(1A2) vs. 2A2	23.2	23.0
	35	1C3+(1C3) vs. 2C3	20.2	20.0
	2:3	36	2S3+(1S3) vs. 3S3	46.6
37		2S3+(1S3) vs. 3S3	46.4	46.0
38		2A1+(1A1) vs. 3A1	46.4	46.0
39		2A2+(2A2) vs. 3A2+(1A2)	46.4	46.0
40		2A2+(1A2) vs. 3A2	46.4	46.0
41		2A3+(2A3) vs. 3A3+(1A3)	46.4	46.0
42		2A3+(1A3) vs. 3A3	46.4	46.0
43		2S3+(2S3) vs. 3S3+(1S3)	40.4	40.0
44		2S3+(1S3) vs. 3S3	40.4	40.0
45		2C3+(1C3) vs. 3C3	40.4	40.0
46		2A1+(1A1) vs. 3A1	40.2	40.0
47		2A1+(1A1) vs. 3A1	23.2	23.0
48		2A3+(2A3) vs. 3A3+(1A3)	23.2	23.0
49		2A3+(1A3) vs. 3A3	23.2	23.0
50		2A2+(2A2) vs. 3A2+(1A2)	23.2	23.0
51		2A2+(1A2) vs. 3A2	23.2	23.0

AREA RATIO	PAIR NO.	WIRE TYPE	WIRE LENGTH(ft)	SPAN (ft)
3:4	52	3A2+(1A2) vs. 4A2	46.4	46.0
	53	3A3+(1A3) vs. 4A3	46.4	46.0
	54	3S3+(1S3) vs. 4S3	40.4	40.0
	55	3C3+(1C3) vs. 4C3	40.4	40.0
	56	3A1+(1A1) vs. 4A1	40.2	40.0
	57	3A1+(1A1) vs. 4A1	23.2	23.0
	58	3A3+(1A3) vs. 4A3	23.2	23.0
	59	3A2+(1A2) vs. 4A2	23.2	23.0
	60	3C3+(1C3) vs. 4C3	20.2	20.0

PART III: The wire type, wire length, and span length for each of the 24 wire pairs which only differ in wire length between the two sets of wires in the same pair.

LENGTH RATIO	PAIR NO.	WIRE TYPE	WIRE LENGTH(ft)	SPAN (ft)
40.2:40.4	1	4S3	40.2, 40.4	40.0
	2	4A2+(2A2)	40.2, 40.4	40.0
	3	4A2	40.2, 40.4	40.0
	4	4A2+(2A3)	40.2, 40.4	40.0
	5	1A2+(2A2)	40.2, 40.4	40.0
	6	1A2+(1A2)	40.2, 40.4	40.0
	7	1A2+(1A2+1A3)	40.2, 40.4	40.0
	8	4A3+(2A3)	40.2, 40.4	40.0
	9	4A3	40.2, 40.4	40.0
	10	1A3+(2A3)	40.2, 40.4	40.0
	11	1A3+(1A3)	40.2, 40.4	40.0
	12	1A3	40.2, 40.4	40.0
	13	4A1	40.2, 40.4	40.0
46.4:46.6	14	2S2	46.4, 46.6	46.0
	15	1S2+(1S2)	46.4, 46.6	46.0
	16	1S2	46.4, 46.6	46.0
	17	1S2+(1C2)	46.4, 46.6	46.0
	18	3S3	46.4, 46.6	46.0
	19	2S3+(1S3)	46.4, 46.6	46.0
	20	1C1	23.2, 23.3	23.0
	21	1C2	23.2, 23.3	23.0
	22	2C3	23.2, 23.3	23.0
	23	1C3	23.2, 23.3	23.0
	24	1C3+(1C3)	23.2, 23.3	23.0

APPENDIX H: IRVINE'S AND SIMPSON'S FORMULAE

PART I: Irvine's static formula [31]

The governing equation for a single span catenary cable hanging statically at the same level at both ends can be expressed as

$$\text{SINH}\left(\frac{wl}{2H} - \frac{wL_0}{2EA}\right) = \frac{wL_0}{2H} \quad (H-1)$$

,where

w = linear unit weight of the cable

H = horizontal tension of the cable

E = modulus of elasticity of the cable

A = cross-sectional area of the cable

L₀ = cable length

l = span length

If both ends are not at the same level as shown in Fig.H, the vertical tension **V** and horizontal tension **H** at left end can be obtained by solving the following two equations simultaneously:

$$l = \frac{HL_0}{EA} + \frac{HL_0}{W} \left[\sinh^{-1} \frac{V}{H} - \sinh^{-1} \frac{V-W}{H} \right] \quad (H-2)$$

$$h = \frac{WL_0}{EA} \left(\frac{V}{W} - 0.5 \right) + \frac{HL_0}{W} \left[\sqrt{1 + \left(\frac{V}{H} \right)^2} - \sqrt{1 + \left(\frac{V-W}{H} \right)^2} \right]$$

,where

l,h=horizontal and vertical distances, respectively, between

both ends of the cable as shown in Fig.H

W =total weight of the cable.

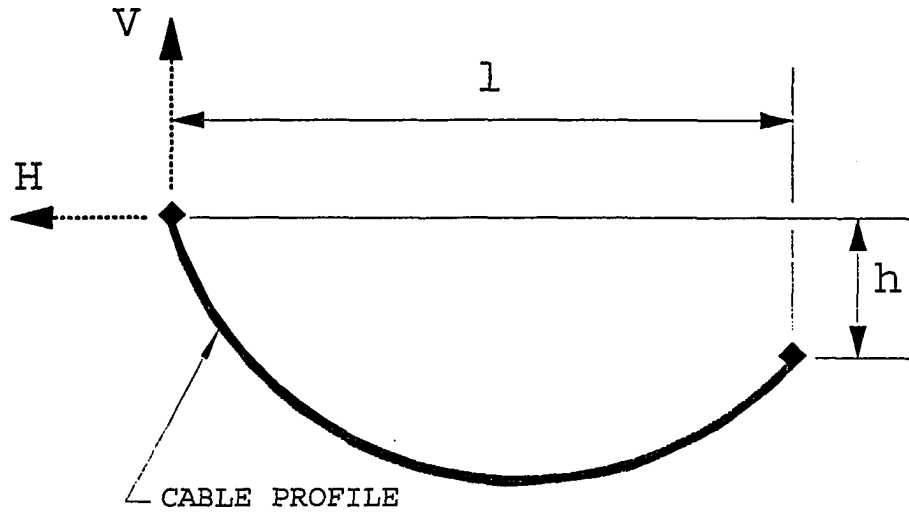


Fig. H: Configuration of a cable element whose ends are not at the same level.

PART II: Simpson's dynamic formula [4]

Simpson's formula for the dynamic support forces of a single-span shallow elastic catenary cable oscillating freely with a small amplitude can be expressed as

$$h = \frac{Hy_0}{\left| -\frac{\theta b_1 H}{\mu m \omega_n^2} + 1 \right|} \left| \frac{b_1}{\mu} \left[1 + \mu \left(1 - \frac{\phi^2}{2} \right) \right] + \frac{4\epsilon\phi}{L_0} \text{SIN}\phi \right|$$

$$v = \frac{Hy_0}{\left| -\frac{\theta b_1 H}{\mu m \omega_n^2} + 1 \right|} \left| \frac{2b_1\epsilon}{\mu} - \frac{2\phi}{L_0} \text{SIN}\phi \right|$$

, where

h = additional horizontal tension in dynamic case with respect to static horizontal tension H

v = additional vertical tension in dynamic case with respect to static vertical tension V

H = static horizontal tension

y_0 = amplitude

$\theta = mg/H$

m = mass per unit length of cable

g = gravity acceleration

$b_1 = \text{COS}\phi / [\epsilon L_0 / (\mu \phi^2)]$

$\phi = [\sqrt{(m/H)}] L_0 \omega_n / 2$

ω_n = natural frequency

$\epsilon = \theta L_0 / 4$

$\mu = H / (EA)$

E = modulus of elasticity

A = cross-sectional area

L_0 =cable length

PART III: Irvine's dynamic formula [31]

Irvine's formula for the dynamic support forces of a single-span taut elastic catenary cable operated under the conditions of free oscillation with a small vertical amplitude and constant additional horizontal tension can be expressed as

$$h = \frac{\omega_n^2 H}{g \left| 1 - \text{SEC} \left(\frac{\omega_n'}{2} \right) \right|} y_0$$

$$v = \sqrt{mH} \omega_n y_0 \left| \text{COT} \left(\frac{\omega_n'}{4} \right) \right| + \left\{ \frac{mg l}{2H} + \sqrt{mH} \omega_n y_0 \left| \text{COT} \left(\frac{\omega_n'}{4} \right) \right| \right\} h$$

,where

h =additional horizontal tension in dynamic case with respect to static horizontal tension H

v =additional vertical tension in dynamic case with respect to static vertical tension V

H =static horizontal tension

y_0 =amplitude

m =mass per unit length of cable

g =gravity acceleration

ω_n =natural frequency

l =span length

$\omega_n' = [\sqrt{(m/H)}] \omega_n l$

APPENDIX I: FIGURES OF SIMILARITY PAIRS OF WIRES

Comparisons of the vertical and horizontal tensions of the prototypes both obtained from the experiment and predicted by the models for the last sixteen pairs of wires in Table 3-18 are shown in Fig. I-1. After considering the length measurement errors, the lower and upper bounds of the prototypes' horizontal tensions obtained by experiment and prediction, respectively, are shown in Fig. I-2.

(a)

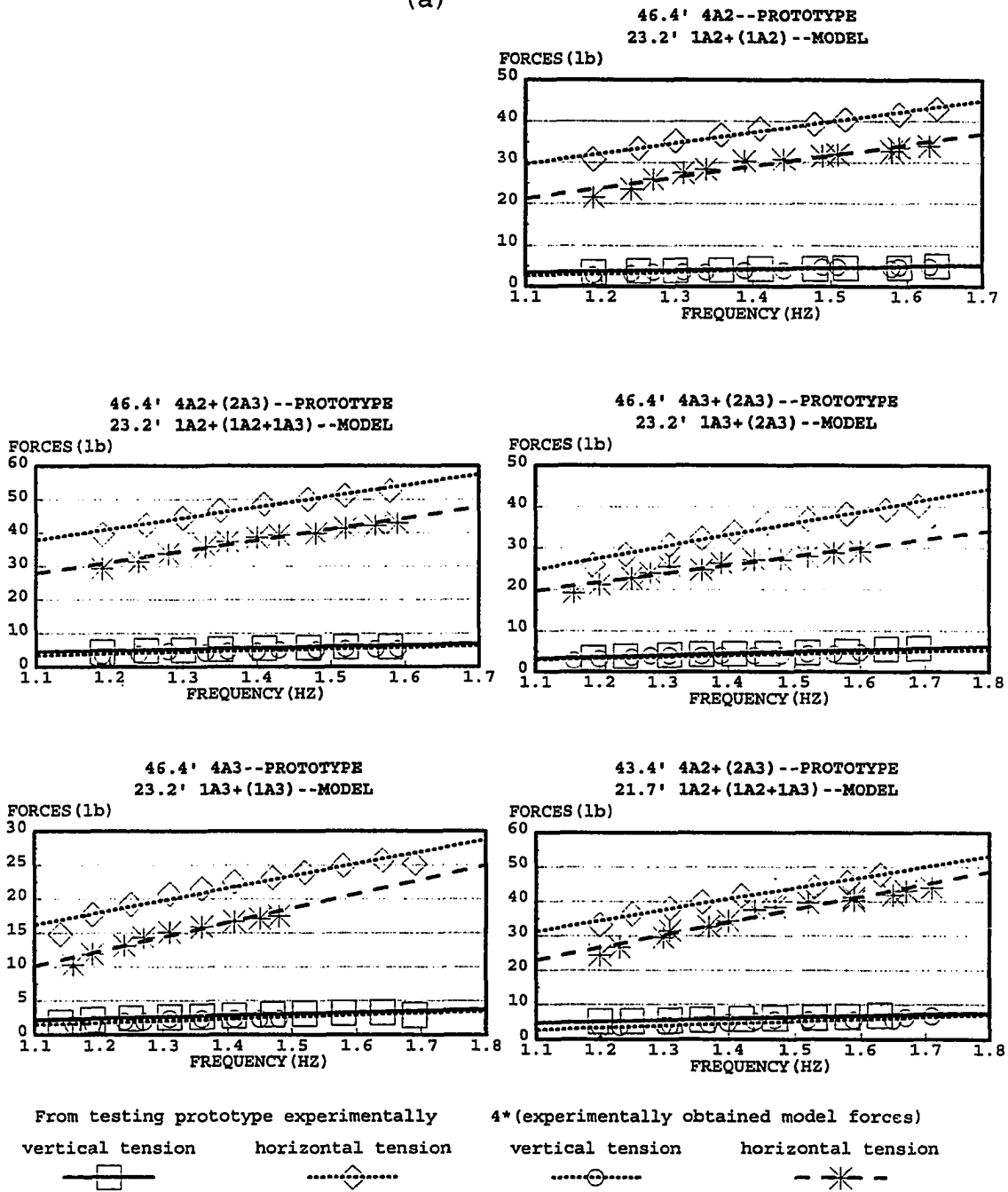
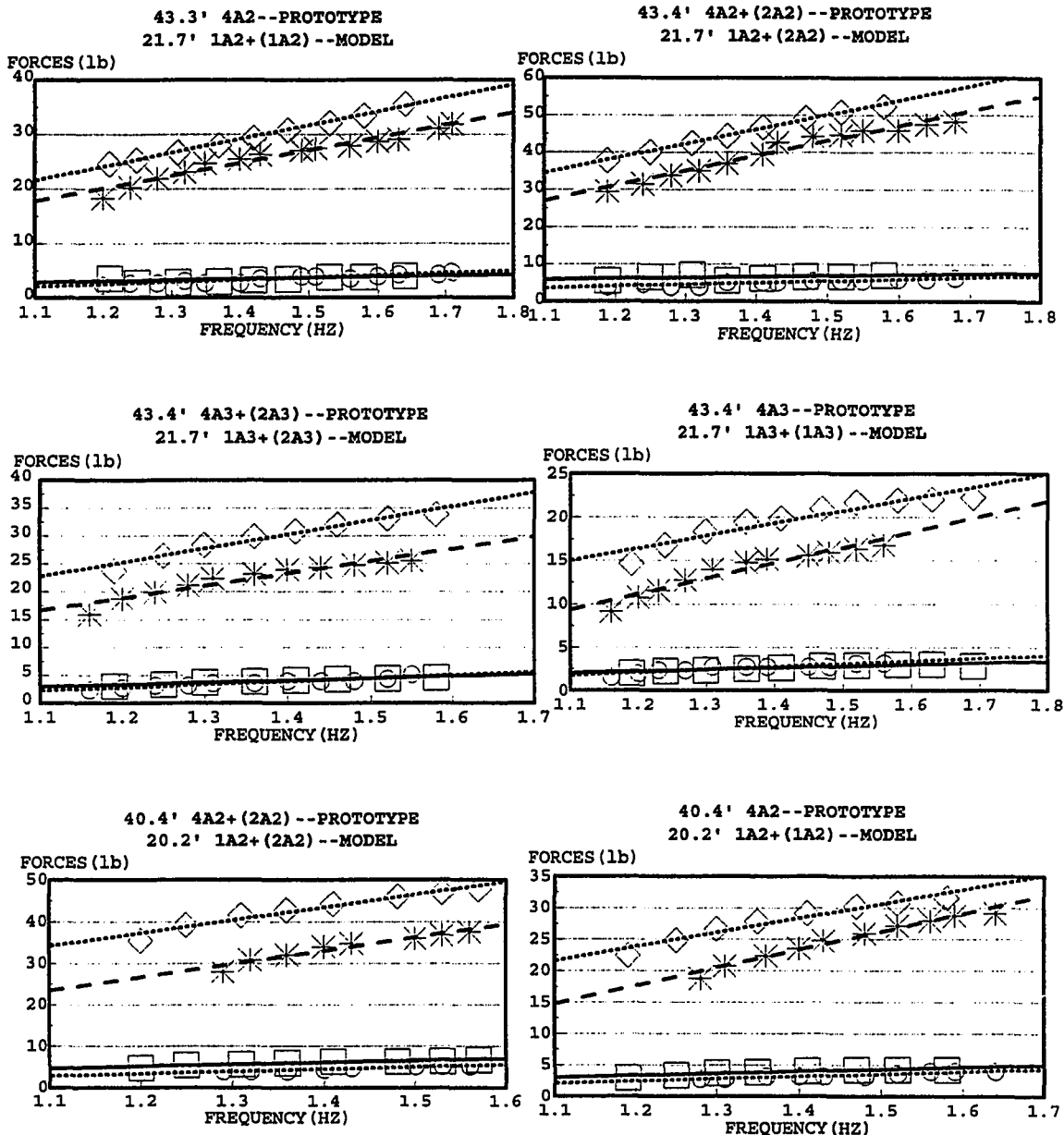


Fig. I-1: Comparison of the vertical and horizontal tensions of the prototype both obtained from the experiment and predicted by the model.

(b)



From testing prototype experimentally 4*(experimentally obtained model forces)

vertical tension horizontal tension vertical tension horizontal tension

□ ◇ ○ *

Fig. I-1: (Continued).

(c)

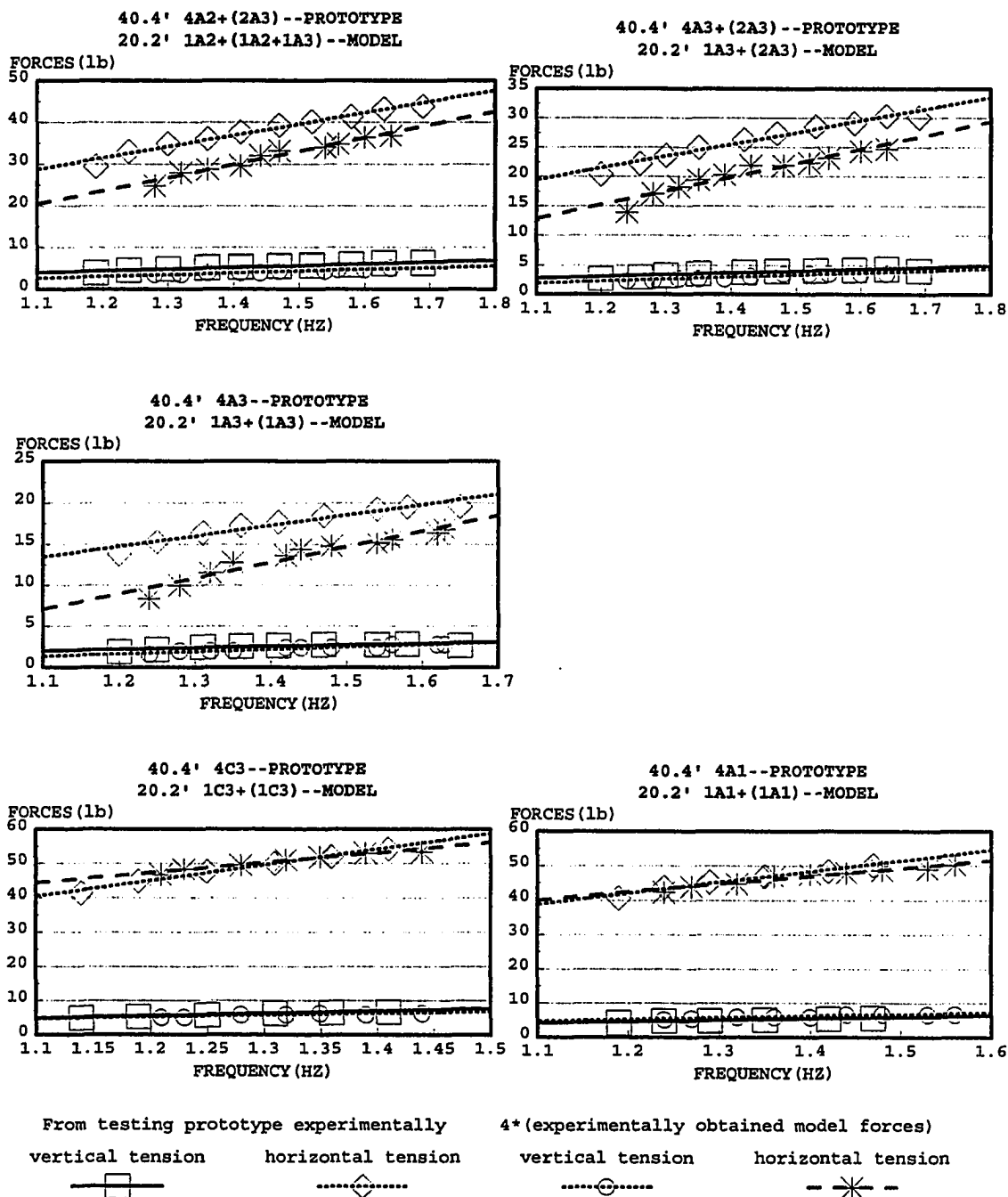


Fig. I-1: (Continued).

(a)

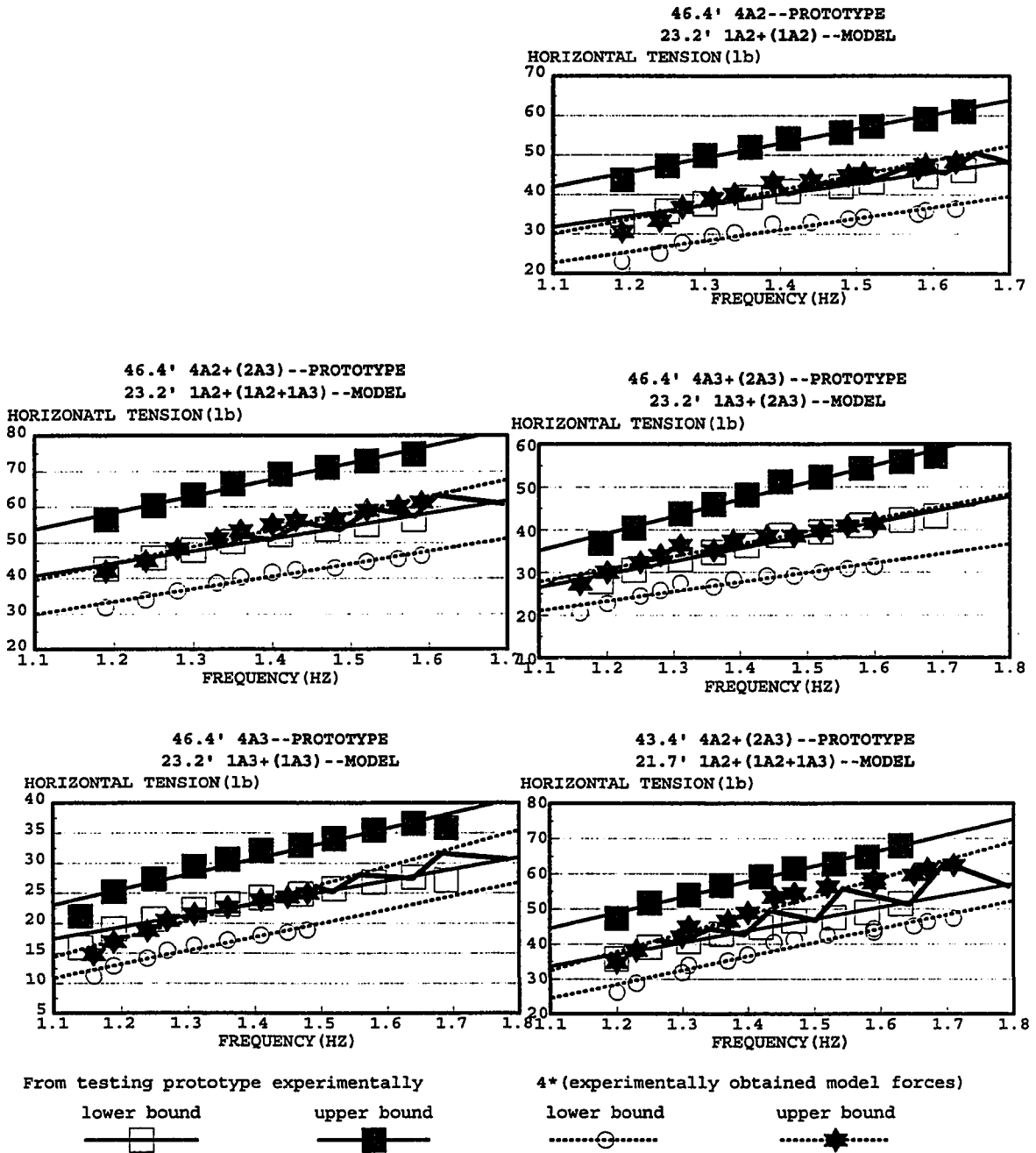


Fig. I-2: Lower and upper bounds of the prototype's horizontal tensions obtained by experiment and prediction, respectively, after considering length measurement error.

(b)

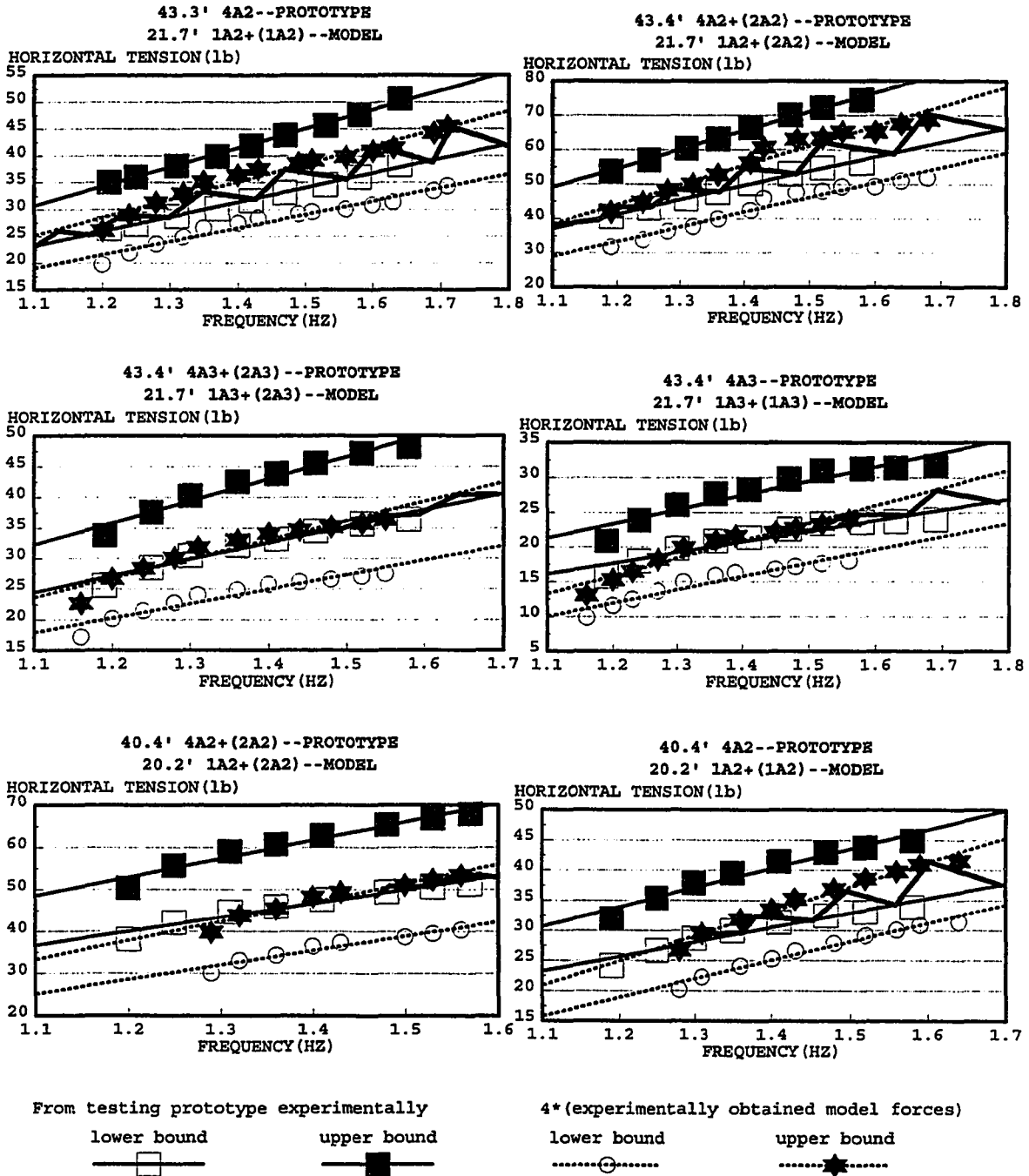
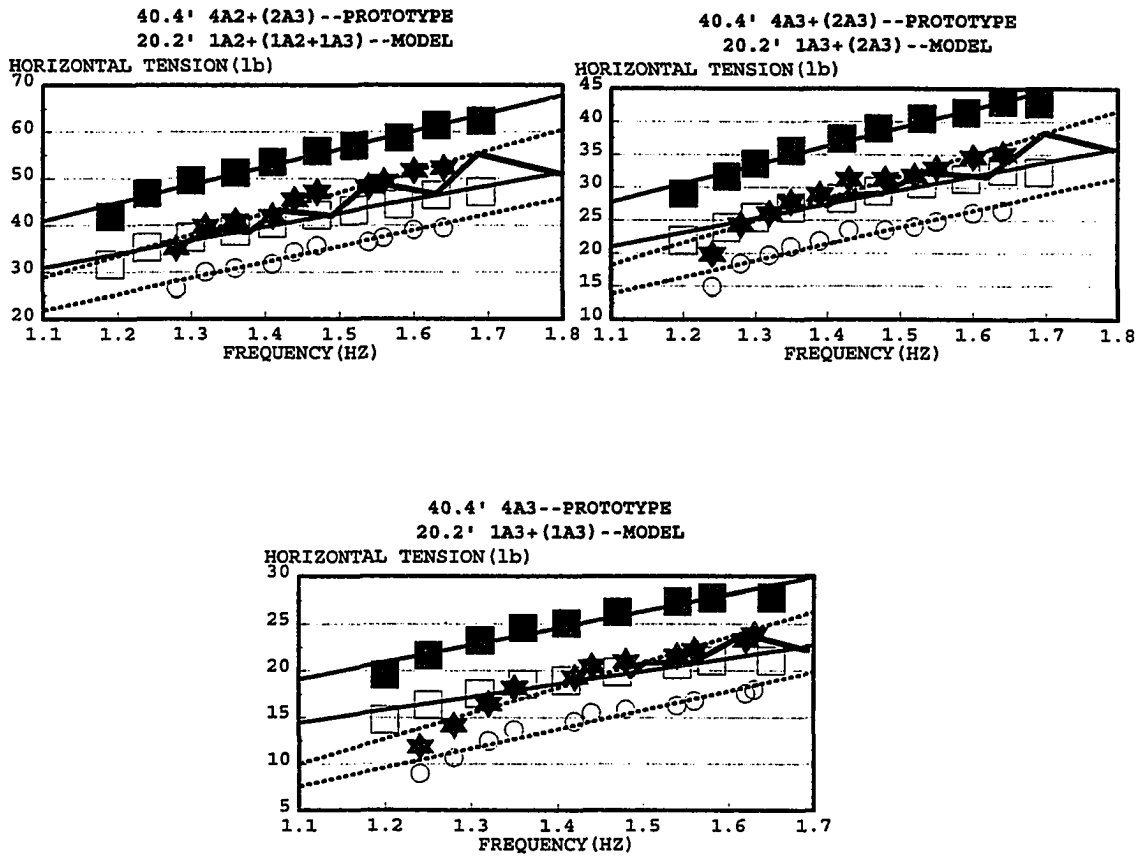




Fig. I-2: (Continued).

(c)



From testing prototype experimentally
 lower bound 
 upper bound 



4*(experimentally obtained model forces)
 lower bound 
 upper bound 

Fig. I-2: (Continued).

REFERENCES

- [1] National Electric Light Association. "Overhead Systems Reference Book.", National Electric Light Association, New York City, NY (1927).
- [2] E.W. Lee. "Nonlinear Forced Vibration of a Stretched String.", British Journal of Applied Physics, Vol. 8, No. 10, pp.411-413 (Oct. 1957).
- [3] Li Li. "Dynamic Loads on Pole Transmission Line Structure from Galloping Conductor.", Master thesis, Iowa State University, Ames, IA (1990).
- [4] A. Simpson. "Determination of the In-plane Natural Frequency of Multispan Transmission Lines by a Transfer-matrix Method.", Proc. IEE, vol 113, No.5, pp.870-880 (May 1966).
- [5] Aluminum Association. "Stress-Strain-Creep Curves for Aluminum Electric Conductor.", Washington, D.C. (1969).
- [6] EPRI. "Transmission Line Reference Book.", Electric Power Research Institute, Palo Alto, California (1979).
- [7] Waltrand A.R. Brinkmann, et al. "Several Local Storm Hazard in the United States: a Research Assessment.", Institute of Behavior Science, the University of Colorado, Boulder, Colorado (1975).
- [8] F. Iliceto, M. Babalioglu, and F. Dabanli, "Report of failure due to ice, wind, and large birds experienced on the 420 kV lines of Turkey", CIGRE, S22-81, pp.50-60 (June 1981).

- [9] Sanjeev Gupta. "Nonlinear Analysis of Transmission Line Structures Subjected to Ice Loads.", Master's thesis, Iowa State University, Ames, IA (1991).
- [10] Den J.P. Hartog. "Mechanical Vibration.", 4th edition, McGraw-Hill, New York, NY (1956).
- [11] A. Simpson. "Wind-induced Vibration of Overhead Power Transmission Lines.", Science Progress Oxford, 68, pp.285-308 (1983).
- [12] A.E. Davison. "Dancing Conductors.", AIEE Transaction, Vol 49, pp.1444-9 (Oct. 1930).
- [13] ANSI. "National Electrical Safety Code.", IEEE Inc., New York, NY (1992).
- [14] Committee on Analysis and Design of Structures of ASCE. "Guidelines for Transmission Line Structure Loading.", ASCE, New York, NY (1984).
- [15] H.H. Farr. "Transmission Line Design Manual.", US Department of Interior, Washington, D.C. (1980).
- [16] J.J. Ratkowski. "Factor Relative to High-Amplitude Galloping.", IEEE pas-87, No.6 (Jun 1968).
- [17] J.J. Ratkowski. "Experiments with Galloping Spans.", AIEE pp.661-669 (Oct. 1963).
- [18] S.G. Krishnasamy. "Wind and Ice Loads on Overhead Transmission Line.", Ontario Hydro Research Review 3, pp.11-18 (Jun 1981).

- [19] C.B. Rawlins. "Analysis of Conductor Galloping Field Observation---Single Conductors." IEEE Transaction on Power Apparatus and Systems, PAS-100, No.8, pp.3744-3753 (Aug. 1981).
- [20] W.D. James, M.A. Baenziger, B. Wouters, Li Li. "Dynamic Loads on Transmission Line structure Due to Galloping Conductors.", Civil and Construction Engineering, Iowa State University, Ames, IA (1991).
- [21] Rural Electrification Administration. "Transmission Line Manual (Mechanical Design).", U.S. Dept. of Agriculture, REA Bulletin 62-1 (May, 1961).
- [22] S. Timoshenko. "Vibration Problems in Engineering.", D. Van Nostrand Company, Inc., New York, NY (1928).
- [23] D.F. Young. "Similitude, modeling, and Dimensional Analysis in Engineering.", Class notes (EM 584), Dept. of Engineering Mechanics and Aerospace Engineering, Iowa State University, Ames, IA (1990).
- [24] Lyman Ott. "An Introduction to Statistical Methods and Data Analysis.", 3rd edition, PWS-KENT Publishing Company, Moston, MA (1988).
- [25] Stephen Timoshenko, "Element of Strength of Materials", fifth edition, Van Nostrand, Princeton, NJ(1968).
- [26] Mardith Baenziger, "Broken Conductor Loads on Transmission Line Structures", Doctoral dissertation, University of Wisconsin-Madison, Madison, WI (1981).

- [27] Brent Wouters, "An Experimental Investigation of the Influence of an Iced-conductor's Characteristics on the Conductor's Tendency to Gallop", Master's Thesis, Iowa State University, Ames, IA (1990).
- [28] Roy R. Craig, Jr. "Structural Dynamics--An Introduction to Computer Method.", John Wiley & Sons, Inc., New York, NY (1981).
- [29] N.C. Barford. "Experimental Measurements: Precision, Error, and Truth.", 2nd edition, John Wiley & Sons, New York, NY (1985).
- [30] Truman L. Kelley. "How Many Figures Are Significant?", Science 60, vol. LX, No. 1562, pp.524 (1924).
- [31] H.M. Irvine. "Cable Structures.", The MIT Press, Cambridge, MA (1981).